The role of hypoxia in urological malignancies



Thesis submitted by
Christopher Blick
Christ Church

For the degree of
Doctor of Philosophy
Department of Medical Oncology
Trinity Term 2012
University of Oxford

Supervisors: Professor Adrian L. Harris
Mr David Cranston

Abstract

Hypoxia, a state of low oxygen, is a feature of most solid tumours as a consequence of poor tumour vascularisation. The mechanisms, which allow cancer cells to survive and continue to grow in hypoxia, are coordinated by the transcription factor HIF. The tumour suppressor gene von Hippel-Lindau (vHL) that targets HIF for degradation is mutated in the vast majority of renal cell carcinomas (RCCs), highlighting the importance of hypoxia to tumour biology. There is, therefore, an important need to understand the adaptive changes mediated by hypoxia and to target this clinically.

One class of genes regulated by HIF are microRNAs (miRNAs). MiRNAs are short, single stranded RNA that primarily inhibit protein expression from target mRNA. The first aim of this project was to identify novel hypoxia regulated miRNAs in bladder cancer and assess their functional significance.

It was found that a number of miRNAs were induced in hypoxic conditions. The hypoxic induction of miR-210 was conserved in all cell lines tested. MiR-145 was found to be highly induced by hypoxia in RT4, a cell line derived from a low-grade, non-muscle invasive tumour. We showed that miR-145 was a novel, HIF target gene with two hypoxia response elements identified within the promoter. Functionally we found that miR-145 induces apoptosis in RT4 cells. MiR-100 was downregulated in hypoxia, but this downregulation did not involve HIF. Regulation of miR-100 was of interest, as it is known to target *FGFR3*, a gene commonly overexpressed or mutated in bladder cancer. Concomitant with a decrease in miR-100, both the mRNA and protein level of *FGFR3* were found to increase in hypoxia in RT4 and RT112 cells. Increased *FGFR3* expression in hypoxia was involved in sustaining activation of the downstream signaling

targets phospho-PKB and phospho-ERK. In addition, we demonstrate a role for *FGFR3* in regulating both 2D and 3D growth and of miR-100 in regulating 3D growth of RT4 cells. We also showed that miR-100 decreased the protein levels of mammalian target of rapamycin (*mTOR*). However, transfection of miR-100 into RT4 cells did not affect the sensitivity of this cell line to rapamycin.

The genetic and biochemical changes that occur in (hypoxic) tumours may alter their responsiveness to chemotherapeutic agents such as rapamycin.

The second aim of this project was to investigate the responsiveness of RCCs to clinically approved chemotherapeutic agents, with the goal of correlating any differences in response to alterations in expression of specific genes.

Although hypoxia regulated miR-100 did not affect sensitivity to rapamycin, we extended these studies and investigated the role of *vHL* status on response of renal cancer cell lines to sorafenib, sunitinib, rapamycin and metformin. We found that the presence of *vHL* increased resistance to rapamycin. Sensitivity to these drugs was also tested in 10 primary cell lines. There was varying sensitivity to these drugs across the cell lines representing the heterogeneity of renal cancer. We analysed the expression of a number of genes in the *mTOR* and hypoxic pathways in these tumours, we found the expression of a known hypoxic gene *REDD1* correlated with sensitivity to rapamycin. *REDD1* expression levels were also higher in tumour tissue when compared to normal renal parenchymal tissue and was associated with other prognostic markers such as CA9, miR-210 and vascular invasion suggesting a role as a diagnostic or prognostic marker and in patient selection for treatment with rapamycin.

Acknowledgements

A great number of people have helped in many different ways towards the completion of this thesis and for this I will always be grateful. I have been incredibly fortunate to receive generous funding from the Royal College of Surgeons of England, The Urology Foundation and UCARE, who supported my first, second and third years of research respectively. I must also thank Cancer Research UK for supporting Professor Harris' laboratory. Much of this funding was acquired through charitable donations and I feel incredibly privileged to have been supported in this way.

I am very grateful to Professor Adrian Harris, as a result of his advice and supervision I have experienced a number of unique opportunities and worked with some incredible people. It has been a privilege to work in his laboratory and I am indebted to him for the great amount of effort he has put into supporting my project. I am also incredibly grateful to David Cranston for offering to be my supervisor. I thank him for his support throughout the last few years, without his backing and belief in my abilities I would not have had this opportunity.

I have been very fortunate to work in Professor Harris' laboratory alongside a number of people from whom I have learnt a great deal. I must particularly acknowledge Anassuya Ramachandran, who has been a great friend and teacher. I thank her for her patience, enthusiasm and 'know how' throughout my time in the lab, without which my time would have undoubtedly been less enjoyable and productive. I must thank those who have given their time to pass on their knowledge and technical skills as well as being friends with whom I have enjoyed many coffee and lunch breaks over the last few years. In particular Simon Wigfield, Rob McCormick, Alan McIntyre, Dean Singleton, Karim Bensaad, Helen Sheldon, Simon Lord and Elena Favaro. I am also grateful to Ioanna Ledaki, Luke Pike, Esther Bridges, Andrew Lomas, John Williams, Dylan Jones and Ulrike Harjes for making the lab such an enjoyable place to work. I am grateful to Helen Turley and Adrian Jubb for their help with immunohistochemistry. To James Catto, David Mole and Margaret Knowles for their advice. To Olga Perestenko for her help with primary cell culture and to Jenny Dollard for her administrative support.

I would also like to thank my family and friends. In particular, my soon to be wife Aoife, who has been extremely understanding and supportive throughout. She most certainly has a lot of time 'owing' as a result of this thesis and I look forward to making that up. Most of all I owe my parents a huge debt of gratitude. They continue to be my most loyal supporters and have always been prepared to go the extra mile on my behalf, I certainly owe my achievements so far to them and for that I will always be grateful.

Abbreviations

%	Percent
3’	The end of the RNA or DNA strand that has the third carbon in the sugar ring of the deoxyribose or ribose at its terminus
4EBP1	Eukaryotic translation initiation factor 4E binding protein1
5’	The end of the DNA or RNA strand that has the fifth carbon in the sugar ring of the deoxyribose or ribose at its terminus
ANOVA	Analysis of variance
BCG	Bacillus Calmette Guerin
CA9	Carbonic anhydrase 9
ccRCC	Clear cell renal cell carcinoma
cDNA	Complementary DNA
ChIP	Chromatin immunoprecipitation
cis	Carcinoma in situ
cm	Centimetres
CT	Computed tomography
DEPC	Diethylpyrocarbonate
DMOG	Dimethyloxallyl glycine
DNA	Deoxyribonucleic acid
dTTP	Thymidine triphosphate
eg	For example
EMT	Epithelial to mesenchymal transition
FFPE	Formalin-fixed, paraffin embedded
FGFR3	Fibroblast growth receptor 3
g	Grams
HCL	Hydrochloric acid
HIF	Hypoxia inducible factor
HIFU	High-intensity focused ultrasound
HRE	Hypoxia response element
HRM	Hypoxia regulated microRNA
HRP	Horseradish peroxidase
IFN-alpha	Interferon- alpha
IHC	Immunohistochemistry
Ki67	Antigen identified by monoclonal antibody Ki67
l	Litre
LDHA	Lactate dehydrogenase A
M	Molar
MAPK	Mitogen activated protein kinases
MI	Muscle invasive
miRNA	MicroRNA
ml	Millilitres
mM	Millimolar
mRCC	Metastatic renal cell carcinoma
MRI	Magnetic resonance imaging
mRNA	Messenger RNA

mTOR	Mammalian target of rapamycin
^{o}C	Degrees Celsius
PBS	Phosphate buffered saline
pH	Power of hydrogen
PHD	Prolyl hydroxylase
PI	Propidium iodide
PI3K	Phosphatidyl inositol kinase
RCC	Renal cell carcinoma
RFA	Radiofrequency ablation
RISC	RNA-Induced Silencing complex
RNA	Ribonucleic acid
rpm	Revolutions per minute
RTK	Receptor tyrosine kinase
RT-qPCR	Quantitative real time polymerase chain reaction
Scr	Scramble
SDS	Sodium dodecyl sulphate
siRNA	Short interfering RNA
TK	Tyrosine kinase
TKI	Tyrosine kinase inhibitors
TNM	Tumour, node, metastasis
UK	United Kingdom
UTR	Untranslated region
VEGF	Vascular endothelial growth factor
vHL	von Hippel-Lindau
ΔΔCT	Delta delta cycle threshold
µg	Microgram
µl	Microlitre
µM	Micromolar

Table of contents

Abstract 2

Acknowledgements 4

Abbreviations 5

Table of contents 7

List of figures 11

List of tables 13

Chapter 1 Introduction and aims of the project 14

1.1. Foreword 14

1.2. The Hallmarks of cancer 15

1.2.1. Sustained cell proliferation 16

1.2.2. Evading growth suppressors 20

1.2.3. Activating invasion and metastasis 21

1.2.4. Enabling replicative immortality 22

1.2.5. Stimulating angiogenesis 23

1.2.6. Resisting apoptosis 23

1.3. Hypoxia 24

1.3.1. Hypoxia and HIF 25

1.3.2. Hypoxia and cancer 27

1.3.3. Hypoxia and the tumour microenvironment 28

1.3.4 Hypoxia, HIF and energy metabolism 29

1.3.5. Therapies targeting hypoxic pathways in urological malignancies 31

1.4 RNA interference and microRNAs 32

1.4.1. miRNAs 32

1.4.2. Biosynthesis 33

1.4.3. Gene silencing by miRNAs 36

1.4.4. miRNAs and cancer 38

1.4.5. miRNAs and hypoxia 40

1.5 Bladder cancer 43

1.5.1. Epidemiology 43

1.5.2. Risk factors 43

1.5.3. Tumour staging 44

1.5.4. Pathogenesis 46

1.5.5. miRNAs in bladder cancer 47

1.5.6. Treatment 49

1.6 Renal cancer 52

1.6.1. Epidemiology and risk factors 52

1.6.2. Tumour diagnosis and staging 53

1.6.3. Pathogenesis 55

1.6.4 Treatment 57

1.7 Aims of project 62

Chapter 2 Materials and Methods 63

2.1 Materials and reagents 63

2.1.1. Plasticware 63

2.1.2. Cell culture reagents 63

2.1.3 Enzymes and kits 63

2.1.4 Primers and TaqMan assays 64

2.1.5. Low density array cards 65
2.1.6 siRNA, microRNA mimics and anti-miRs 65
2.2 Methods *66*
2.2.1 Routine cell culture 66
2.2.2 Primary cell culture 68
2.2.3 Long term cell storage 69
2.2.4 Exposure of cells to hypoxia 69
2.2.5 RNA extraction and quantification 70
2.2.6 Reverse transcription of mRNA 71
2.2.7 Reverse transcription of miRNA 71
2.2.8 Quantitative PCR 71
2.2.9 Normalisation and quantification of gene expression 72
2.2.10 Protein extraction and quantification 73
2.2.11 SDS-poly acrylamide gel electrophoresis 74
2.2.12. Immunohistochemistry 76
2.2.13. DNA extraction 76
2.2.14. Transfection of small RNA 77
2.2.15. Transduction of shRNA constructs 77
2.2.16 Chromatin immunoprecipitation 77
2.2.17 Flow cytometry 78
2.2.18 Luciferase assay 79
2.2.19 SRB assay 79
2.2.20 Spheroid growth 80
2.2.21 Drug treatment 80
2.2.22 Statistical analysis 81

Chapter 3 Hypoxia regulated miRNAs and the role of miR-145 in bladder cancer. 82

3.1. Introduction *82*
3.1.1. Hypoxia in bladder cancer 82
3.1.2. microRNAs in bladder cancer 82
3.2 Results *85*
3.2.1 Normalisation of controls 85
3.2.2. Analysis of known hypoxia regulated microRNAs in bladder cancer cell lines 87
3.2.3. MicroRNA-210 88
3.2.4. MicroRNA-155 88
3.2.5. microRNA-193b 93
3.2.6. microRNA-503 93
3.2.7. microRNA-100 98
3.2.8. microRNA-424 98
3.2.9. Low density microarray analysis of RT4 and T24 cell lines in hypoxia 104
3.2.10. Validation of RT4 array data 109
3.2.11 Validation of T24 array data 115
3.2.12. Hypoxic and *p53* regulation of miR-145 121
3.2.13. Identification of hypoxic response elements for miR-145 123
3.2.14. The role of miR-145 in apoptosis and the myc pathway 125
3.2.15. The effect of miR-145 on apoptosis 127
3.3 Discussion *130*
3.3.1. Hypoxia regulated miRNAs that may be part of a core signature 130
3.3.2. Hypoxia regulated miRNAs that may be unique to bladder cancer 132
3.3.3. The role of miR-145 in non- invasive bladder cancer 136
3.3.4. Conclusion 138

Chapter 4 The hypoxic regulation of *FGFR3* expression via *HIF-1α* and miR-100. 140
4.1 Introduction *140*
4.1.1. Molecular alterations in bladder cancer 140
4.1.2. FGFR3 in disease 140
4.2 Results *143*
4.2.1. Hypoxic regulation of miR-100 expression 143
4.2.2. Hypoxic regulation of *FGFR3* mRNA expression 146
4.2.3. The hypoxic regulation of FGFR3 protein 148
4.2.4. Identification of hypoxia response elements in FGFR3 150
4.2.5. A role for miR-100 regulating *FGFR3* levels in RT4 cells 152
4.2.6. miR-100 and FGFR3 regulation of downstream targets and cell growth 154
4.2.7. The effects of FGFR3 and miR-100 on 2-D and 3-D cell growth 156
4.2.8. Immunohistochemistry of FGFR3 in bladder cancer samples 159
4.3 Discussion *161*
4.3.1 The hypoxic regulation of FGFR3 161
4.3.2. miR-100 regulation of FGFR3 162
4.3.3. Mechanisms of FGFR3 and miR-100 regulation 162
4.3.4. Translational relevance 164
4.3.5. Conclusion 165

Chapter 5 The role of vHL mutation and hypoxia regulated genes in predicting sensitivity to targeted therapies in renal cancer. 167
5.1. Introduction *167*
5.1.1. vHL and renal cancer 167
5.1.2. Targeted therapies in renal cancer 168
5.2. Results *172*
5.2.1. The effect of hypoxia on miR-100 expression in renal cancer cell lines 172
5.2.2. Sensitivity of vHL null and competent RCC4 cells to rapamycin 175
5.2.3. Sensitivity of vHL null and competent RCC4 cells to sunitinib 177
5.2.4. Sensitivity of vHL null and competent RCC4 cells to sorafenib 179
5.2.5. Sensitivity of vHL null and competent RCC4 cells to metformin 179
5.2.6. Sensitivity of 786-0 cells to chemotherapeutic agents 182
5.2.7. Sensitivity of UMRC2 cells to chemotherapeutic agents 184
5.2.8. Sensitivity of HUVEC cells to chemotherapeutic agents 186
5.2.9. Summary 186
5.2.10. Sensitivity of primary renal cancer cell lines to targeted therapies 188
5.2.11. Comparison of historic and primary cell lines 197
5.2.12. Genes involved in the hypoxic and mTOR pathways in renal cancer 198
5.2.13. Analysis of gene expression data from renal cancer cell lines 201
5.2.14. Gene co-expression in primary cell lines 209
5.2.15. Gene expression and rapamycin sensitivity 211
5.2.16. REDD1 expression in renal cancer cell lines 211
5.2.17. REDD1 expression and clinical data 214
5.3. Discussion *219*
5.3.1. miR-100 in renal cancer 219
5.3.2. vHL mutation and drug sensitivity 220
5.3.3. Does the absence of competent vHL effect gene expression? 222
5.3.3. Correlation of gene expression 227
5.3.4. Can gene expression predict sensitivity to rapamycin? 228
5.3.5. The role of REDD1 in renal cancer 229
5.3.6 Conclusion 230

Chapter 6 Conclusions and future plans **232**
6.1. Hypoxia regulated miRNAs in bladder cancer *232*
6.2. The role of vHL mutation and hypoxia regulated genes in predicting sensitivity to targeted therapies *234*
Publications and presentations **237**
References **238**

List of figures

Figure 1-1 The hallmarks of cancer **16**
Figure 1-2 *PKB* and *ERK/MAPK* pathways **19**
Figure 1-3 MicroRNA biosynthesis **35**
Figure 1-4 Summary of the mTOR pathway **61**
Figure 2-1 Characterisation of cell lines **67**
Figure 3-1 Selection of control gene for miRNA experiments **86**
Figure 3-2 Regulation of miR-210 by hypoxia in bladder cell lines **89**
Figure 3-3 miR-210 expression in cells treated with DMOG **90**
Figure 3-4 Regulation of miR-155 by hypoxia in bladder cell lines **91**
Figure 3-5 miR-155 expression in cells treated with DMOG **92**
Figure 3-6 Regulation of miR-193b by hypoxia in bladder cell lines **94**
Figure 3-7 miR-193b expression in cells treated with DMOG **95**
Figure 3-8 Regulation of miR-503 by hypoxia in bladder cell lines **96**
Figure 3-9 miR-503 expression in cells treated with DMOG **97**
Figure 3-10 Regulation of miR-100 by hypoxia in bladder cell lines **99**
Figure 3-11 miR-100 expression in cells treated with DMOG **100**
Figure 3-12 Regulation of miR-424 by hypoxia in bladder cell lines **101**
Figure 3-13 miR-424 expression in cells treated with DMOG **102**
Figure 3-14 Profiling of hypoxia regulated miRNAs in RT4 and T24 cells **107**
Figure 3-15 MicroRNAs upregulated in hypoxia in RT4 and T24 cells **108**
Figure 3-16 Regulation of miR-145 by hypoxia in bladder cell lines **110**
Figure 3-17 Regulation of miR-518-3p by hypoxia in bladder cell lines **111**
Figure 3-18 Regulation of miR-125a-3p by hypoxia in bladder cell lines **112**
Figure 3-19 Regulation of miR-519d by hypoxia in bladder cell lines **113**
Figure 3-20 Regulation of miR-708 by hypoxia in bladder cell lines **114**
Figure 3-21 Hypoxic regulation of miR-518f in bladder cell lines **116**
Figure 3-22 Regulation of miR-150 by hypoxia in bladder cell lines. **117**
Figure 3-23 Regulation of miR-200a by hypoxia in bladder cell lines **118**
Figure 3-24 Regulation of miR-15a by hypoxia in bladder cell lines **119**
Figure 3-25 Regulation of miR-99a by hypoxia in bladder cell lines **120**
Figure 3-26 HIF-1α and p53 regulation of miR-145 in RT4 cells **122**
Figure 3-27 Identification of putative hypoxia response elements for miR-145 **124**
Figure 3-28 The role of miR-145 in c-myc and p21 expression **126**
Figure 3-29 Effects of miR-145 expression on apoptosis in RT4 cells **129**
Figure 4-1 Hypoxic regulation of miR-100 and targetting of *FGFR3* **145**
Figure 4-2 Regulation of *FGFR3* mRNA by hypoxia in bladder cancer cell lines **147**
Figure 4-4 Identification of putative HRE in FGFR3 **151**
Figure 4-5 Regulation of *FGFR3* levels by miR-100 **153**
Figure 4-6 Regulation of ERK and PKB signaling by FGFR3 and miR-100 **155**
Figure 4-7 Impact of FGFR3 and miR-100 on RT4 cell viability **157**
Figure 4-8 Effect of FGFR3 and mimic miR-100 upon 3-D growth of RT4 spheroids **158**
Figure 4-9 Immunohistochemistry of FGFR3 **160**
Figure 5-1 miR-100 regulation by hypoxia **174**
Figure 5-4 Sorafenib sensitivity in RCC4 cells **180**
Figure 5-5 Metformin sensitivity in RCC4 cells **181**
Figure 5-6 Drug sensitivity in 7860 cells **183**
Figure 5-7 Drug sensitivity in UMRC2 cells **185**
Figure 5-8 Drug sensitivity in HUVEC cells **187**
Figure 5-9 Primary renal cancer cell lines **189**
Figure 5-10 Drug sensitivity of primary renal cancer cell lines **191**
Figure 5-11 Drug sensitivity in primary renal cancer cell lines **193**
Figure 5-12 Comparison of drug sensitivities in renal cancer cell lines **196**
Figure 5-13 Gene expression in RCC4 and 7860 cells **202**
Figure 5-14 Gene expression in cell lines 17511.11, 27877.10 and 35236.10 **204**
Figure 5-15 Gene expression from cell lines 36993.10, 04134.10 and 5711.10 **205**
Figure 5-16 Gene expression in cell lines 00929.11, 09885.11 and 34484.11 **206**

Figure 5-17 Gene expression from cell line 35285.11 **207**
Figure 5-18 Rapamycin, the mTOR pathway and integration of REDD1 and AMPK signaling **212**
Figure 5-19 REDD1 expression in RCC4 and 7860 cells **213**
Figure 5-20 REDD1 correlation with rapamycin sensitivity and expression in tumours **215**
Figure 5-21 REDD1 expression and tumour variables **217**
Figure 5-22 REDD1 knockdown and rapamycin sensitivity **218**

List of tables

Table 1-1 Hypoxia regulated miRNAs 41
Table 1-2 TNM classification of bladder cancer 46
Table 1-3 Altered miRNA expression in bladder cancer [126] 48
Table 1-4 EAU guidelines, scoring for progression and recurrence 50
Table 1-5 EAU guidelines for treatment for non-muscle invasive bladder cancer 2011 51
Table 1-6 Bosniak classification of renal cysts 54
Table 1-7 TNM classification of renal cancer 54
Table 2-1 Cell lines and reagents 68
Table 3-1 microRNAs up or downregulated depending on vHL mutation 87
Table 3-2 Summary of miRNA expression in response to hypoxia in bladder cancer 104
Table 3-3 Results from flow cytometry. 128
Table 4-1 Correlation of miR-100 and the metagene signature 144
Table 4-2 Number and stage of tumours stained for FGFR3 and CA9 159
Table 5-1 IC50 values for primary renal cancer cells 195
Table 5-2 Sensitivity of renal cancer cells to targeted therapies 198
Table 5-3 Genes selected for analysis in renal cancer cell lines 200
Table 5-4 Gene expression in primary cell lines 208
Table 5-5 Correlation of gene expression 210
Table 5-6 Correlation of gene expression with rapamycin sensitivity 211

Chapter 1 Introduction and aims of the project

1.1. Foreword

Cancer is one of the leading causes of death worldwide, with an estimated 8 million people dying from this disease each year [1]. Cancer is primarily a diagnosis associated with increasing age and therefore as life expectancy increases so to will the incidence of this disease. Cancer is characterized by uncontrolled cell growth and the loss or alteration of homeostatic mechanisms, which under normal conditions limit cell growth and induce cell death in times of stress. It is the loss of control, and the ability to develop mechanisms to avoid cell death, which allow cancer cells to survive and proliferate in harsh conditions. The cause of cancer is multifactorial, activation of oncogenes and inhibition of tumour suppressor genes contribute to altered regulation of the cell cycle leading to sustained cell growth. The interaction between cancer cells, their microenvironment and surrounding stroma is particularly important to growth and contributes to tumour heterogeneity.

This introduction begins by describing certain features common to all cancers. I then discuss hypoxia as a pathological state that can enhance oncogenesis. The role of a novel class of regulators of gene expression, microRNAs (miRNAs) will also be discussed. Where appropriate, these sections will be discussed in the context of bladder and renal cancers, which are the focus of this thesis. Finally, I will outline the aims of the work undertaken herein.

1.2. The Hallmarks of cancer

Cancer is a multi-step process where normal cells sustain genetic damage over a prolonged period of time, which along with inherent susceptibilities, leads to the manifestation of the transformed phenotype. In 2000, Hanahan and Weinberg described 6 hallmarks that are applicable to all cancer types - sustained proliferative signaling, resisting cell death, evading growth suppressors, activating invasion and metastasis, inducing angiogenesis and enabling replicative immortality [2](Figure 1.1). More recently metabolic reprogramming and evading the immune system have been included as emerging hallmarks of cancer [3].

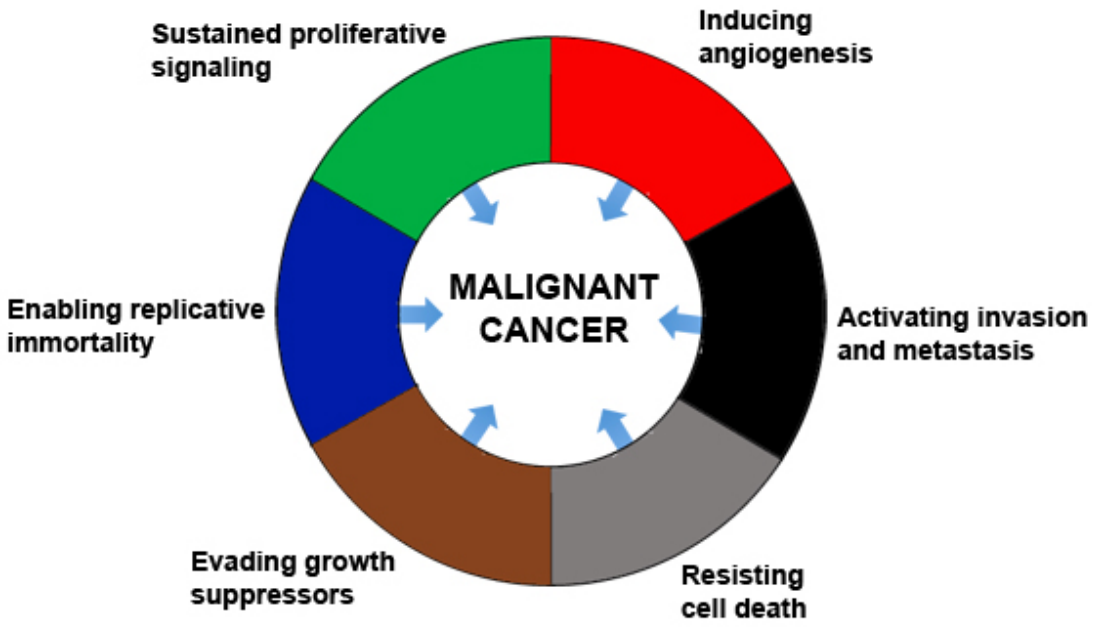


Figure 1-1 The hallmarks of cancer

1.2.1. Sustained cell proliferation

All cells require growth signals (mitogenic signals) to proliferate; cancer cells are no exception and must have continuous growth stimulatory signals to survive. Many cancers produce their own growth factors, such as TGFα and EGF, which act as autocrine messaging cues and permit growth independent of the surrounding environmental influences. The growth factors act on cells primarily via cell surface receptor tyrosine kinases (RTKs). Ligand binding to RTKs leads to

receptor phosphorylation; for example, ligand binding to IGFR1 leads to autophosphorylation of tyrosines 1131, 1135 and 1136 which serve as binding sites for the insulin receptor substrate (IRS) 1 to 4 [4]. Phosphorylated receptors then activate intracellular signaling pathways (see below) that lead to cell proliferation.

Through mutations, the need for extracellular growth factors can be bypassed by the constitutive activation and independent regulation of downstream signaling. Mutations in growth factor receptors are a common mechanism of continued signaling in many cancer types. For example, the activation of *FGFR3* by overexpression or mutation is common in bladder cancer [5]. The mutation spectrum of *FGFR3* range from those that induce ligand independent receptor dimerisation and signaling to those that activate the kinase domain [6]. The role of *FGFR3* in bladder cancer is discussed further in Chapter 4.

In addition to mutations of receptors and overexpression of ligands, sustained proliferation can occur by the constitutive activation of intracellular signaling pathways. Arguably the most characterised intracellular oncogenic pathways are those mediated by the extracellular receptor activated kinases (ERK) (also known as mitogen activated protein kinases (MAPK)) and the phosphatidylinositol 3- kinase (PI3K) pathway.

1.2.1.1. The ERK/MAPK Signaling Pathway

The ERK/MAPK signaling pathway is, in essence a phosphorylation relay system. The pathway is initiated by the activation of the small GTP binding protein RAS by RTKs or adaptor proteins in the receptor complex such as IRS. Activated RAS

activates the first serine/threonine kinase in the cascade, the MAP kinase kinase kinase (MAPKKK) RAF. RAF in turn phosphorylates and activates the dual specificity MAP kinase kinase (MAPKK) MEK; MEK tyrosine phosphorylates the final tyrosine kinase in the cascade, ERK (p42/44 MAPK) (Figure 1.2) [7]. Activated ERK in turn phosphorylates a number of proteins, including transcription factors required for cell proliferation. The importance of the *ERK/MAPK* pathway in oncogenesis is highlighted by the fact that mutation in components of this pathway occur in approximately 30% of cancers [8]. Indeed, mutations in *RAS* are documented in approximately 20% of bladder cancers [9].

1.2.1.2. The PI3 Kinase Signaling Pathway

The phosphatidylinositol 3-kinase (*PI3K*) pathway is another signaling pathway commonly affected by somatic mutations or gene amplifications leading to increased cancer cell proliferation. There are 3 classes of PI3Ks of which class I PI3Ks act downstream of receptor tyrosine kinases (RTKs). Class I PI3Ks are composed of a regulatory p85 subunit and a catalytic p110 subunit [10]. Via its phospho-tyrosine binding SH2 domain, the p85 subunit localizes PI3K to the activated receptor and plasma membrane [11]. At the plasma membrane, PI3K phosphorylates its preferred substrate phosphoinositide (4,5) bisphosphate (PIP2) to phosphoinositide (3,4,5) triphosphate (PIP3). PIP3 serves as a binding site for proteins that have phospho-lipid binding domains such as pleckstrin homology (PH) and FYVE domains [12]. Two proteins that contain PH domains are PDK1 and AKT; both proteins are recruited to the plasma membrane where PDK1 phosphorylates AKT at threonine 308, causing partial activation [13]

(Figure 1.2). Full AKT activation requires additional phosphorylation on serine 473 by the mTORC2 complex; this is discussed further in Chapter 1.6.4.2 Activated AKT phosphorylates many downstream target genes to inhibit cell cycle arrest and apoptosis and promote cell growth, thereby leading to increased cell survival and proliferation [10]. PI3K signaling is often activated in cancers by mutations in either the p85 or p110 subunits of *PI3K* or by mutations in *AKT1*.

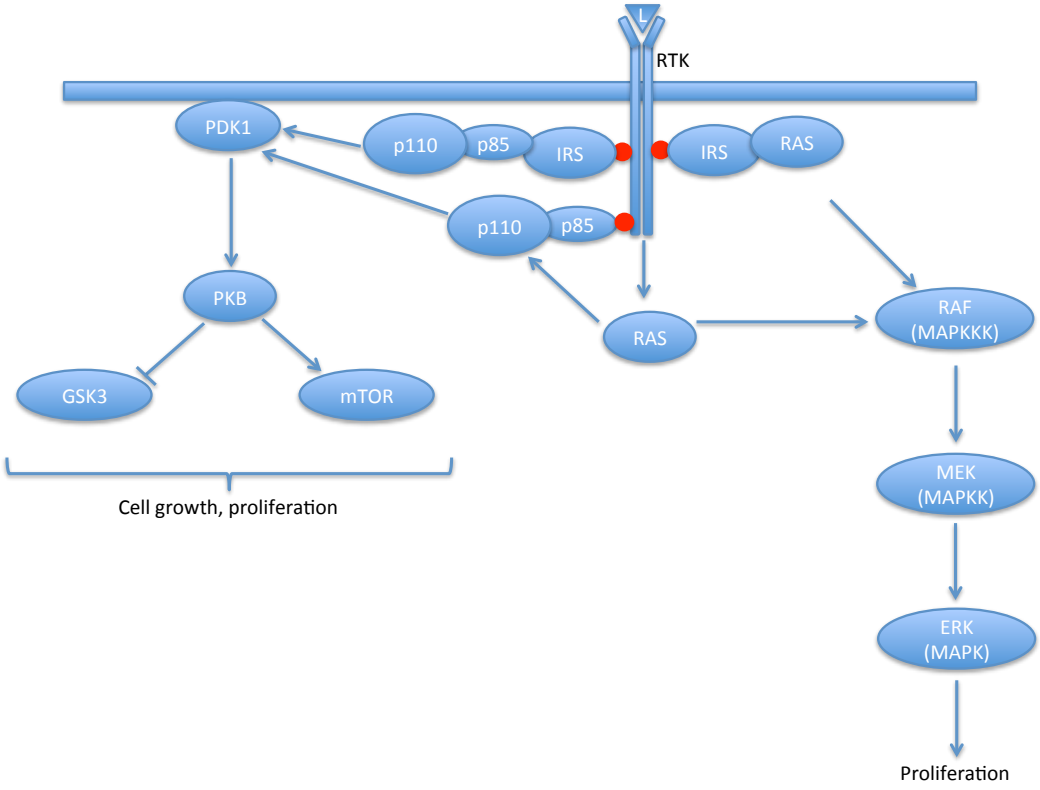


Figure 1-2 *PKB* and *ERK/MAPK* pathways

L= ligand, RTK= Receptor Tyrosine Kinase

1.2.2. Evading growth suppressors

In normal cells, proliferative signals are countered by events such as contact inhibition so that proliferation is coupled almost completely to tissue requirements. Cancer cells, on the other hand, are largely insensitive to normal growth restrictive cues; loss of sensitivity to growth inhibitory pathways is a prerequisite for continued cancer cell survival. A large number of tumour suppressors exist to limit cell growth and mutation of tumour suppressors can alter regulation and entry into the cell cycle and subsequent cell division. Perhaps the most frequently mutated gene in the cancer genome is the tumour suppressors *p53*. The *p53* gene encodes a transcription factor whose levels are normally held in check by the ubiquitin ligase MDM2. Under conditions of stress, MDM2 is sequestered, thereby allowing p53 to lead to the transcription of its target genes including *p21, NOXA, PUMA* and *PIG3* eventually causing cell cycle arrest, senescence or apoptosis. Mutations in *p53* have been documented in around 40% of bladder cancers, although they are more common in high grade tumours [14, 15].

The retinoblastoma protein (Rb) binds to, and sequesters the E2F transcription factor in quiescent cells. Upon growth factor stimulation, CYCLIN:CYCLIN dependent kinase (CDK) complexes hyperphosphorylate Rb, eventually leading to its dissociation from E2F, which is then free to lead to the transcription of genes required for cell cycle progression. Inactivating mutations in *Rb* that prevent its binding to E2F have been documented in around 35% of bladder cancers [16] and alterations in either or both of *p53* and *Rb* are associated with a poor prognosis in bladder cancer [17].

Proteins that negatively regulate the ERK and PI3K pathways are also considered tumour suppressors as they inhibit growth stimulatory pathways. A key negative regulator of PI3K signaling is the protein and lipid phosphatase PTEN. PTEN is responsible for the dephosphorylation of phosphatidyl-inositol 3,4,5 triphosphate (PIP3) to PIP2, reversing the phosphorylation event mediated by PI3K signaling, thereby limiting the activation of PKB. Mutations in *PTEN* leads to the aberrant activation of the pro-mitotic pathway PI3K [18].

1.2.3. Activating invasion and metastasis

In the majority of cases, it is not always the biology of the primary tumour that is associated with mortality but rather the presence of metastases at distant sites. Of all the aspects of cancer biology, metastasis is perhaps the least well understood. Metastasis is a multistep process in which cancer cells must first detach from their primary tumour, migrate through the surrounding tissue, intravasate into the vasculature, survive and finally extravasate from the vasculature, invade and colonise the secondary site. Activating invasion and metastasis or more simply progression of disease is complex and involves the induction of epithelial-to-mesenchymal transition (EMT) of cancer cells, degradation of the basement membrane, loss of cell polarity and remodeling of the actin cytoskeleton in cancer cells to allow them to invade [19]. The induction of matrix metalloproteases (MMP) and urokinase-type plasminogen activator aids in the dissolution of the extracellular matrix and regulation of *RHO*, RAC and CDC42 signaling affects cell motility. A key mechanism for EMT is due to a shift in cadherin expression/function. E-CADHERIN is primarily expressed by epithelial

cells and downregulation of E-CADHERIN is one of the features of the epithelial-to-mesenchymal transition (EMT) that occurs in invasive cancer cells. Abnormal expression of cadherins in bladder cancer has been shown to promote an invasive phenotype and may act as the primary mediator of invasion and metastasis [20].

1.2.4. Enabling replicative immortality

It was noted in the 1960s that normal cells cultured *in vitro* have limited replicative potential. This is known as the Hayflick limit and dependent on the length of telomeres at either end of each chromosome. With each cell division, the telomeres shorten and once a minimum telomere length is reached, the vast majority of cells permanently exit from the cell cycle and enter a state of replicative senescence. A small number of cells do continue to proliferate but as telomeres continue to shorten, chromosome end fusion occurs and leads to genomic instability that triggers apoptosis [21].

To maintain telomere length, stem cells and cells during embryonic development express the enzyme telomerase; adult human cells do not express this enzyme and so are subject to replicative senescence. A feature of most, if not all cancers, is that they re-express telomerase. Increased telomerase activity has been shown in renal cancers when compared to normal tissue and also thought to be associated with disease progression [22]. In some tumours an alternative lengthening of telomeres (ALT) mechanism is active, the precise mechanism appears to be tumour type dependent. These alternative mechanisms are thought to operate through DNA repair and recombination processes [23].

1.2.5. Stimulating angiogenesis

The ability of tumours to promote the growth of new blood vessels has been the focus of targeted therapies in urological cancers in addition to other cancer types. Angiogenesis, the formation of new blood vessels from the existing vasculature, is a process that normally occurs in events such as wound healing. However, it is also a feature of cancer, which provides malignant cells with nutrients and a system to remove waste products. The activation of many oncogenes in cancer cells leads to the expression of pro-angiogenic growth factors such as vascular endothelial growth factor (VEGF), platelet derived growth factor (PDGF) and fibroblast growth factor (FGF). These growth factors, acting via their receptors, activate the PI3K-AKT-mTOR pathway and the RAS-RAF-MEK-ERK pathways that promote endothelial cell activation, growth and migration, which ultimately lead to angiogenesis. In addition, the immune response produced at the site of a tumour can also promote angiogenesis. It is known that angiogenesis can occur very early in the development of a tumour, making it an important therapeutic target and the subject of ongoing trials [24].

1.2.6. Resisting apoptosis

The ability of cells to resist apoptosis is another key component of tumourigenesis. Apoptosis is an “ordered” process during which cells undergo programmed cell death in an organized manner. Apoptosis can be initiated either from extracellular or intracellular signals. Extracellular apoptotic signals include the ligands FASL and TNF acting on cells via the receptors FAS and TNFR

respectively. In addition the apoptotic cascade can also be initiated by events within a cell such as DNA damage or oxidative stress. This intracellular apoptotic initiation machinery acts on the mitochondria and is regulated by the BCL-2 family of proteins. Under normal conditions the pro-apoptotic proteins including BAX, BAK and BAD are held in check by anti-apoptotic proteins that include BCL-2 and BCL-X_L. Upon cellular damage that cannot be repaired, the activity of anti-apoptotic genes is inhibited by another subfamily of the BCL-2 proteins, the BH3 only proteins. The pro-apoptotic proteins are present in the mitochondrial membrane, activation of these proteins leads to their oligomerization and the permealisation of the membrane. This occurs either through rupture of the membrane or clustering of proteins which forms a pore through which cytochrome C release occurs followed by caspase activation, DNA condensation and regulated fragmentation and membrane blebbing [25].

Excessive growth factor signaling causes normal cells to undergo apoptosis; cancer cells must circumvent this checkpoint to survive. The tumour suppressor p53 triggers apoptosis by inducing the expression of the BH3 only proteins PUMA and NOXA; loss of *p53* function in cancer, therefore, also serves to prevent apoptosis. Cancer cells also suppress expression of pro-apoptotic BAX and BAK and increase expression of the anti-apoptotic proteins BCL-2 and BCL-X_L, thereby holding the apoptotic cascade in check [26].

1.3. Hypoxia

Oxygen diffusion is limited to 100-180μM from source before it is entirely metabolised [27]. Adaptation to conditions of low oxygen tension is crucial for

normal cells to survive conditions of stress such as tissue ischemia. Such is the nature of growing tumours that cancer cells are likely to be exposed to hypoxia as they grow further from their native blood supply. It is the ability of cancer cells to adapt and survive in low oxygen, which in many ways distinguishes these cells from normal cells.

1.3.1. Hypoxia and HIF

The activation of hypoxia inducible factors (HIFs) is the main regulatory mechanism in oxygen homeostasis. HIF is a heterodimer formed of an α and a β subunit. The β subunit is the constitutively expressed aryl hydrocarbon receptor nuclear translocator (ARNT). Three HIF-α isoforms exist, HIF-1α, HIF-2α and HIF-3α. HIF-1α has four functional domains. At the amino (N) terminus is the bHLH/PAS domain involved in dimerization and DNA binding. The central region of the protein has the two oxygen dependent degradation domains (ODDD), the N-terminal ODDD (NODDD) and the C-terminal ODDD (CODDD). Overlapping with the CODDD is the first of two transactivation domains (TADs) involved in transcriptional activation, the N-terminal TAD (N-TAD). At the C-terminal of the protein lies the second TAD, the C-TAD. HIF-2α has a similar structure to HIF-1α. Although HIF-3α has a CODDD and can be regulated by hypoxia, it lacks the C-TAD and alternative splicing generates variants that antagonize HIF-1α activity [28].

As mentioned above, HIF-1β is constitutively expressed. However, the expression of the α subunit is regulated in a manner that depends on both oxygen and iron. Regulation of the stability of the α subunit is mediated by a

family of prolyl hydroxylases (PHDs). Three PDHs have been identified that are responsible for mediating the turnover of the α subunit – PHD1 (EGLN2), PHD2 (EGLN1) and PHD3 (EGLN3). It is thought that PHD2 is the key player in regulating HIF-α levels. The PHDs are exquisitely dependent on oxygen, α-ketoglutarate and iron for their activity and are responsible for hydroxylating a proline residue in each of the ODDDs – in the case of HIF-1α, these are Pro402 in the NODDD and Pro564 in the CODDD [29]. The hydroxylated residues on the HIF-α subunits are recognized by the product of the von Hippel-Lindau (*vHL*) gene. The vHL protein is the recognition component of a ubiquitin ligase complex that includes elongin B, elongin C, Cullin2 and RBX. Recognition of HIF-α by this complex leads to its ubiquitination and subsequent proteosomal degradation. In addition to hydroxylation of proline residues, the α subunit is also hydroxylated on an asparagine residue in the C-TAD; in the case of HIF-1α, this is Asn803. Asparagine hydroxylation is mediated by factor inhibiting HIF (FIH), which like the PHDs, requires oxygen, α-ketoglutarate and iron for its activity. Hydroxylation in the C-TAD prevents the association of HIF with the transcriptional co-activator p300, thereby dampening HIF mediated transcription [30].

In hypoxic conditions, the lack of oxygen inhibits PHD and FIH activity. Thus HIF-α is no longer degraded and, therefore, dimerises with HIF-β and becomes transcriptionally active. Once active, the HIF complex binds to target genes at sites with the recognition sequence 5'RCGTTG-3", so called "hypoxia response elements", which lead to the upregulation of these genes. It is thought that as many as 1-5% of all genes in the human genome can be expressed in response to

hypoxia in a cell/tissue specific manner [31]. In the normal physiological setting HIF activation allows the body to adapt to low oxygen levels for example by inducing the expression of erythropoietin to increase red blood cell production and VEGF to promote angiogenesis. However, in pathological settings such as cancer, hypoxia can lead to the upregulation of many genes involved in angiogenesis, invasion, metastasis and cell survival [32].

1.3.2. Hypoxia and cancer

Previously, I discussed the hallmarks of cancer; hypoxia is involved in the regulation of each of these hallmarks through a number of complex mechanisms [33]. Firstly hypoxia, via HIF induces a number of growth factors such as *EGF*, *IGF-1, IGF-2* and *PDGF* [34], which allows activation of oncogenic signaling pathways. HIF potently induces the expression of BNIP3 [35], a protein that possesses an atypical BH3 domain. The role of BNIP3 in hypoxia is controversial. Early work suggested that overexpression of BNIP3 was responsible for the induction of apoptosis [36]; however, more recent work suggests that it may be involved in hypoxia induced autophagy/mitophagy, as a protective mechanism to reduce reactive oxygen species [37]. In renal cancer BNIP3 is associated with hypoxic induction of apoptosis and alterations in this gene or parts of the apoptosis pathway in renal cancer provides a survival advantage for cancer cells [38].

It is thought that tumour hypoxia is one of the most important features for tumour cell dissemination and progression of disease to invasion and metastasis [39]. In general, hypoxic tumours are more aggressive and associated with a

worse prognosis. HIF induces the expression of many enzymes that modify the extracellular matrix including MMP2 and lysyl oxidase, thereby promoting cancer cell invasion. HIF also leads to the induction of the transcriptional repressors SNAIL and TWIST1, which in turn suppress the expression of E-CADHERIN and promote EMT [40].

Hypoxia has been shown to induce the expression of telomerase in a manner that is dependent on either reactive oxygen species production [41] or activation of MAPK [42], thereby contributing to replicative immortality. Finally, hypoxia can also synergise with existing genetic mutations in cancer cells to enhance oncogenesis. For example, activation of PI3K signaling and increased mTOR activity increases the translation of *HIF-1*α and the subsequent hypoxic response [32, 43]; this is discussed further in Chapter 5. Furthermore, while low oxygen tension is the primary activator of the HIF pathway, growth factors (e.g. insulin, EGF, PDGF) and cytokines (e.g. TNF alpha, interleukin-1 beta) have also been shown to initiate the HIF pathway [44, 45].

1.3.3. Hypoxia and the tumour microenvironment

In the majority of cancers and in the case of renal cancer in particular it is perhaps the hypoxia activation of angiogenic pathways in the stroma that is of most interest [46]. Renal tumours are highly vascular and this is in part due to the activation of HIF. HIF upregulates VEGF expression, a potent chemoattractant for endothelial cells to promote the formation of new blood vessels [47]. Other pro-angiogenic factors induced by hypoxia include PDGF and FGF. There is also some evidence that hypoxia suppresses expression of the angiogenic inhibitor thrombospondin-1 [48].

In order for tumours to grow, cancer cells must be able to survive and proliferate in the tumour microenvironment. The tumour microenvironment is a complex system including a large number of cell types and is thought to be critical in modeling the response to therapy. Hypoxic regions of a tumour are also nutrient starved due to poor vascularization. One major consequence of hypoxia is that the pH of the extracellular environment of cancer cells drops. The reasons for this are two-fold. Firstly, HIF induces the expression of carbonic anhydrase 9 (CA9) [49], which causes hydration of CO_2 molecules to carbonic acid. *CA9* is a HIF-1 α responsive gene, which allows hypoxic cancer cells to buffer their intracellular pH to near neutral conditions necessary for their biosynthetic reactions. CA9 plays a significant role in cancer adaptation to hypoxic environments and hence may be involved in tumour progression [50]. These findings not only make CA9 protein an integral marker for hypoxia but also an attractive target for therapy [51].

Secondly, hypoxia favours glycolysis, leading to the production of lactate as a by-product that lowers the extracellular pH (see below). The ability to survive in low pH is characteristic of cancer cells [52] and conversely increased lactate in the extracellular environment may promote oncogenesis by suppressing the immune system, enhancing cell migration and serving as an energy source for surrounding, normoxic cancer cells [53].

1.3.4 Hypoxia, HIF and energy metabolism

The basic unit of energy in a cell is ATP and the primary source of this is the metabolism of glucose. The first step in this process is glycolysis, the breakdown

of glucose to pyruvate with a net gain of two molecules of ATP. Under aerobic conditions when oxygen is available, pyruvate enters the Krebs cycle, resulting in the generation of multiple metabolic intermediates and the reducing agents NADH and $FADH_2$. These in turn enter the electron transport chain (ETC) and ultimately lead to a net yield of 36 molecules of ATP. Thus, under conditions of normal oxygen tension, most cells utilize glucose via the Krebs cycle to maximize ATP generation. Under hypoxic conditions, when oxygen is low, or anaerobic conditions, when there is no oxygen, the Krebs cycle and ETC are not utilized. Thus, all the ATP generated in a cell in these conditions comes from glycolysis.

HIF co-ordinates the expression of a number of genes that allows the cell to adapt to hypoxia more efficiently. Under hypoxic conditions, cells must take up more glucose, as they are not efficiently producing ATP. Indeed, the propensity of cancer cells to absorb glucose is the basis of FDG-PET imaging in cancer. HIF directly induces the expression of the glucose transporter GLUT1, thereby allowing the cells to take up glucose. HIF also induces the expression of the enzyme lactate dehydrogenase A (LDHA), that catalyses the conversion of pyruvate to lactate, and of the transporter MCT4, that facilitates the transport of lactate outside the cell [54].

An unusual observation is that in many cancers, even under normal oxygen tension, cells preferentially undergo glycolysis. This aerobic glycolysis was first observed by the biochemist Otto Warburg in 1924 and is termed the Warburg effect. Although energetically inefficient, glycolytic metabolism appears to provide a survival advantage by allowing adaption to nutrient poor conditions and providing metabolic intermediates that are used for other cellular processes [54]. The switch from oxidative phosphorylation to glycolysis is coordinated by

various oncogenes and tumour suppressor genes and one key gene involved in this process is HIF [55].

1.3.5. Therapies targeting hypoxic pathways in urological malignancies

The HIF pathway mediates a number of processes critical to tumourigenesis and therefore it is an obvious therapeutic target. Strategies to target hypoxia and the HIF pathway include directly targeting HIF, targeting the activity of HIF target genes or other cellular pathways into which the hypoxic response is integrated.

The expression of HIF can be decreased with the antisense RNA EZN-2698 [56] or by using digoxin to inhibit its translation [57]. The inhibitor hypericin forces poly-ubiquitination and degradation of heat shock protein 90 (HSP90) [58]. HIF is a HSP90 client protein and therefore treatment with hypericin also decreases HIF levels and has shown to have an antiangiogenic and antitumour effect [59]. Alternatively, drugs that activate PHDs [60] and p53 [61] have also been shown to decrease HIF levels. Other reagents such as echinomycin and chetomin have been shown to inhibit HIF transcriptional activity by inhibition of HIF binding to DNA and interference between HIF-1 and its coactivator p300 respectively [62, 63].

Some HIF target genes are also being explored as therapeutic targets. CA9 activity can be inhibited by a number of classes of drugs that reverse extracellular environment acidification and tumour growth. Perhaps the most characterised HIF target gene of therapeutic importance is VEGF. Inhibition of VEGF activity either with the blocking antibody bevacizumab or with VEGFR inhibitors such as sorafenib and sunitinib are of clinical importance and have

been approved by the FDA for the treatment of multiple cancer types including, metastatic renal cell carcinoma. These inhibitors are discussed later in this chapter and in chapter 5.

Finally, targeting other cellular pathways can impact upon the activation of HIF. The best characterized of these is the inhibition of the mTOR pathway using rapamycin and its analogues. The *mTORC1* complex has been shown to enhance translation of HIF-α transcript levels; its inhibition attenuates HIF levels and subsequent activation of its targets [64]. In metastatic renal cell carcinoma, mTOR inhibitors have been shown to be a safe and effective therapy [65]. The role of mTOR inhibitors is discussed in Chapter 5.

1.4 RNA interference and microRNAs

1.4.1. miRNAs

Mechanisms that regulate gene expression transcriptionally by affecting promoter activity or post translationally by protein modifications are well established. Over the last 20 years evidence has emerged that a potent mechanism for regulating gene expression post transcriptionally exists and is termed RNA interference (RNAi). RNAi is a highly conserved process that is triggered by double stranded RNA (dsRNA). The major source of endogenous dsRNAs are microRNAs (miRNAs).

MiRNAs are small (18-22 nucleotides) non coding, single stranded RNAs. The first miRNA (lin-4) was discovered in 1993 in *Caenorhabditis elegans (C.elegans)* [66]. MiRNA let-7 was subsequently discovered in *C. elegans* and found to be highly conserved in a wide range of organisms [67], leading to the realisation

that miRNA are a prevalent group of molecules important for regulating gene expression.

MiRNA genes are found dispersed across the hμMan genome either as single genes or more commonly as gene clusters giving rise to the large polycistrionic transcripts from which individual miRNAs are processed. About 40% of all hμMan micro-RNAs are co-transcribed as clusters of up to eight miRNAs per transcript. A large proportion of miRNAs are encoded within mRNA introns, the remainder are located within exons or the 3'UTR of mRNA [68] and are co-transcribed with the gene in which they reside [69].

1.4.2. Biosynthesis

1.4.2.1. Formation of pre-cursor miRNA (Pre miRNA)

MiRNA genes are transcribed by RNA polymerase II forming long primary RNAs (pri-miRNAs). These contain a 5' CAP structure and are polyadenylated at the 3' end. A central feature of these molecules is that they have imperfect repeat sequences that allow the RNA to fold back on itself as a hairpin structure. Within the nucleus, this hairpin of the pri-microRNA is recognised and cleaved by a microprocessor complex consisting of the RNase III-nuclease, Drosha and the double stranded RNA binding protein DiGeorge syndrome critical region 8 (DGCR8). Processing by Drosha yields the 60-70 nucleotide hairpin structure, which is known as the precursor miRNA (pre-miRNA) (Figure 1.3).

1.4.2.2. Export of pre-miRNA to the cytoplasm and formation of miRNA

Exportin5 along with cofactor Ran GTP actively exports the pre- miRNA from the nucleus into the cytoplasm. The pre-miRNA then undergoes further cleavage by another RNase III-endonuclease DICER with its ds-RNA binding partner, the transactivating response RNA binding protein (TRBP). TRBP recruits the human Argonaute protein (AGO2) to the DICER complex and hence a minimal RNA induced silencing complex (RISC) is formed. In some cases, AGO2, which has RNase H-like endonuclease activity, can also help with processing of the pre-miRNA. Cleavage by DICER and AGO2 results in a double-stranded RNA (dsRNA) molecule which is a short lived, asymmetric duplex, one strand of which will be the mature miRNA with the other strand being the passenger strand or miR*. The mature miRNA gets loaded into the miRISC complex in which Argonaute (Ago) proteins are the key effector molecules [70] (Figure 1.4).

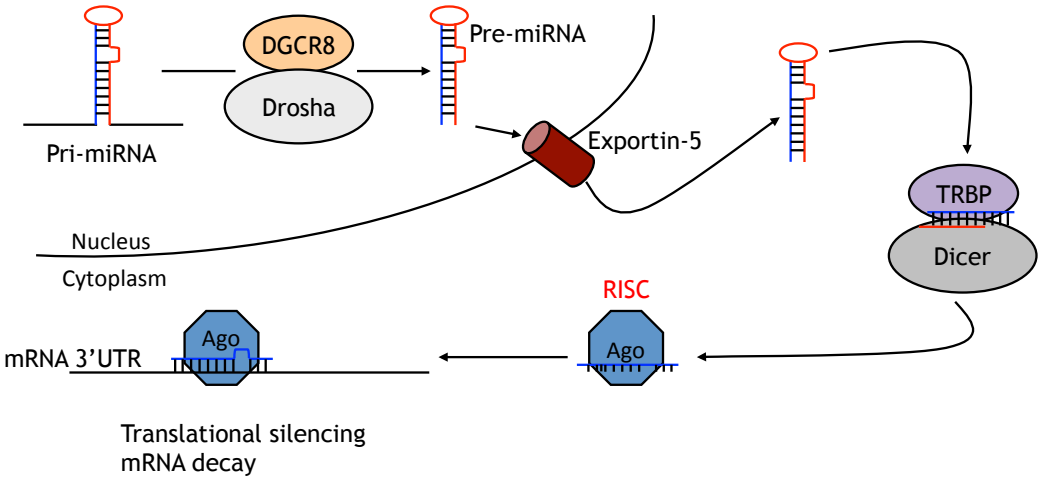


Figure 1-3 MicroRNA biosynthesis

1.4.2.3. Non-canonical miRNA generation

Although sequential processing by Drosha and Dicer represent the canonical pathway for miRNA synthesis, alternative processing strategies have recently been identified. One such example of this is the generation of mirtrons. Mirtrons are derived from introns of genes, with the cleavage of the 5' end of the intron and debranching of the lariat producing the hairpin pre-miRNA. Thus, the initial processing of mirtrons is independent of the activity of Drosha but is rather dependent on splicing. These pre-miRNA are then processed by Dicer to generate the dsRNA from which the mature miRNA will be derived.

In contrast to mirtrons, miR-451 is thought to be generated in a Drosha dependent but Dicer independent mechanism [71]. Cleavage by Drosha generates the short hairpin pre-miRNA structure that is loaded directly into the Ago2 protein for further processing. At present, it is unclear how widespread this mode of miRNA production is.

In addition to these alternative mechanisms, miRNA can also be generated by further processing of both small nucleolar RNAs (snoRNAs) and transfer RNAs (tRNAs). Finally, in some cases, endogenous shRNA can be generated that are transcribed and loaded directly into Dicer [72], utilizing a mechanism that is routinely used to generate exogenous shRNA in molecular biology.

1.4.3. Gene silencing by miRNAs

The cellular components required to execute gene silencing by miRNA are also needed for efficient knockdown of gene expression mediated by short interfering RNA (siRNA). The end result of miRNA processing by Drosha and/or Dicer is an imperfect dsRNA molecule. On the other hand, synthetic siRNA routinely used to knockdown gene expression are a perfectly complementary dsRNA.

In the minimal RNA induced silencing complex (RISC), TRBP recruits the effector Argonaute protein to the DICER complex. In humans, the Argonaute family of proteins has 8 members, AGO1-4 and PIWIL1-4. All Argonaute family proteins contain an RNA binding PAZ domain and a PIWI domain that shares some homology to RNAse H. However, to date, only AGO2 in man has been shown to cleave mRNA. Indeed, RISC complexes into which AGO2 has been incorporated can also process the pre-miRNA. Of the RNA duplex (either miRNA or siRNA),

one strand is incorporated into the RISC complex and is known as the guide strand and is used to target mRNA; the complementary strand, also known as the passenger strand or miR* is often degraded. However, the choice of guide strand from the duplex is not fixed and in some cases, the passenger strand can be incorporated into the RISC complex in a context dependent manner.

The majority of mRNA targeted by the RISC complex become concentrated at distinctive cytoplasmic sites known as processing bodies (p- bodies) and it is at these sites that miRNA/siRNA mediate their cellular functions [73].

RNAi mediated by siRNA is primarily based on perfect complementarity between the guide strand the target mRNA. In contrast, miRNAs exhibit partial complementarity to their target sequence, with selection largely dependent on binding of a 6-8bp "seed" sequence at the 5' end of the miRNA to its target mRNA. Binding sites for miRNA are often found in the 3' untranslated region (UTR) of mRNA. Where perfect complementarity exists between the guide miRNA strand and the target mRNA, such as in the case of siRNA, and AGO2 is incorporated into the RISC complex and endonuclease cleavage of the target mRNA occurs, leading to its degradation. Some human miRNAs have near perfect homology to their targets and binding results in degradation of mRNA in a process similar to that of the siRNA pathway. However, the majority of miRNAs only have limited sequence homology to their target mRNA and effect gene silencing primarily by inhibiting protein translation.

miRNAs may affect translational efficiency via RISC-miRNA mediated translational silencing in one of three ways – by inhibiting the initiation or elongation of ribosomal protein synthesis, by premature termination of translation or by immediate proteolytic degradation of the newly synthesised

protein. The mechanisms by which miRNA impact on translation have not been fully elucidated but binding of the RISC complex to the 3'UTR is thought to prevent circularisation of the mRNA that is required for efficient translation [74]. MiRNA targeting of mRNA also leads to the destabilisation of the latter, by the removal of the 3' poly-A tail and 5'CAP, leading to transcript decay [75].

The limited complementarity of miRNAs to their target mRNA has hampered efforts to identify potential target mRNAs using computational methods. Calculations suggest that there may be over 1000 miRNA genes in the mammalian genome, which may regulate up to 30% of the protein coding genes indicating few cellular processes are not affected by miRNAs [76, 77].

MiRNAs have been shown to be involved in a variety of developmental and metabolic cellular processes such as cell proliferation, cell differentiation, metabolism, apoptosis, and stem cell maintenance. Many miRNAs have tissue specific expression profiles suggesting they fulfil roles in tissue specialisation and/or tissue maintenance.

1.4.4. miRNAs and cancer

Alterations in miRNA expression are evident in the majority of human cancers. A significant percentage of miRNA genes are located at chromosomal fragile sites or minimal regions of loss of heterozygosity and amplification in cancer [78]. MiRNA profiling experiments revealed that many miRNAs are abnormally expressed in clinical cancer specimens. The analysis of the expression profile in six different solid cancers demonstrated that a group of 21 commonly deregulated miRNAs, including miR-21, the miR-17-92 cluster and miR-191 were

over expressed in the examined cancer types [79]. These changes in miRNA expression are not necessarily always causative as many other changes occur in cancer cells, which may influence miRNA expression such as genomic rearrangements, abnormalities in miRNA processing genes and disrupted epigenetic regulation of miRNAs [80]. However, miRNAs have been implicated in all the hallmarks of cancer discussed above.

The miR-17-92 cluster is a target of the MYC oncogene and is amplified in many solid tumours. Members of this cluster are known to inhibit the pro-apoptotic transcription factor E2F1 [81], the lipid phosphatase PTEN and the pro-apoptotic protein BIM [82], thereby leading to cancer cell survival. MiRNAs can also behave as tumour suppressors. The miRNA let-7 negatively regulates RAS expression [83]; low expression of let-7 correlates with poor prognosis in lung cancer and head and neck squamous cell carcinoma patients [84]. The miR-15-16 cluster, which downregulates FGF2 and FGFR1, is deleted in a large proportion of B-cell chronic lymphocytic leukaemia, as well as in multiple myeloma and prostate cancer [85].

MicroRNAs have been associated with the regulation of apoptosis in various tumours. For example, miR-34a, which is often lost in neuroblastoma, downregulates the anti-apoptotic gene BCL-2 [86] and the histone deacetylase SIRT1 [87], all of which leads to apoptosis. MiR-125b can also downregulate BCL-2, leading to the induction of apoptosis [38]. The miR-200 family is well documented to affect EMT and cancer cell invasion by targeting the ZEB proteins [88]. The ZEB family of transcriptional repressors inhibit the expression of E-CADHERIN and therefore, promote EMT; elevated levels of miR-200, thus suppress EMT [88]. The levels of miR-200 are decreased during EMT and in

tumours such as aggressive lung and prostate cancer. In contrast, miR-373 and miR-520c promote migration by suppressing the expression of the hyaluronan receptor CD44; increased expression of miR-373 has been reported in breast cancer metastasis samples [89].

A number of miRNAs have been linked with pro and anti-angiogenic pathways. MiR-378 has been shown to promote angiogenesis by inhibiting the tumour suppressor SUFU, which induces the expression of VEGF [90]. Whereas other miRNAs have anti-angiogenic effects such as miR-221 which targets C-KIT and inhibits angiogenesis [91]. Finally, miRNAs have been associated with senescence, either directly for example by miR-138 regulation of telomerase [92] or indirectly for example the miR-290 regulation of DNA methylation and telomerase expression [93].

1.4.5. miRNAs and hypoxia

Hypoxia also leads to the differential regulation of miRNA, which may contribute to cell survival in these conditions (see chapter 1.3). A number of studies have looked at the hypoxic regulation of miRNA expression using high throughput strategies. Hua et.al performed miRNA microarray analysis on the nasopharyngeal cell line CNE after treatment with the hypoxia mimetic DFOM [94]; six miRNA were found to be induced after this treatment (Table 1.1). Kulshreshtha et al exposed 4 cancer lines to 0.2%O_2 and performed microarray analyses for differential miRNA expression at various time points [95]. Twenty-three upregulated miRNAs were identified in at least two cell lines, and were together termed the hypoxia regulated microRNAs (HRMs) (Table 1.1). HREs were identified in miR-210 and miR-26a-2. Finally, HIF-1α was found to have a

dominant effect on inducing miR- 24 and miRNA-181c, whilst HIF-2 has a greater effect on miR-26a-1 [69]. Bruning et al performed a miRNA microarray analyses of Caco-2 colorectal cancer cells after exposure to 1%O_2 for varying lengths of time [96]; 17 miRNA were found to be induced by hypoxia, including several members of the let-7 family (Table 1.1).

Hua et.al. 2006 [94]	Kulshreshtha et.al. 2007 [95]	Bruning et.al. 2011 [96]
miR-155	**miR-103-1**	**miR-1246**
miR-210	**miR-106a**	**miR-923**
miR-188	**miR-107**	**let-7e**
miR-181b	**miR-125b-1**	**miR-210**
miR-30d	**miR-181a-1**	**let-7c**
miR-151	**miR-181a-2**	**miR-193b***
	miR-181b-1	**miR-638**
	miR-181b-2	**miR-1275**
	miR-181c	**miR-192***
	miR-192	**miR-374b**
	miR-195	**let-7d**
	miR-21	**let-7b**
	miR-210	**miR-215**
	miR-213-5p	**miR-155**
	miR-23a	**let-7f**
	miR-23b	**miR-26b**
	miR-24-1-3p	**let-7a**
	miR-26a-1	
	miR-26a-2	
	miR-26b	
	miR-27a	
	miR-30b	
	miR-93-1	

Table 1-1 Hypoxia regulated miRNAs

The hypoxic induction of miR-210 has been observed in all cells tested to date (Table 1.1) including primary cells [97], suggesting that it is an integral part of the response to this stress. However, the induction of other miRNAs in response to hypoxia is variable and is likely to occur in a cell/tumour type specific manner.

Nevertheless, hypoxic induction of miR-155 has been reported in CNE [94], lung cancer [98] and Caco-2 cells where an HRE has been identified in the promoter of this gene [96]. Finally, miR-424 has been shown to be induced by hypoxia in endothelial cells [99].

In addition to miRNA being induced in response to hypoxia, the expression of a number of miRNA can also be inhibited after exposure to low oxygen. The mechanism of downregulation is less clear and although HIF is known to be a transcriptional repressor, it is likely that in some cases downregulation may occur via HIF independent pathways. In renal tubular epithelial cells, miR-34a expression is decreased by hypoxia [100]. After 8hrs of exposure to hypoxia, the levels of miRNA-155, miRNA-106a, miRNA-135a, miRNA-17-3p, miRNA-199a-5p, and miRNA-203, miR-135a and miR-199a-5p were found to be decreased in endothelial cells [101]. The expression of miR-20b was decreased by hypoxia in a number of cell lines [102]. Hua et al found miR-20b, miR-26b, miR-15b, let-7g, miR-224, let-7a, let-7d, miR-16, let-7f, miR-30b, miR-20a, let-7c and let-7e to be decreased in DFOM treated CNE cells [94].

The analysis of HRMs and their targets has established links between HRMs and a number of cellular pathways involved in tumourigenesis, such as cell proliferation, for example by miR-21 regulation of PTEN [103] and apoptosis by let-7e through regulation of CASPASE 3 [104].

1.5 Bladder cancer

1.5.1. Epidemiology

In the United Kingdom, approximately 10,000 people are diagnosed with bladder cancer and 5,000 people die from this disease each year. It is the most common tumour in the urinary system and in the UK it is the 4th most common cancer in men and the 11th most common cancer in women [105]. The incidence of bladder cancer has fallen in some reports by up to 40% since the early 1990s [106]. There is a male predominance with a male: female ratio of 5:2. Bladder cancer is a disease associated with increasing age and the incidence peaks in the 70-80 year age group [107].

1.5.2. Risk factors

The most common risk factor for bladder cancer is smoking which is thought to be associated with approximately 65% of male and 30% of female bladder cancers. Current evidence suggests that duration of smoking is the most important factor. However, cigarette smoke can act as a late stage carcinogen with those who stop smoking for at least 20 years having a higher risk of bladder cancer than non- smokers, suggesting an early-stage irreversible effect [108].

A number of chemicals have been associated with an increased risk of developing bladder cancer. Historically, workers in the dye, rubber, chemical and paint industries may have been exposed to carcinogens such as benzene compounds and arylamines. The carcinogens β-napthylamine, 4-aminobiphenyl, polcyclic aromatic hydrocarbons and N-nitroso compounds are all linked with bladder cancer. However, their involvement in bladder cancer has diminished, as

exposure is less common due to stricter health and safety regulations governing their use.

In addition to exposure to carcinogens, infections are also implicated in the development of bladder cancer. Chronic irritation resulting from recurrent infections or indwelling catheters is associated with an increased risk of developing squamous cell carcinoma (SCC) of the bladder.

In areas such as North East Africa and the Middle East where schistosomiasis is endemic, chronic irritation from bilharzial eggs is associated with a 5-fold increase in the risk of bladder cancer. Schistosomiasis can lead to development of SCC and there is typically a lag phase of 30 years between initial parasite infection and bladder cancer presentation, which occurs at a median age of 46 years.

1.5.3. Tumour staging

In Europe and North America, the majority (90%) of cases of bladder cancer are derived from the epithelial layer of the bladder called the urothelium and are termed transitional cell carcinomas [109]. The remaining 10% consists of adenocarcinoma, SCC and rare tumours such as neuroendocrine, sarcoma and small cell carcinomas [110]. In parts of the world where schistosomiasis is prevalent, squamous cell carcinoma accounts for 65% of bladder cancer cases; however, this incidence is decreasing with an increase in urothelial bladder cancer as sanitation improves but smoking and the use of pesticides increases [111].

In 2004, the World Health Organisation (WHO) published a standardized classification system for bladder cancer [112]. At the time of diagnosis, bladder cancer is staged by the depth of invasion of the growing tumour. Ta tumours are confined to the urothelial layer where the tumour arises, T1 tumours have spread into the subepithelial connective tissue, T2 tumours have invaded through to the muscularis propria, T3 tumours have spread to the perivesical tissue and T4 tumours have spread beyond the bladder to neighbouring organs such as the prostate or the uterus (Table 1.2). Pathological staging is determined by the TNM classification system, which considers the tumour characteristics (T), the nodal status (N) and metastatic disease (M) (Table 1.2). Ta and T1 tumours are termed non-muscle invasive (NMI) bladder cancer, while tumours that are T2 or greater are termed muscle invasive (MI) bladder cancer. In addition, there are three grades of bladder cancer, depending on the degree of de-differentiation and nuclear morphology, with grade 1 being the most differentiated and grade 3 being the least. Based on this classification system, TCC can either be defined as urothelial papilloma, papillary urothelial neoplasm of low malignant potential, low-grade papillary urothelial carcinoma or high-grade papillary urothelial carcinoma.

Tumour characteristics	Nodal status
Tx Primary tumour cannot be assessed	**Nx** Regional lymph nodes not assessed
T0 No evidence of primary tumour	**N0** No regional lymph node metastasis
Ta non-invasive papillary carcinoma	**N1** Metastasis in a single pelvic lymph node
Tis Carcinoma in situ	**N2** Metastasis in multiple pelvic lymph nodes
T1 Tumour invades subepithelial connective tissue	**N3** Metastasis in a common iliac lymph node
T2 Tumour invades muscle **T2a** Tumour invades superficial muscle **T2b** Tumour invades deep muscle	Metastatic disease
T3 Tumour invades perivesical tissue **T3a** microscopically **T3b** macroscopically	**M0** No distant metastasis
T4 Tumour invades surrounding organs **T4a** Tumour invades prostate, uterus or vagina **T4b** Tumour invades pelvic or abdominal wall	**M1** Distant metastasis

Table 1-2 TNM classification of bladder cancer

1.5.4. Pathogenesis

It is generally accepted that NMI and MI bladder cancer have distinct underlying aetiologies. NMI cancer is characterised by increased expression and activating mutations of *FGFR3*, the PI3 kinase pathway and *RAS* [113, 114]. The role of *FGFR3* in NMI is discussed further in Chapter 4.1.2. In NMI, the PI3 kinase pathway can be activated by mutations in the p110α catalytic subunit (*PIK3CA*). Mutations in *PIK3CA* have been identified in 15-25% of Ta/T1 tumours [115]. Furthermore, mutations in *PIK3CA* are more common in low grade compared to high grade bladder cancer [116]. Some evidence suggests that mutations in *FGFR3* and *PIK3CA* occur simultaneously in the same samples [117]. Mutations in the small GTP binding protein *RAS* have also been reported in around 10% of bladder tumours [118]. Early studies suggested that *RAS* mutations were more prevalent in low grade Ta/T1 tumours [118], although larger studies are needed

to confirm this. Interestingly, mutations in *FGFR3* and *RAS* appear to be mutually exclusive of each other [115, 118].

In addition to these, Ta tumours exhibit LOH of the long arm of chromosome 9, 9q [119]. A number of tumour suppressor genes are found on chromosome 9q including tuberous sclerosis 1 (*TSC1*), deleted in bladder cancer 1 (*DBC1*) and *PATCHED 1* (*PTCH1*) [120, 121]. Further to LOH, mutations in *TSC1* have been identified in around 15% of bladder cancer, irrespective of tumour stage or grade [115, 117].

In contrast to the mutation spectrum in NMI bladder cancer, MI bladder cancer appear to have frequent mutations in in *TP53*, *RB* and *PTEN* genes. Mutations in *TP53* have been detected in around 10% of Ta but 60% of T2 bladder cancers suggesting that it is associated with more advanced stage tumours [14, 122]. In the majority of cases, the occurrence of *p53* and *FGFR3* mutations are mutually exclusive [14, 122]. MI bladder cancers also have a high incidence of loss of heterozygosity of *PTEN* and *Rb*, although the second allele in each case is rarely mutated [123].

1.5.5. miRNAs in bladder cancer

The first study to examine miRNA expression in bladder cancer was published by Gottardo et al in 2007 [124], in which miRNA expression from 25 bladder tumour and 2 normal bladder samples was analysed. They found miRNAs 223, 26b, 221, 103, 185, 23b, 203, 17-5p, 23a and 205 to be upregulated in bladder tumours when compared to normal urothelium. In an attempt to apply miRNA expression profiling in more clinically relevant setting, Neely et al concluded that

the ratio between the expression of the known oncomiR, miR-21 and miR-205 could differentiate between invasive and non invasive bladder cancers, suggesting there may be a role for miRNAs as a marker in bladder cancer [125]. Since then a number of studies have used microarray techniques and sequencing to classify bladder tumours based upon their miRNA expression. A systematic review published in 2011 summarised a number of miRNAs aberrantly expressed in bladder cancer (Table 1.3).

miRNA	Target pathway
Upregulated	
miR-129	Signal transduction, protein expression
miR-221	Apoptosis
Downregulated	
miR-1/133a/218	Cytoskeleton
miR-19a	Apoptosis and mTOR pathway
miR-30a-3p/133a/199a	Differentiation
miR-34a	Cell cycle control
miR-99a/100	Proliferation
miR-101	Gene expression
miR-125b	Apoptosis and proliferation
miR-145/133a	Cytoskeleton
miR-145	Signal transduction
miR-200/205	EMT
miR-200 family	EMT

Table 1-3 Altered miRNA expression in bladder cancer [126]

As expression is cell type specific it is likely that the functional effects of miRNAs also follow this pattern. The miRNA cluster 143-145 has been found to be downregulated in bladder cancer and thought to act as a tumour suppressor, in part through the regulation of plasminogen activator inhibitor-1 (PAI-1), which is known to be upregulated in a number of solid tumours [127]. MiR-143 has also

been shown to target cyclooxygenase 3, the expression of which is associated with increased grade and stage of TCC [128]. MiR-145 is known to induce apoptosis in both a caspase dependent and independent manner and inhibit growth through the targeting of FSCN1 in bladder cancer cell lines [129, 130].

Members of the miR-200 family, associated with EMT, have been found to be downregulated in advanced bladder cancer [131].

There is also evidence that miRNA expression may provide a non-invasive method of diagnosis and surveillance as miRNAs can be detected in urine. Relative expression of miRNAs 126 and 152 has a sensitivity of 72% and a specificity of 82% in the diagnosis of bladder cancer [132], more recently miR-96 and 183 were found to be significantly higher in patients with urothelial cancer and expression levels of these miRNA fell following tumour resection [133].

1.5.6. Treatment

Treatment for bladder cancer is dependent on the grade and stage of the cancer. Patients will initially undergo a transurethral resection of the bladder tumour (TURBT). This procedure is performed to enable tissue diagnosis but also aims to remove the tumour in its entirety. Understaging of tumours occurs in approximately 1-15% of cases [134] and therefore a second resection is recommended in all cases where the initial diagnosis is either high grade or stage T1 and above.

Treatment can be subdivided depending on the stage of the tumour.

1.5.6.1. Non-muscle invasive bladder cancer

Non-muscle invasive cancer, although not lethal has a high incidence of recurrence and progression [135]. The risk of recurrence or progression can be estimated by considering the number of tumours present at the time of initial resection, the tumour size, the stage and grade of the tumour and the presence of concurrent carcinoma in situ (CIS) [136]. This information is converted into a score as shown in Table 1.4, which predicts a low, intermediate or high risk of recurrence and progression [136].

Factor	Recurrence	Progression
Number of tumours		
Single	0	0
2-7	3	3
≥8	6	3
Tumour diameter		
<3 cm	0	0
≥ 3 cm	3	3
Prior recurrence rate		
Primary	0	0
≤ 1 recurrence/year	2	2
> 1 recurrence/year	4	2
Category		
Ta	0	0
T1	1	4
Concurrent CIS		
No	0	0
Yes	1	6
Grade (WHO1973)		
G1	0	0
G2	1	0
G3	2	5
Total score	0-17	0-23

Table 1-4 EAU guidelines, scoring for progression and recurrence

Recurrence score 0=low risk, 1-9=intermediate risk, 10-17=high risk.

Progression score 0=low risk, 2-6=intermediate risk, 14-23=high risk

Immediately after initial tumour resection a single instillation of intravesical chemotherapy has been show to reduce the recurrence rates by 11.7% in patients with de novo tumours [137]. Mitomycin C, epirubicin and doxorubicin have all been used to good and equal effect. In patients at low risk of recurrence this is often the only treatment required. Those patients at intermediate risk may benefit from repeated instillations aimed to prevent disease recurrence rather than progression [138]. Intravesical Bacillus Calmette Guerin (BCG) immunotherapy is used in patients considered at intermediate and high risk of progression. It has been shown to reduce the chance of both recurrence and progression [139, 140]. While BCG is given as a course lasting between 6 weeks and 18 months, the optimal number and frequency of instillations has not been agreed.

Current recommendations for treatment are shown in Table 1.5

Category	Low	Intermediate	High
Recurrence	1 immediate instillation of chemotherapy	1 immediate instillation followed by further instillations of chemotherapy or BCG depending on risk of progression	1 immediate instillation of chemotherapy followed by either chemotherapy or a minimum of 1 year of BCG
Progression	1 immediate instillation of chemotherapy	1 immediate instillation of chemotherapy, followed by a minimum of 1 year of BCG or further chemotherapy	BCG for at least 1 year or cystectomy

Table 1-5 EAU guidelines for treatment for non-muscle invasive bladder cancer 2011

1.5.6.2. Muscle invasive bladder cancer

Those patients diagnosed with muscle invasive disease may be considered for neoadjuvant cisplatin based chemotherapy. Neoadjuvant chemotherapy (NC) in bladder cancer is associated with a 5% overall survival benefit at 5 years and in up to 40% of cases the cystectomy specimen is staged T0 [141]. There are concerns regarding the delay to cystectomy as a result of NC; however, evidence suggests that a wait of less than three months is unlikely to alter outcome [142]. Radical cystectomy and urinary diversion is recommended in patients with T2-T4a, N0, M0 bladder cancer, in high-risk patients with recurrent disease, BCG failures, carcinoma in situ and extensive papillary disease. In patients not deemed fit or those who refuse cystectomy, radical radiotherapy is an alternative option.

1.6 Renal cancer

1.6.1. Epidemiology and risk factors

Renal cell cancer (RCC) accounts for approximately 9,000 cancer diagnoses and 4,000 deaths in the UK each year and represents 2-3% of all cancers. There is a male predominance of 3:2 and the peak incidence is in the 65-69 year age group. While the incidence of renal cancer has increased over the last 30 years, it is thought that this may be due to better imaging and detection of incidental tumours [142].

Worldwide, the highest rates of renal cancer occur in North America and Europe and the lowest occur in Africa and Asia. Few risk factors have been proven;

however smoking, obesity, diabetes and hypertension have been associated with an increased risk of RCC. The use of phenacetin based analgesia is associated with increased risk of developing RCC and in women, parity is also associated with increased risk.

The majority of renal cancers are adenocarcinomas, which arise from the renal parenchyma; however, approximately 10% originate from the renal pelvis and are transitional cell carcinomas. Traditionally, RCC can be divided into 5 main subgroups of – clear cell, papillary, chromophobe, collecting duct, and unclassified RCC. Clear cell RCC make up the majority of cases of RCC diagnosed (75-80%) and have a characteristic clear cytoplasm. Papillary RCC account for around 10-15% of cases diagnosed and are characterized by a papillary growth pattern, with areas of necrosis including both tubular papillary and solid architecture. Papillary RCC can be divided into Type 1, characterised by small cells and a pale cytoplasm and Type 2, characterised by large cells and eosinophilic cytoplasm. Chromophobe RCC account for around 4-5% of cases diagnosed with cells characterised by pale and granular cytoplasm.

1.6.2. Tumour diagnosis and staging

Currently more than 50% of RCCs are detected incidentally and very few present with the triad of haematuria, flank pain and an abdominal mass. Approximately 30% of patients present with paraneoplastic conditions such as hypercalcaemia.

In the most part the diagnosis of a renal mass is made radiologically and renal masses can be either solid or cystic. Masses are characterized by CT, MRI or ultrasound. A CT of the chest abdomen and pelvis is used to stage renal cancers.

To predict the malignant potential of renal cysts the Bosniak system has been adopted (Table 1.6).

Bosniak	Features	
I	Simple benign cyst with a hairline thin wall which does not contain septa, calcification or solid components, the cyst does not enhance with contrast	Benign
II	Benign cyst that may contain a few hairline-thin septa, fine calcification may be present in the wall or septa. Uniformly high-attenuation lesions of <3cm, which do not enhance	Benign
IIF	Contain hairline thin septa; there may be minimal thickening of the septa or wall. The cyst may contain calcification; there is no contrast enhancement. Also includes intrarenal non enhancing high attenuation lesions >3cm	A small proportion are malignant
III	Indeterminate cystic masses that have thickened irregular walls or septa in which enhancement can be seen	Malignant in >50%, surgery or close follow up recommended
IV	Malignant cystic lesions containing enhancing soft-tissue components	Surgery recommended

Table 1-6 Bosniak classification of renal cysts

Tumour characteristics	Nodal status
Tx Primary tumour cannot be assessed	**Nx** Regional lymph nodes not assessed
T0 No evidence of primary tumour	**N0** No regional lymph node metastasis
T1 Tumour ≤ 7cm limited to the kidney T1a Tumour ≤4cm, limited to kidney T1b Tumour >4cm but ≤ 7cm in greatest dimension	**N1** Metastasis in a single regional lymph node
T2 Tumour >7cm, limited to the kidney T2a Tumour >7cm but ≤10cm T2b Tumour >10cm, limited to kidney	**N2** Metastasis in more than 1 regional lymph node
T3 Tumour extends into major veins, adrenals or perinephric tissue, not beyond Gerota's fascia T3a Tumour extends into renal vein or its branches, perirenal and/or renal sinus fat T3b Tumour extends into vena cava below diaphragm T3c Tumour extends into vena cava above diaphragm or invades wall of vena cava Tumour invades subepithelial connective tissue	**Distant Metastasis**
T4 Tumour extends beyond Gerota's fascia	M0N0 distant metastasis M1 Distant metastasis

Table 1-7 TNM classification of renal cancer

A number of factors have been suggested as predictors of prognosis in renal cell carcinoma. Firstly the subtype of the tumour; chromophobe has a better prognosis than papillary, which in turn has a more favourable prognosis when compared to clear cell. Fuhrman grade, sarcomatoid features, microvascular invasion, tumour necrosis and invasion of the collecting system are all considered to be negative prognostic indicators. Other relevant variables include performance status, cachexia, anaemia and localized symptoms.

1.6.3. Pathogenesis

Macroscopically, a number of gross chromosomal changes are associated with RCC. Clear cell RCC is characterized by deletions of chromosomes 3p, 6q, 8p, 9p and 14q as well as duplications of 5q22. Papillary RCC are characterized by chromosomal trisomy of 3q, 7, 12, 16, 17 and 20. Chromophobe RCC have loss of chromosomes 1, 2, 6, 10, 13, 17 and 21 [143].

On a finer genetic level, the most frequently mutated gene in RCC is *vHL*. The Knudson hypothesis explains the pathogenesis of familial cancers where the inheritance of a mutated tumour suppressor gene is followed by a second mutational event involving the wild type allele, which leads to malignancy [144]. Familial von Hippel-Lindau disease is an autosomal dominant syndrome characterized by mutations in one copy of the *vHL* gene followed by loss or mutation of the second allele, leading to a predisposition to benign and malignant tumours such as retinal haemangioblastoma, RCC, pheochromocytoma, and pancreatic tumours. The *vHL* gene is located in chromosome 3p25.3, a region that is frequently deleted in clear cell RCC. In

addition, mutations in *vHL* occur in around 60-80% of cases of sporadic clear cell RCC. The vHL protein forms the recognition component of a ubiquitin ligase complex that binds to the hydroxylated HIF-1α subunit and targets it for degradation in normoxia (see Chapter 1.3.1). Thus, mutations in vHL in RCC lead to constitutive activation of the HIF pathway thereby promoting various processes including angiogenesis.

Duplication of chromosome 7 is a feature of about 75% of papillary renal cell carcinoma. Two key genes on this chromosome are the receptor tyrosine kinase *C-MET* and its ligand hepatocyte growth factor (*HGF*). Mutations in *C-MET* are associated with hereditary papillary RCC and found in around 10% of cases of sporadic papillary RCC [145, 146].

In addition to these well characterized genes, mutations in the tumour suppressor fumarate hydratase, which encodes the enzyme in the Krebs cycle responsible for the conversion of fμmarate to malate, are associated with hereditary leiomyomatosis RCC [147]; these tumours also have overexpression of HIF-1α. Furthermore, germline mutations in the folliculin gene (*FLCN*) lead to renal tumours in Birt -Hogg-Dube syndrome [148]. More recently, mutations in the histone demethylase *JARID1C* and the methylase *SETD2* have been reported in around 3% of cases of clear cell RCC [149, 150]. Finally, mutations in *PBRM1*, a component of the chromatin remodeling complex, have been reported in around 40% of cases of clear cell RCC [149].

1.6.4 Treatment

Wherever possible nephron-sparing surgery is recommended as this is known to have similar oncological outcomes to radical surgery. Where this is not possible, radical nephrectomy either by open or laparoscopic surgery is recommended.

In the management of small renal masses, surveillance and minimally invasive treatments such as RFA, cryoablation, laser ablation and high intensity focused ultrasound (HIFU) have been considered.

A large number of patients are either diagnosed with or progress to metastatic disease. The prognosis for metastatic RCC is poor with a median survival of 10-12 months. Treatment is mainly palliative, incorporating surgery with adjuvant medical therapy [151]. Before the advent of targeted therapies, the standard chemotherapeutic agents for the treatment of renal cancer were cytokines such as interleukin-2 (IL-2) and interferon (IFN). Although IL-2 can achieve remission in a subset of patients, toxicity associated with treatment restricts its use in only fit patients [152].

More recently, an understanding of the biology associated with vHL mutation has guided the development and choice of targeted therapies in the management of renal cancer. Stabilization of HIF results in the upregulation of target genes such as *VEGF, TNF-a* and *PDGF* that are strongly implicated in angiogenesis; inhibitors of these pathways are, therefore, likely to be of clinical benefit to patients.

1.6.4.1. Targeting tyrosine kinase pathways

The new generation inhibitors generally fall into two classes - those that bind to the ligands and prevent initiation of signaling or those that bind to the signaling

receptors and inhibit their activity. Bevacizumab, a humanized monoclonal antibody against VEGF, belongs to the first class and has been shown to improve progression free survival (PFS) when given in combination with IFN compared to IFN alone [153].

Many of the growth factors implicated in oncogenesis act via cell surface receptors with tyrosine kinase activity. Two small molecule tyrosine kinase inhibitors that have become the mainstay in the treatment of metastatic renal cancer are sorafenib and sunitinib. Sorafenib inhibits the kinase activities of the cell surface receptor tyrosine kinases VEGFR2, VEGFR3, PDGFR-b, c-KIT and RET, as well as the serine threonine kinase RAF [154]. It has been shown to improve PFS in patients unresponsive to cytokine therapy [155, 156]. Sunitinib inhibits the kinase activity of VEGFR, PDGFR-a, PDGFR-b, c-KIT and RET [157]. In a phase III clinical trial, it was found to improve PFS by 6 months compared to cytokine therapy alone [158]. Pazopanib targets VEGFR, PDGFR and C-KIT and was found to improve PFS compared to the placebo group in a phase III clinical trial [159]. Thus, sunitinib, pazopanib and bevacizumab now represent first line therapies in the treatment of low and intermediate risk patients with RCC and sorafenib is recommended as second line treatment for metastatic RCC after cytokine failure [160].

1.6.4.2. Targeting the mTOR pathway

A central metabolic pathway that is proving to be an important therapeutic target in cancer, and RCC in particular, is the mammalian target of rapamycin (mTOR)[160, 161]. The protein kinase mTOR integrates signals from growth

factors, amino acids and oxygen availability [162] to positively regulate cell growth through a number of processes including protein synthesis and turnover[163]. In mammals, two mTOR complexes exist- mTORC1 and mTORC2 [164]. While the kinase mTOR is shared, the complexes differ by the presence of the proteins RAPTOR or RICTOR respectively. The drug rapamycin primarily inhibits the activity of the mTORC1 complex (Figure 1.4). The presence of this selective inhibitor has meant that most work in the field to date has looked at uncovering the cellular function of mTORC1.

In the uninduced state, mTOR signaling is held in check by a complex of tuberous sclerosis complex (TSC) proteins, TSC1 and TSC2, which binds to the mTOR co-activator RHEB and inhibit its activity. Growth factor signaling activates the PI3 kinase pathway and leads to activation of the kinase PKB (AKT) (see Chapter 1.2). Activated PKB phosphorylates TSC2 on multiple residues and inhibits the ability of the TSC complex to antagonise RHEB function. RHEB, is an obligate co-activator of mTOR and with inhibition of the TSC complex, is able to associate with, and promote signaling from mTORC1 [165] (Figure 1.4).

The two main targets of mTORC1 are the ribosomal protein p70 S6 kinase (p70S6K) and 4EBP1. Phosphorylation of p70S6K leads to its activation and subsequent phosphorylation of the ribosomal S6 protein, thereby promoting ribosome biogenesis and translation initiation. Phosphorylation of 4EBP1 by mTORC1 inhibits its association with the EIF4E, thereby allowing the latter for assemble the translation initiation complex [166]. Thus, the net effect of mTORC1 activation is increased protein translation, leading to cell growth (Figure 1.4).

Much less is known about signaling by mTORC2. In contrast to mTORC1, the TSC complex appears to promote the activity of mTORC2. mTORC2 has been shown to be the kinase responsible for Ser-473 phosphorylation on PKB/AKT, a prerequisite for its full activation. In addition, the mTORC2 complex appears to play a role in cell migration [167], however the extent and importance of its functions is currently unclear.

In the context of insulin signaling, it has previously been shown that activated mTORC1/p70S6K inhibits PI3K signaling and PKB activation. This occurs at the level of IRS-1; p70S6K phosphorylates the IRS-1 on residues that then prevent the binding of the p85 subunit of PI3K [168, 169]. A somewhat contradictory observation is that treatment with rapamycin can lead to an increase in PKB phosphorylation on Ser-473 within a few hours in some cell types [170]. The mechanism by which this occurs is unclear, although it appears to require the insulin receptor [170] and PI3K signaling [171]. In addition, prolonged treatment with rapamycin also prevents assembly and activity of mTORC2 [172]. Two rapamycin analogues have now been approved for the treatment of renal cancer. Temsirolimus is recommended as first line treatment and everolimus is recommended as second line treatment after failure of tyrosine kinase inhibitors.

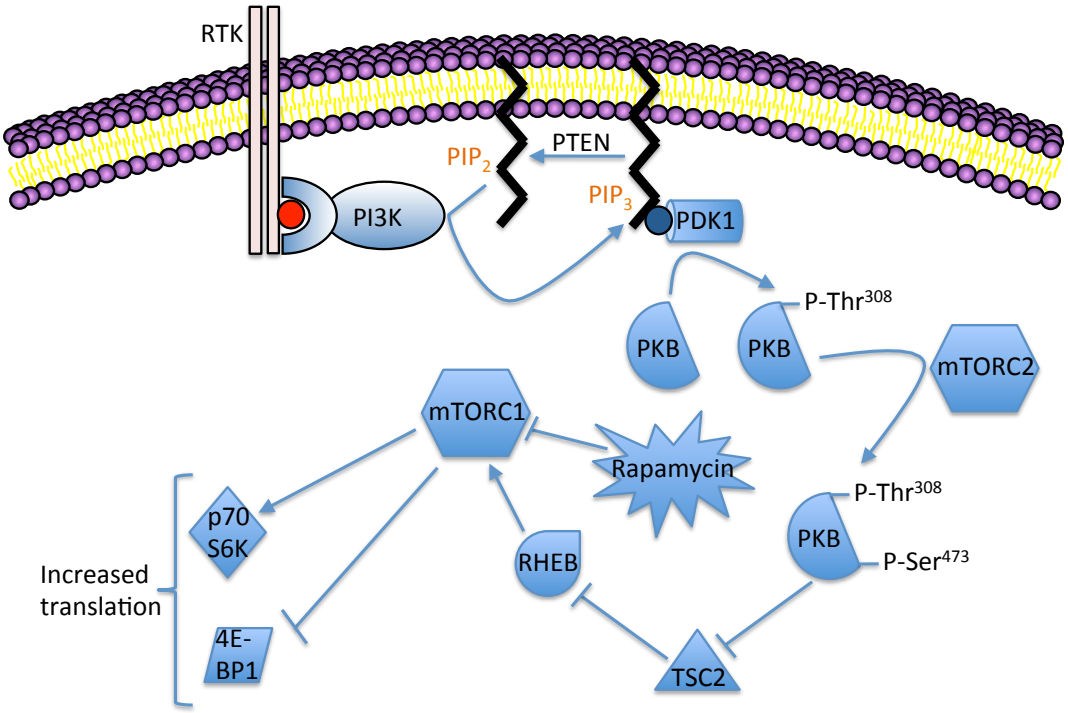


Figure 1-4 Summary of the mTOR pathway

1.7 Aims of project

The work in this thesis has focused on urological malignancies and bladder and renal cancer in particular. As miRNAs represent a novel class of molecules involved in gene regulation, the first aim was to identify hypoxia regulated miRNAs in bladder cancer and evaluate their functional significance and this is covered in Chapter 3. Furthermore, our previous work suggested that miR-100 may be of functional significance in bladder cancer. Thus, in Chapter 4, I investigated the hypoxic regulation of miR-100, its effects on *FGFR3* expression, downstream signaling and effects on cell viability. Although targeted therapies are now in routine use in the management of RCC, responses to these agents vary. The focus of Chapter 5 was to investigate the response of primary and established RCC lines to chemotherapeutic agents currently used in the treatment of RCC. Furthermore, expression profiling of selected genes was also performed in the primary RCC cultures, to identify markers (including vHL mutation) that may predict sensitivity to targeted therapies in RCC.

Chapter 2 Materials and Methods

2.1 Materials and reagents

2.1.1. Plasticware

All plasticware was purchased from Corning (Corning, US).

2.1.2. Cell culture reagents

The cell dissociation agent trypsin-EDTA, the antibiotics penicillin/streptomycin and the cell culture media Dulbecco's Modified Eagle Medium (DMEM), McCoy's 5A, RPMI 1640, HAMS F12, and the Keratinocyte-serum free media with supplements rEGF and BPE were obtained from Invitrogen (Grand Island, USA). Foetal calf serum (FCS) was obtained from PAA Laboratories (Austria). The cell dissociation agents Dornase alfa and Collagenase IV were obtained from Sigma-Aldrich (St Louis, USA). The trypsin inhibitor was obtained from Sigma-Aldrich.

2.1.3 Enzymes and kits

The High Capacity cDNA synthesis kit, Taqman Universal mastermix and miRNA reverse transcription kit were purchased from Applied Biosystems (Foster City, USA). The Sybr Green mastermix (SensiMix) was obtained from Bioline (London, UK). The EZ-ChIP kit was purchased from Millipore (Billerica, MA, USA).

2.1.4 Primers and TaqMan assays

Primers were purchased from Invitrogen. All primers were of standard, de-salted purity. miRNA TaqMan assays were purchased from Applied Biosystems.

Primer sequences are as follows:

ACTIN_F: ATTGGCAATGAGCGGTTC,

ACTIN_R: GGATGCCACAGGACTCCAT,

CAIX_F: CTTGGAAGAAATCGCTGAGG,

CAIX_R: TGGAAGTAGCGGCTGAAGTC,

FGFR3_F: GCCTCCTCGGAGTCCTTG

FGFR3_R: CGAAGACCAACTGCTCGTG

REDD1_F: CTGGAGAGCTCGGACTGC

REDD1_R: TCCAGGTAAGCCGTGTCTTC

FGFR3 HRE1_F: AGCAGATGGCCTTTTCCTTGTGAG

FGFR3 HRE1_R: ATGCCGCGGAGCTGAACCCTGTGG

FGFR3 HRE2_F: GCCGTCCTGCCCTCCTCCACCTGA

FGFR3 HRE2_R: CGCTCCGGCTCGCTGTCC

miR-145 HRE1_F: GTGAATGAGGCCGTGAACAGAGAC

miR-145 HRE1_R: CATGTCCACGGTTCTAGTTTCTTG

miR-145_HRE2_F: AGCACCGGGGGCAGGTCAAG

miR-145_HRE2_R: GGCATTTTTAAGCAGCTGGCACTG

CA9 HRE_F: GTCCATGGCCCCGATAACCTTCTG

CA9 HRE_R: GGGGCAACCTCTGGGGATGGAC

UBC ChiP_F: TTGCTGGCAAATATCAGACG

UBC ChiP_R: GCAAGACCATCACCCTTGAG

2.1.5. Low density array cards

For the expression profiling of around 350miRNA in RT4 and T24 cells, Low Density miRNA Arrays, Pool A was purchased from Applied Biosystems. For the mRNA expression profiling done in RCC cell lines, Low Density Arrays were custom designed with TaqMan assays for the genes listed in Table 5.3 spotted in triplicate. The arrays had ACTIN, HPRT1, RPL11 and 18S ribosomal RNA spotted on as internal control genes.

2.1.6 siRNA, microRNA mimics and anti-miRs

SiRNA against HIF-1α, HIF-2α, p53 and an individual control siRNA were synthesised by Eurogentec (Liege, Belgium).

The siRNA sequences are as follows:

siHIF-1α: UCAAGUUGCUGGUCAUCAG

siHIF-2α: UAACGACCUGAAGAUUGAA

sip53: GACUCCAGUGGUAAUCUAC

Scr: ACGACACGCAGGUCGUCAU

The pooled siGENOME siRNA against FGFR3, the pooled siGENOME siRNA control, miRNA mimics and anti-miRs and appropriate controls were all purchased from Dharmacon (Lafayette, CO).

2.2 Methods

2.2.1 Routine cell culture

The cell lines HT1376, RT4, RT112, T24, 786-0 and RCC4 were obtained from Cancer Research UK Cell Services. Cell lines 7860, RCC4 and UMRC2 empty vector and *+vHL* were characterized by western blotting for the presence of HIF-1 and HIF-2 (Figure 2.1) The cell lines 97-7 and h-TERT were kindly provided by Dr. Margaret Knowles (Leeds Institute of Molecular Medicine, Leeds, UK). UMRC2 cells were kindly provided by Dr. Johannes Schödel (Henry Wellcome Building for Molecular Physiology, Oxford, UK). The characteristics and culture conditions for the above cell lines are listed in Table 2.1.

All cell lines were passaged by washing with phosphate buffered saline (PBS) and dissociated by incubation with 2mLs trypsin-EDTA at 37^{o}C for 5-10 minutes. For all cell lines except h-TERT, the trypsin was stopped by adding 8mLs of complete culture media (with FCS); for h-TERT cells, the trypsin was stopped by adding the trypsin inhibitor (100µL of a 1% solution per mL of trypsin diluted in culture media). Cells were pelleted by centrifugation at 750g for 4 minutes, resuspended in complete culture media and counted with an automated Coulter counter.

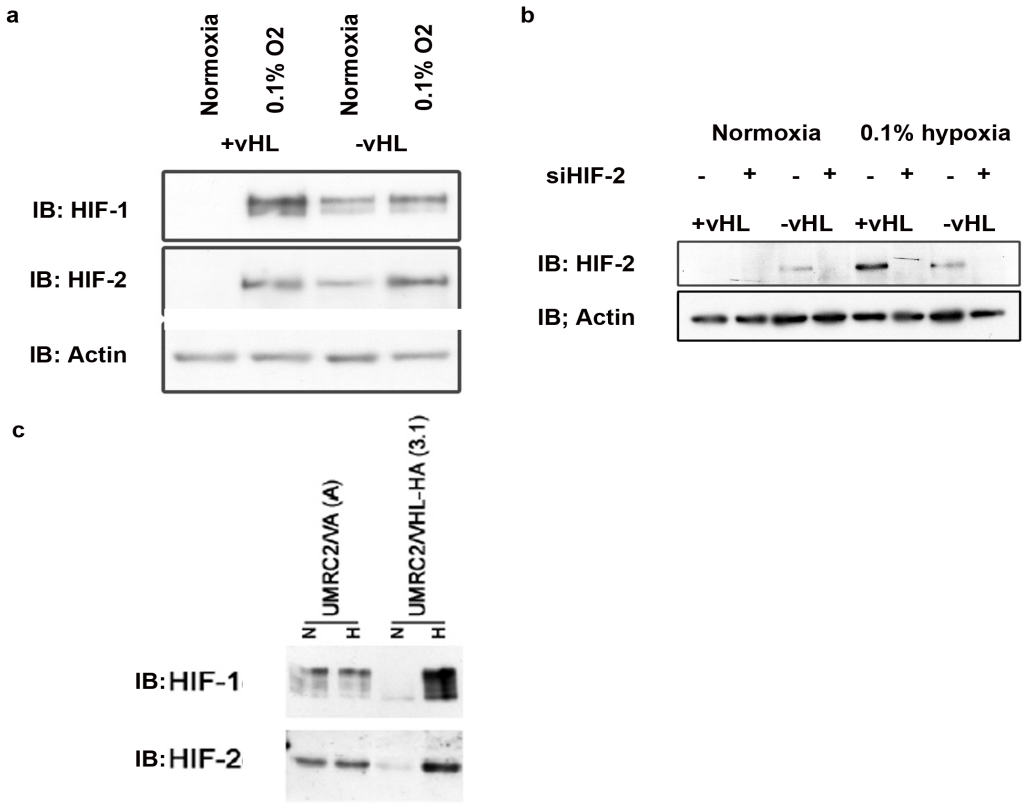


Figure 2-1 Characterisation of cell lines

(a) Protein expression of HIF-1α and HIF-2α in RCC4 cells with vHL and RCC4 cells (empty vector) in normoxia and hypoxia. (b) Protein expression of HIF-1α and HIF-2α in 7860 cells with vHL and 7860 cells (empty vector). Also shown are cells with HIF-2α knockdown. (c) Protein expression of HIF-1α and HIF-2α in UMRC2 cells transfected with an empty vector (VA) or vHL.

Cell line	Characteristics	Culture medium
RT-4	Transitional cell papilloma Overexpress wild type FGFR3	McCoy's 5a medium supplemented with 2mM L-glutamine and 10% FCS
RT-112	Transitional cell carcinoma G2 Overexpress wild type FGFR3	RPMI 1640 media supplemented with 2mM L-glutamine and 10% FCS
T-24	Transitional cell carcinoma G3 Express mutant HRAS and p53	DMEM 5a medium, 2mM L-Glutamine, 10% FCS
HT-1376	Transitional cell carcinoma G3 Mutated p53	DMEM, 2mM L-Glutamine, 10% FCS
97-7	Non-invasive bladder cancer cell line S249C mutant FGFR3 cells	F12 (Hams medium), L-Glutamine, 10% FCS
h-TERT	Telomerase immortalised normal urothelial cells	KFSM keratinocyte medium (Life technologies, Inc, Paisley, Scotland)
786-0	Renal call adenocarcinoma, +VHL and empty vector	DMEM, 2mM L-Glutamine, 10% FCS
RCC4	Renal call adenocarcinoma, +VHL and empty vector	DMEM, 2mM L-Glutamine, 10% FCS
UMRC2	Renal call adenocarcinoma, +VHL and empty vector	DMEM, 2mM L-Glutamine, 10% FCS
Primary renal cells		DMEM, 2mM L-Glutamine, 10% FCS

Table 2-1 Cell lines and reagents

2.2.2 Primary cell culture

Renal tumour tissue or normal renal cortex was taken from nephrectomy specimens immediately after surgery at the Churchill hospital, Oxford, UK. A portion of the tissue was snap frozen in liquid nitrogen for DNA extraction. The remaining tissue was dissected and cut into 2mm cubes using a sterile scalpel. The tissue was incubated with a dissociation mix containing 4.9ml of RPMI 1640,

50ul of Dornase alfa and 50ul of Collagenase IV in a gentleMACS C Tube and the tissue was disrupted on a gentleMACS Dissociator (Miltenyi Biotec, Auburn, USA) according to the manufacturer's instructions. The suspension was passed through a 70µm cell strainer and the clarified cell suspension was centrifuged at 750g for 4 minutes. The cells were resuspended and plated in a vented tissue culture flask with a 25cm^2 growth surface area. Cells were allowed to reach 80% confluence before being passaged. Primary cells were used from passages 2-6.

2.2.3 Long term cell storage

For cryopreservation, cells were harvested in the exponential phase of growth. Cells were suspended at a concentration of 1*10^{6}cells/ml in FCS with 10% dimethylsulphoxide (DMSO; Sigma-Aldrich, UK) and aliquoted in 1mL aliquots in cryovials. Cryovials were placed in a cryo-freezing container ("Mr. Frosty") (Thermo Fisher Scientific Rochester, US) that had an isopropanol reservoir and was then placed in a -80^{o}C freezer to achieve a freezing rate of -1^{o}C/minute. Two to seven days after freezing, cells were transferred to liquid nitrogen for long term storage. Frozen cells were rapidly thawed at 37^{o}C in a water bath, added to 5mls of media and then centrifuged at 750g for 4 minutes. The cell pellet was resuspended and plated into a new culture flask.

2.2.4 Exposure of cells to hypoxia

Cells were exposed to mild hypoxia (1%O_2) by placing them in a hypoxic incubator (MiniGalaxy A, RS Biotech, Scotland, UK). To attain moderate hypoxia (0.1%O_2), cells were placed in a hypoxic workstation (In Vivo$_2$, Ruskinn

Technology, Bridgend, UK). For all experiments done with hypoxia, parallel cell cultures were maintained in normoxic conditions (5% CO_2, 37°C, 21% O_2). All experiments were done in triplicate from independent cell cultures. To reproduce the effects of hypoxia we also used dimethyloxalylglycine (DMOG) (Sigma-Aldrich, St Louis, USA). DMOG is a cell permeable competitive inhibitor of HIF-α prolyl hydroxylases and leads to the stabilisation of HIF. DMOG was added to the culture medium at the start of the incubation period to make a final concentration of 1mM.

2.2.5 RNA extraction and quantification

Up to $1*10^7$ cells were lysed in 1ml of Trizol (Invitrogen). The aqueous and organic phases were separated by adding 200µL of chloroform per mL of Trizol, shaking vigourously and then centrifuging at 13000g at 4°C for 15 minutes. The supernatant (aqueous phase) was removed and placed in a new 1.5ml tube, 500ul of isopropanol was then added, the contents were mixed by inversion and left at room temperature for 10 minutes. This was then centrifuged at 14,000rpm @4°C for 10 minutes. The supernatant was removed and the remaining pellet was washed in 1ml of 75% ethanol in DEPC treated water (Ambion, USA). This was then centrifuged at 7,500rpm @4°C for 5 minutes. The supernatant was removed and the pellet left to air dry for 5 minutes before being resuspended in 100ul of DEPC treated water.

RNA purity and quantity were confirmed using the NanoDrop ND-1000 spectrophotometer (Thermo Scientific, MA, USA).

2.2.6 Reverse transcription of mRNA

Total RNA was reverse transcribed to cDNA using the High Capacity Reverse Transcription Kit. Briefly, each reaction contained 2μg of total RNA, 4mM dNTPs, random primers, 1X reverse transcription buffer and 5 units of the Multiscribe reverse transcriptase in a final reaction volume of 20μL. The assembled reaction was incubated in a thermal cycler programmed with the following temperature profile – 25°C for 10 minutes, 37°C for 120 minutes, 85°C for 5 seconds followed by an indefinite hold at 4-12°C. The cDNA was diluted by adding 200μL of sterile water and either used immediately or stored at -20°C.

2.2.7 Reverse transcription of miRNA

MiRNAs present in total RNA were reverse transcribed using the miRNA Megaplex Pool A Version 3.1. One microgram of total RNA was reverse transcribed in a total reaction volume of 7.5μL with 1X Megaplex RT buffer, 1X Megaplex RT primers, 3mM $MgCl_2$, 2.5mM dNTPs, 75 units of Multiscribe reverse transcriptase and 0.25 units of RNAse inhibitor. RNA was reverse transcribed with the following cycling conditions in a thermal cycler – 40 cycles of 16°C for 2 minutes, 42°C for 1 minute and 50°C for 1 second followed by an incubation at 85°C for 5 minutes and finally an indefinite hold at 4-12°C. After completion, 6μL of the reaction was diluted with the addition of 444μL of sterile water and was either used immediately or stored at -20°C.

2.2.8 Quantitative PCR

Quantitative PCR (qPCR) analyses were performed either on a Rotor-Gene 3000

(Corbett Research, Qiagen, West Sussex, UK) or 7900HT Fast Real Time PCR System (Applied Biosystems).

For individual gene expression at the transcript level, cDNA samples were interrogated by qPCR using the Sybr Green chemistry. Each reaction consisted of 1X SYBR Green mastermix, 300nM of each primer and 2µL of the diluted cDNA in a final reaction volume of 10µL. Cycling conditions were as follows – 95°C for 15 minutes for Taq polymerase activation, followed by 50 cycles of 95°C for 15 seconds and 60°C for 60 seconds. To confirm that a single product was obtained during the amplification, a dissociation curve analysis was performed at the end of the run. Thermal conditions for the dissociation curve were as follows - 95°C for 15 seconds, 60°C for 20 seconds and a slow ramp (1% of the standard ramp rate; approximately 20 minutes) to 95°C. For each target, every sample was analysed in triplicate.

For qPCR of individual miRNAs, each reaction consisted of 1X TaqMan Universal PCR mastermix, 2µL of the diluted miRNA cDNA pool and 1X Taqman primers/probe mix in a total reaction volume of 10µL. cycling conditions were as described for the SYBR Green analysis above with the exception that a dissociation curve analysis was not performed. For each target, every sample was analysed in triplicate.

2.2.9 Normalisation and quantification of gene expression

For gene expression at the transcript level, expression of the gene of interest was normalized to the expression of β-ACTIN (*ACTB*) in that sample. For expression of miRNA, expression of the miRNA of interest was normalized to the expression

of RNU44. In both cases, expression was quantified using the ΔCT method (also known as the comparative CT method). The formula for calculating relative expression is as follows [173].

Target quantity=2^-((CT miRNA of interest)-(CT control miRNA)).

The ΔCT method assumes that the amplification efficiency of the primers for the miRNA/gene of interest and control miRNA/gene are almost identical. The TaqMan primers/probes from Applied Biosystems are designed to have close to 100% amplification efficiencies. Furthermore, the amplification efficiencies of the primers used for qPCR for chromatin immunoprecipitation (ChIP) were also tested by constructing a standard curve for each primer pair and found to be close to 100% (data not shown). The amplification efficiency of all other primers was assumed to be 100%. In the majority of cases data is presented as fold change relative to a calibratory sample (with an expression value of 1).

2.2.10 Protein extraction and quantification

Whole cell lysates were prepared using the urea lysis buffer (6.2 M urea, 5mM DTT, 1% sodium dodecyl sulphate (SDS), 10% glycerol, 10mM Tris-Cl, pH 6.8) with added protease (Roche, Indiana, USA) and phosphatase (Sigma-Aldrich) inhibitors. The tissue culture dishes were placed on ice, the culture medium aspirated and the cells washed once with ice cold PBS. Cells were lysed with the appropriate volume of lysis buffer (200μL per 6-cm dish, scaled according to surface area) with gentle scraping with a cell scraper. The lysate was then passed through a 21-gauge needle until the sample was homogenized.

Protein quantification was performed with the Bio-rad Dc System (Bio-rad, Hertfordshire, UK). Protein lysates were diluted 1:3 and assayed in duplicate. A

standard curve was constructed with bovine serum albumin (BSA) at concentrations of 0, 0.125, 0.25, 0.5, 1.0 and 2μg/μL in duplicate. Reagent A* was made by adding 20μL of reagent S to 1mL of reagent A. 25ul of reagent A* was then added to each well with sample/standard curve. Finally, 200μL of reagent B was added to each well and the colour allowed to develop for 20 minutes at room temperature. An optical plate reader was used to measure absorbance at 690nm.

2.2.11 SDS-poly acrylamide gel electrophoresis

Proteins were detected by SDS-poly acrylamide gel electrophoresis (SDS-PAGE) and Western blot analysis. Proteins were separated on a 10% acryalmide /bis resolving gel (acrylamide/bis ratio 37.5:1, 375mM Tris-Cl (pH 8.8), 0.1% SDS polymerized with TEMED and ammonium persulphate (APS)) overlaid with a 4% stacking gel (acrylamide/bis ratio 37.5:1, 125mM Tris-Cl (pH 6.8), 0.1% SDS polymerized with TEMED and APS) by electrophoresis (electrophoresis buffer - 250mM glycine, 25mM Tris, 0.1% SDS) at 120V for 90 minutes. The proteins were then transferred from the gel to a methanol activated PVDF membrane with a semi-dry transfer after equilibration of the gel, membrane and filter paper in transfer buffer (transfer buffer – 20% methanol in electrophoresis buffer).

PVDF membranes were blocked with either 5% low-fat milk or 5% BSA in wash buffer (25mM Tris, 150mM sodium chloride, 2.8mM potassium chloride, 0.05% Tween-20) and incubated with primary antibodies overnight at 4^{o}C. The following day, the membranes were washed three times, each for 10 minutes, with wash buffer and then incubated with HRP-conjugated secondary antibodies diluted in 5% low-fat milk in wash buffer for one hour at room temperature. ECL

(GE Healthcare, Amersham, UK) was used as the chemiluminescent substrate and the signal was visualized by exposing to film. Where required, membranes were stripped with the Pierce Stripping Buffer (Thermo Fisher Scientific) before being reprobed with a new antibody. Primary antibodies were diluted 1:500-1:1000, secondary antibodies were diluted 1:1000; secondary antibodies were purchased from DAKO, sources of primary antibodies are given in Table 2.2.

Antibody	Origin	Source	WB	IHC
CA9	Mouse	In house	1:1000	1:50
HIF-1	Mouse	BD transduction Laboratories	1:1000	
HIF-2	Mouse	AbD Serotec	1:500	
mTOR	Rabbit	Cell signaling Technology	1:500	
P70S6K	Rabbit	Cell signaling technology	1:500	
Phosph-p70 S6 Kinase	Rabbit	Cell signaling Technology	1:500	
Total ERK	Rabbit	Cell Signaling Technology	1:1000	
Phospho-ERK	Rabbit	Cell Signaling Technology	1:1000	
Phospho-PKB (Ser473)	Rabbit	Cell Signaling Technology	1:1000	
Total PKB	Rabbit	Cell Signaling Technology	1:1000	
Phospho-MYC	Rabbit	Cell Signaling Technology	1:1000	
MYC	Mouse	Santa Cruz	1:1000	
P21	Rabbit	Cell Signaling Technology	1:1000	
β -Actin	Mouse	Sigma	1:500	
FGFR3	Rabbit	Cell signaling technology	1:500	1:50

Table 2-2 Antibodies

2.2.12. Immunohistochemistry

Immunohistochemistry was performed by Dr. Helen Turley and Dr. Adrian Jubb. In brief, 5µm sections were cut from paraffin embedded tissue or cell pellets. Sections were de-waxed followed by antigen retrieval, blocking and then incubation with primary and secondary antibodies.

2.2.13. DNA extraction

DNA extraction was extracted from frozen tumour material using the Qiagen Gentra Puregen kit. In brief, tumour tissue was crushed with a mortar and pestle in liquid nitrogen. To 5-10mg of this crushed tissue, 300µL of cell lysis solution was added and the mix was heated to 65^{o}C for 30 minutes. To aid protein digestion, 1.5µL of proteinase K was added and the mix incubated overnight at 55^{o}C. The following day 1.5µL of RNAse A solution was added and this was incubated at 37^{o}C for 30 minutes. Samples were rapidly cooled by placing on ice for 1 minute. Proteins were precipitated by adding 100µL of protein precipitation solution, mixed by vortexing and centrifuged at maximum speed for 3 minutes to pellet the protein. DNA was precipitated from the supernatant by adding 300µL of isopropanol and pelleted by centrifugation at maximum speed for 3 minutes. The DNA pellet was then washed with 70% ethanol and then solubilised by adding 200µL of DNA hydration solution and incubating at 65^{o}C for 1 hour. DNA quantity and purity was measured using the Nanodrop.

Sequencing of the DNA samples for mutations in the three exons of vHL was performed by Dr Claire Taylor at the Leeds Institute of Molecular Medicine.

2.2.14. Transfection of small RNA

Cells were transiently reverse transfected with small RNA (siRNA, miRNA mimics and anti-miRs) using the Oligofectamine transfection reagent (Invitrogen) according to the manufacturer's instructions. Briefly, lipid:oligonucleotide complexes were made in 200µL of OptiMEM (Invitrogen) with 6uL of Oligofectamine and 20nM final concentration of small RNA. Cells were plated at a density of $3*10^5$ cells per 6cm dish (in 1.8mLs of media) to which the complexes were added. The following day, the medium was changed and the cells treated as appropriate.

2.2.15. Transduction of shRNA constructs

Lentiviral particles encoding five different shRNA sequences against REDD1, along with lentiviral particles encoding a control shRNA sequence were purchased from Sigma-Aldrich. The shRNA were in the pLKO.1 plasmid backbone with puromycin resistance. Cells were plated at a density of $2*10^6$ cells in vented culture flask with a $75cm^2$ surface area. The following day, cells were transduced with lentiviral particles. Two days later, cells were selected with 2µg/mL puromycin to select for cells into which the lentivirus particles had integrated. The knockdown of REDD1 was confirmed by qPCR.

2.2.16 Chromatin immunoprecipitation

ChIP assays were performed using the EZ-ChIP Kit (Millipore) as per the manufacturers instructions. Briefly, RT4 cells were either incubated in normoxia or $0.1\%O_2$ for 24 hours. DNA was crosslinked with 1% paraformaldehyde, excess

paraformaldehyde was quenched with 125mM glycine and the cells harvested by scraping. Cells were resuspended in SDS lysis buffer with protease inhibitors to get a cell suspension at $2*10^7$ cells/mL. To shear genomic DNA, 350µL of the cell suspension was sonicated with 12 pulses of 10 seconds. Sheared DNA was pre-cleared with protein G beads and immunoprecipitation was performed with anti-HIF-1α and α-RNA polymerase II antibodies using 100µL of sheared DNA per antibody. After overnight incubation, antibodies with bound chromatin were purified with protein G beads, the protein:DNA complexes eluted and then the crosslinks reversed to release the sheared genomic DNA.

2.2.17 Flow cytometry

RT4 cells were reverse transfected with mimic-100 or anti-miR-100 as described above and either kept in normoxia or placed in 0.1%O_2. On day 3, 4 and 5, cells were harvested with trypsin and pelleted. Cells were stained with annexin-V-AlexaFluor647 (Invitrogen) (5µL) and propidium iodide (Invitrogen) (50µg/mL) in 100µL of annexin V binding buffer (BD Pharmagen) for 15 minutes at room temperature. After incubation, 400µL of annexin V staining buffer was added to each sample, cells were placed on ice and then analysed by flow cytometry using a Cyan ADP Flow Cytometer (Beckman Coulter). Data collection and analysis was performed using Summit version 1 (DAKO). Cell debris was gated on the forward and side scatter plots. The voltage on the FL1 (488nm) and FL3 (613nm) channels was adjusted to acquire data for annexin V and propidium iodide respectively.

2.2.18 Luciferase assay

MCF7 cells were plated at a density of 30 000 cells per well of a 48-well plate in 200μL of penicillin/streptomycin free culture media. The following day, cells were transfected with mimic ctrl or mimic-100, 50ng pRL-TK and 50ng of either the control pSSG_3 untranslated region (UTR) plasmid or the pSSG_3 plasmid with the partial 3'UTR of *FGFR3* (SwitchGear Genomics). Briefly, complexes were formed in a volume of 50uL with Lipofectamine 2000 (Invitrogen), the indicated DNA and miRNA mimics at 20nM final concentration for 20 minutes at room temperature. 50ul of DNA/LF2000 complexes were added to each of the appropriate 48-wells, complexes were left for 4-6 hours, the media was then aspirated and replaced with 250uL of fresh media. Two days after transfection, cells were lysed with 150uL of 1X passive lysis buffer (Promega, Madison, USA). For each condition, 30uL of the lysates was placed in triplicate in an opaque, white 96-well plate. Injectors 1 and 2 were set to sequentially dispense 100ul of LAR II and Stop and Glo reagent. Measurements were made with a 1-2 second delay and a 5-10 second read time. Using a reagent injector, Initially 100ul of LARII (Promega) was dispensed and firefly luciferase activity read. Then Stop and Glo (Promega) was dispensed and Renilla luciferase activity read.

2.2.19 SRB assay

For the viability of RT4 after transfection with siRNA or miRNA mimics, cells were reverse transfected and plated at the indicated densities. The following day, the media was aspirated, fresh media added and the cells placed in either normoxia or hypoxia for the indicated time. For the drug treatment, cells were

plated in a 96 well plate at 2000 cells per well overnight. Varying dilutions of drugs were added the following day. Cells were then cultured for between 24 and 96 hours. The medium was discarded and 100ul of cold TCA added to each well. The plates were then placed at 4^{o}C for 30 minutes to fix protein, the TCA was washed off with water and plates dried overnight. The following day 100ul of 0.4% SRB was added to each well and incubated at room temperature for 15 minutes. Unbound SRB was then washed of with 1% acetic acid. The plates were dried and SRB solubilized in 100ul of 10mM Tris and placed on a shaker for 5 minutes. Absorbance was then measured at 540nM in triplicates and IC50 was calculated from the result of log absorbance.

2.2.20 Spheroid growth

RT4 cells were reverse transfected as described above. The following day, cells were plated at a density of 5000 cells per well of a non-adherent 96 well plate (Costar), centrifuged at 750g for 5 minutes and then returned to the incubator, with a media change on day 3. Spheroids photographed on days 3, 5 and 7 after plating, with the diameter of the spheroid used to calculate its volume.

2.2.21 Drug treatment

Sorafenib (Selleck, UK) was diluted in DMSO to a stock dilution of 100mM. Sunitinib (Selleck) was diluted in DMSO to a stock dilution of 100mM. Metformin (Calbiochem) was diluted in medium to a stock concentration of 1M. Rapamycin (Sigma) was acquired prediluted in DMSO at a stock concentration of 2.74mM.

2.2.22 Statistical analysis

Unless otherwise noted, all statistical analyses were performed with the Students T-test. In cases where multiple groups were being assessed, ANOVA testing rather than T-tests would have been more appropriate.

Chapter 3 Hypoxia regulated miRNAs and the role of miR-145 in bladder cancer.

3.1. Introduction

3.1.1. Hypoxia in bladder cancer

The activation of hypoxia regulated genes is involved in bladder cancer initiation, progression and invasion [174-176]. Regions of hypoxia have been shown in both superficial and invasive bladder tumours with colocalisation of the hypoxic markers CA9 and *VEGF* on the luminal surface of superficial tumours, the periphery of necrotic areas and in hypoxic cores found in larger solid tumours [175, 177]. Levels of HIF-1α expression correlate with VEGF expression, microvessel density and *ki67* proliferation index confirming the importance of the hypoxic response on angiogenesis and proliferation in both superficial and invasive urothelial cancers [178, 179]. Immunohistochemistry performed on bladder cancer specimens has shown a correlation between the expression of HIF-1α and advancing tumour stage and grade [180]. Increased expression of HIF-1α is associated with poor prognosis and has been shown to predict recurrence and progression in bladder cancer [177, 179, 181].

3.1.2. microRNAs in bladder cancer

The characterisation of miRNAs differentially regulated in bladder cancer has been the focus of recent studies aiming to establish a role of miRNAs as diagnostic and prognostic markers. Current evidence suggests that more miRNAs are downregulated, rather than upregulated in bladder cancer and it is the loss of

regulation by miRNAs which has a greater role in tumourigenesis [182]. Hypoxia induced alterations in expression of miRNAs may either block the translation of mRNA targets or cause mRNA degradation. To date no studies have investigated the effect of hypoxia on the regulation of miRNAs in bladder cancer. Hypoxia regulated miRNAs (HRMs) have been identified in other cancer types; miR-210 is currently acknowledged as the most hypoxia regulated miRNA and is consistently upregulated as a result of HIF activation across a number of different tumour types.

Comparison of miRNAs reported to be hypoxia regulated by Kulshreshtha et al with those known to have altered expression in bladder cancer reveals miRNAs 15a, 21, 30b, 93, 125b, 141, 214 and 373 as potential HRMs in bladder cancer [183, 184]. MiRNAs regulated by hypoxia in other tumour types such as miR-21 and 99a have shown high expression in invasive bladder cell lines and relative expression of miRNAs 200c, 141 and 30b has been used to differentiate between non invasive and invasive disease [185]. In a study of 106 bladder tumours, miR-21 expression was higher in tumour tissue and a high miRNA-21:miRNA-205 ratio was associated with invasive bladder cancer. MiR-21 is reported to target and down regulate PTEN causing activation of the PI3K and AKT pathways [125, 185]. In the same study, miRNA-143 and miR-145 expression was found to be lower in tumours than normal tissue [186]. MiR-145 expression is reported to be down regulated in colon, prostate, lung and ovarian cancers, in bladder cancers low expression is associated with a poor prognosis [129, 187, 188]. This significant down regulation has identified miR-145 as one of the most notable tumour suppressor miRNAs. A number of targets of miR-145 have been identified such as C-MYC, SOX2 and OCT4 [189]. Interestingly, miR-145 has

also been reported to post transcriptionally regulate the HIF-1 target gene BNIP3 in prostate cancer. Mir-145, a known target of p53, inhibits growth, invasion and metastasis and induces apoptosis through caspase dependent and independent apoptosis and reduced expression of miR-145 has been shown to occur early in tumour development [129, 190-192]. Immunohistochemistry of miR-145 in bladder cancer showed homogenous but reduced staining compared to normal tissue in papillary tumours, heterogenous expression in muscle invasive tumours and in carcinoma *in situ* miR-145 was absent [129].

The primary aim of this chapter was to identify hypoxia regulated miRNAs in bladder cancer. We found that miR-145 is significantly upregulated by hypoxia in RT4 cells and therefore the second aim of this chapter was to establish the functional significance of this upregulation in low grade, non-muscle invasive bladder cancer.

3.2 Results

3.2.1 Normalisation of controls

Small nuclear RNAs (snoRNAs) are used as control genes for the normalisation of miRNAs when acquiring expression data using real-time qPCR. In our experiments we used the Taqman megaplex miRNA pool A, which includes the three snoNAs RNU44, RNU48 and U6. Our group has previously shown that variation in snoRNA expression exists amongst tumour type and also as a result of exposure to hypoxia [193]. Therefore to establish the most appropriate control gene for normalizing microRNA expression we used Genorm version 3.2 to calculate an gene stability measure (M) value to establish the most consistently expressed control gene [193, 194].

We analysed expression data for RNU44, RNU48 and U6 in RT4 cells in normoxia and hypoxia in three separate experiments. All three snoRNAs had low M values; the most stable gene was found to be RNU44 with an M value of 0.04 (Figure 3.1). We confirmed the stability of the internal control genes by looking at the expression of miR-210 as a positive control. Equivalent hypoxic upregulation of miR-210 was seen when using all three control genes. As RNU44 had the lowest M value, this was chosen as the control gene for all further experiments (Figure 3.1).

a

Replicate	RNU44	RNU48	U6	Normalisation factor
Normoxia R1	23.6	23.0	17.7	0.97
Hypoxia R1	25.1	22.9	18.9	1.01
Normoxia R2	24.9	22.7	19.4	1.02
Hypoxia R2	25.6	23.1	19.6	1.04
Normoxia R3	25.1	22.0	18.3	0.99
Hypoxia R3	23.9	21.7	18.6	0.97
M<0.5	0.04	0.05	0.05	

b

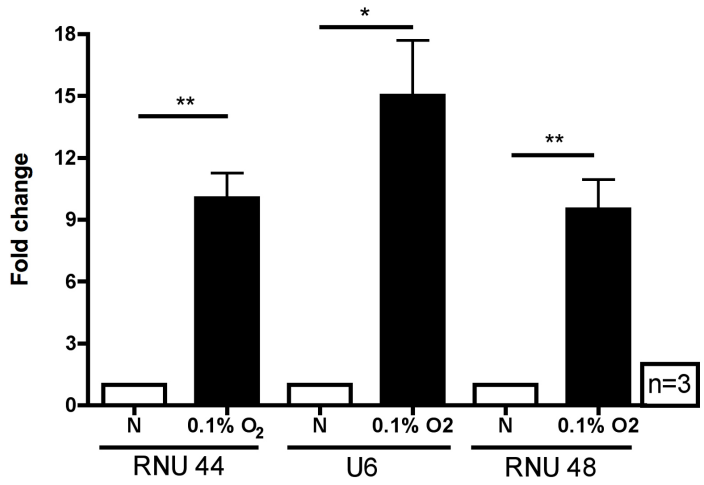


Figure 3-1 Selection of control gene for miRNA experiments

(a) GeNorm (version 3.2) software was used to establish the most stable control gene to be used in future experiments. The lowest M value identifies the most stable gene [188, 189]. (b) RT4 cell were cultured in normoxia and 0.1% O_2 for 24 hours, miR-210 expression was quantified using the three control genes RNU44, U6 or RNU48. Statistical significance: * $p<0.05$, ** $p<0.01$, *** $p<0.001$.

3.2.2. Analysis of known hypoxia regulated microRNAs in bladder cancer cell lines

Our group has previously identified a number of miRNAs with altered expression based upon *vHL* mutation in renal cancer (Table 3.1). As *vHL* mutation leads to the constitutive expression of HIF and mimics hypoxia, we used miRNAs found to be up or down regulated in this analysis as the basis for our initial experiments.

	Agilent		**Illumina**		**Solexa**	
ID	Log FC	Adj. P. val	Log FC	Adj. P. val	Log FC	Adj. P.val
hsa miR-210	2.69	4.60E-14	1.23	0.02	4.39	4.61
hsa miR-155	1.92	2.91E-12	1.32	3.55E-05	2.77	2.98
hsa miR-193b	0.6	3.40E-05	0.36	0.01	1.85	1.79
hsa miR-152	0.5	3.94E-05	2.62	4.77E-05	N F	N F
hsa miR-23b	-1.46	6.81E-09	-0.79	0.02	N F	N F
hsa miR-148a	-0.85	1.84E-06	-3.31	5.51E-05	-4.06	-3.84
hsa miR-145	-0.73	1.90E-05	-1.86	4.77E-05	-4.05	-4.03
hsa miR-503	-0.89	1.90E-05	-1.12	0.01	-0.71	-0.26
hsa miR-143	-0.41	1.90E-05	-4.64	8.17E-08	N F	N F
hsa miR-224	-0.68	0.02	-1.1	0.02	N F	N F
hsa miR-9*	-0.09	0.03	-1.17	0.04	N F	N F
hsa miR-100	-0.69	0.02	-0.61	0.04	-0.43	-0.49
hsa miR-424	-1.49	9.10E-07	-0.53	0.03	-1.54	-1.63

Table 3-1 microRNAs up or downregulated depending on vHL mutation

Unpublished results from our group used with permission of Carme Camps. Data shows expression of miRNAs in RCC4 cells (*vHL* null) versus RCC4 cells (+*vHL*) In 3 different platforms the Agilent, Illumina and Solexa array systems. The fold change shows the effect of the absence of *vHL*in normoxia. MiRNAs 210, 155 and 193b are upregulated across all three platforms. MiRNAs 424, 100 and 503 are consistently downregulated across three platforms.

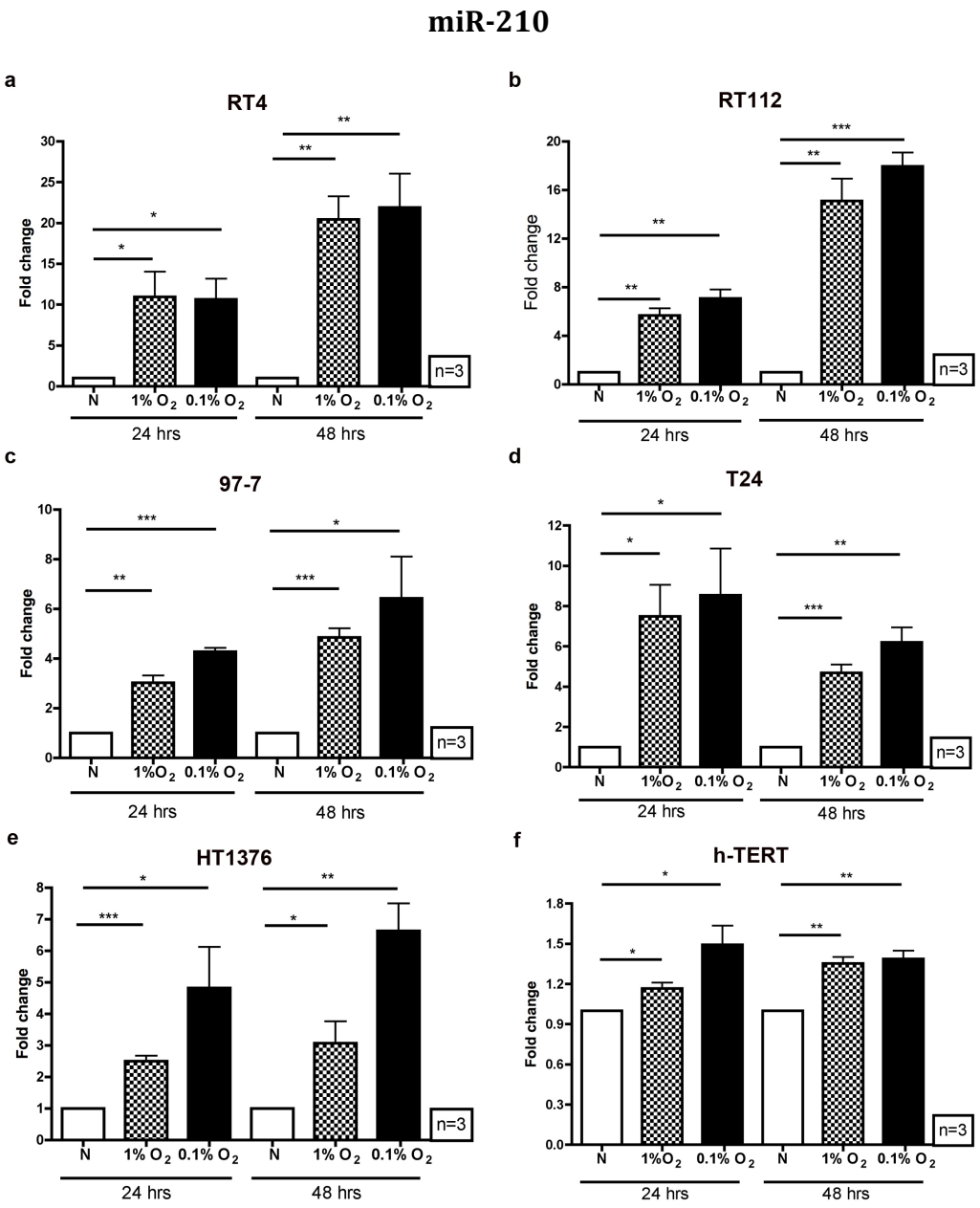
We decided to focus on the three most up and down regulated miRNAs across all three platforms - miRNAs 210, 155, 193b, 503, 424 and 100 were chosen. We screened 5 bladder cancer cell lines RT4, RT112, 97-7, T24 and HT1376 and the immortalized bladder urothelium line h-TERT. We quantified the expression of the chosen miRNAs relative to RNU44 in normoxia, 1% O_2 and 0.1% O_2 at 24 and 48 hours.

3.2.3. MicroRNA-210

MiR-210 was upregulated in hypoxic conditions across all 6 cell lines (Figure 3.2). Although there was significant upregulation in the normal urothelial cell line h-TERT, the fold change difference was much lower than seen in other cell lines. To confirm the HIF dependent induction of miR-210 we treated cells with DMOG in normoxia (Figure 3.3). The hypoxic upregulation of miR-210 in cells treated with DMOG was matched in all cell lines except h-TERT.

3.2.4. MicroRNA-155

Although miR-155 was elevated in *vHL* null RCC4 cells, it was downregulated in RT4 and RT112 cells in response to hypoxia (Figure 3.4). However, this was not consistent at both 24 and 48 hours nor at different extremes of hypoxia and indeed, treatment of RT4 or RT112 cells with DMOG had no effect on miR-155 expression (Figure 3.5). As the fold changes seen are very small (10-20%), they are likely to be within the error of the experiment and, therefore, not significant.



	RT4	RT112	97-7	T24	HT1376	h-TERT
Normoxia	31.0	30.1	28.5	30.3	28.5	26.5
0.1% O_2	27.8	25.1	25.5	27.2	25.8	26.0
Normoxia	23.5	24.3	25.5	25.5	25.8	24.2
0.1% O_2	23.3	24.0	24.8	25.6	25.5	24.2

Figure 3-2 Regulation of miR-210 by hypoxia in bladder cell lines

(a) RT4, (b) RT112, (c) 97-7, (d) T24, (e) HT1376 and (f) h-TERT cells were cultured in normoxia, 1% O_2 and 0.1% O_2 for 24 and 48 hours. Data are presented as mean ± standard error. Statistical significance: * $p<0.05$, ** $p<0.01$, *** $p<0.001$. Median CT values for miR-210 (black) and RNU44 (red) in normoxia and 0.1% O_2 after 24 hours incubation are shown in the table at the bottom of the figure. These CT values for RNU44 are also relevant in Figures 3.4, 3.6, 3.8, 3.10 and 3.12.

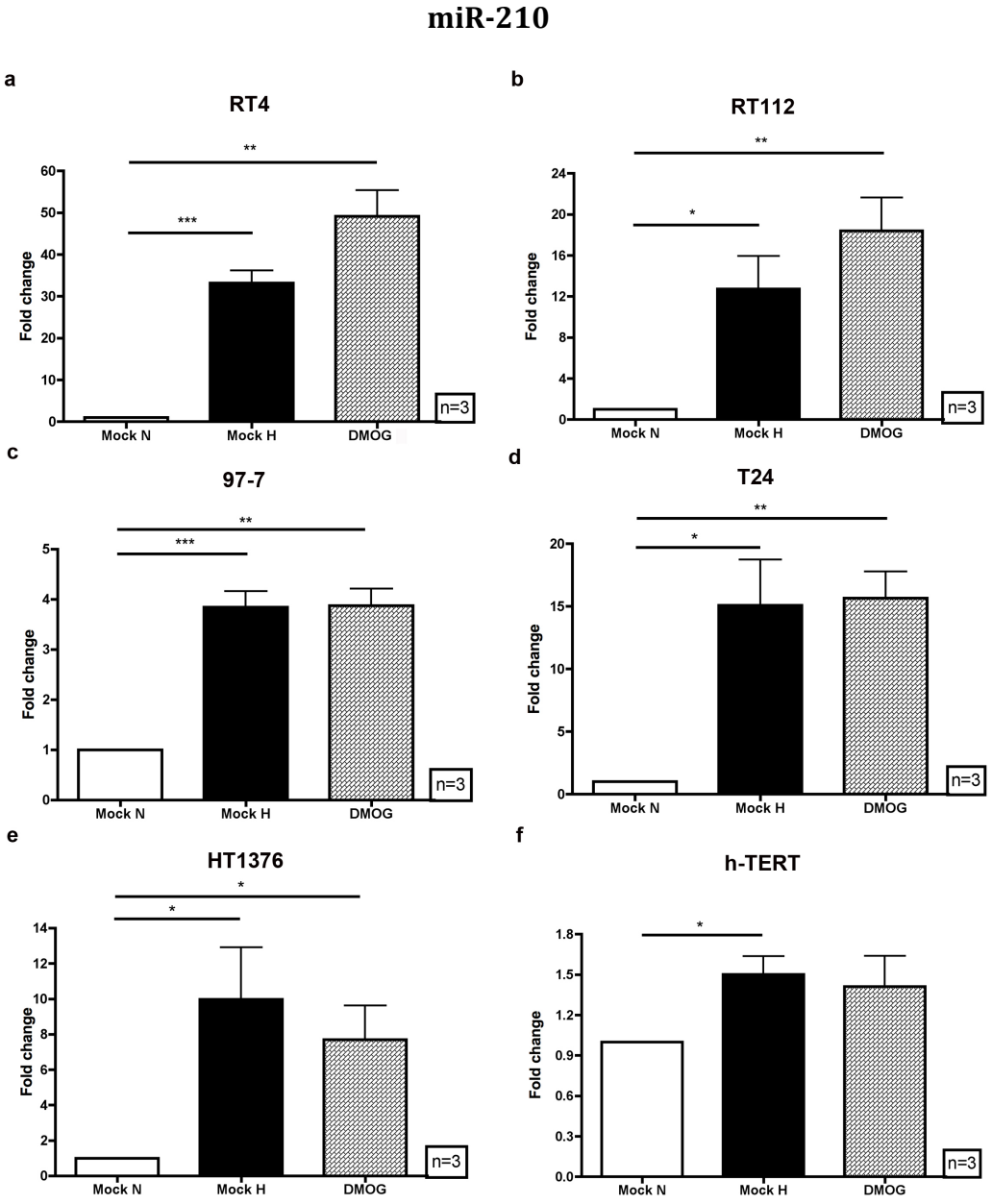
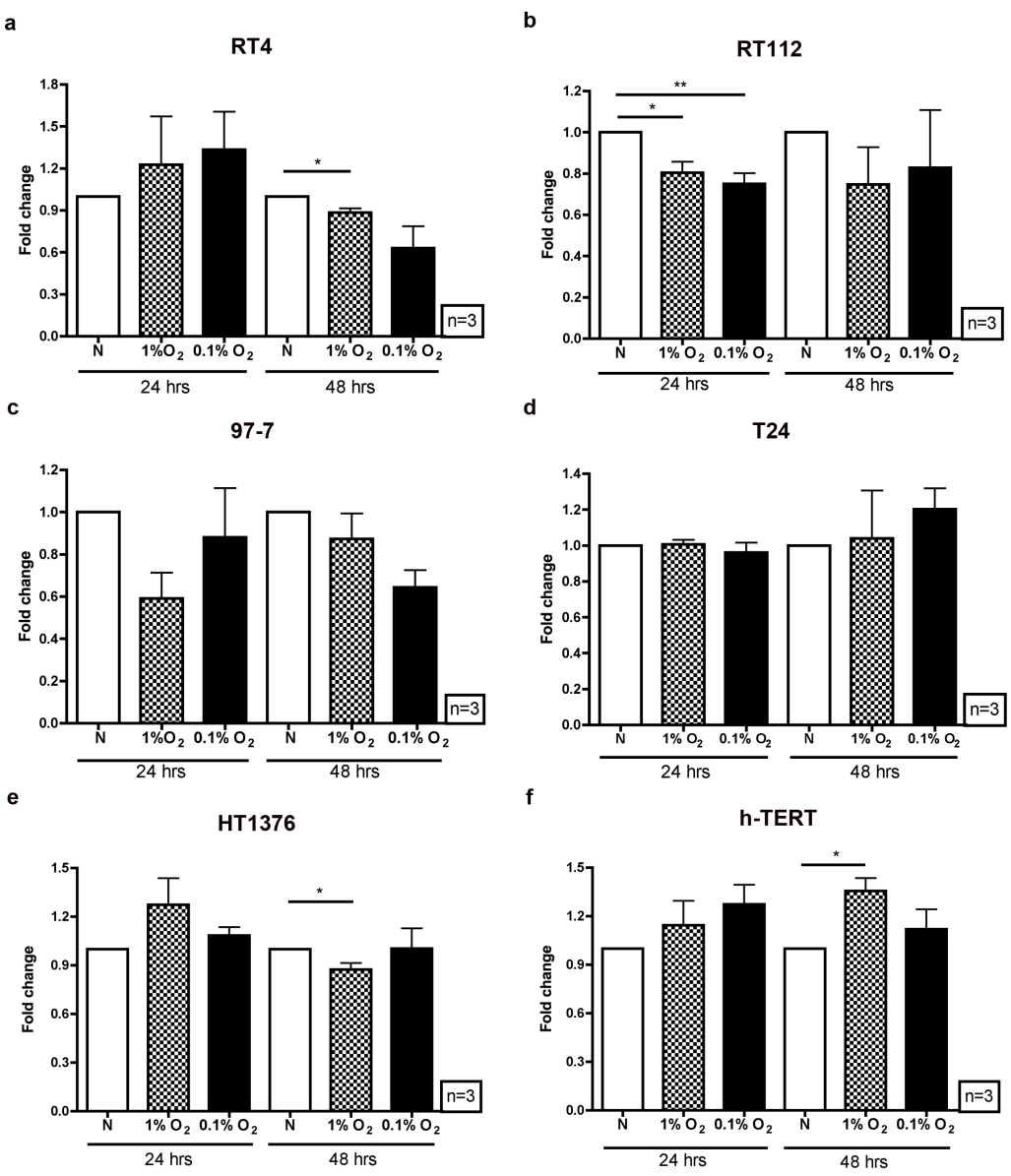


Figure 3-3 miR-210 expression in cells treated with DMOG

(a) RT4, (b) RT112, (c) 97-7, (d) T24, (e) HT1376 cells and (f) h-TERT cells were cultured in normoxia, 0.1% O_2, and in normoxia with 1mM DMOG for 24 hours. Data are presented as mean ± standard error. Statistical significance: * $p<0.05$, ** $p<0.01$, *** $p<0.001$.



	RT4	RT112	97-7	T24	HT1376	h-TERT
Normoxia	35.3	30.6	35.5	25.1	36.5	32.4
0.1% O_2	37.7	30.9	35.7	25.1	37.7	32.8

Figure 3-4 Regulation of miR-155 by hypoxia in bladder cell lines

(a) RT4, (b) RT112, (c) 97-7, (d) T24, (e) HT1376 and (f) h-TERT cells were cultured in normoxia, 1% O_2 and 0.1% O_2 for 24 and 48 hours. Data are presented as mean ± standard error. Statistical significance: * $p<0.05$, ** $p<0.01$, *** $p<0.001$. Median CT values for normoxia and 0.1% O_2 after 24 hours are shown in the table at the bottom of the figure.

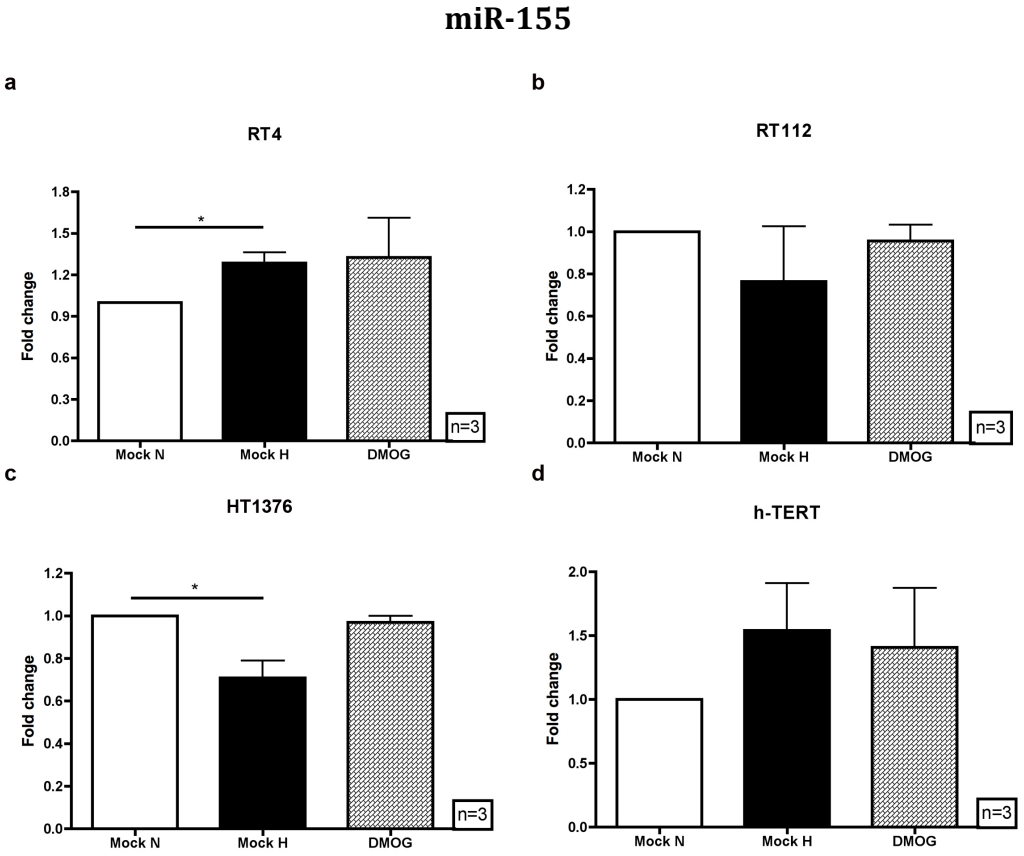


Figure 3-5 miR-155 expression in cells treated with DMOG

(a) RT4 cells, (b) RT112, (c) HT1376 and (d) h-TERT cells were cultured in normoxia, 0.1% O_2, and in normoxia with 1mM DMOG for 24 hours. Data are presented as mean ± standard error. Statistical significance: * $p<0.05$, ** $p<0.01$, *** $p<0.001$.

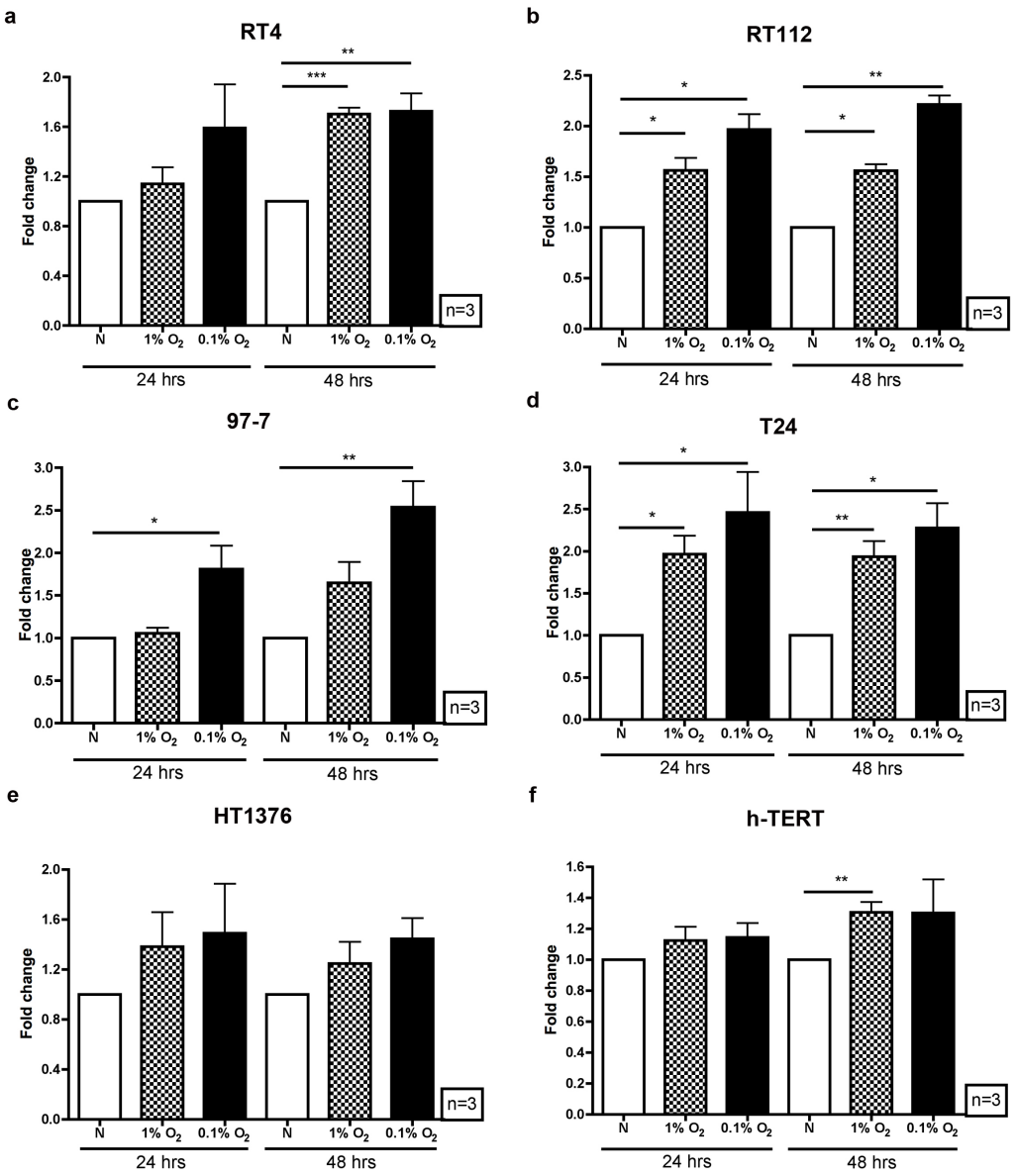
3.2.5. microRNA-193b

MicroRNA 193b was upregulated in *vHL* null RCC4 cells and in agreement with this was increased by hypoxia in RT4, RT112, 97-7 and T24 cell lines (Figure 3.6). Upregulation was more consistent after 48 hours when the average fold change was between 2 and 3 in 0.1% O_2. The effect of hypoxia was less at 1% O_2 suggesting the upregulation of miR-193b expression occurs later and requires lower levels of oxygen. Treatment of cells with DMOG also increased miR-193b expression in RT112, 97-7 and T24 cells (Figure 3.7). Modest upregulation of miR-193b was seen in h-TERT cells at 48 hours (Figure 3.6) but this was not reproduced with DMOG treatment (Figure 3.7).

3.2.6. microRNA-503

MicroRNA-503 expression was decreased in *vHL* null RCC4 cells. The expression of this miRNA could not be detected in RT4, RT112, 97-7 and HT1376 cells. Although modest downregulation of miR-503 was detected in T24 cells, more pronounced downregulation was evident in h-TERT (Figure 3.8).

Downregulation was also seen in these cell lines when treated with DMOG in normoxia (Figure 3.9), suggesting that it was mediated by HIF.



	RT4	RT112	97-7	T24	HT1376	h-TERT
Normoxia	25.3	23.5	24.2	26.2	23.0	25.2
0.1% O_2	25.0	22.7	23.7	24.9	22.5	24.8

Figure 3-6 Regulation of miR-193b by hypoxia in bladder cell lines

(a) RT4, (b) RT112, (c) 97-7, (d) T24, (e) HT1376 and (f) h-TERT cells were cultured in normoxia, 1% O_2 and 0.1% O_2 for 24 and 48 hours. Data are presented as mean ± standard error. Statistical significance: * $p<0.05$, ** $p<0.01$, *** $p<0.001$. Median CT values for normoxia and 0.1% O_2 after 24 hours are shown in the table at the bottom of the figure.

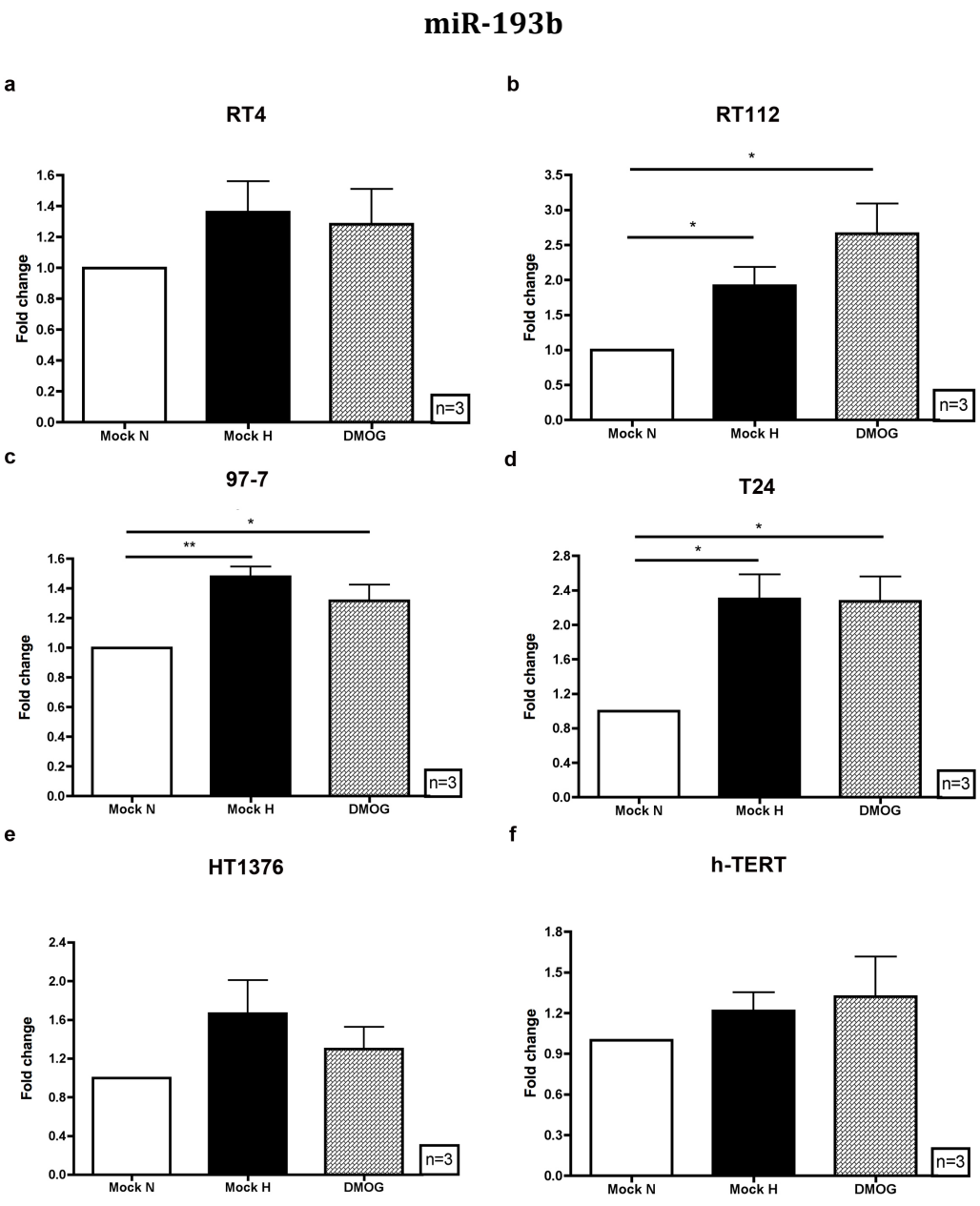
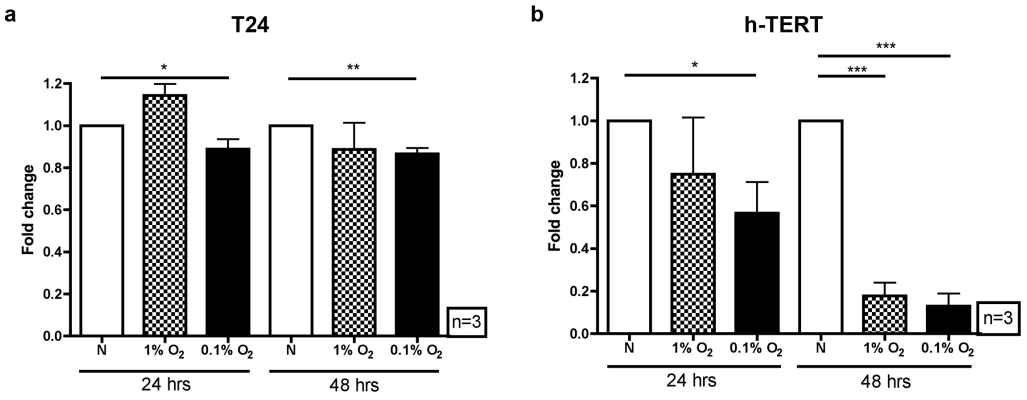


Figure 3-7 miR-193b expression in cells treated with DMOG

(a) RT4, (b) RT112, (c) 97-7, (d) T24, (e) HT1376 and (f) h-TERT cells. Cells were cultured in normoxia, 0.1% O_2, and in normoxia with 1mM DMOG for 24 hours. Data are presented as mean ± standard error. Statistical significance: * $p<0.05$, ** $p<0.01$, *** $p<0.001$.

miR-503



	T24	h-TERT
Normoxia	35.3	36.8
0.1% O_2	35.5	37.4

Figure 3-8 Regulation of miR-503 by hypoxia in bladder cell lines

(a) T24 and (b) h-TERT cells were cultured in normoxia, 1% O_2 and 0.1% O_2 for 24 and 48 hours. Data are presented as mean ± standard error. Statistical significance: * $p<0.05$, ** $p<0.01$, *** $p<0.001$. Median CT values for normoxia and 0.1% O_2 after 24 hours are shown in the table at the bottom of the figure. Data for RT4, RT112, 97-7 and HT1376 cells is not shown due the low expression of miR-503 in these cell lines.

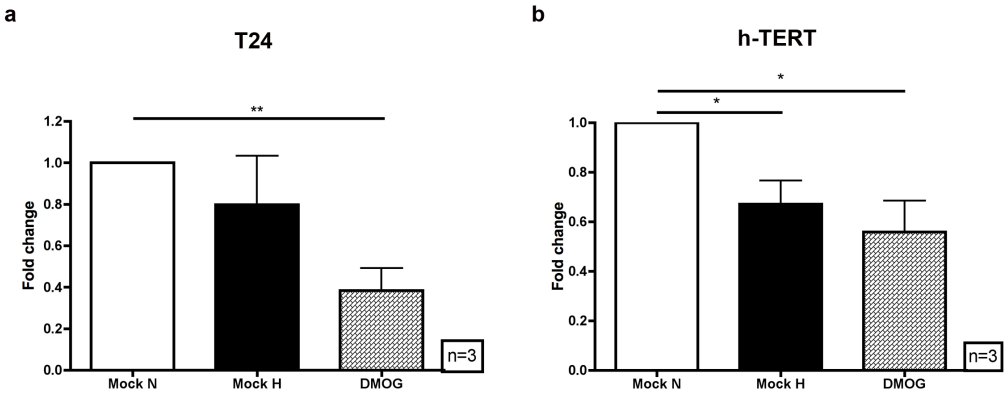


Figure 3-9 miR-503 expression in cells treated with DMOG

(a) T24 and (b) h-TERT cells were cultured in normoxia, 0.1% O_2 and in normoxia with 1mM DMOG for 24 hours. Data are presented as mean ± standard error. Statistical significance: * $p<0.05$, ** $p<0.01$, *** $p<0.001$.

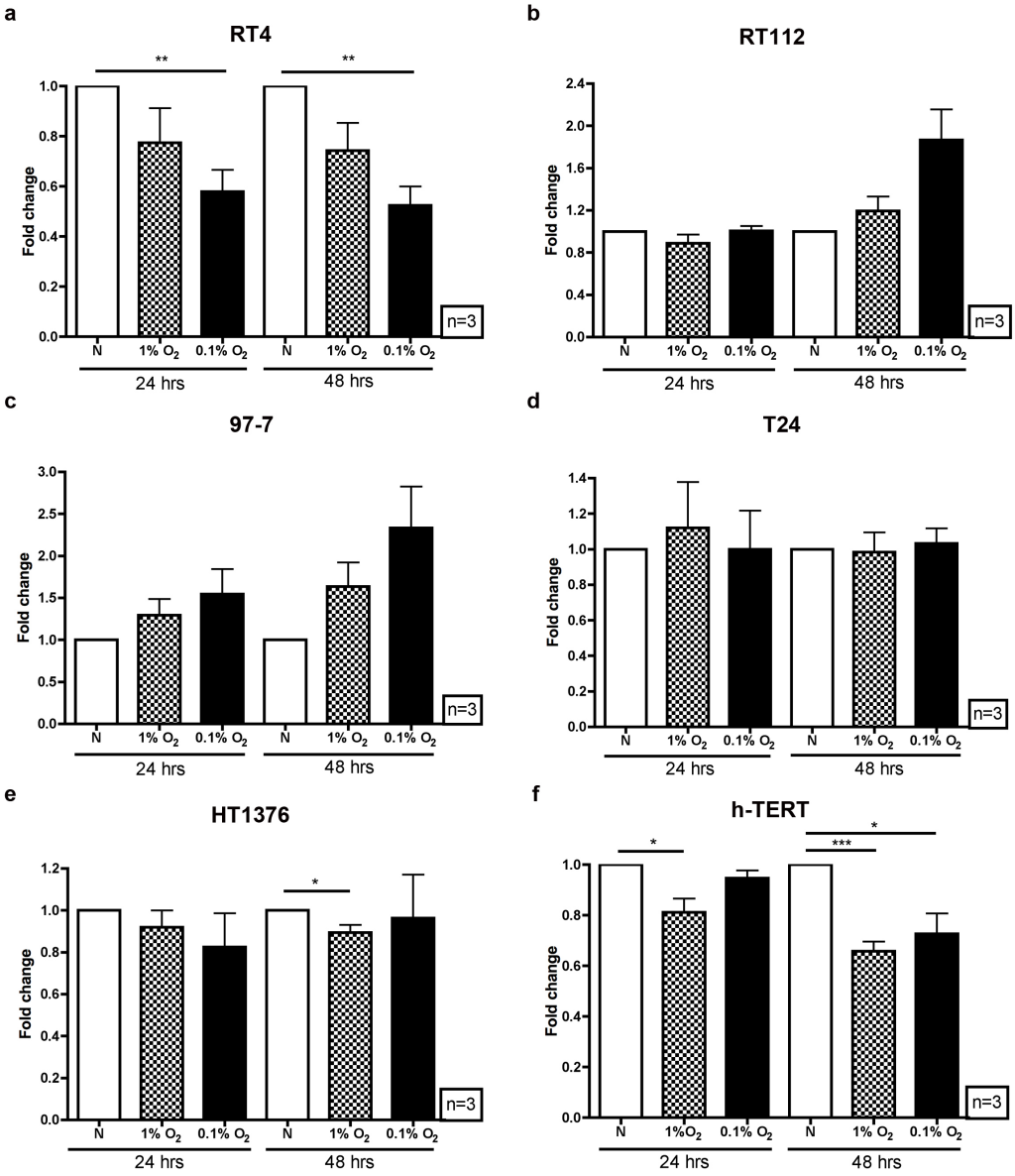
3.2.7. microRNA-100

MiR-100 was downregulated as a result of *vHL* mutation in RCC4 cells. In bladder cancer cell lines we found significant downregulation in RT4 and h-TERT and modest downregulation in HT1376 cells (Fig 3.10). In RT112 and 97-7 cells there is a trend suggesting increased miR-100 expression at 48hrs in 0.1% O_2 although this is not significant. In RT4 cells there was an approximately 2-fold downregulation and this effect was seen at both 24 and 48 hours and also in varying levels of hypoxia. Downregulation of miR-100 in cells treated with DMOG was not seen suggesting the hypoxic downregulation may occur due to a HIF independent mechanism (Figure 3.11).

3.2.8. microRNA-424

MiR-424 was downregulated in vHL null RCC4 cells. In contrast, significant induction was observed in RT112, 97-7 and T24 cells (Figure 3.12). miR-424 was downregulated in HT1376 and h-TERT cell lines but only at 48 hours and 1% O_2. DMOG treatment led to modestly increased expression of miR-424 in 97-7 and T24 cells (Figure 3.13).

miR-100



	RT4	RT112	97-7	T24	HT1376	h-TERT
Normoxia	32.4	30.9	29.6	23.6	26.7	24.3
0.1% O_2	33.1	30.9	28.1	23.6	27.1	25.1

Figure 3-10 Regulation of miR-100 by hypoxia in bladder cell lines

(a) RT4, (b) RT112, (c) 97-7, (d) T24, (e) HT1376 and (f) h-TERT cells were cultured in normoxia, 1% O_2 and 0.1% O_2 for 24 and 48 hours. Data are presented as mean ± standard error. Statistical significance: * $p<0.05$, ** $p<0.01$, *** $p<0.001$. Median CT values for normoxia and 0.1% O_2 after 24 hours are shown in the table at the bottom of the figure.

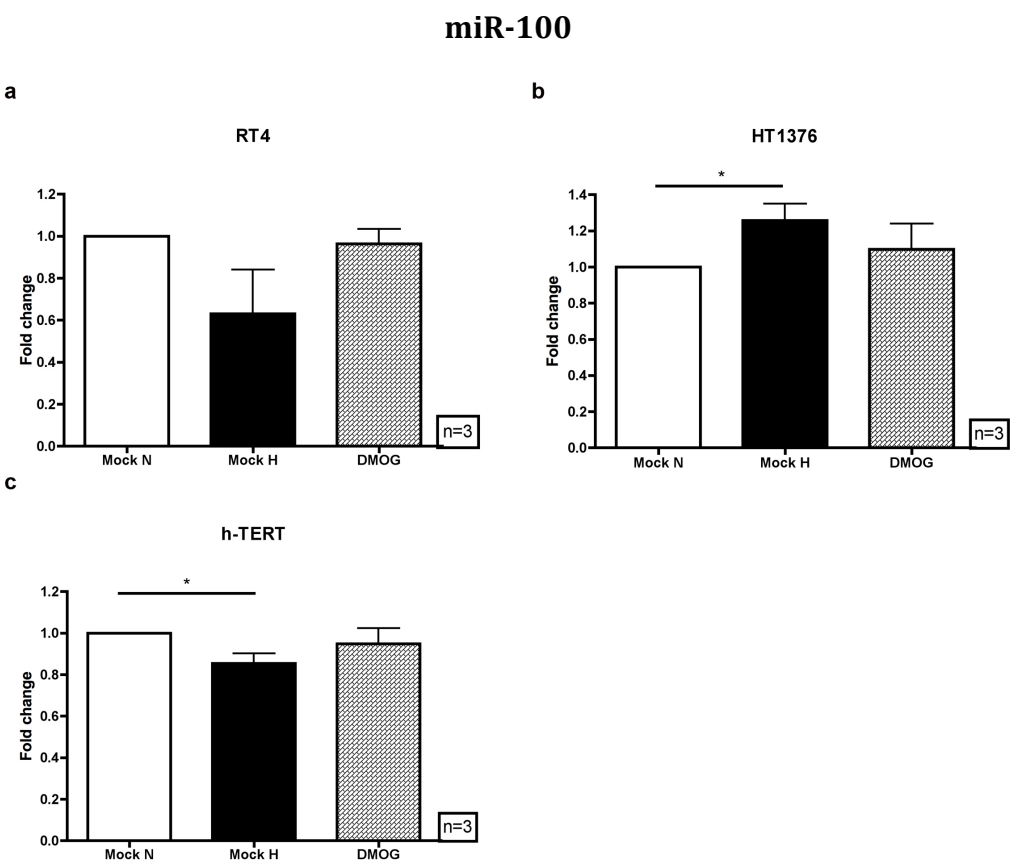
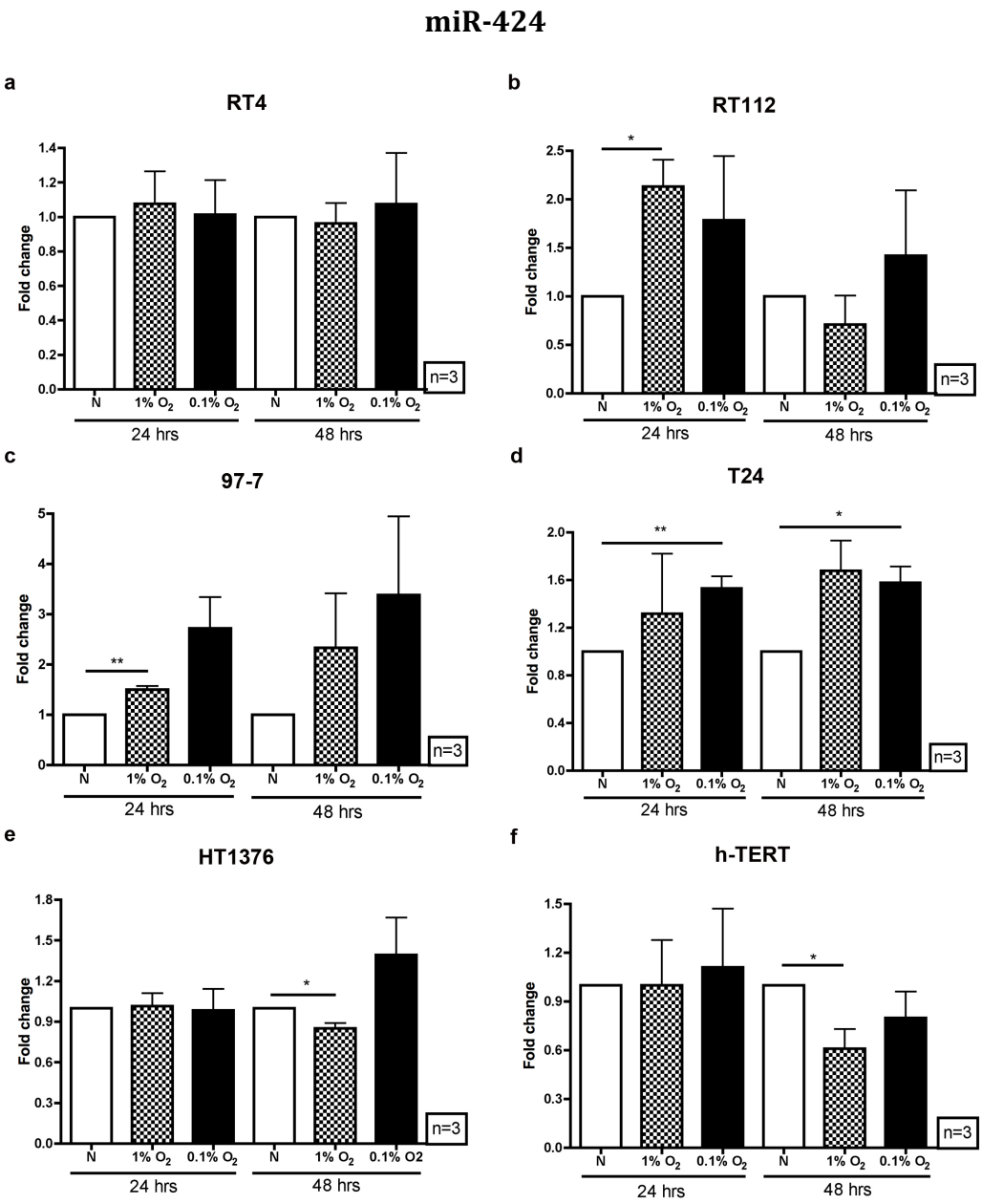


Figure 3-11 miR-100 expression in cells treated with DMOG

(a) RT4, (b) RT112, (c) 97-7, (d) T24, (e) HT1376 and (f) h-TERT cells were cultured in normoxia, 0.1% O_2, and in normoxia with 1mM DMOG for 24 hours. Data are presented as mean ± standard error. Statistical significance: * $p<0.05$, ** $p<0.01$, *** $p<0.001$.



	RT4	RT112	97-7	T24	HT1376	h-TERT
Normoxia	32.5	35.3	29.6	34.3	31.6	30.2
0.1% O_2	32.3	34.4	28.1	33.8	31.5	29.9

Figure 3-12 Regulation of miR-424 by hypoxia in bladder cell lines

(a) RT4, (b) RT112, (c) 97-7, (d) T24, (e) HT1376 and (f) h-TERT cells were cultured in normoxia, 1% O_2 and 0.1% O_2 for 24 and 48 hours. Data are presented as mean ± standard error. Statistical significance: * $p<0.05$, ** $p<0.01$, *** $p<0.001$. Median CT values for normoxia and 0.1% O_2 after 24 hours are shown in the table at the bottom of the figure.

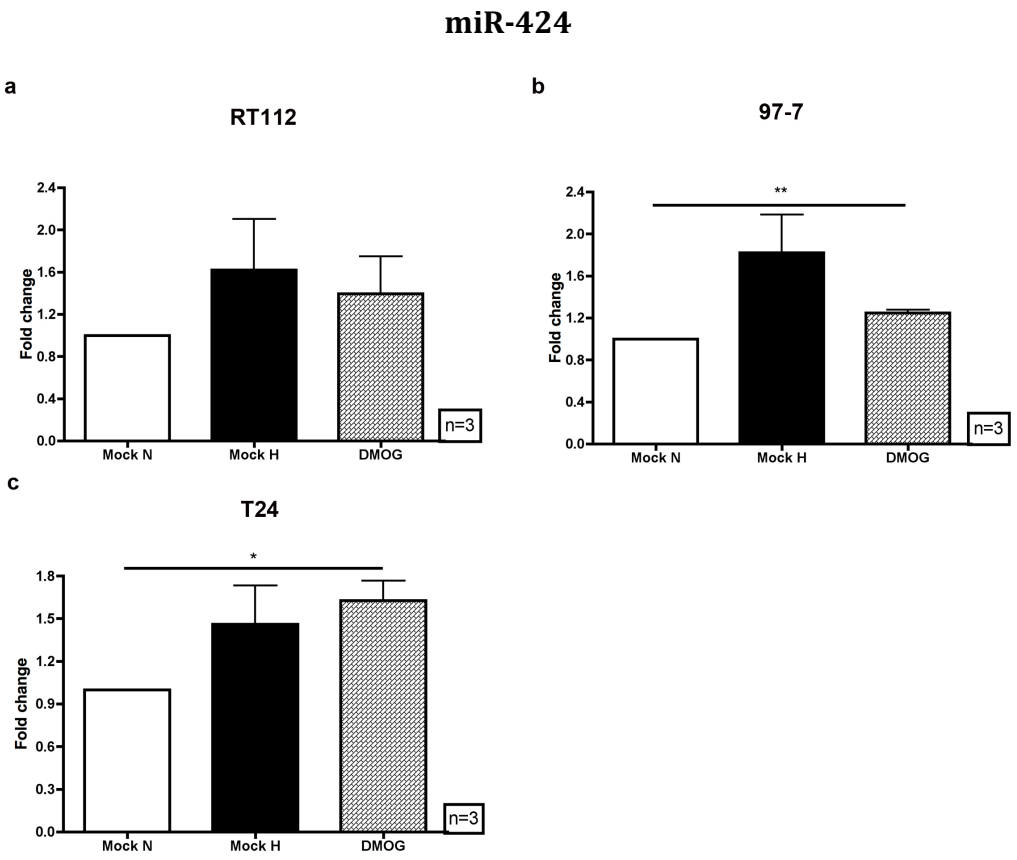


Figure 3-13 miR-424 expression in cells treated with DMOG

(a) RT112, (b) 97-7 and (c) T24 cells were cultured in normoxia, 0.1% O_2, and in normoxia with 1mM DMOG for 24 hours. Data are presented as mean ± standard error. Statistical significance: * $p<0.05$, ** $p<0.01$, *** $p<0.001$.

Summary

We examined the hypoxic regulation of 6 miRNAs found to be regulated by *vHL* mutation in RCC4 renal cancer cells. The findings are summarized in table 3.2.

The hypoxic upregulation of miR-210 seen in all bladder cell lines agrees with published data that this miRNA is hypoxia regulated and it is likely miR-210 is involved in a generic hypoxic response in both physiological and pathological processes. miR-155 was commonly downregulated suggesting the hypoxic upregulation in RCC4 cells is cell line or perhaps tumour type dependent.

miR-193b was upregulated by hypoxia in 5 out of 6 cell lines and in HT1376 upregulation was seen but not significant.

None of those microRNAs found to be downregulated in the absence of *vHL* in RCC4 cells were consistently downregulated in bladder cell lines suggesting this effect is tumour type specific. It has been suggested that downregulation of miRNAs in hypoxia may occur via HIF independent pathways, this is more likely to increase the intertumour variation as key genes vary between tumours [195].

Cell line	Duration of incubation	Oxygen	miR-210	miR-155	miR-193b	miR-503	miR-100	miR-424
RT4	24hours	1% O_2	0.033	ns	ns	-	ns	ns
		0.1% O_2	0.021	ns	ns	-	0.008	ns
	48hours	1% O_2	0.001	0.019	<0.001	-	ns	ns
		0.1% O_2	<0.001	ns	0.007	-	0.003	ns
RT112	24hours	1% O_2	0.001	0.019	0.044	ns	ns	0.015
		0.1% O_2	0.001	0.008	0.024	ns	ns	ns
	48hours	1% O_2	0.002	ns	0.012	ns	ns	ns
		0.1% O_2	<0.001	ns	0.005	ns	ns	ns
97-7	24hours	1% O_2	0.002	0.028	ns	-	ns	0.015
		0.1% O_2	<0.001	ns	0.039	-	ns	ns
	48hours	1% O_2	<0.001	ns	ns	-	ns	ns
		0.1% O_2	0.032	0.013	0.007	-	ns	ns
T24	24hours	1% O_2	0.014	ns	0.012	ns	ns	ns
		0.1% O_2	0.031	ns	0.038	0.029	ns	0.007
	48hours	1% O_2	0.001	ns	0.007	ns	ns	ns
		0.1% O_2	0.002	ns	0.019	0.005	ns	0.012
HT1376	24hours	1% O_2	0.001	ns	ns	-	ns	ns
		0.1% O_2	0.057	ns	ns	-	ns	ns
	48hours	1% O_2	0.040	0.032	ns	-	0.042	0.016
		0.1% O_2	0.003	ns	ns	-	ns	ns
h-TERT	24hours	1% O_2	0.016	ns	ns	ns	0.025	ns
		0.1% O_2	0.025	ns	ns	0.040	ns	ns
	48hours	1% O_2	0.002	0.011	0.009	<0.001	0.001	0.031
		0.1% O_2	0.003	ns	ns	<0.001	0.025	ns

Table 3-2 Summary of miRNA expression in response to hypoxia in bladder cancer

Relative expression of miRNAs 210, 193b, 155, 503, 100 and 424 in 6 bladder cell lines after 24 and 48 hours incubation at 1% or 0.1% O_2 when compared to that of normoxic samples. Data are presented as p values in miRNAs upregulated (red) and downregulated (green).

3.2.9. Low density microarray analysis of RT4 and T24 cell lines in hypoxia

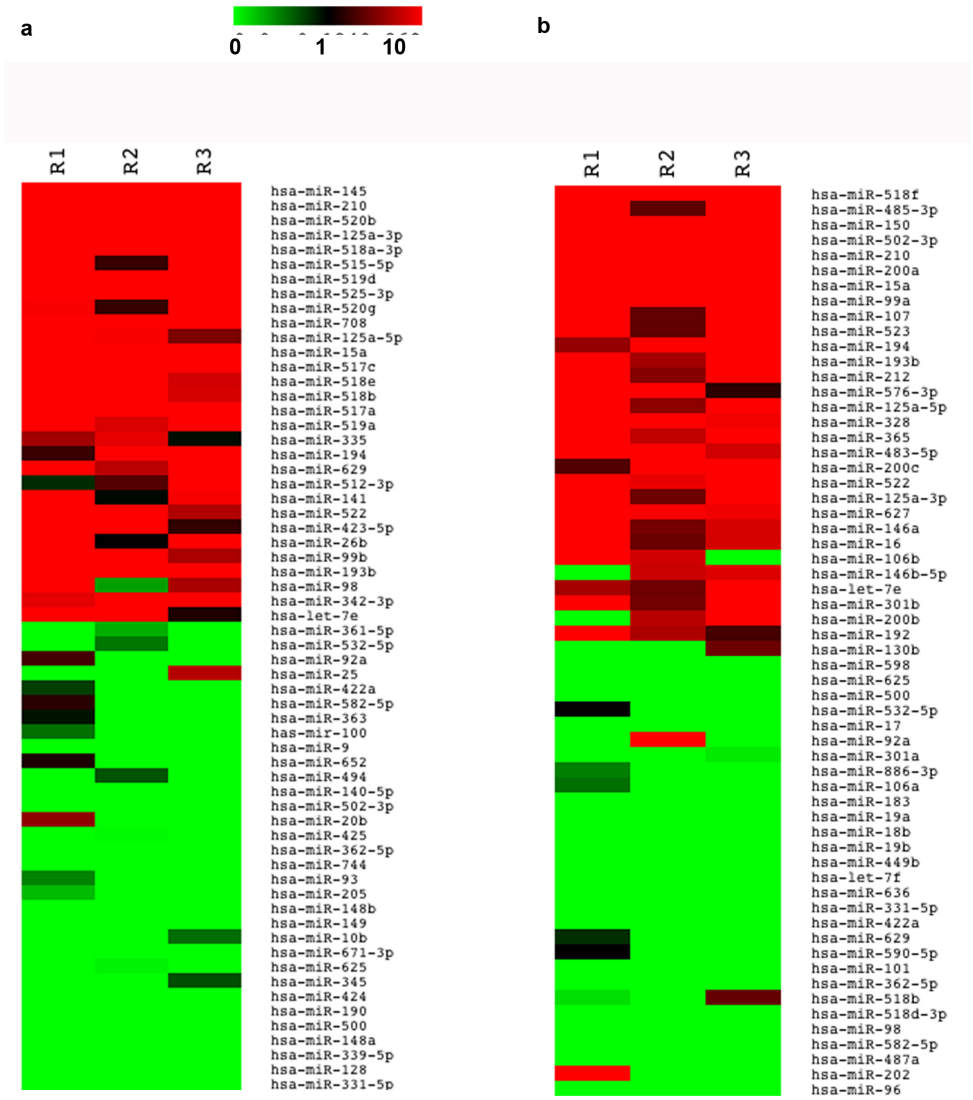
Access to the Applied Biosystems Low Density TaqMan array platform enabled us to screen for a greater number of microRNAs regulated by hypoxia. To identify some whose expression may be unique to bladder cancer, we analysed

the expression of 384 miRNAs in the TaqMan miRNA pool A in the non-invasive cell line RT4 and the invasive cell line T24. For each cell line, the study was performed in triplicate; the expression values are normalized to RNU44 and presented as fold change relative to normoxia. MiRNAs with CT values >40 in both normoxia and hypoxia were excluded. We reasoned that the 30 most up and downregulated miRNAs for each cell line are likely to be true hits and not false positives; these are presented in Figures 3.14a.

The expression data from RT4 cells showed that miR-145 was the most upregulated microRNA in hypoxia followed by miR-210. Of note is that a number of miRNA belonging to the C19MC cluster on chromosome 19 including miR-518a-3p, 515-5p and 525-3p amongst others were found to be upregulated (Figure 3.14a) [196, 197]. Included in the most downregulated miRNAs were miR-331-5p and 128 and in RT4 cells the previously validated miR-100 (Figure 3.14a).

Comparing the 30 most hypoxia upregulated miRNA in RT4 and T24, 7 were upregulated in both (Figure 3.15a). However, a number of the differentially regulated genes are unique to each cell line (Figure 3.14). This may be due to the differences between the molecular pathways involved in these two forms of bladder cancer that these two cell lines represent. Those miRNAs found to be upregulated in T24 include miR-150. In addition, three members of the miR-200 family including miR-200a, 200b and 200c are upregulated in T24 cells in response to hypoxia. The median fold change of the top 10 most upregulated miRNAs in each cell line from the three replicates is show in Figure 3.15b. Only three miRNAs are upregulated more than 10 fold in hypoxia, these are miR-145, miR-210 and miR-518f. To validate the findings of these arrays we analysed the

hypoxic regulation of the ten most upregulated miRNAs from both cell lines using individual miRNA assays. The chosen miRNAs were: miRs 145, 518-3p, 125a-3p, 519d, 708, 525-3p, 517a, 519a, 335, 518f, 150, 200a, 15a, 99a, 107, 194 and 212.

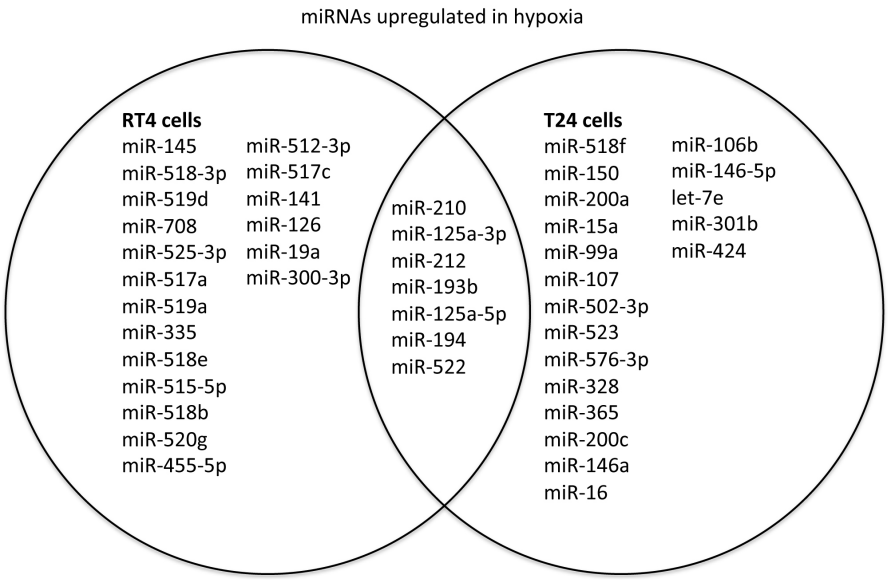


a **b**

Figure 3-14 Profiling of hypoxia regulated miRNAs in RT4 and T24 cells

The expression of miRNAs was examined in (a) RT4 cells and (b) T24 cells after exposure to normoxia or 0.1% hypoxia for 24 hours. Expression was profiled using the Applied Biosystems Pool A Version 3.1 TaqMan Low Density array. The expression data represents the effect of hypoxia on expression of each miRNA in the three independent experiments. The 30 most up and downregulated miRNAs with CT values <40 are shown. The colour scheme range can be seen at the top of this figure.

a



b

	RT4 cells	Fold change (median n=3)		T24 cells	Fold change (median n=3)
1	miR-145	68.7	1	miR-518f	36.3
2	miR-210	15.4	2	miR-150	9.4
3	miR-518-3p	7.9	3	miR-210	5.9
4	miR-125a-3p	5.7	4	miR-200a	5.2
5	miR-519d	5.6	5	miR-15a	5.0
6	miR-708	4.7	6	miR-99a	4.6
7	miR-525-3p	3.5	7	miR-107	4.4
8	miR-517a	2.3	8	miR-194	3.4
9	miR-519a	2.9	9	miR-193b	2.6
10	miR-335	2.4	10	miR-212	2.4

Figure 3-15 MicroRNAs upregulated in hypoxia in RT4 and T24 cells

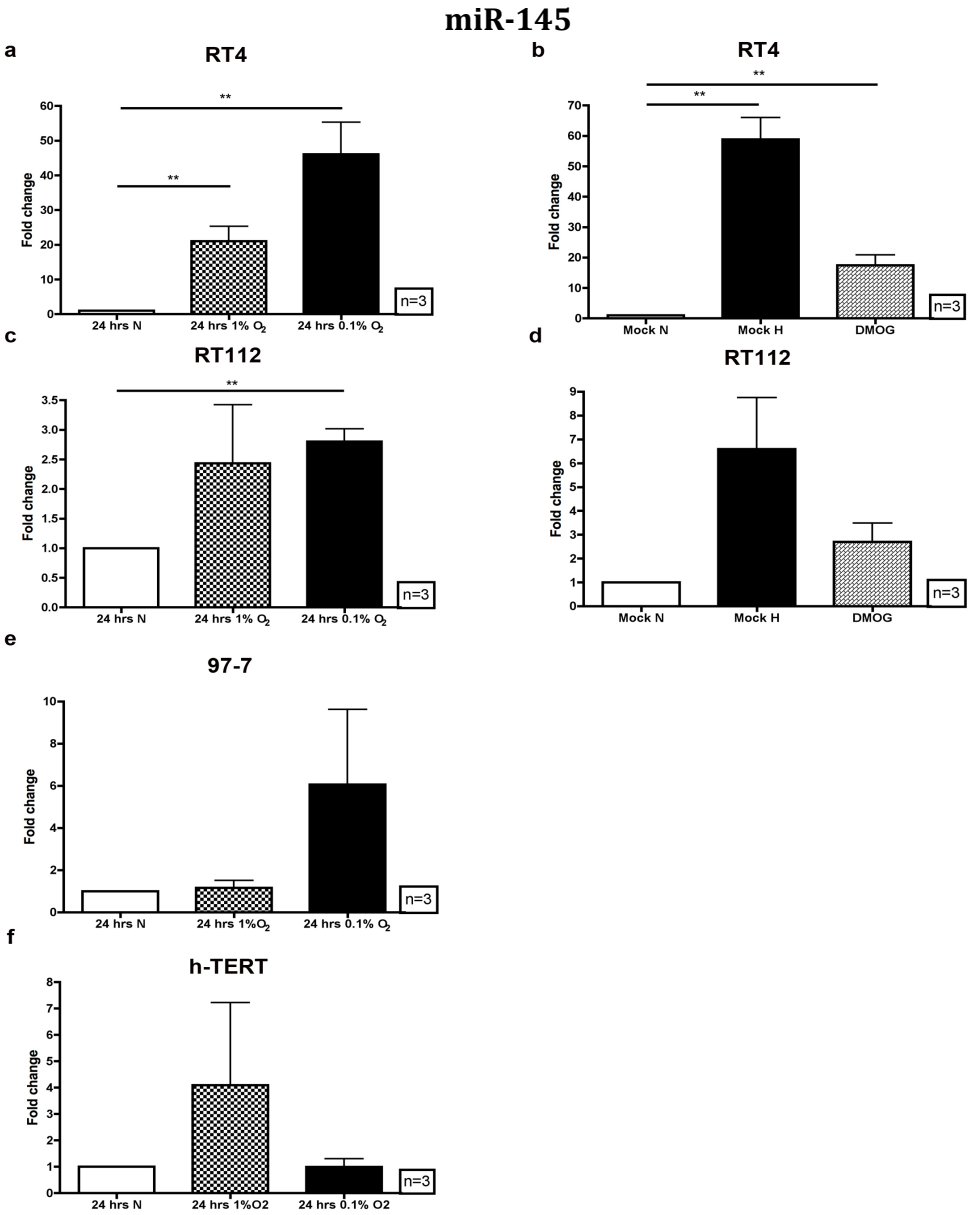
a) This figure combines those miRNAs found to be upregulated by hypoxia in RT4 and T24 cells. This figure combines array data in figures 3.14 with results shown in figures 3.1-3.13. b) The top 10 miRNAs upregulated in hypoxia are shown in b. The median fold change from 3 replicates is also shown.

3.2.10. Validation of RT4 array data

Those miRNAs found to be upregulated in RT4 cells were examined in 3 superficial (RT4, RT112 and 97-7) and 1 normal (h-TERT) cell lines.

MiR-145 was significantly upregulated in RT4 cells with on average 44-fold upregulation (Figure 3.16). There was also upregulation seen in cells treated with DMOG in normoxia suggesting a HIF dependent induction in hypoxia. Hypoxic induction was also seen in RT112 cells, however the fold change was much lower and was not seen in 1%O_2. There was no change in 97-7 cells and h-TERT cells.

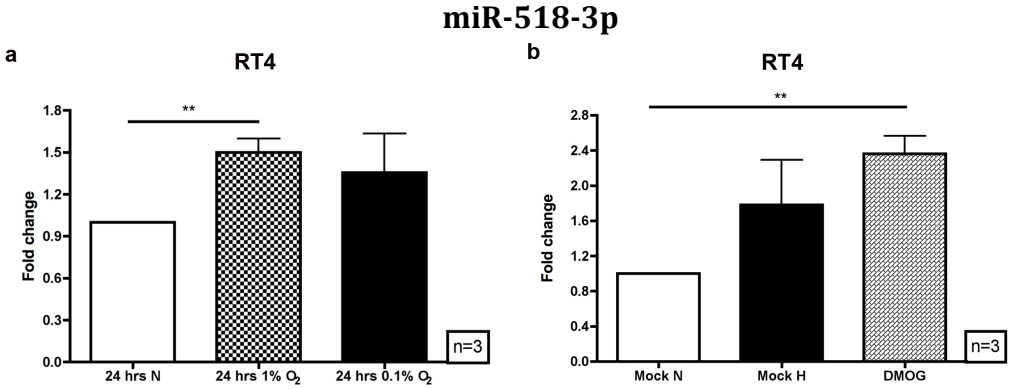
MiRNA-518-3p was modestly upregulated in RT4 cells but in other cell lines the basal levels of expression were too low for analysis (Figure 3.17). DMOG treatment of these cells also led to upregulation suggesting HIF dependent regulation. There was upregulation of miR-125a-3p in RT4 and RT112 cells but this was not reproduced in 97-7 and h-TERT cells (Figure 3.18). Upregulation of this miRNA following treatment with DMOG did not achieve statistical significance. The hypoxic upregulation of miR-519d seen in the array data was not reproduced in the individual experiments in any of the 4 cell lines tested (Figure 3.19). MiR-708 was upregulated in both RT4 and RT112 cells but interestingly downregulation was seen in h-TERT cells (Figure 3.20). In general the hypoxic regulation of miRNAs in RT4 and RT112 cells were similar and were consistent with those seen in the array data although the fold changes seen in the array data were higher than those seen in the individual assays.



	RT4	RT112	97-7	h-TERT
Normoxia	38.7	35.1	44.3	39.5
0.1% O_2	32.3	34.0	43.6	40.2
Normoxia	24.8	24.3	26.8	24.2
0.1% O_2	24.4	24.0	26.0	24.2

Figure 3-16 Regulation of miR-145 by hypoxia in bladder cell lines

(a) RT4, (c) RT112, (e) 97-7 and (f) h-TERT cells were incubated in normoxia, 1% O_2 or 0.1% O_2 for 24 hours. (b) RT4 and (d) RT112 cells treated with 1mM DMOG in normoxia. Data are presented as mean ± standard error. Statistical significance: * $p<0.05$, ** $p<0.01$, *** $p<0.001$. Median CT values for miR-145 (black) and RNU44 (red) in normoxia and 0.1% O_2 after 24 hours are shown in the table at the bottom of the figure. The CT values for RNU44 also relevant for Figures 3.17-3.20.

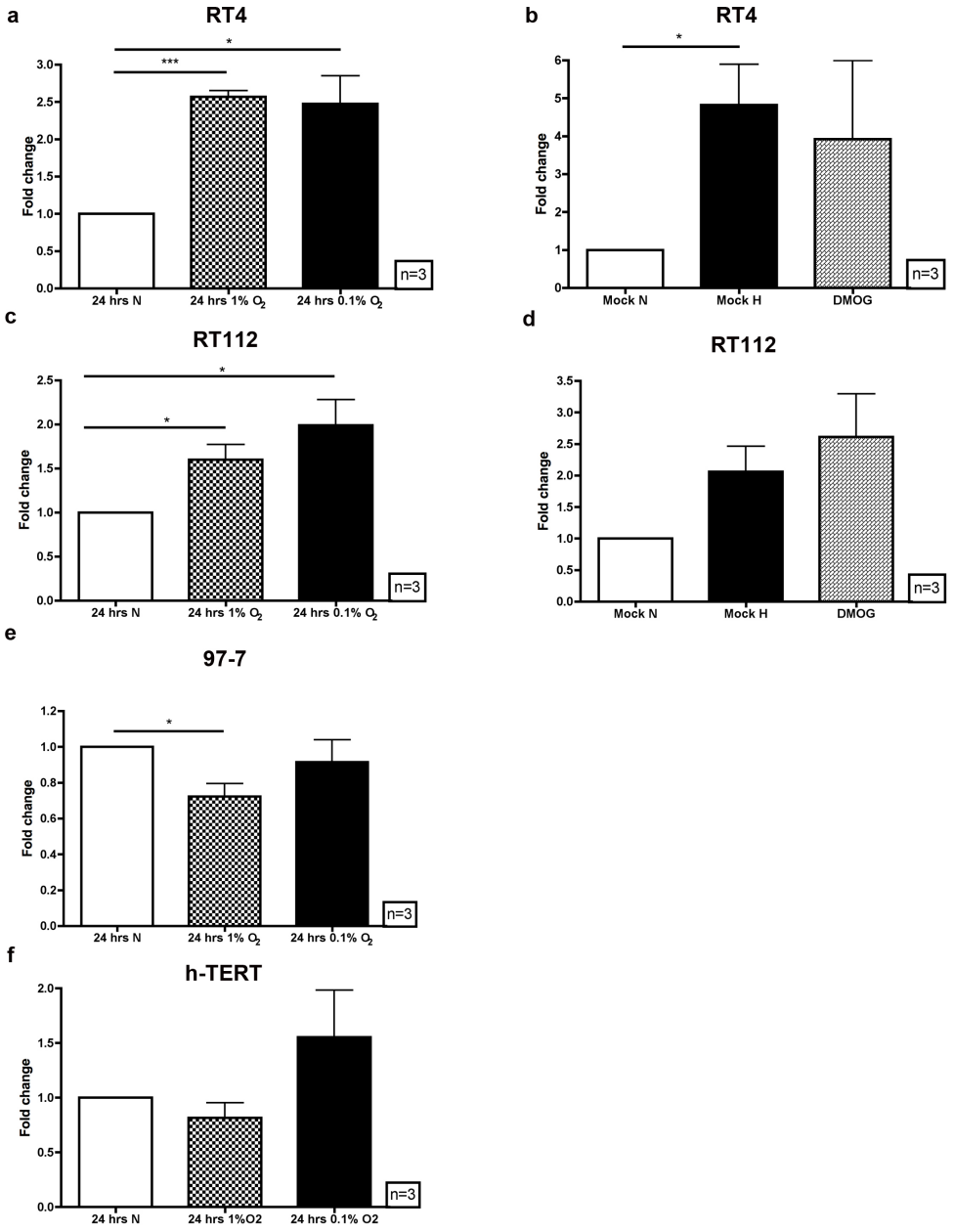


	RT4
Normoxia	34.9
0.1% O_2	34.8

Figure 3-17 Regulation of miR-518-3p by hypoxia in bladder cell lines

(a) RT4 cells were incubated in normoxia, 1%O_2 or 0.1%O_2 for 24 hours. (b) RT4 cells were treated with 1mM DMOG in normoxia in 24 hours. Data are presented as mean ± standard error. Statistical significance: * $p<0.05$, ** $p<0.01$, *** $p<0.001$. Median CT values for normoxia and 0.1% O_2 after 24 hours are shown in the table at the bottom of the figure. Results from RT112, 97-7 and h-TERT cells are not shown due to the low expression of this miRNA in these cell lines.

miR-125a-3p

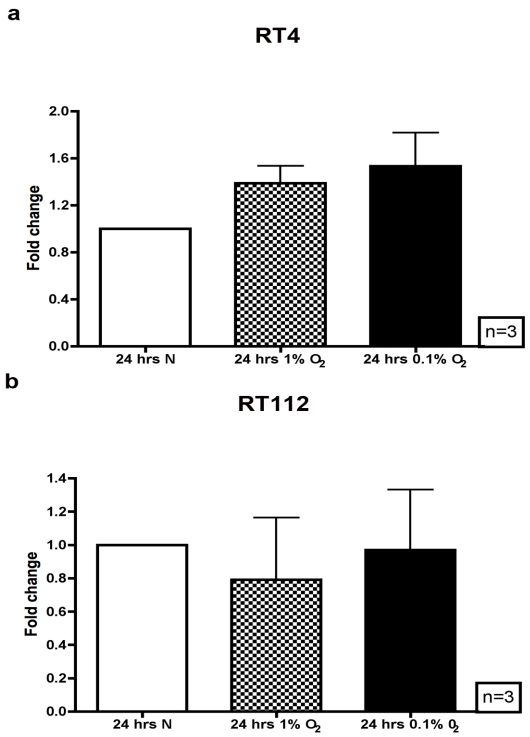


	RT4	RT112	97-7	h-TERT
Normoxia	34.6	36.4	35.7	35.6
0.1% O_2	33.9	35.1	36.1	35.0

Figure 3-18 Regulation of miR-125a-3p by hypoxia in bladder cell lines

(a) RT4, (c) RT112, (e) 97-7 and (f) h-TERT cells were incubated in normoxia, 1% O_2 or 0.1% O_2 for 24 hours. (b) RT4 and (d) RT112 cells were treated with 1mM DMOG in normoxia for 24 hours. Data are presented as mean ± standard error. Statistical significance: * $p<0.05$, ** $p<0.01$, *** $p<0.001$. Median CT values for normoxia and 0.1% O_2 after 24 hours are shown in the table at the bottom of the figure.

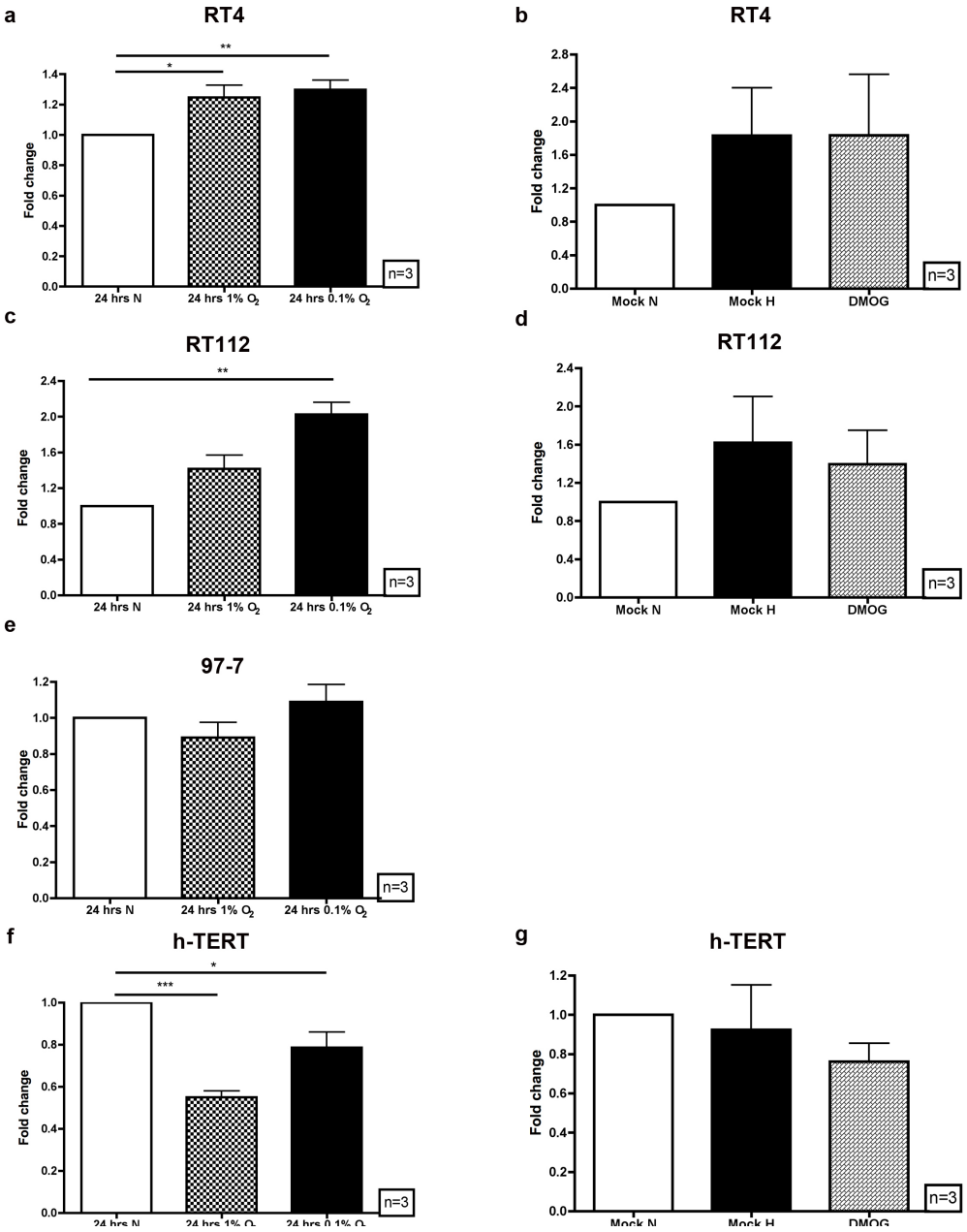
miR-519d



	RT4	RT112
Normoxia	31.3	36.3
0.1% O_2	30.8	36.5

Figure 3-19 Regulation of miR-519d by hypoxia in bladder cell lines

(a) RT4 and (b) RT112 cells were incubated in normoxia, 1% O_2 or 0.1% O_2 for 24 hours. Data are presented as mean ± standard error. Statistical significance: * $p<0.05$, ** $p<0.01$, *** $p<0.001$. Median CT values for normoxia and 0.1% O_2 after 24 hours are shown in the table at the bottom of the figure. Data from 97-7 and h-TERT cells are not shown due to the low expression of these miRNAs in these cell lines.



	RT4	RT112	97-7	h-TERT
Normoxia	29.5	34.8	34.8	26.8
0.1% O_2	28.4	33.7	35.3	27.4

Figure 3-20 Regulation of miR-708 by hypoxia in bladder cell lines

(a) RT4 (c) RT112, (e) 97-7 and (f) h-TERT cells were incubated in normoxia, 1% O_2 or 0.1% O_2 for 24 hours. (b) RT4, (d) RT112 and (g) h-TERT cells were treated with 1mM DMOG in normoxia for 24 hours. Data are presented as mean ± standard error. Statistical significance: * $p<0.05$, ** $p<0.01$, *** $p<0.001$. Median CT values for normoxia and 0.1% O_2 after 24 hours are shown in the table at the bottom of the figure.

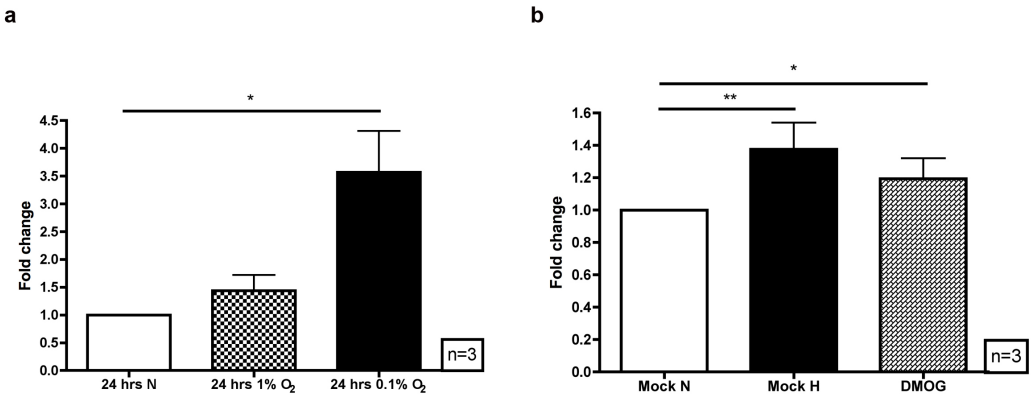
3.2.11 Validation of T24 array data

Those miRNAs found to be upregulated in T24 cells were examined in 2 high grade (T24 and HT1376) and 1 normal urothelial (h-TERT) cell lines. Although miR-518f expression was significantly upregulated in T24 cells (Figure 3.21), the magnitude of upregulation was much lower than the array data. No induction of miR-518f was seen in HT1376 cells and expression levels were too low in normoxia to be recorded.

MiR-150 did not appear to be induced by hypoxia in the individual experiments (Figure 3.22). Hypoxic induction of miR-200a was seen in T24 cells but downregulation was seen in h-TERT cells (Figure 3.23). Expression levels were too low in HT1376 cells for analysis. MiR-15a was upregulated in T24 cells but there were no changes in HT1376 and h-TERT (Figure 3.24). A similar pattern was seen in the expression of miR-99a with upregulation seen in T24 cells but not reproduced in HT1376 cells.

In general the upregulation of miRNAs seen from the array data was reproduced in the individual assays, where this did not occur this could be explained by the low expression levels of the individual miRNA.

miR-518f

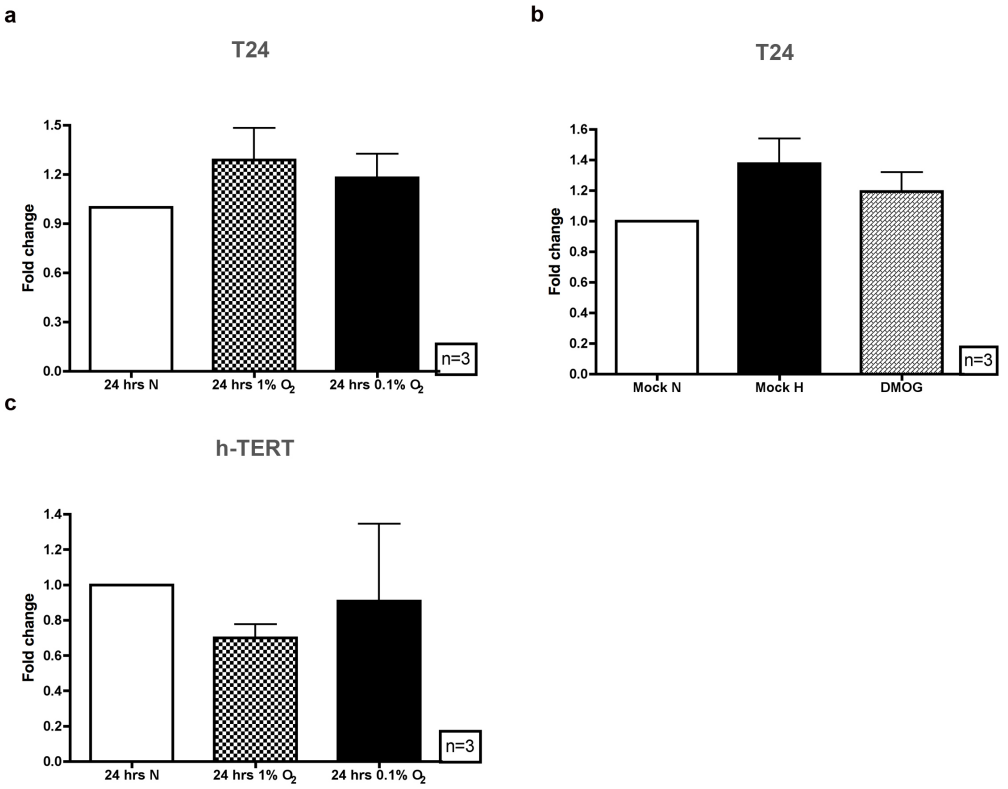


	T24	HT1376	h-TERT
Normoxia	40.9	Not detected	Not detected
0.1% O_2	39.4	Not detected	Not detected
Normoxia	24.0	25.8	24.2
0.1% O_2	24.1	25.5	24.2

Figure 3-21 Hypoxic regulation of miR-518f in bladder cell lines

a) T24 cells were incubated in normoxia, 1% O_2 or 0.1% O_2 for 24 hours. (b) T24 cells were treated with 1mM DMOG in normoxia for 24 hours. Data are presented as mean ± standard error. Statistical significance: * $p<0.05$, ** $p<0.01$, *** $p<0.001$. Median CT values for miR-518f (black) and RNU44 (red) in normoxia and 0.1% O_2 after 24 hours are shown in the table at the bottom of the figure. The CT values for RNU44 are also relevant for Figures 3.22-3.25.

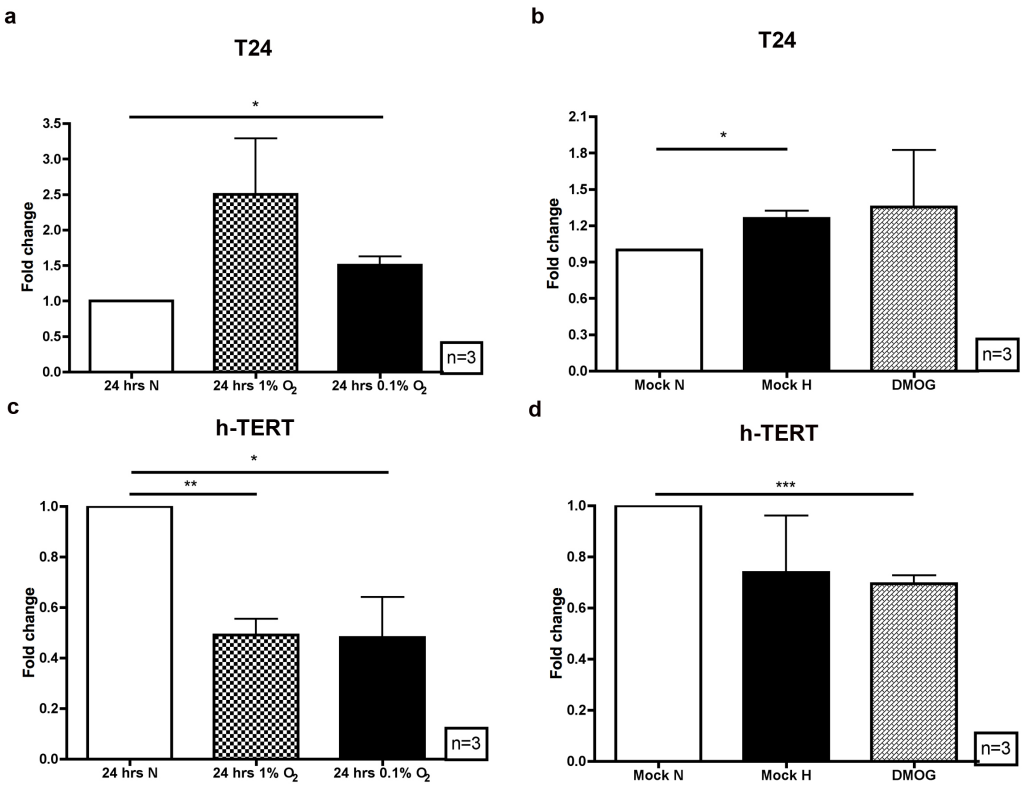
miR-150



	T24	h-TERT
Normoxia	35.6	37.5
0.1% O_2	35.5	37.9

Figure 3-22 Regulation of miR-150 by hypoxia in bladder cell lines.

(a) T24 cells, (c) h-TERT cells, Cells were incubated in normoxia, 1% O_2 or 0.1% O_2 for 24 hours. (b) T24 cells were treated with 1mM DMOG for 24 hours in normoxia. Data are presented as mean ± standard error. Statistical significance: * $p<0.05$, ** $p<0.01$, *** $p<0.001$. Median CT values for normoxia and 0.1% O_2 after 24 hours are shown in the table at the bottom of the figure. Data for HT1376 cells are not shown due to the low levels of expression of this miRNA in this cell line.

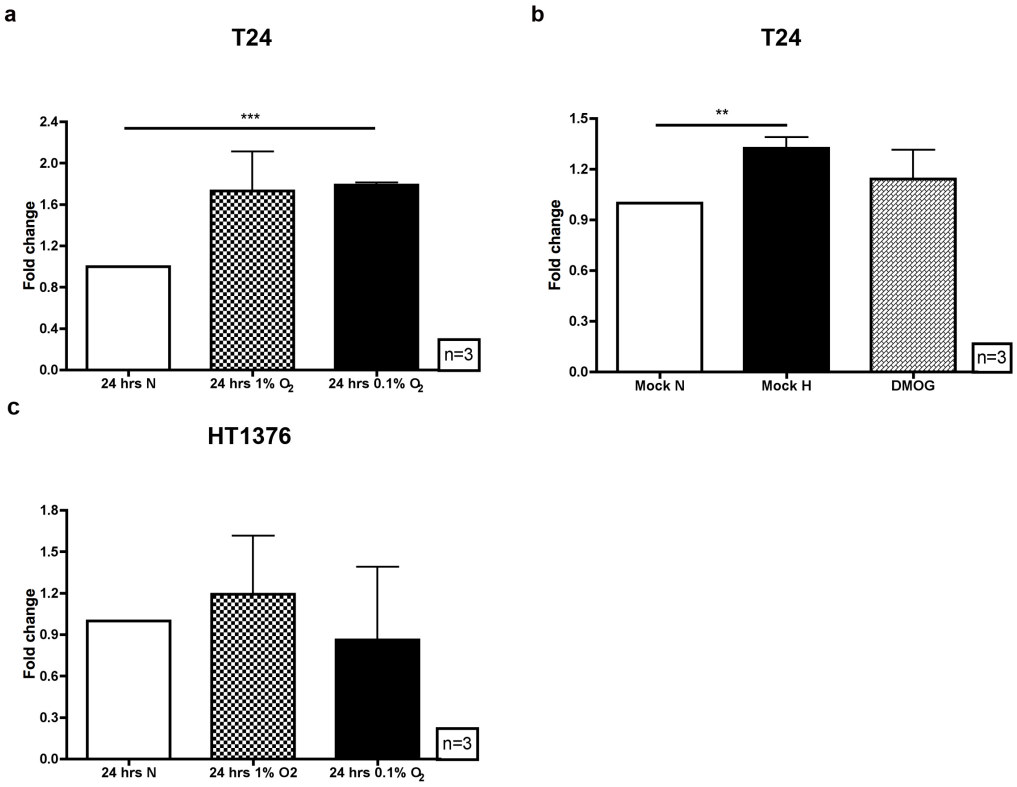


	T24	h-TERT
Normoxia	35.8	29.9
0.1% O_2	35.2	30.2

Figure 3-23 Regulation of miR-200a by hypoxia in bladder cell lines

(a) T24 and (c) h-TERT cells were incubated in normoxia, 1% O_2 or 0.1% O_2 for 24 hours. (b) T24 and (d) h-TERT cells were treated with 1mM DMOG in normoxia for 24 hours. Data are presented as mean ± standard error. Statistical significance: * $p<0.05$, ** $p<0.01$, *** $p<0.001$. Median CT values for normoxia and 0.1% O_2 after 24 hours are shown in the table at the bottom of the figure. Data for HT1376 cells are not shown due to the low levels of expression of this miRNA in this cell line.

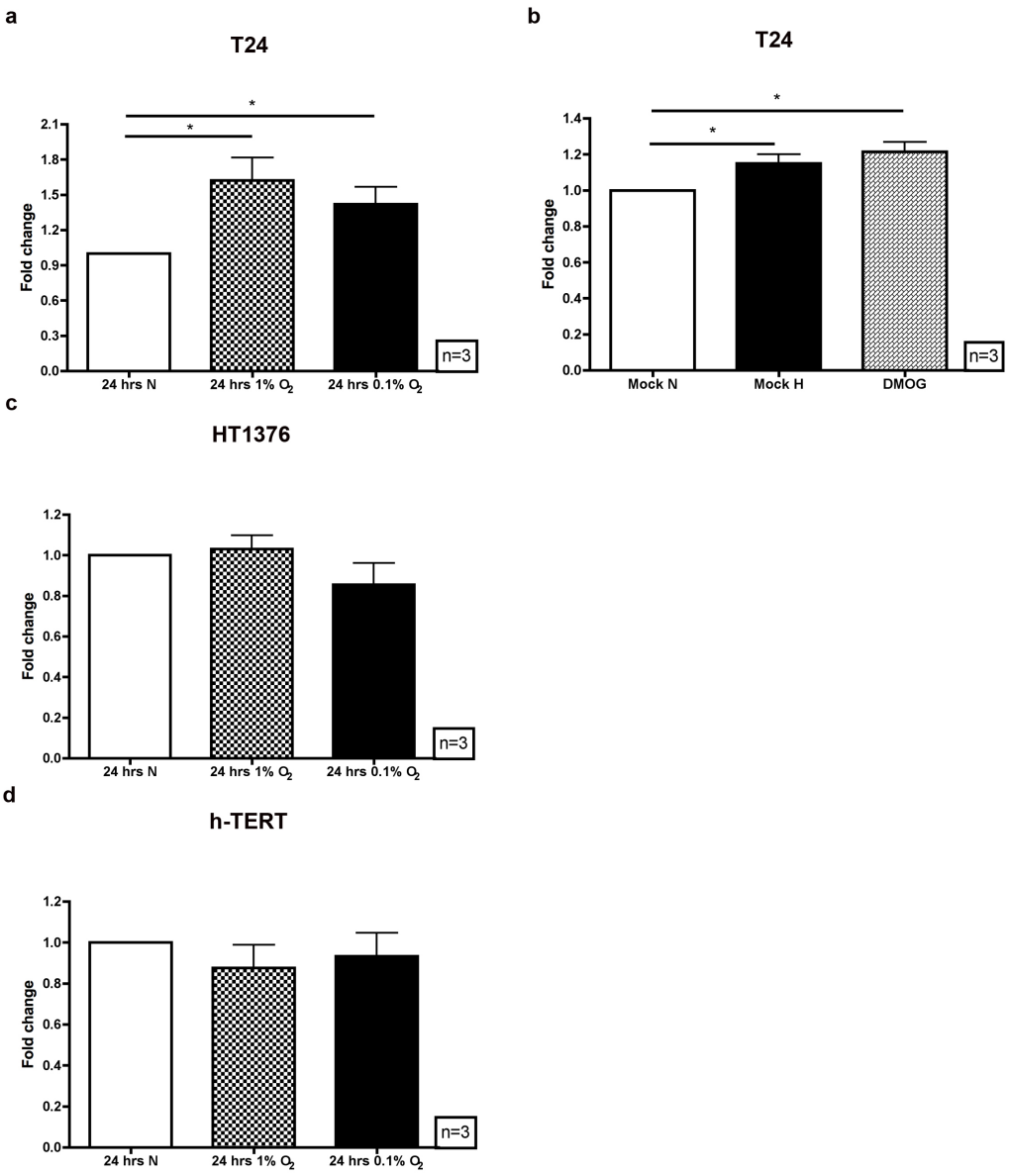
miR-15a



	T24	HT1376
Normoxia	36.0	34.7
0.1% O_2	35.0	35.5

Figure 3-24 Regulation of miR-15a by hypoxia in bladder cell lines

(a) T24 cells, (c) HT1376 cells, Cells were incubated in normoxia, 1% O_2 or 0.1% O_2 for 24 hours. (b) T24 cells were treated with 1mM DMOG in normoxia for 24 hours. Data are presented as mean ± standard error. Statistical significance: * $p<0.05$, ** $p<0.01$, *** $p<0.001$. Median CT values for normoxia and 0.1% O_2 after 24 hours are shown in the table at the bottom of the figure. Data for h-TERT cells are not shown due to the low levels of expression of this miRNA in this cell line.



	T24	HT1376	h-TERT
Normoxia	24.3	28.1	26.2
0.1% O_2	23.8	28.3	26.0

Figure 3-25 Regulation of miR-99a by hypoxia in bladder cell lines

(a) T24, (c) HT1376 and (d) h-TERT cells were incubated in normoxia, 1% O_2 or 0.1% O_2 for 24 hours. (b) T24 cells were treated with 1mM DMOG in normoxia for 24 hours. Data are presented as mean ± standard error. Statistical significance: * $p<0.05$, ** $p<0.01$, *** $p<0.001$. Median CT values for normoxia and 0.1% O_2 after 24 hours are shown in the table at the bottom of the figure.

3.2.12. Hypoxic and *p53* regulation of miR-145

The dramatic upregulation of miR-145 in RT4 cells, which was also confirmed by the individual assay was interesting as this miRNA is known to be controlled by p53 and also known to be a tumour suppressor gene [192]. As this hypoxic induction was only preserved in the least malignant cancer cell line we hypothesized that this upregulation could potentially be a protective mechanism preventing uncontrolled cell growth in the presence of hypoxia. As RT4 is the only bladder cancer cell line we used with wild type *p53* we also aimed to identify whether the presence of wild type p53 may promote this hypoxic induction.

Initially we cultured RT4 cells in normoxia and 0.1% O_2 and knocked down either *HIF-1* α or *HIF-2* α (Figure 3.26). RNU44 was used as the control gene and the expression of known HIF target miR-210 was a positive control. MiR-145 was induced in hypoxia in a *HIF-1* α dependent manner. The positive control miR-210 is also a HIF-1α target gene (Figure 3.26a and b). Knockdown of *p53* alone did not significantly reduce miR-145 expression in hypoxia (Figure 3.26c). Also of note, *p53* knockdown decreased miR-210 expression in hypoxia (Figure 3.26d and f), perhaps suggesting an alternative pathway for miR-210 hypoxic regulation. It is possible that a combined knockdown of *HIF* and *p53* may further reduce miR-145 expression, to deduce this we would need to perform a separate *HIF-1* knockdown in parallel to the experiments performed here. We would also need to confirm *p53* and *HIF1/2* knockdown by either mRNA quantification using PCR or protein quantification by western blot.

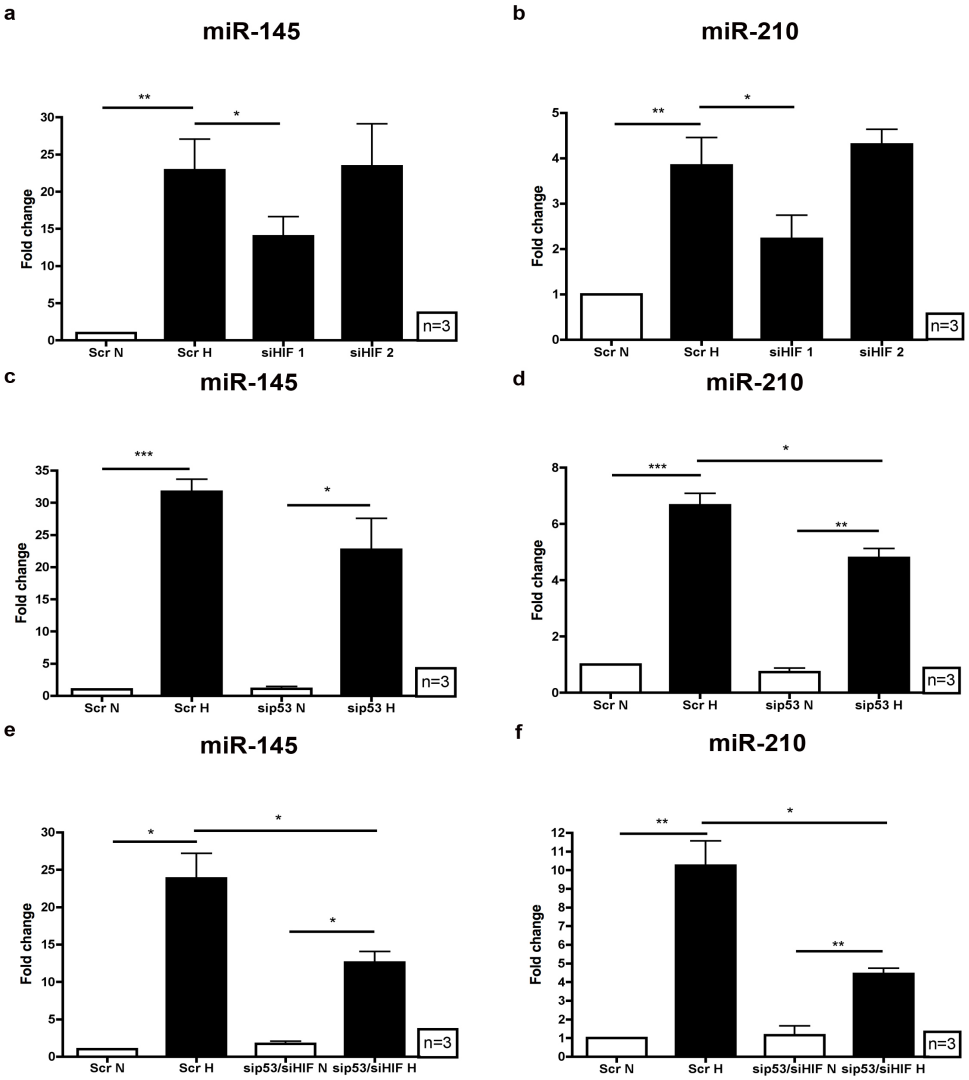


Figure 3-26 HIF-1α and p53 regulation of miR-145 in RT4 cells

	Scr N	Scr H	siHIF1	siHIF2	Sip53 N	Sip53 H	Si comb. N	Si comb. H
RNU44	23.9	24.2	22.8	22.3	24.3	24.4	24.6	24.5
miR-210	31.7	27.3	29.6	27.8	32.5	27.6	32.8	27.2
miR-145	37.7	28.0	31.3	27.7	37.6	33.4	36.7	33.7

Regulation of miR-145 and miR-210 expression by HIF and p53. MiR-145 levels were examined in RT4 cells after exposure to 24 hrs of 0.1% hypoxia in combination with (a) *HIF-1α* knockdown, (b) *p53* knockdown or (c) a combination of both *HIF-1α* and *p53* knockdown (comb.). Data are presented as fold change relative to the normoxic sample at each time point. MiR-210 levels were examined in RT4 cells after exposure to 24hrs of 0.1% hypoxia in combination with (b) *HIF-1α* knockdown, (d) *p53* knockdown or (f) a combination of both *HIF-1α* and *p53* knockdown. Data are presented as fold change relative to the scramble in normoxia. Statistical significance: * $p<0.05$, ** $p<0.01$. Mean ± standard error. The median CT values are shown in the table below.

3.2.13. Identification of hypoxic response elements for miR-145

We used Matinspector and identified two putative HIF response elements (HREs) within the promoter region of miR-145 with 2 RCGTG motifs (Figure 3.27a). To confirm that they were true HIF binding sites, we performed a chromatin immunoprecipitation (ChIP) experiment with HIF-1α and RNA polymerase II. As a positive control, we used the HRE of *CA9*. In response to hypoxia, there was a marked enrichment of the *CA9* HRE with both the HIF-1 α and RNA polymerase II antibodies (Figure 3.27b). Similarly, miR-145 HRE1, which is closer to the transcription start site, was also enriched with both HIF-1α and RNA polymerase II. MiR-145 HRE2 was only enriched in HIF-1α samples (Figure 3.27b). In contrast, the negative control *UBC* was not enriched in normoxia or hypoxia with either antibody. Therefore the hypoxic induction of miR-145 would appear to be a direct effect of HIF-1 α activation.

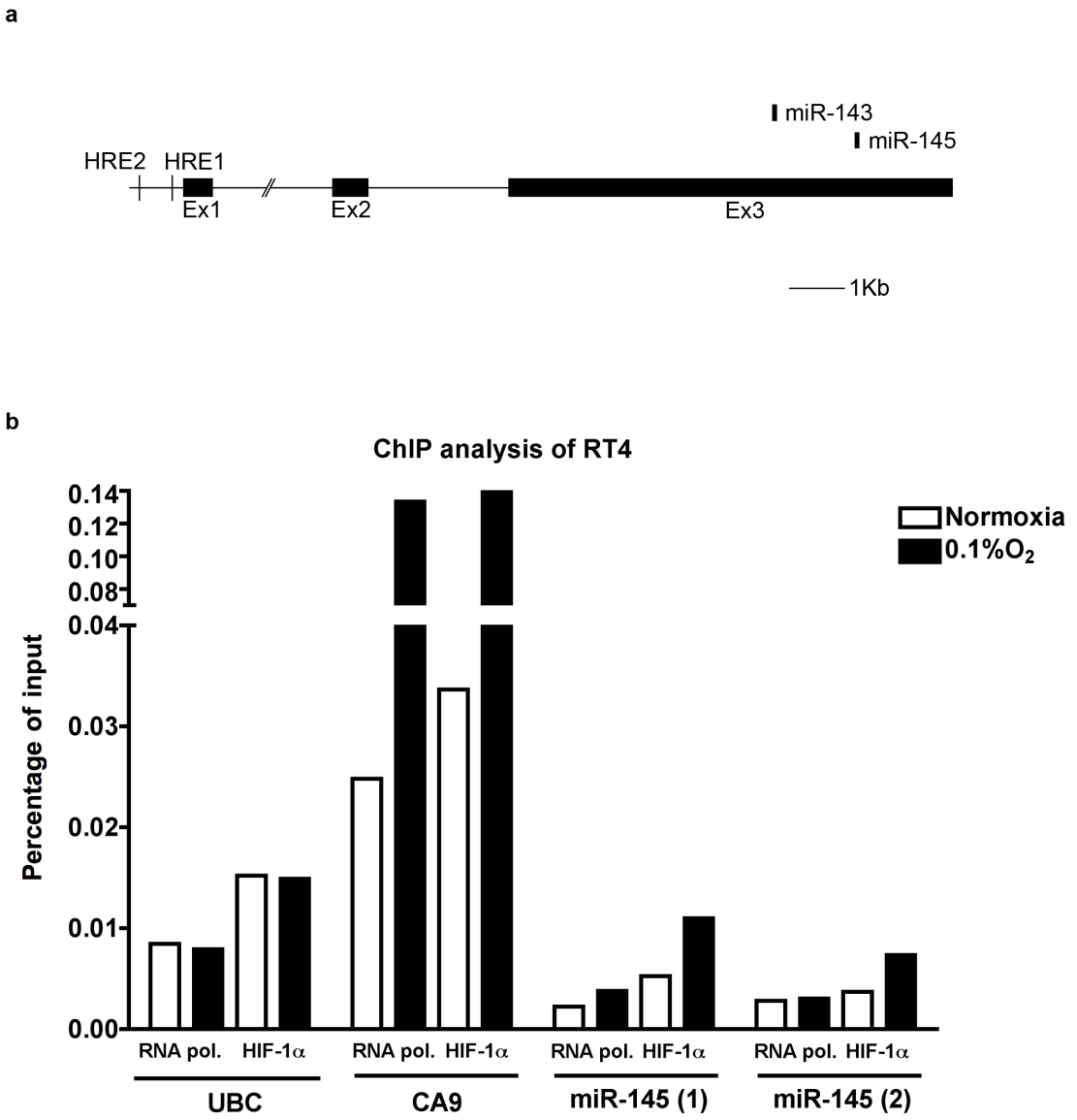


Figure 3-27 Identification of putative hypoxia response elements for miR-145

(a) Relative position of the two HREs in the promotor relative to the exons of the transcript from which miR-145 is processed. (b) ChIP analyses were then performed with antibodies against RNA polymerase II and HIF-1α in normoxia or hypoxia. *UBC* was the negative control and *CA9* was the positive control. Data is presented as % of input and is representative of three independent experiments.

3.2.14. The role of miR-145 in apoptosis and the myc pathway

MiR-145 is known to target *C-MYC* [192] and it is, therefore, possible that overexpression of miR-145 seen in hypoxia may downregulate C-MYC and hence inhibits the function of this oncogene. To test this hypothesis we transfected RT4 cells with both mimic miR-145 and antimiR-145 and analysed *C-MYC* mRNA and protein expression. First we quantified miR-145 and miR-210 to demonstrate the mimic-145 and anitmiR-145 transfection and the hypoxic response respectively. RNU44 was used as the internal control, cells were transfected and lysed after 3, 4 and 5 days incubation in either normoxia or 1% O_2 (Figure 3.28a). Interestingly the transfection of cells with mimic miR-145 caused a down regulation of miR-210 expression (Figure 3.28b), suggesting that miR-145 may be involved in the regulation of miR-210.

We found no evidence that either the *C-MYC* mRNA (Figure 3.28c) or protein (Figure 3.28e) was regulated by miR-145. Similarly, miR-145 did not appear to affect the levels of p21 mRNA (Figure 3.28d) or protein (Figure 3.28f). Although hypoxia led to an increase in transcript levels of both *C-MYC* (Figure 3.28c) and *p21* (Figure 3.28d), this was not translated to the protein levels (Figure 3.28e and f respectively).

.

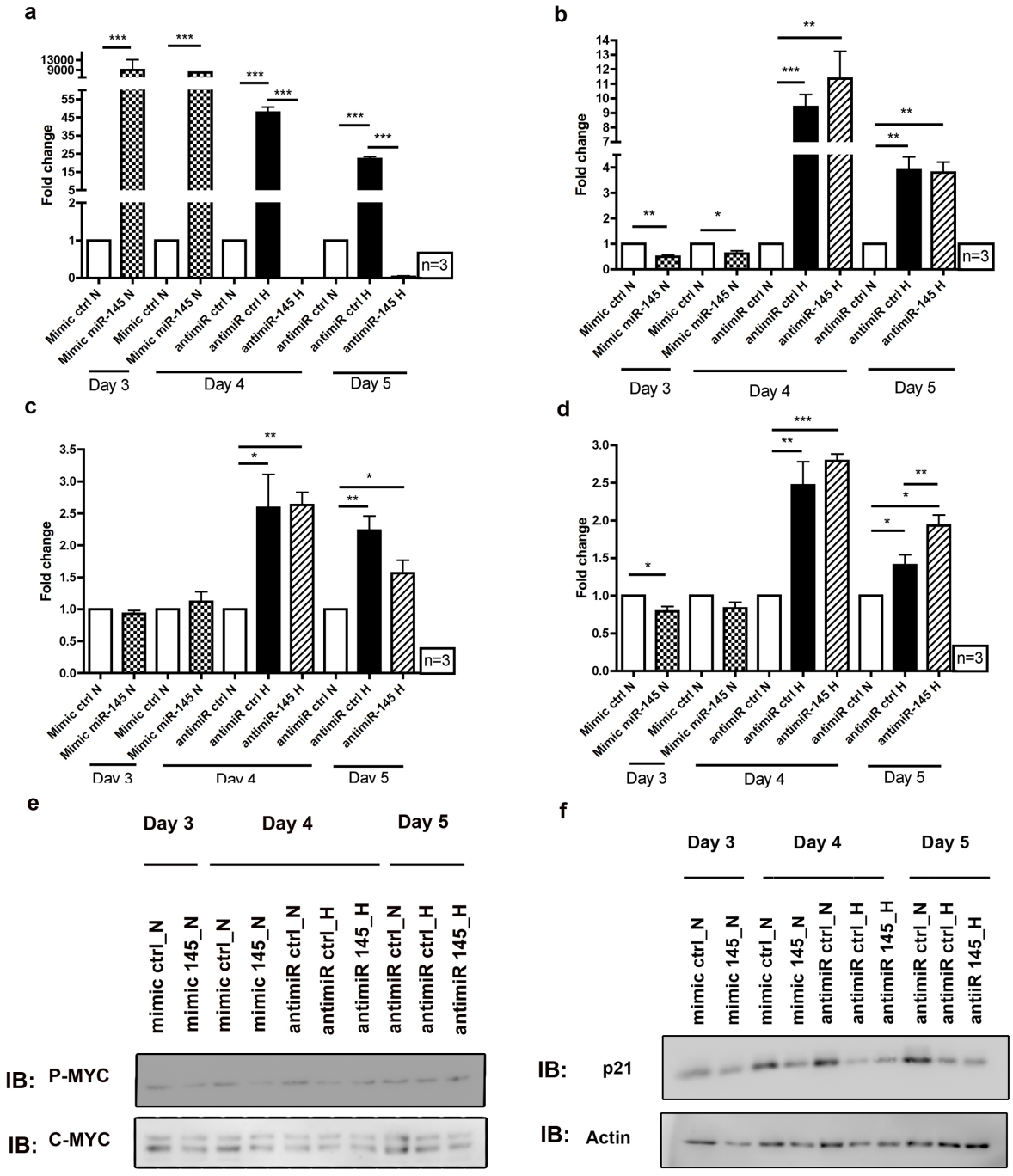


Figure 3-28 The role of miR-145 in c-myc and p21 expression

RT4 cells were transfected with either scramble, mimic miR-145 or antimiR-145 and cultured for 3-5 days in normoxia or 0.1% O_2. (a) miR-145, (b) miR-210, (c) *C-MYC* and (d) *p21* mRNA expression after transfection of mimic or antimiR-145 and incubation in normoxia or 0.1% O_2. (e) Western blot of phospho and total C-MYC and (f) Western blot of p21 in RT4 cells transfected with mimic or antimiR-145 and incubation in normoxia or 0.1% O_2.

3.2.15. The effect of miR-145 on apoptosis

MiR-145 has been shown to induce caspase dependent and independent apoptosis in other tumour types. We therefore aimed to establish whether miR-145 also affected apoptosis in RT4 cells. Cells were transfected with mimic miR-145 or antimiR-145 and incubated in either normoxia or 0.1% O_2 for 3-5 days.

We used flow cytometry for annexin V and PI to quantify the cell population undergoing apoptosis in each condition. Following transfection with mimic-miR-145 we found that the viable cell population (quadrant R5) decreased from 74.5% to 67.5% (Figures 3.29a and b). Concomitantly, there was an increase in the apoptotic population (quadrant R3) from 5.1% to 9.3% and an increase in the necrotic population (quadrant R4 from 10.8% to 14.2%). This suggests that miR-145 does have a role in apoptosis in RT4 cells.

For the comparison in hypoxia we can see a much larger population in quadrant R4 staining positive for both annexin V and PI in the anti-miR-control sample (35.1%) (Figure 3.29d); this is likely due to the cellular response to hypoxia after prolonged exposure. Upon transfection of antimiR-145, the fraction of cells in quadrant R4 drops to 23.4% and there is an increase in the percentage of viable cells (quadrant R5; 58.3% in anti-miR-control versus 68.5% in anti-miR-145) (Figure 3.29e) suggesting a reduction in cell death as a result of miR-145 knockdown. We were unable to detect any differences in levels of cleaved- PARP, another marker of apoptosis (Figure 3.29f).

	Mimic ctrl N	Mimic 145 N	
R3 (apoptotic)	5.1	9.3	
R4 (necrotic)	10.8	14.2	
R5 (viable)	74.5	67.5	
R6 (other)	9.5	9.0	
	Antimir ctrl N	**Antimir ctrl H**	**Antimir-145 H**
R3 (apoptotic)	3.6	2.4	3.5
R4 (necrotic)	15.2	35.1	23.4
R5 (viable)	78.9	58.3	68.6
R6 (other)	2.2	4.2	4.4

Table 3-3 Results from flow cytometry.

Values are presented as percentages. The data are presented graphically in Figure 3.29

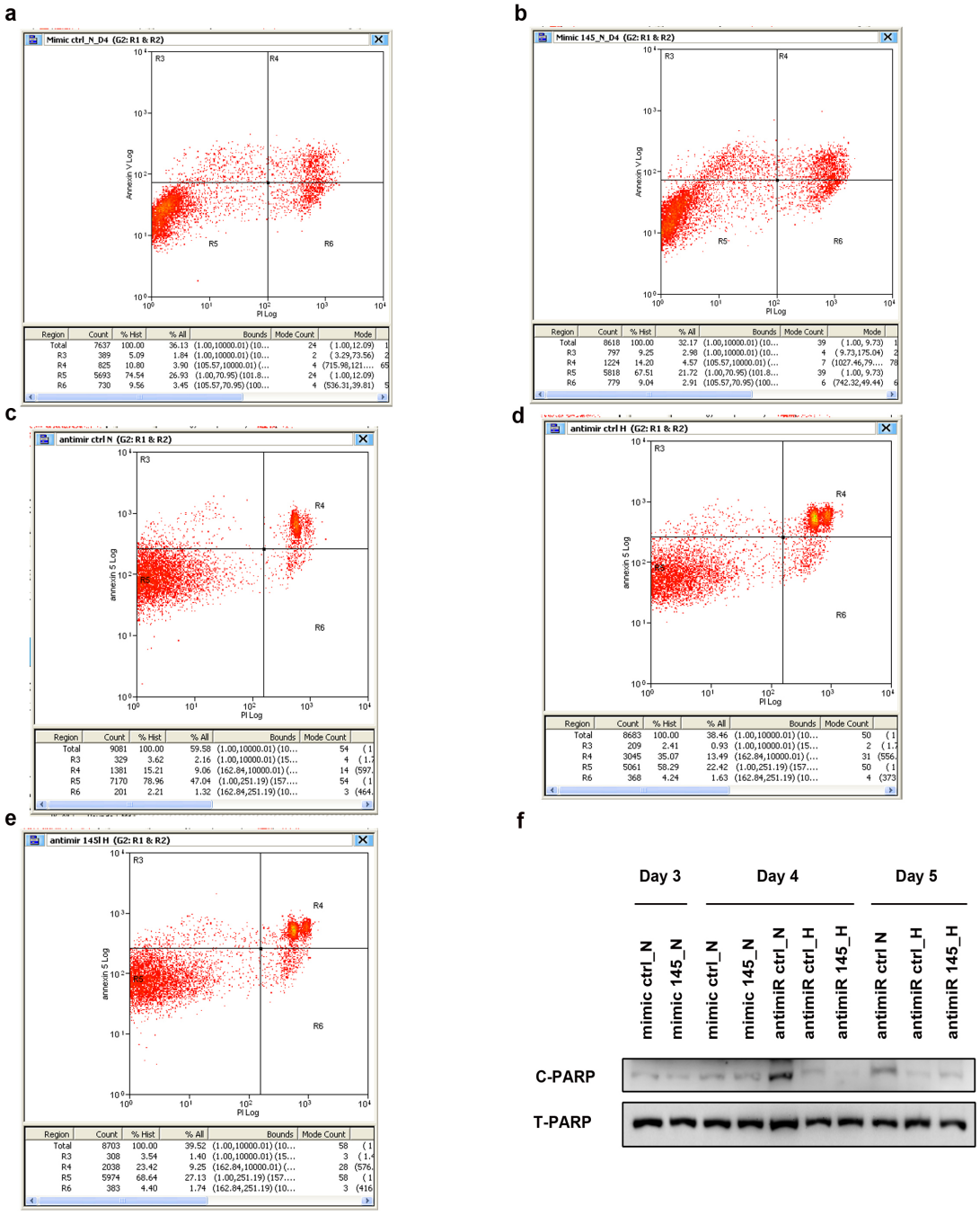


Figure 3-29 Effects of miR-145 expression on apoptosis in RT4 cells

RT4 cells were transfected with either control (a) mimic control or (b) mimic -145 for four days in normoxia and assayed for apoptosis by annexin V staining and flow cytometry analyses. RT4 cells were transfected with either antimiR control in (c) normoxia, (d) hypoxia or (e) anti-miR-145 in hypoxia for five days and assayed for apoptosis by annexin V staining and flow cytometry analyses. (f) RT4 cells were transfected with mimic or antimiR-145 and lysates were probed for cleaved PARP.

3.3 Discussion

3.3.1. Hypoxia regulated miRNAs that may be part of a core signature

The network of miRNAs involved in regulating cellular processes is complex as one gene can be targeted by a number of miRNAs and conversely a single miRNA can target multiple genes. MiRNAs can act as tumour suppressors or oncogenes in their own right. A number of miRNAs have been associated with various signaling pathways in bladder cancer and proven to be up and down regulated in both non-invasive and invasive bladder cancer. Those involved in regulation of p53 and FGFR3 are of particular importance as these genes are often mutated over overexpressed in invasive and non-invasive disease respectively.

Hypoxia and the activation of the HIF pathway is well described in bladder tumours and also recognized as a predictor for disease progression in superficial bladder cancer[177]. Hypoxia regulated miRNAs are thought to be integral in the hypoxic response and regulate both pathological and physiological responses to hypoxia. With the exception of miR-210, which is widely accepted as the most consistently upregulated hypoxia regulated miRNA, variations in expression data amongst different tumour types has led us to believe that the hypoxic response has a considerable 'tumour specific' element.

We initially used miRNA regulated by *vHL* mutation in RCC4 cells to identify targets that may be differentially regulated by hypoxia in bladder cancer. As in other tumours miR-210 was consistently upregulated in hypoxia in all bladder cell lines. While the induction of miR-210 by hypoxia is universal and also observed in the immortalized normal urothelium line h-TERT, it is exaggerated in cancer cell lines as the magnitude of induction was much lower in h-TERT.

This may suggest that the hypoxic response in cancer cells is reinforced by additional signaling pathways, for example mTOR [198].

Another miRNA whose expression is induced by loss of vHL in RCC4 and hypoxia in bladder cancer is miR-193b. MiR-193b expression was increased by exposure to hypoxia or DMOG in 4/5 bladder cancer lines and in the normal urothelium line. This was also borne out in the low density arrays done on RT4 and T24 cells, where miR-193b was induced in both lines. This would suggest that miR-193b might be a HIF target gene; further work may involve looking at its expression after *HIF-1* α knockdown and looking for putative HREs in its promoter. Although there are few known direct actions of this miRNA, it is known to target urokinase-type plasminogen and its loss of function through mutations in the miRNA processing machinery can lead to increased expression of UKPA in hepatocellular and breast cancer cells promoting cell migration, invasion and metastasis [199, 200]. MiR-193b is thought to act as a tumour suppressor in prostate cancer where increased expression significantly reduced the growth of prostate cancer cell lines and regulates *CYCLIN D1* and cell proliferation in melanoma [201].

Although miR-155 expression was found to be increased by *vHL* mutation in RCC4, it was not induced by hypoxia in the bladder cancer cell lines. In addition, although miR-424 was found to be decreased in *vHL* null RCC4 cells, its expression was either unchanged to induced in response to hypoxia in bladder cancer cell lines. This may highlight cell line or cancer type specific miRNA that are regulated by hypoxia; indeed, this is expected as miRNA expression profiles can be used for cancer classification [184].

MiR-503, whose expression was decreased by *vHL* mutation in RCC4 cells, was undetectable in 4/5 bladder cancer cell lines. In T24 and h-TERT cells, decreased expression was seen in response to hypoxia and DMOG treatment. Not much is known about the targets of miR-503. MiR-503 expression has been shown to be induced during muscle differentiation and to cause cell cycle arrest [202]. MiR-503 has also been shown to decrease migration in hepatocellular carcinoma [202]. It is likely that hypoxic down regulation of miR-503 would have different effects in the invasive T24 and normal h-TERT cells and it may warrant further investigation.

RCC4 cells null for *vHL* had lower levels of miR-100. In the immortalized normal epithelial line h-TERT and in the low invasive RT4 cells, decreased miR-100 levels were seen, suggesting this effect is associated with 'less malignant' cell types in bladder cancer (Figure 3.9). In Chapter 4 we discuss the potential role of decreased miR-100 in hypoxia, particularly in the context of regulating FGFR3 signaling.

3.3.2. Hypoxia regulated miRNAs that may be unique to bladder cancer

We hypothesized that exposure to hypoxia may lead to changes in miRNA expression that would be unique to bladder cancer. We, therefore, performed low density miRNA profiling to look at he expression of 384 miRNA in response to hypoxia in RT4 and T24 cells. Of the 25 miRNA that were most highly induced in both cell lines, 7 were in common. These included the well characterised miR-210 and miR-193b, which we have discussed in this chapter and found to be robust hypoxia responsive genes. Additional miRNA found in common included

miR-125a-3p, miR-125a-5p and miR-212. Indeed, we could validate the hypoxic induction of miR-125a-3p in RT4 and RT112 cells using individual assays. MiR-125a-3p and miR-125a-5p are derived from the same stem loop structure of pre-miR-125a [203]. MiR-125a-5p is an independent prognostic indicator in gastric cancer but not previously described as a miRNA involved in bladder cancer tumourigenesis [204]. MiR-212 has not been associated with bladder cancer but reduced levels of miR-212 expression are reported to increase HB-EGF and resistance to cetuximab in breast cancer [205]. These miRNA may, therefore, represent common HRMs in bladder cancer.

The expression of a number of miRNA in response to hypoxia appeared to be in a tumour type dependent manner. For example, the hypoxic induction of miR-145 and miR-708 observed in RT4 cells was also seen in the non-muscle invasive line RT112. These may represent hypoxia responsive miRNA in non-muscle invasive bladder cancer, although work on additional cell lines would be required to confirm this. MiR-708, previously reported to be upregulated in bladder cancer has been shown to induce apoptosis through the suppression of *ZEB2* and *BMI1*, which regulate *E CADHERIN* and also its target *SURVIVIN*. *In vivo* experiments demonstrated a significant reduction in tumour size in mice treated with miR-708 [206, 207].

One of the most interesting findings was the upregulation of a number of miRNAs belonging to the chromosome 19 miRNA cluster, almost half of the 25 most hypoxia upregulated miRNAs in RT4 cells belong to this cluster. The same pattern was not seen in T24. We could validate the expression of one of these, miR-518-3p, with individual assays in RT4. The chromosome 19 miRNA cluster is amplified in aggressive brain tumours, and associated with development

although its precise role is not currently understood [208]. Various miRNAs in this cluster have been investigated, in a study by Yoshitomi et al miRNAs 517a and 520g (both part of the 520 cluster) were found to be induce apoptosis in bladder cancer cells through the regulation of *AREG* and *BCLAF1* and their loss of function was thought to be due to epigenetic silencing secondary to DNA methylation [209]. The C19MC cluster has been reported to be upregulated in undifferentiated human stem cells and known to target genes involved in the modification and maintenance of chromatin function [196]. The observation that multiple miRNA from this cluster are expressed may suggest that the entire cluster is hypoxia responsive in RT4 cells. It would be interesting to investigate their expression on additional non-muscle invasive bladder cancer cell lines.

By and large, there were no similarities between T24 and HT1376 cells except for miR-210 and miR-193b suggested that the upregulated miRNAs in T24 cells are cell line specific and not to high grade bladder cancer. We could validate the expression of miR-99a, 200a and 15a in response to hypoxia in T24 cells with individual assays. MiR-99a is down regulated in a number of cancers, it is known to target *FGFR3* and *mTOR* and overexpression of this miRNA is known to limit the tumourigenicity of cell lines [210].

Of interest is that three miRNA in the miR-200 family, miR-200a, 200b and 200c, were all found to be induced by hypoxia in T24 cells. The miR-200 family is well documented to target the *ZEB* transcription factors that are activators of the epithelial to mesenchymal transition phenotype [211] . It is therefore, possible that hypoxic regulation of miR-200 is part of the regulatory loop that controls invasion and metastasis in invasive bladder cancer cells.

We could not validate the hypoxic induction of miR-518f and miR-150 with individual assays. In the case of the former, this discrepancy is most likely due to the low levels of expression of miR-518f with CT values of 40, suggesting the hypoxic induction seen in the array data may have been due tot the very low levels of miR-518f in normoxia (Figure 3.21). Low levels of miR-150 have been found to correlate with poor response to chemotherapy and prognosis in colorectal cancer [212]; it may be worthwhile investigating this miRNA in additional invasive bladder cancer cell lines.

The most downregulated miRNAs were miR-331-5p and miR-128, both of these miRNAs when downregulated have been associated with increased resistance to chemotherapy in leukaemia and breast cancer respectively. It has been suggested that miR-128 may act as a tumour suppressor miRNA and low levels may promote invasion and tumour growth [213-215].

Thus, we are not surprised by the variations in miRNA expression in hypoxia firstly because the different bladder phenotypes represented by the RT4 and T24 cells but also the difference in mutations of key genes such as *p53* and *FGFR3*. Interestingly many of the hypoxia regulated miRNAs in RT4 cells have been found to be involved in pro-apoptotic pathways in bladder cancer and other tumours. It is possible that hypoxia in non invasive tumours initiates a cascade mediated by hypoxia regulated miRNAs to maintain the papillary phenotype, limit growth and prevent invasion. Further studies would be required to test this hypothesis.

We decided to focus the remaining work in this chapter on the role of miR-145 in non muscle invasive cancer. The dramatic 40-50 fold upregulation seen in

hypoxia is the greatest induction we discovered amongst all miRNAs in bladder cancer cell lines.

3.3.3. The role of miR-145 in non- invasive bladder cancer

We found that miR-145 was the most induced hypoxia regulated miRNA, upregulation occurred in a *HIF-1α* dependent manner and we identified 2 hypoxia response elements on the promotor region of miR-145. The HRE closest to the transcription start site, HRE1, was enriched with both the RNA polymerase II antibody and the HIF-1 α antibody while the HRE that was further away (HRE2) was only enriched with the HIF-1α antibody. This would be expected as the RNA polymerase would only bind to sites close to where transcription would begin. As a positive control *CA9* was shown to be highly enriched in hypoxia with both antibodies. *CA9* HRE is highly responsive to HIF and leads to upregulation of more than a thousand fold in hypoxia so the dramatic enrichment seen with *CA9* is to be expected.

We hypothesized that a possible explanation for the absence of hypoxic miR-145 induction in the other cell lines is the presence of *p53* mutation in other lines, whereas RT4 cells have wild type *p53*. Although *p53* knockdown alone did not affect hypoxic induction of miR-145, the double knockdown of both *p53* and *HIF-1* α led to decreased expression, suggesting that the two transcription factors synergise, although knockdown of *p53* and *HIF-1α* individually would be required to confirm this. Indeed *HIF-1* α has previously been shown to stabilize wildtype *p53* and leads to its transcriptional activation [216]. Further evidence for a synergy between *HIF* and *p53* comes from examining the levels of miR-210-

knockown of *p53* attenuates hypoxic miR-210 induction. A similar observation has recently been reported in mouse embryonic fibroblasts where loss of p53 attenuated the hypoxic induction of miR-210 [217]. It has also been shown that p53 leads to overexpression of miR-107, which in turn targets and leads to the downregulation of HIF-1β. The synergy between HIF and p53 warrants further investigation.

Reduced expression of miR-145 has been reported in colorectal, ovarian and breast cancers, this observation led to speculation it may be a putative tumour suppressor [191, 192]. The hypoxic regulation of miR-145 has not previously been described, and would, therefore, represent a novel HRM. Chen et al found that miR-145 targets *BNIP3*, *BNIP3* is a HIF-1 α target and the authors concluded that the miR-145 regulation of BNIP3 demonstrated a HIF independent mechanism of post transcriptional regulation. We did not examine the hypoxic induction of miR-145 in prostate cancer cell lines but it may be that the pathway is actually HIF dependent as we have found. These authors also found that upregulation of p53 induced miR-145 expression. Another group found that p53 transcriptionally regulates miR-145 expression and miR-145 in turn targets c-MYC. Although we were unable to confirm this link in RT4 cells it is likely that the down regulation of *c-MYC* occurs as a result of a number of regulatory pathways rather than miR-145 alone [192].

MiR-145 has previously been shown to induce apoptosis in T24 cells [129],. We have shown that miR-145 expression and its regulation by hypoxia are involved in the regulation of apoptosis in RT4 cells as well. MiR-145 has been shown to mediate both caspase dependent and caspase independent apoptosis in bladder cancer [129]. PARP cleavage is primarily a result of caspase activity [218]. In the

bladder cancer cell line SW780, miR-145 was shown to lead non-caspase dependent apoptosis as the broad spectrum caspase inhibitor zVAD-fmk did not inhibit this process [129]. Thus, it is possible that PARP cleavage was not observed in RT4 cells as the non-classical apoptosis pathway was activated. Further work is needed to test this hypothesis.

Evidence suggests that miR-145 has a role as a tumour suppressor through a number of mechanisms including the previously mentioned regulation of *C-MYC* and suppression of *mucin 1* thereby preventing invasion [191]. The miR-145 is targeted and suppressed by the RAS signaling pathway; in turn, miR-145 targets *RREB1* and *KRAS* in pancreatic cancer and overexpression of miR-145 suppresses growth and invasion in breast cancer cell lines [191, 219]. It is possible that the loss of miR-145 induction in hypoxia may have an anti-apoptotic effect in the other cell lines examined, however this requires further analysis.

3.3.4. Conclusion

Identification of HRMs and establishing their role in tumourigenesis has a number of potential clinical benefits. We have already mentioned that miRNAs and relative expression of miRNAs have been used to sub classify different forms of cancer. We have previously shown that miR-210 has a role not only as a marker of hypoxia but also as a prognostic marker in breast cancer. In line with other studies, miR-210 is robustly induced in hypoxia in bladder cancer lines. Lower levels of induction were observed in normal bladder urothelial lines suggesting that additional pathways may be responsible for augmenting hypoxic induction of miR-210. Additionally, we have shown in this chapter that miR-193b

is also a robust hypoxia regulated gene in bladder cancer cells. We have also shown that miR-100 is suppressed by hypoxia; in Chapter 4, we discuss miR-100 dependent regulation of *FGFR3* levels, and the consequences of modulating this pathway. Additional miRNA that may be part of a bladder cancer HRM signature are miR-125a-5p, miR-125a-3p and miR-212. Specifically in low grade bladder cancer, we have shown that miR-145 is a robustly induced, novel HIF target gene and that miR-145 contributes to apoptosis in RT4 cells. Hypoxic induction of miR-145 may suggest a good prognosis as the loss of this effect may contribute to enhanced cell growth.

Chapter 4 The hypoxic regulation of *FGFR3* expression via *HIF-1 α* and miR-100.

4.1 Introduction

4.1.1. Molecular alterations in bladder cancer

The majority (90%) of cases of bladder cancer are derived from the urothelium [109]. Most cases (70-80%) of bladder cancer are low-grade non-muscle invasive (NMI) cancers comprising Ta and T1 tumours. Muscle invasive (MI) cancers encompass stage T2 and beyond and account for 20-30% of bladder cancer. NMI cancer is associated with a low incidence of progression (10-20%) but a high recurrence rate (70%) [105, 220]. Thus, although not fatal, NMI cancer requires long term monitoring of patients and regular surveillance and in the US bladder cancer is the most expensive cancer per patient to manage from diagnosis to death [221].

It is generally accepted that NMI and MI bladder cancer have distinct underlying etiologies. While MI cancer is associated with inactivating mutations in *TP53*, *RB* and *PTEN* genes, NMI cancer is characterised by increased expression and activating mutations of *FGFR3*, *H-RAS* and *PI3K* [113, 114].

4.1.2. FGFR3 in disease

FGFR3 is one of four members of the FGFR family of receptor tyrosine kinases that serve as cell surface receptors for the FGF ligands. Structurally, it consists of a ligand binding extracellular domain with three immunoglobulin repeats, a single transmembrane domain and cytoplasmic tail with tyrosine kinase domain.

After ligand binding, the receptors dimerise and transphosphorylate each other to fully activate their kinase activity. Activated FGFR3 leads to the activation of multiple signalling pathways including the ERK/MAPK cascade and PI3K signalling [222]. Germ line mutations in *FGFR3* are associated with skeletal abnormalities. Mutations in *FGFR3* have been reported in patients with achondroplasia and hypochondroplasia. The majority of mutations identified to date are thought to confer a gain of function phenotype that allows the receptor to either signal in the absence of a ligand or enhances signalling upon ligand binding signalling [222]. One study has identified a loss of function mutation in *FGFR3* in patients with CATSHL syndrome, which is characterised by tall stature and hearing loss [223].

In addition to skeletal defects, *FGFR3* also plays an important role in the pathogenesis of bladder cancer, and in particular, in NMI bladder cancer. Mutations in *FGFR3* have been found in around 70% of NMI bladder cancer and in around 20% of MI bladder cancer [5, 14, 224]. The spectrum of activating mutations found in *FGFR3* in bladder cancer are identical to those implicated in skeletal abnormalities. Perturbations in *FGFR3* in bladder cancer can also occur by deregulated expression. Upregulation of FGFR3 protein expression has been reported in NMI bladder cancer [225] and expression has been found to decrease with increasing stage with 80% of pTa tumours, 70% of pT1 tumours and 50% of pT2 tumours [6, 225]. One study has correlated mutation status to FGFR3 immunostaining across both NMI and MI bladder cancer, 85% of mutant tumours, the majority of which were low stage, also showed overexpression of FGFR3 [6]. In addition, 54% of MI bladder cancer had either a mutation or overexpression of *FGFR3*. The high levels of both wild type and mutated *FGFR3*

found in bladder tumours suggests both are involved in bladder cancer tumourigenesis. Currently the mechanisms of upregulation aren't known. It should be noted that mutations in *FGFR3* have been reported in other cancers including multiple myeloma [226]and cervical cancers [227].

In the previous chapter we identified a number of hypoxia regulated miRNAs in bladder cancer. One possibility is that miRNAs are involved in the regulation of *FGFR3* expression. We have previously reported that *FGFR3* is targeted by miRNAs 99a and miR-100 [184]. We have already found that miR-100 is downregulated in bladder cancer and in hypoxia. The aim of this chapter was to determine the role of hypoxia and miR-100 on regulating *FGFR3* expression and signaling in bladder cancer cell lines.

4.2 Results

4.2.1. Hypoxic regulation of miR-100 expression

To determine whether miR-100 plays a role in the hypoxic regulation of *FGFR3* levels, we examined miR-100 expression in RT4 cells after exposure to hypoxia. Exposure to hypoxia for 24 and 48hrs led to a significant decrease in miR-100 levels in RT4 (Figure 4.1a). The hypoxic suppression of miR-100 could not be reversed by knocking down either HIF-1α or HIF-2α (Figure 4.1b). To determine whether there was a correlation between miR-100 and hypoxia *in vivo*, we used a breast cancer series on which both mRNA and microRNA microarray profiling had been performed [67]. Using this and independent tumours series, we have generated an *in vivo* hypoxia metagene signature whose median expression is a robust indicator of tumour hypoxia [228, 229]. We, therefore, examined the relationship between miR-100 expression and the tumour hypoxia score *in vivo.* In breast cancer tumour samples, we found a significant inverse correlation between miR-100 expression and tumour hypoxia score (Figure 4.1c). Metagene signatures have also been derived for tumour proliferation, immune response and invasion. MiR-100 expression showed an inverse correlation with the proliferation and immune response scores but a positive correlation with invasion (Table 4.1). To confirm miR-100 targets *FGFR3*, we performed a luciferase assay using a plasmid in which the 3'UTR of the *FGFR3* transcript was fused to the 3'end of the open reading frame of firefly luciferase. Co-transfection with mimic miR-100 caused a significant reduction in expression (Figure 4.1d) confirming *FGFR3* as a target of miR-100.

Spearman	Hypoxia	Proliferation	ERS1 signaling	ERBB2 signaling	Invasion	Immune Response	Apoptosis
Correlation Coefficient	-0.33	-0.66	-0.11	-0.10	0.28	-0.24	-0.13
Sig. (2-tailed)	0.01	0.01	0.12	0.14	0.00	0.00	0.06
N	207	207	207	207	207	207	207

Table 4-1 Correlation of miR-100 and the metagene signature

Data were provided by Francesca Buffa. The metagene signatures were derived from three head and neck and five breast cancer cell lines. These signatures represent functional grouping of genes through analysis of *in-vivo* co-expression patterns.

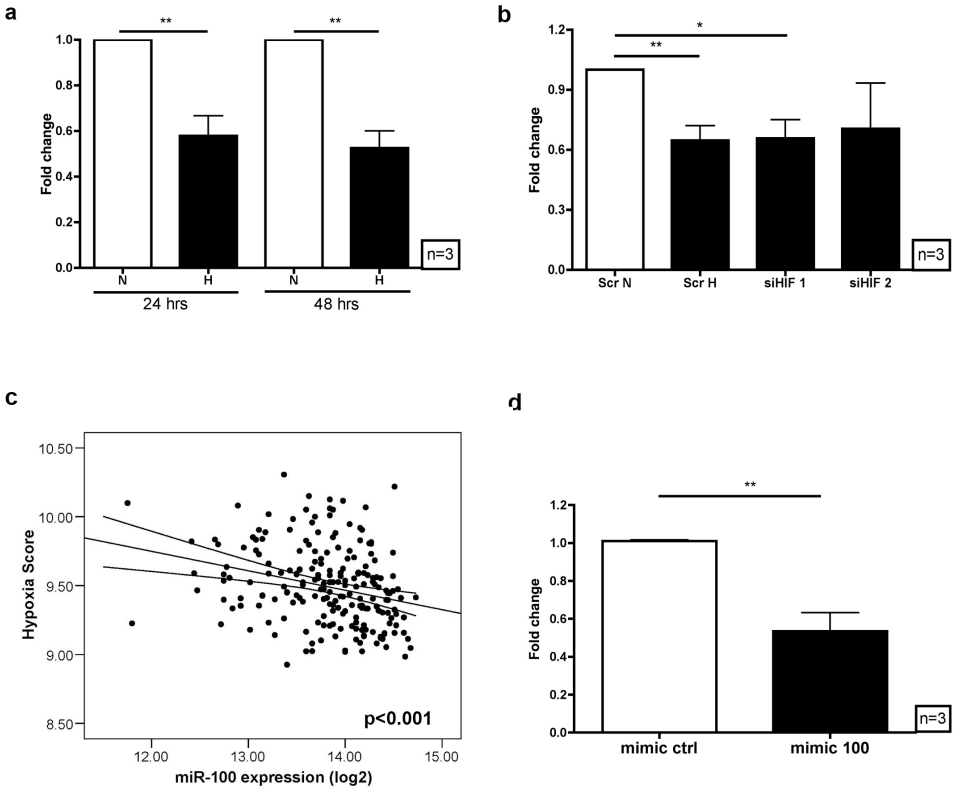


Figure 4-1 Hypoxic regulation of miR-100 and targetting of *FGFR3*

Regulation of miR-100 expression by hypoxia. (a) MiR-100 levels were examined in RT4 cells after exposure to 24 or 48hrs of hypoxia. Data are presented as fold change relative to the normoxic sample at each time point. (b) MiR-100 levels were examined in RT4 cells after exposure to hypoxia, in combination with either *HIF-1α* or *HIF-2α* knockdown, for 24hrs. Data are presented as fold change relative to the scramble in normoxia. (c) Correlation of miR-100 levels to tumour hypoxia, as measured by the median hypoxia score, in 219 breast cancer specimens (correlation co-efficient=0.334, p<0.0001). (d) Luciferase assay performed in MCF7 cells, data are presented as fold change relative to mimic control. Statistical significance: * p<0.05, ** p<0.01. Mean ± standard error.

4.2.2. Hypoxic regulation of *FGFR3* mRNA expression

As miR-100 is downregulated in hypoxia and is known to target *FGFR3* we first aimed to establish the effects of hypoxia on *FGFR3* expression. The expression of *FGFR3* mRNA was investigated in three non-invasive bladder cell lines (RT4, RT112 and 97-7) and 1 invasive cell line (T24) after exposure for 24 and 48 hours to normoxia or 0.1% O_2 hypoxia (Figure 4.2). In RT4 cells there was a 2 fold induction at 24 hours and a 4 fold induction at 48 hours, in RT112 cells a 2-2.5 fold induction was seen at 24 and 48 hours respectively. In 97-7 cells *FGFR3* expression levels did not change at 24 hours but were reduced at 48 hours when compared to hypoxia. *FGFR3* expression in T24 cells is not shown due to the low levels of expression. As a positive control we used the known hypoxia induced gene *CA9* and as expected *CA9* expression was significantly upregulated at both 24 and 48 hours in all cell lines.

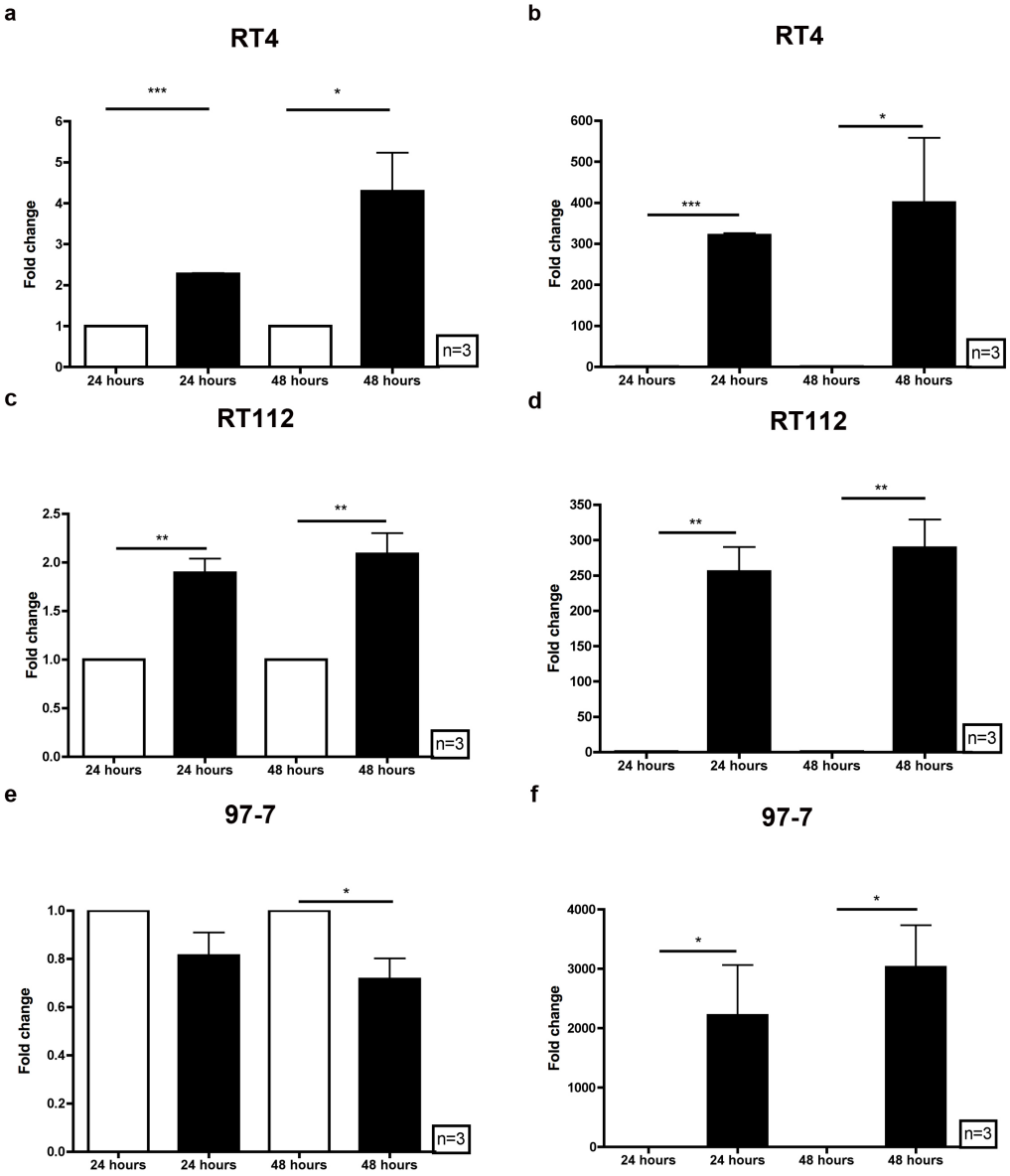


Figure 4-2 Regulation of *FGFR3* mRNA by hypoxia in bladder cancer cell lines

(a-b) RT4,(c-d) RT112 and (e-f) 97-7 cells were incubated in normoxia or 0.1% O_2 for 24 hours and 48 hours. *FGFR3* (a,c and e) and *CA9* (b,d and f) mRNA expression relative to *ACTIN* is presented as fold change. Data are presented as mean ± standard error. Statistical significance: * $p<0.05$, ** $p<0.01$, *** $p<0.001$.

4.2.3. The hypoxic regulation of FGFR3 protein

First we validated the FGFR3 antibody by knocking down FGFR3 in RT4 cells in normoxia and hypoxia (Figure 4.3a). Having demonstrated an increase in expression levels of *FGFR3* mRNA in hypoxia we then looked at expression of FGFR3 protein after 24 hours incubation in normoxia and 0.1% O_2. In both RT4 and RT112, increased expression of FGFR3 protein was observed (Figure 4.3b). In 97-7 cells, FGFR3 was expressed in both normoxic and hypoxic conditions but further induction in hypoxia was not seen. In contrast, no expression of FGFR3 was detectable in T24.

To confirm the hypoxic regulation of FGFR3 expression we treated RT4 cells with DMOG, a PHD inhibitor that leads to HIF stabilisation in normoxia. We found that concomitant with this stabilisation of HIF was an increase in levels of both *FGFR3* mRNA (Figure 4.3c) and protein (Figure 4.3d) in RT4 cells. We next sought to determine the HIF dependence of *FGFR3* expression. Knocking down *HIF-1*α expression but not *HIF-2*α expression significantly decreased *FGFR3* mRNA (Figure 4.3e) and protein (Figure 4.3f) after exposure to hypoxia. Therefore, *HIF-1* α regulates the hypoxic induction of FGFR3 in RT4 cells.

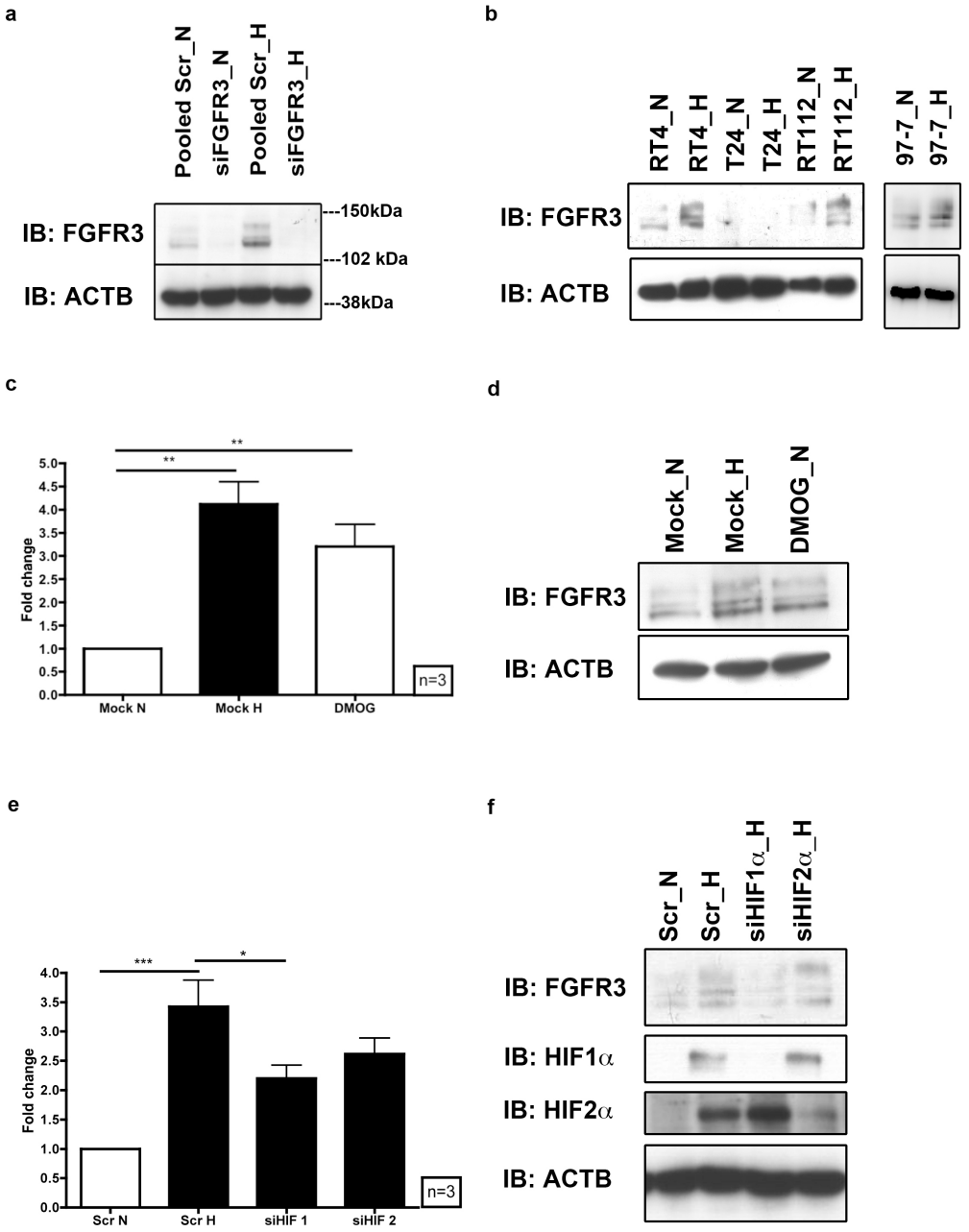


Figure 4-3 Hypoxic regulation of FGFR3 in bladder cell lines

(a) RT4 cells were cultured in normoxia and 0.1% O_2, cells and transfected with either scramble or siFGFR3. (b) Four bladder cancer lines were cultured in either normoxic or hypoxic conditions for 24hrs and probed for the expression of FGFR3 protein. (c) mRNA levels of *FGFR3* were examined in RT4 cells after 24hrs of exposure to normoxia (white bars), hypoxia (black bar) or with the hypoxia mimetic DMOG. Data are presented as fold change relative to mock in normoxia. (d) FGFR3 protein levels were investigated in RT4 cells after exposure to normoxia, hypoxia or the hypoxia mimetic DMOG. (e) mRNA levels of *FGFR3* were examined in RT4 cells after exposure to hypoxia, in combination with either *HIF-1α* or *HIF-2α* knockdown, for 24hrs. Data are presented as fold change relative to the scramble in normoxia. (f) FGFR3 protein levels in RT4 cells were examined after exposure to hypoxia in combination with either *HIF-1α* or *HIF-2α* knockdown, for 24hrs. Statistical significance: * $p<0.05$, ** $p<0.01$, *** $p<0.001$. Mean ± standard error.

4.2.4. Identification of hypoxia response elements in FGFR3

We used MatInspector [230] to identify putative HIF response elements within the promoter region of FGFR3 and identified two putative RCGTG motifs (Figure 4.4). However, neither of these sites were enriched when chromatin immunoprecipitations were performed with HIF-1α (Figure 4.4b). The positive control *CA9* immunoprecipitated with both RNA polymerase and HIF-1a antibodies in hypoxia. Thus, although we found *FGFR3* mRNA and protein regulation to be HIF-1α dependent we were unable to identify a HIF response element.

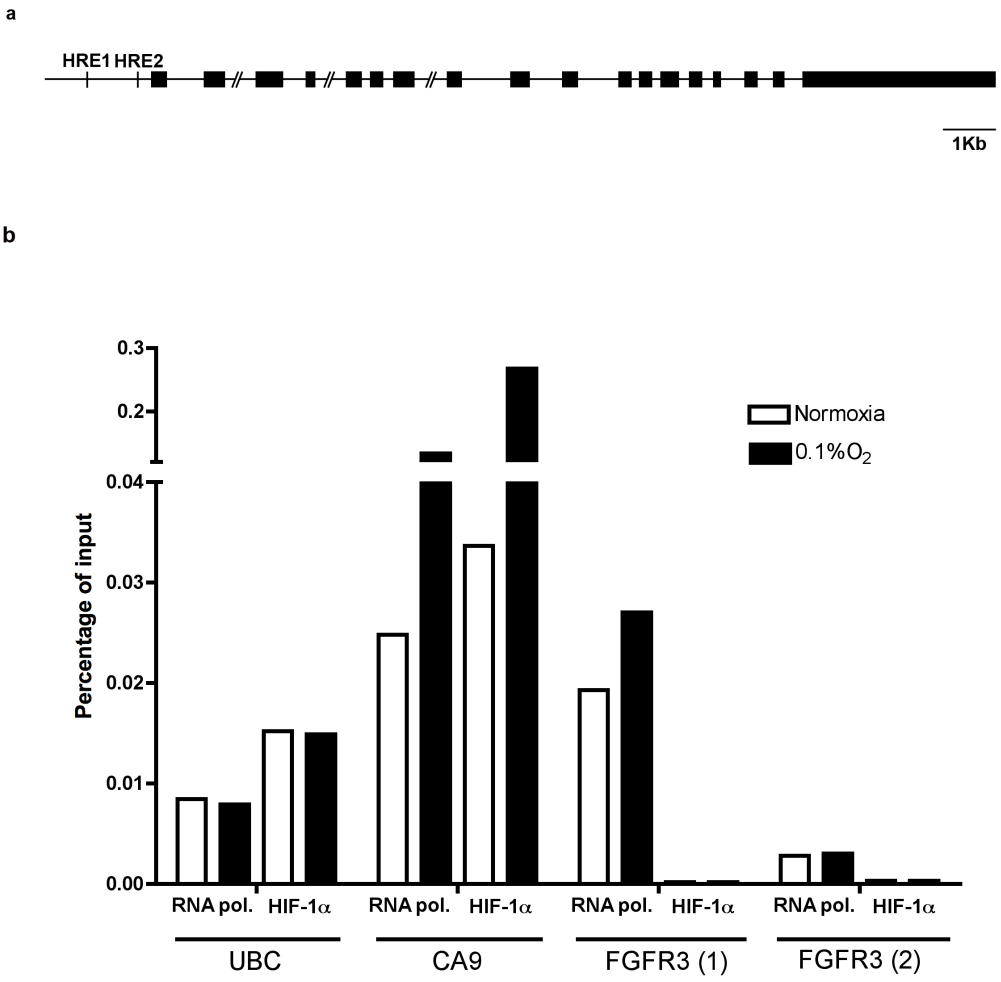


Figure 4-4 Identification of putative HRE in *FGFR3*

a) Relative position of the putative HREs in the *FGFR3* promoter. (b) ChIP analyses were performed with antibodies against RNA polymerase II and HIF-1α in normoxia or hypoxia. *UBC* was the negative control and *CA9* was the positive control. Data is presented as % of input and is representative of three independent experiments.

4.2.5. A role for miR-100 regulating *FGFR3* levels in RT4 cells

It has previously been shown that the MYC oncogene suppresses transcription from the miR-100 locus [231]. As FGFR3 signaling can activate MYC [232], we investigated whether FGFR3 signaling in hypoxia was responsible for reducing miR-100 levels. However, knocking down *FGFR3* levels in RT4 did not affect miR-100 levels (data not shown).

By transfecting RT4 cells with either mimic-100 or anti-miR-100, the biological relevance of miR-100 on regulating *FGFR3* expression in bladder cancer was further investigated. The transfection of mimic-100 into RT4 cells inhibited the hypoxic induction of *FGFR3* mRNA (Figure 4.5a). In addition, there was also a downregulation of FGFR3 protein expression after mimic-100 transfection (Figure 4.5b). Importantly, while transfection of RT4 cells with anti-miR-100 in normoxia did not increase *FGFR3* mRNA levels (Figure 4.5c), FGFR3 protein levels were increased after transfection of anti-miR-100 (Figure 4.5d). Thus, endogenous levels of miR-100 play a role in regulating FGFR3 protein levels in RT4 cells.

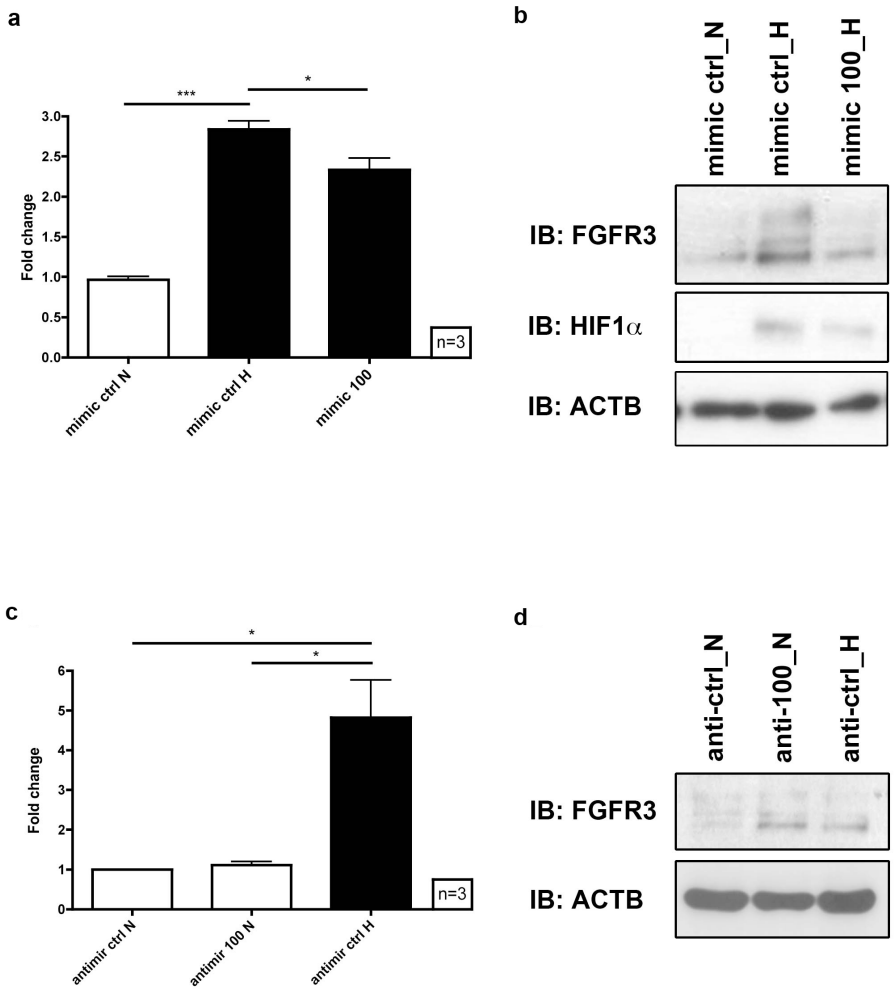


Figure 4-5 Regulation of *FGFR3* levels by miR-100

a) mRNA levels of *FGFR3* were examined in RT4 cells after exposure to hypoxia and in combination with mimic-100 transfection. Data are presented as fold change relative to mimic-ctrl in normoxia. (b) FGFR3 protein levels were examined in RT4 cells after exposure to hypoxia and in combination with mimic-100 transfection. (c) *FGFR3* mRNA levels were investigated in RT4 cells after transfection with anti-miR-ctrl in normoxia and hypoxia or anti-miR-100 in normoxia. Data are presented as fold change relative to anti-miR-ctrl in normoxia. (d) FGFR3 protein levels were examined in RT4 cells after transfection with anti-miR-ctrl in normoxia and hypoxia or anti-miR-100 in normoxia. Statistical significance: * $p<0.05$, *** $p<0.001$. Mean ± standard error.

4.2.6. miR-100 and FGFR3 regulation of downstream targets and cell growth

Activation of FGFR3 initiates signalling cascades in the cell primarily mediated by ERK (p42/44MAPK) and PKB (AKT) [233]. Therefore, the effects of FGFR3 and miR-100 on the activation of these downstream pathways was next investigated. FGFR3 knockdown reduced phosphorylation of both Ser-473-PKB (Figure 4.6a) and Thr202/Tyr204-ERK1/ERK2 (Figure 4.6b). For loss of Ser-473 phosphorylation on PKB, this effect was more prominent under hypoxic conditions, where knocking down FGFR3 led to an almost complete loss of phosphorylation (Figure 4.6a). Similarly, in hypoxia, transfection of mimic-100 caused a decrease in phosphorylation of both PKB and ERK (Figures 4.6c and d). Thus, increased levels of FGFR3 play an important role in maintaining ERK and PKB signalling in hypoxia.

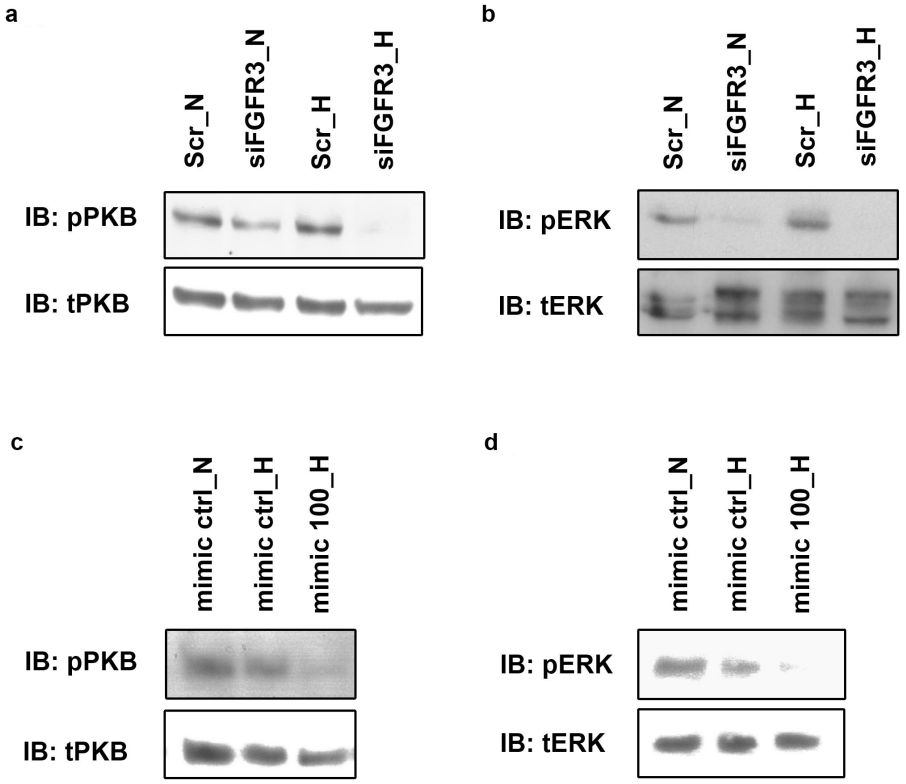


Figure 4-6 Regulation of ERK and PKB signaling by FGFR3 and miR-100

(a) Phosphorylation of S473 on PKB was examined in RT4 cells after knocking down *FGFR3* and exposing cells to normoxia or hypoxia for 24hrs. (b) The dual phosphorylation of ERK-1 on T202/Y204 (or ERK-2 on T185/Y187) was examined in RT4 cells after knocking down FGFR3 and exposing cells to normoxia or hypoxia for 24hrs. (c) Phosphorylation of S473 on PKB was examined in RT4 cells after transfecting mimic-ctrl in normoxia or hypoxia or mimic-100 in hypoxia. (d) The dual phosphorylation of ERK-1 on T202/Y204 (or ERK-2 on T185/Y187) was examined in RT4 cells after transfecting mimic-ctrl in normoxia or hypoxia or mimic-100 in hypoxia.

4.2.7. The effects of FGFR3 and miR-100 on 2-D and 3-D cell growth

It is well established that ERK and PKB activation are potent mitogenic signals. We therefore investigated the effects of miR-100 and FGFR3 on cell viability. In 2-dimensional growth in 96-well plates, hypoxia led to a significant decrease in proliferation of RT4 cells at all cell densities (Figure 4.7). At the highest cell density (4000 cells), knockdown of FGFR3 suppressed the hypoxic growth of RT4 cells even further (Figure 4.7e), and there was a similar trend towards this at the other cell densities (Figure 4.7a and c). In contrast, transfection of mimic-100 did not affect the 2-D growth of RT4.

To assess the effects of FGFR3 and miR-100 on 3-dimensional growth, RT4 cells were transfected with the appropriate siRNA/mimics and grown as spheroids. FGFR3 knockdown significantly reduced the 3-D growth of RT4 cells at 3, 5 and 7 days incubation (Figure 4.8a). Transfection of mimic-100 also significantly reduced spheroid volume of RT4 cells at 5 and 7 days (Figure 4.8b). Images of the spheroids are shown in Figure 4.8c and d.

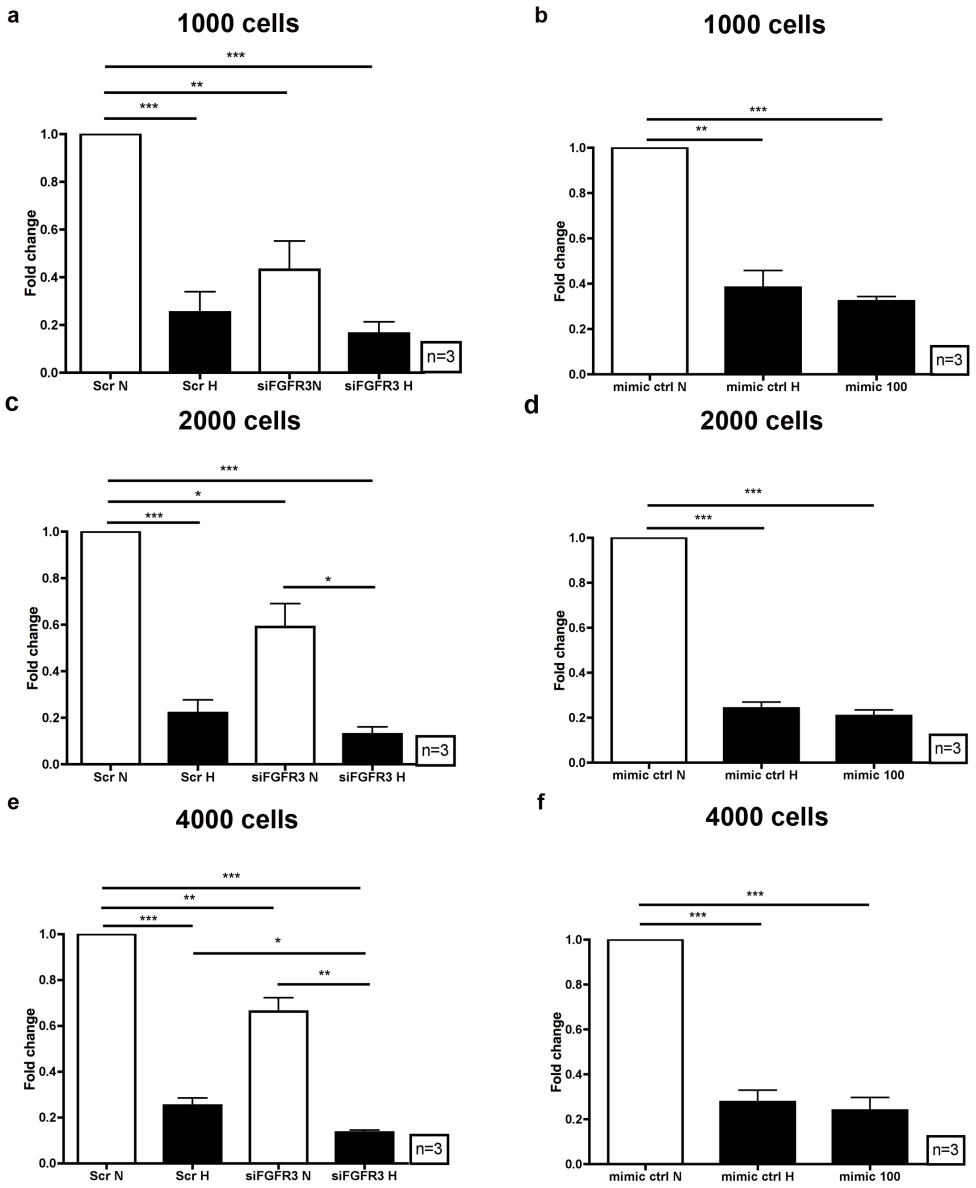


Figure 4-7 Impact of FGFR3 and miR-100 on RT4 cell viability

(a, c and e) Cell viability of RT4 was assayed with the SRB assay after knocking down *FGFR3* and exposing 1000, 2000 and 4000 cells to normoxia (white bars) or hypoxia (black bars) for 72hrs. Absorbance is presented relative to the scramble in normoxia. (b, d and f) Cell viability of RT4 was assayed with the SRB assay after transfecting mimic-100 and exposing 1000, 2000 and 4000 cells to normoxia (white bars) or hypoxia (black bars) for 72hrs. Statistical significance: * $p<0.05$, ** $p<0.01$, *** $p<0.001$. Mean ± standard error.

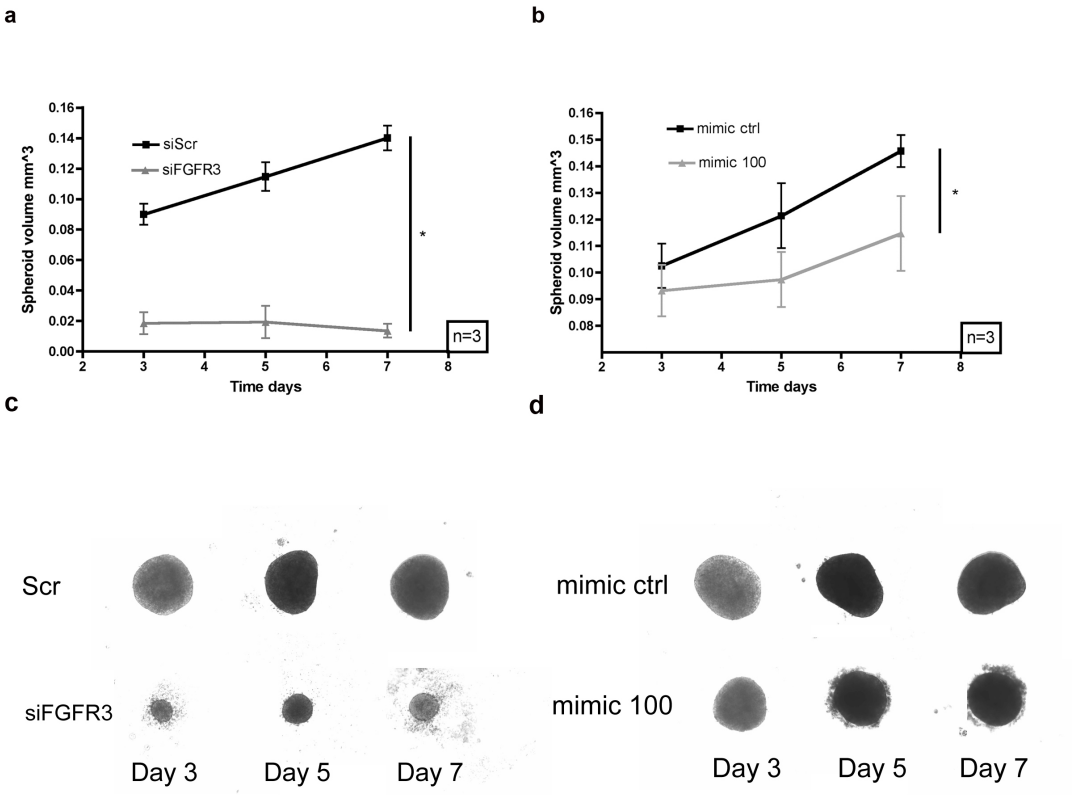


Figure 4-8 Effect of FGFR3 and mimic miR-100 upon 3-D growth of RT4 spheroids

a-b) 3-D spheroid growth of RT4 cells after knocking down *FGFR3* (triangular data points) compared to scramble transfected cells (square data points). Measurements were taken at 3, 5 and 7 days. 30 spheroids were grown in each condition and the mean size was used for calculations. Each experiment was performed in triplicate. c-d) RT4 cells were grown as spheroids and images of representative spheroids were taken at 3, 5 and 7 days. Statistical significance: * $p<0.05$, ** $p<0.01$, *** $p<0.001$. Mean ± standard error.

4.2.8. Immunohistochemistry of FGFR3 in bladder cancer samples

We examined 44 bladder tumour specimens for FGFR3 expression to determine whether FGFR3 colocalises with the known hypoxia regulated gene CA9. The tumour characteristics are shown in Table 4.2. Staining and scoring was performed by Adrian Jubb. First the FGFR3 antibody was validated by staining for FGFR3 by immunohistochemistry. Cell pellets were made from RT4 cells transfected with either Scr or siFGFR3 siRNA; the siFGFR3 cell pellet (Figure 4.9b) had almost no staining compared to the Scr transfected cell pellet (Figure 4.9a), confirming the specificity of the antibody. FGFR3 positive staining was seen in 14/25 non invasive samples and 12/19 invasive samples (Table 4.2). In those cases where FGFR3 positive staining was seen >75% of the specimen stained positive for FGFR3 and therefore colocalisation with CA9 which typically stains positive at the luminal surface of non invasive tumours could not be easily assessed. We did see focal colocalisation in 2 samples (Figure 4.9 c-d, e-f). FGFR3 staining does not exclusively colocalise with hypoxic regions; in a number of samples the staining intensity was stronger in hypoxic areas suggesting there may be an element of hypoxic upregulation *in vivo.*

	Inverted papilloma	pTa	>T1	Total
Number of cases	3	22	19	44
FGFR3 positive	0	14	12	26

Table 4-2 Number and stage of tumours stained for FGFR3 and CA9

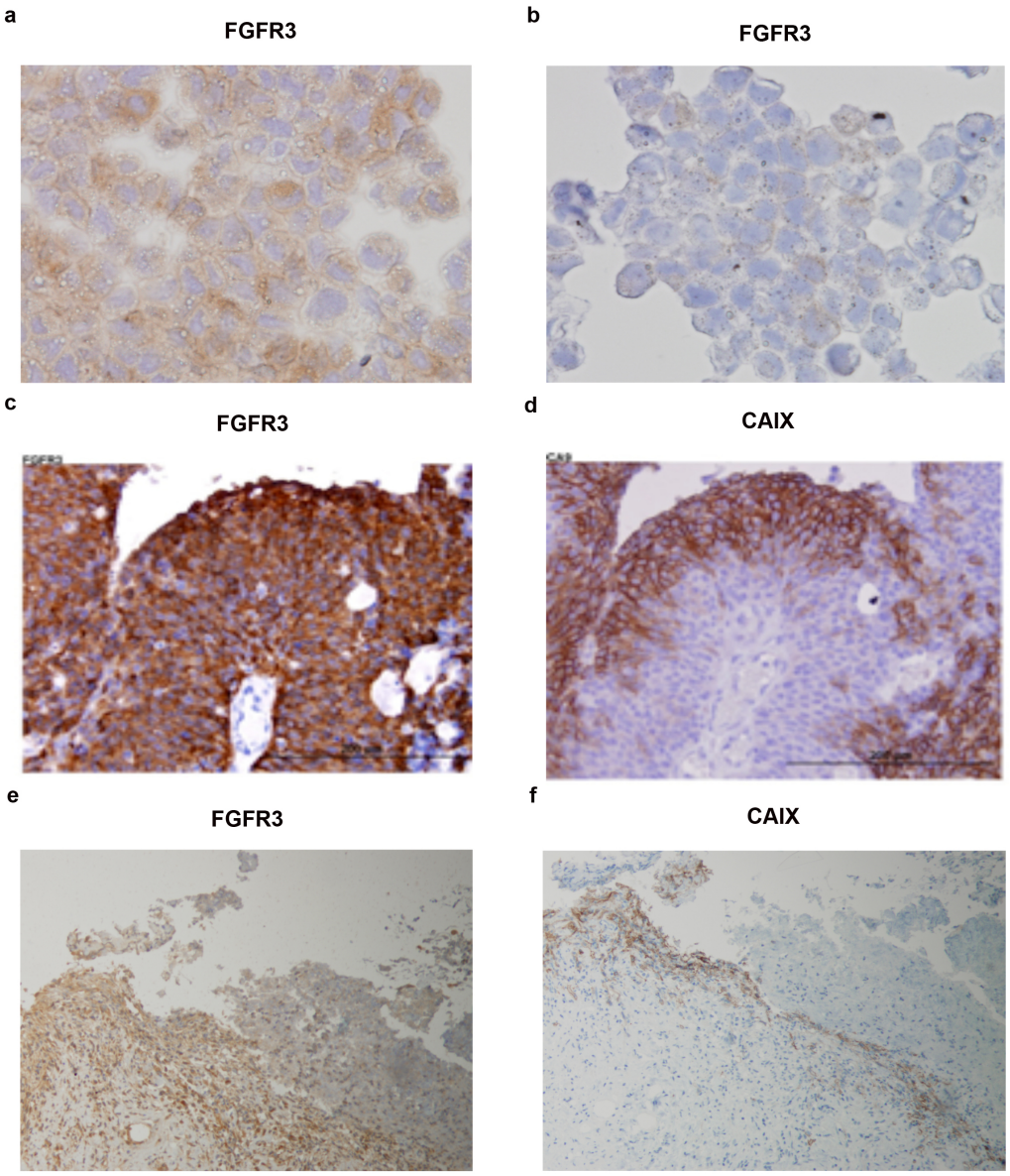


Figure 4-9 Immunohistochemistry of FGFR3

a) RT4 cells were transfected with scramble siRNA were cultured in hypoxia and stained for FGFR3. (b) RT4 cells were transfected with siFGFR3 and cultured in hypoxia and stained for FGFR3. A grade 1 pTa tumour was then stained for (c) FGFR3 and (d) CA9. A second grade 1 Ta tumour was also stained for (e) FGFR3 and (f) CA9.

4.3 Discussion

4.3.1 The hypoxic regulation of FGFR3

Hypoxia is an important aspect of tumour biology. It is known that in addition to its effects on metabolic reprogramming, hypoxia can lead to the activation of RTK pathways such as signaling by EGFR [234, 235]. In addition, HIF-1α has been shown to directly target the *C-MET* RTK for transcriptional induction [236]. In this chapter, we show for the first time that FGFR3 is induced in bladder cancer cell lines by hypoxia in a manner that is dependent on HIF-1α. Alterations in FGFR3 are a key event in bladder cancer, either by mutation or by increased expression in non muscle invasive and invasive bladder cancers [6]. Tumour hypoxia may represent an additional mechanism for increased levels of FGFR3 in bladder cancer. Hypoxic regulation of FGFR3 may also be relevant in other tumours that have also been shown to express FGFR3 including myeloma, head and neck [233] and liver cancer [237]. The coordinated regulation of FGFR3 expression by additional pathways warrants further investigation as p73 and p63, members of the p53 family of transcription factors, have been shown to induce FGFR3 transcription [238].

At present, we have not been able to identify a functional HRE in the promoter region of FGFR3. Chromatin immunoprecipitation with HIF-1 followed by high throughput sequencing has recently been performed to identify HREs in MCF7 cells [239]; no putative HREs were identified for FGFR3 in that cell line (David Mole, personal communication). While this does not mean that no HREs exist for FGFR3 as hypoxic induction and HIF binding are likely to be cell line specific, at

present it would appear that the increase in *FGFR3* mRNA and FGFR3 protein that occurs in hypoxia is not due to direct transcriptional activation by HIF.

4.3.2. miR-100 regulation of FGFR3

To further understand the potential mechanisms by which FGFR3 levels may be increased under hypoxia, we chose to investigate the role of the microRNA-100. We have previously shown that miR-100 can target FGFR3 and that the expression of these two molecules at the mRNA levels were negatively correlated in bladder cancer[184]. In this chapter, we found that miR-100 levels decreased after exposure of RT4 cells to hypoxia. As no comparable data set of matched miRNA and mRNA gene expression data is available for bladder cancer, we interrogated our own breast cancer data series for regulation of miR-100. Importantly, *in vivo*, the expression of miR-100 was anti-correlated to tumour hypoxia in breast cancer, suggesting that the ability of hypoxia to decrease miR-100 levels occurs in other tumour types as well. Indeed aberrant expression of miR-100 has been reported in ovarian, renal, prostate and bladder cancers [240, 241].

4.3.3. Mechanisms of FGFR3 and miR-100 regulation

The mechanism of downregulation of hypoxia regulated genes, and miRNAs in particular, is unclear. Recent work suggests that genes downregulated under hypoxia are not direct targets of HIF [242]. Intriguingly, the hypoxic decrease of miR-100 was not affected by knockdown of either *HIF-1α* or *HIF-2α*. In the previous chapter, we showed the hypoxic suppression of miR-100 could not be

recapitulated by treating cells with the HIF stabilizing agent DMOG in normoxia (Figure 3.11). Thus, it would appear that the ability of hypoxia to downregulate miR-100 expression is not HIF dependent. While the majority of cellular responses to hypoxia are mediated by HIF, a number of HIF independent events in hypoxia have been reported. For example, the induction of heme oxygenase-1 under hypoxia in Chinese hamster ovary cells is independent of HIF [243, 244]. Furthermore, the hypoxic induction of ICAM-1 in monocytes is dependent on NF-κB and not HIF [245]. Recently, in *C.elegans* neurons, hypoxia was shown to regulate glutamate receptor trafficking in a manner that was independent of HIF-1, but involved the activity of the *C. elegans* PHD orthologue *egl-9* [246]. It is likely one of the other stress response pathways is be responsible for regulating the expression of a subset of genes under hypoxia [247], as has been reported for heme oxygenase-1 [248]. Regardless, we have found that miR-100 expression in RT4 cells contributes to the regulation of FGFR3 levels as transfection of anti-miR-100 is capable of increasing FGFR3 levels in normoxia and introduction of mimic-100 decreases FGFR3 levels in hypoxia.

Functionally, FGFR3 and miR-100 are responsible for regulating cell proliferation of RT4 cells. Of note is the observation that knocking down FGFR3 expression in RT4 cells led to a dramatic decrease in cell viability in normoxia and hypoxia, concomitant with a decrease in the activation of PKB and ERK signaling. Thus, even in cells expressing *FGFR3* without a point mutation (such as RT4), autocrine and/or paracrine signaling clearly play an indispensible role in cell viability. Indeed, a recent study using small molecule inhibitors against FGFR3 led to a significant decrease in viability of a number of bladder cell lines expressing FGFR3 without point mutation[249]. We found knockdown of FGFR3

had a more dramatic effect on reducing the phosphorylation of ERK and PKB in cells exposed to hypoxia compared to their normoxic counterparts. This strongly suggests that increased levels of FGFR3 plays a crucial role in maintaining the viability of RT4 cells exposed to hypoxia.

The role of miR-100 was found to be more subtle [250], with a decrease in cell viability observed in 3-D cultures but not 2-D growth. Thus, the role of miR-100 is more pronounced in stressful cellular conditions, when nutrient supply is perhaps more limiting and oxygen gradients are steeper. A single miRNA is likely to regulate the expression of multiple target genes, although the effect on each may be subtle. In addition to *FGFR3*, other targets of miR-100 include polo-like kinase 1 (*PLK1*) [251] and the phosphatase *RBSP3* [252]. In addition, miR-100 has recently been shown to target *mTOR* in clear cell ovarian cancer [240]. Thus, under more severe conditions of 3-D growth, miR-100 is likely to play an important role in regulating cell proliferation and viability by targeting additional pathways, such as mTOR [253], which plays a key role during stress. On a related point, downregulation of miR-100 may be one mechanism that contributes to keeping the mTOR pathway active under hypoxic conditions.

4.3.4. Translational relevance

The high incidence of overexpression and mutation of FGFR3 in bladder cancer has led to speculation FGFR3 may have a role as a diagnostic and prognostic marker. FGFR3 mutations can be detected in genomic DNA isolated from urine; however this investigation is not widely performed. The bladder cancer phenotype associated with FGFR3 mutation is one with a low rate of progression

and recurrence, however overexpression of wild type FGFR3 has not been linked with clinical outcome [225, 254].

The role of FGFR3 in the treatment of bladder cancer has not yet been established. Both mutant and wild type FGFR3 have been targeted by small molecule inhibitors, neutralizing antibodies and targeted therapies [249, 255, 256] and these strategies have been successful in inhibiting cell proliferation and inducing cell cycle arrest *in vitro* and *in vivo*. These therapies are known to target other receptor tyrosine kinases and it is not clear to what extent these are off target effects. Normal urothelial cells appear to be unresponsive to FGFR3 inhibitors [249]. The specific nature of targeted therapies and the two distinct molecular pathways in bladder cancer will inevitably require the development of biomarkers to aid in patient selection. It is possible that microRNAs and in the case of *FGFR3*, miR-100 could be used to target and inhibit the expression of FGFR3.

4.3.5. Conclusion

In this chapter, we have shown for the first time, hypoxic regulation of FGFR3 that is partly dependent on suppression of miR-100 expression. This represents a novel mechanism for regulating FGFR3 in bladder cancer that may provide an additional mechanism for increased expression of this growth promoting pathway that could contribute to the pathogenesis of this disease. The link with hypoxia may explain the strong association with the papillary phenotype, where it has been shown that the luminal cells away from the vascular core are hypoxic. This may provide selection for upregulation of FGFR3 and maintenance of the

papillary phenotype. FGFR3 overexpression may provide a positive effect by preventing progression to muscle invasive disease. The use of therapies targeting FGFR3 may lead to the loss of this potentially protective mechanism and require additional studies. Finally, miR-100 is known to target *mTOR*. Thus, downregulation of miR-100 may in part be responsible for maintaining mTOR activity in hypoxia but may also affect the sensitivity of cells to the inhibitor rapamycin, as has been reported for clear cell ovarian cancer [253]. In the next chapter, we will look at whether exposure of primary bladder cancer cells to hypoxia and established renal cancer cell lines with vHL mutations have altered sensitivity to drugs, including rapamycin.

Chapter 5 The role of vHL mutation and hypoxia regulated genes in predicting sensitivity to targeted therapies in renal cancer.

5.1. Introduction

5.1.1. vHL and renal cancer

The cellular outcomes of hypoxia are primarily mediated by the heterodimeric transcription factor HIF. Under normoxic conditions the α subunits are hydroxylated on two proline residues by a family of oxygen and α-ketoglutarate dependent prolyl hydroxylases [257] (see also Chapter 1.3.1). The hydroxylated α subunits are recognized by a ubiquitin ligase complex that leads to its ubiquitination and subsequent degradation by the 26S proteasome. A key component of the ubiquitin ligase complex is the product of the von Hippel-Lindau (*vHL*) gene that recognizes the hydroxylated proline residues on the α subunit. Under hypoxic conditions, prolyl hydroxylase activity is impaired, leading to HIF stabilization and the transcription of HIF target genes involved in invasion, metabolism, angiogenesis and apoptosis [32].

Hypoxia is a feature of many solid cancers as a consequence of poor tumour vascularization and a concomitant decrease in oxygen delivery. Increased tumour hypoxia is associated with resistance to chemotherapeutic drugs and worse overall disease free survival [258]. The importance of hypoxia and the HIF pathway in cancer is further highlighted by the high frequency of mutations of the tumour suppressor gene *vHL* in renal cell cancer (RCC) [259-261]. The majority of clear cell RCCs have lost *vHL* function, either as a consequence of

mutation or promoter silencing [260]. However, despite the conservation of this genetic change, the clinical outcome varies markedly across patients and is likely to reflect the differential regulation of downstream pathways, as well as additional mutations [162].

Although the heterogeneity of renal cancers is well described, much of the current work in the field makes use of established, historic cell lines that may not accurately reflect actual tumours. While a number of groups have established primary tumour cell lines *in vitro* from nephrectomy specimens [262], the sensitivity of these primary cell lines against targeted therapies have not previously been tested.

5.1.2. Targeted therapies in renal cancer

The prognosis for metastatic RCC is poor. Traditional chemotherapy in this disease has involved the use of cytokines; however, these are toxic and only effective in a small number of patients. Over last 5 years, a new generation of targeted therapeutic agents that more selectively inhibit pathways activated in cancer have been approved in the management of RCC. These include bevacizumab, a monoclonal antibody that binds to and sequesters VEGF, and small molecule inhibitors such as such as sorafenib, sunitinib and pazopanib that inhibit oncogenic kinases (see Chapter 1.6.4. for a discussion on these drugs).

5.1.2.1 Integration of the mTOR pathway and hypoxia

Activation of the mTOR signaling pathway leads to new protein synthesis (Figure 1.5 and 5.18), a process that is energy intensive. Under hypoxic conditions, the mTORC1 pathway must be attenuated as an adaptive mechanism to low oxygen, nutrient supply and energy levels.

The integration of mTOR signaling and hypoxia occurs at two levels. In the first instance, hypoxia, induces the expression of the REDD proteins (regulated in development and DNA damage response). Two isoforms of the REDD protein exist, encoded by two different genes. REDD1 is a HIF target gene [198], whose expression is induced under hypoxia as well as in response to other stress signals. The REDD proteins are inhibitors of mTOR signaling. Although their mechanism of action is not fully elucidated, it is thought that one possibility is that they compete with TSC1/2 for binding to the cytoplasmic protein 14-3-3. This, therefore, leads to the release of TSC1/2, which can then inhibit mTOR [263] (Figure 5.18). The ability of hypoxia to regulate REDD1 induction and mTOR activity appears to be dependent on the stress-sensor protein Ataxia-Telangiectasia Mutated (ATM) as suppression of phosphorylation of the mTORC1 targets p70S6K and 4EBP1 were lost in ATM knockout mouse embryonic fibroblasts [264].

The second point of crosstalk between mTOR signaling and hypoxia is at the point of HIF translation. Signaling from mTOR has been shown to contribute to the maintenance of HIF-1 levels in hypoxia [64]. The 5'UTR of the HIF-1α transcript contains a terminal polyoligopyrimidine (5'-TOP) sequence. Activation of p70 S6Kinase by mTORC1, and subsequent phosphorylation of the ribosomal S6 protein prioritises the translation of mRNA with these 5'-TOP

sequences (including many ribosomal proteins); in some cases, 5'-TOP dependent translation can account for as much as 60% of HIF-1α protein levels [265]. It is also possible that the mTOR pathway is in part regulated by prolyl hydroxylase domain containing proteins, a group of proteins that are well recognized as playing an integral role in the HIF activation pathway [266]. Increased activity of the mTOR pathway has been found in a number of cancers [161, 163]. In addition, renal cancer cells in which vHL had been knocked down were highly sensitive to growth inhibition by the mTOR inhibitor, rapamycin [267], therefore, suggesting that targeting the mTOR pathway may be useful in the treatment of renal cancer. The rapamycin analogues temsirolimus and everolimus have now been approved as first line therapy for the treatment of metastatic RCC (see Chapter 1.6.4 for a discussion). In the clinical setting mTOR inhibitors are metabolized to rapamycin, for example the trough plasma levels of Serolimus are in the range of 4-20nM [268]. Under the dosing schedule approved by the FDA for renal cell cancer, administration of the rapamycin analogue temsirolimus results in peak sirolimus levels of 72nM [269].

5.1.2.2. The role of the AMPK pathway in cancer

Another pathway important for controlling cellular metabolism that may play an important role in cancer is that mediated by the AMP-activated protein kinase (AMPK). AMPK is a trimeric protein complex with a catalytic α subunit and regulatory β and γ subunits. Under conditions of stress, the ratio of ATP to AMP in a cell drops; AMP binds to the γ subunit and protects an activating

phosphorylation mediated by LKB1. Activated AMPK inhibits ATP consuming pathways in a cell, chief among them being mTORC1. Inhibition of the mTORC1 complex is achieved by phosphorylation of the pathway inhibitor TSC2 by AMPK [270]. AMPK has also been shown to directly phosphorylate RAPTOR causing subsequent inhibition of mTORC1 and cell cycle arrest [271]. The importance of AMPK signaling is highlighted by the fact that loss of function mutations in *LKB1* are causal in Peutz-Jeghers syndrome, which is characterized by predisposition to cancer, and have also been documented in around 40% of non-small cell lung cancer [272]. Recently, treatment of renal cancer cells with the AMPK activators AICAR or metformin was found to decrease cell viability of RCC cell lines [273], suggesting that activating AMPK may be a useful therapeutic tool in the management of renal cancer. In fact activation of AMPK through the use of metformin is currently being investigated in a number of cancers including breast, head and neck and renal cancers [274-276].

To enable clinicians to maximize the effectiveness of treatment, there is a significant clinical need for more accurate and patient specific diagnostic tests and prognostic markers. Detailed investigations to accurately diagnose RCC tumour characteristics that predict disease recurrence, progression or metastasis have not been performed to date. The aim of this chapter was to identify biomarkers in RCC tumours that may correlate/predict response to chemotherapeutic drugs used in the treatment of this disease. We began by looking at a potential link with miRNA expression, and in particular, miR-100 as it has been shown to target mTOR. We then performed drug response studies on established renal cancer cell lines and subsequently on cultures of primary renal tumours to better assess the response of tumours *in vivo* to these agents. The

vHL status of these primary tumours was also assessed. We investigated the mRNA expression of a number of genes involved in the hypoxic, mTOR and general cell proliferation pathways to determine whether their expression correlated with *vHL* mutation status and response to targeted therapy agents.

5.2. Results

5.2.1. The effect of hypoxia on miR-100 expression in renal cancer cell lines

Previously, miR-100 was found to be downregulated by hypoxia in the bladder cancer cell line RT4 (Figure 3.10 and Figure 4.1). MiR-100 suppresses mTOR expression in these cells (Figure 5.1a) [253]. Therefore, we investigated a potential role for miR-100 in renal cancer and sensitivity to rapamycin. The expression of miR-100 expression in the renal cancer cell lines RCC4 and 786-0 was first examined. The expression of miR-100 was not regulated by hypoxia in either cell line, irrespective of *vHL* status (Figure 5.1b,d). However, in 786-0 cells, miR-100 expression was significantly lower in *vHL* null cells (Figure 5.1d). Hypoxia regulated miR-210 was used as a positive control and was induced by hypoxia in *vHL* competent RCC4 and 786-0 cells (Figure 5.1 c, e). In *vHL* null RCC4 cells, high levels of miR-210 expression were seen in both normoxia and hypoxia due to the constitutive activation of HIF-1α (Figure 5.1c). In 786-0 cells, only modest upregulation of miR-210 was evident in *vHL* null cells compared to their *vHL* competent counterparts (Figure 5.1e). Our group has previously found miR-100 to be downregulated in renal tumour samples when compared with normal renal tissue (Figure 5.1f produced by Robert McCormick unpublished).

Finally, transfection of mimic-100 did not affect the sensitivity of the bladder cancer cell line, RT4, to rapamycin (data not shown).

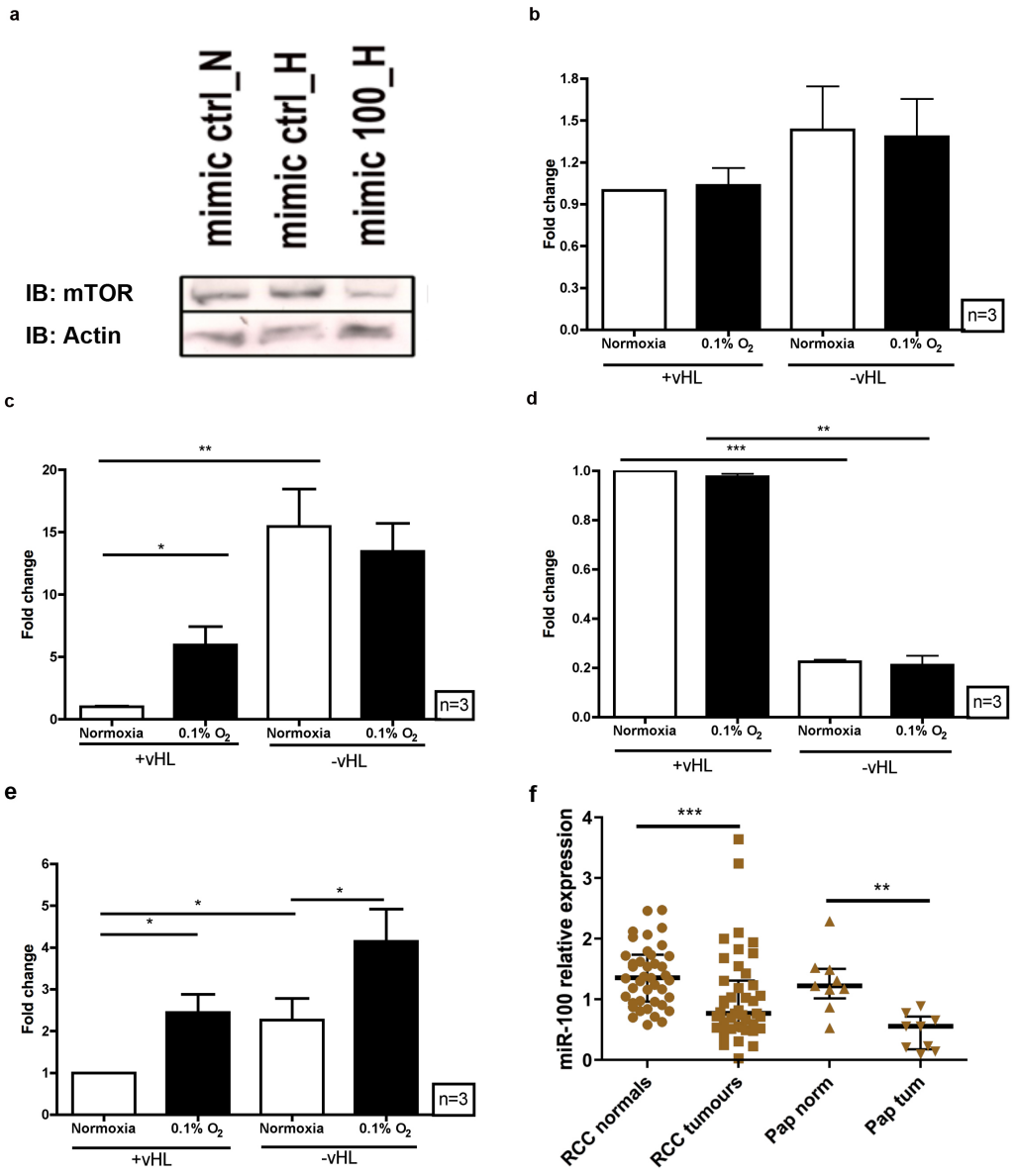


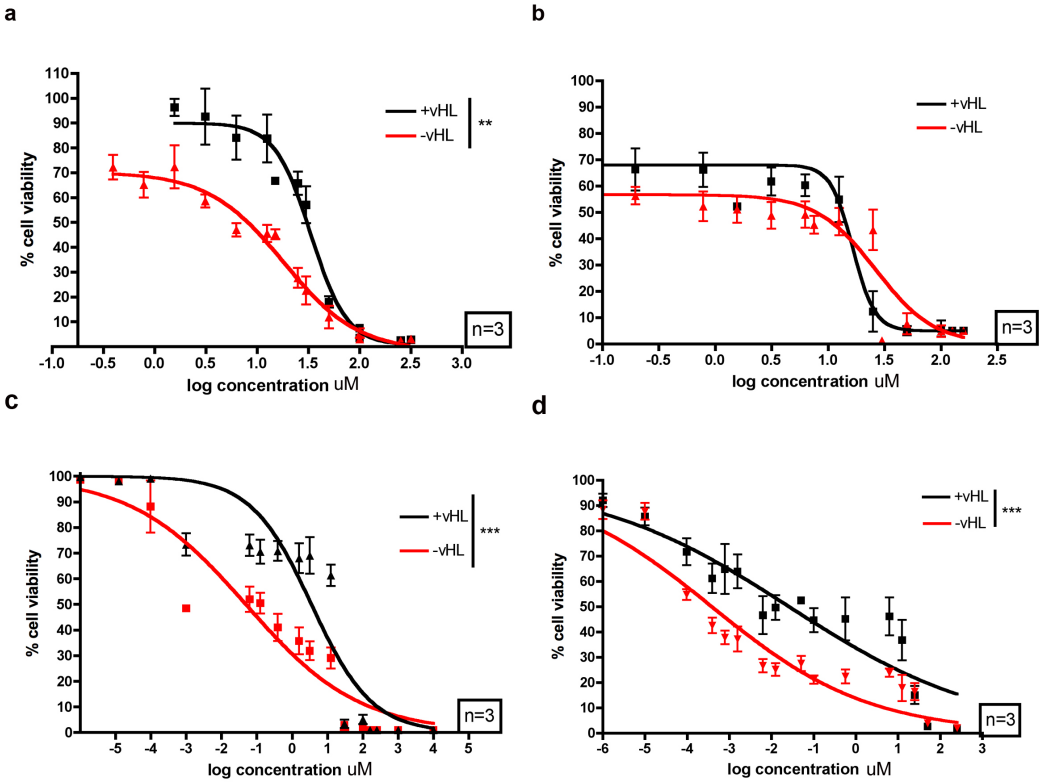
Figure 5-1 miR-100 regulation by hypoxia

(a) Western blot of mTOR expression in RT4 cells transfected with either mimic control or mimic-miR-100 and exposed to normoxia or 0.1%O_2 for 24 hours. MiR-100 levels were examined in (b) RCC4 and (d) 786-0 cells after exposure to 24 hours of normoxia or 0.1% O_2. MiR-210 levels were examined in (c) RCC4 and (e) 786-0 cells after exposure to 24 hours of normoxia or 0.1%O_2. Data is presented as fold change relative to expression in the *+vHL* sample of each cell line in normoxia. (f) MiR-100 expression in matched normal and renal tumour samples separated into clear cell (RCC) and papillary (pap) tumours. Statistical significance: * $p<0.05$, ** $p<0.01$, ***$p<0.001$. Mean ± standard error.

We next investigated the effect of *vHL* mutation on the sensitivity of RCC to a number of chemotherapeutic agents currently employed in the treatment of this disease - rapamycin, sorafenib, sunitinib and metformin. Initial work was carried out with the established RCC lines RCC4, 786-0 and UMRC2, and subsequently sensitivity was investigated in primary RCC cell lines. SRB assays were performed to assess cell viability.

5.2.2. Sensitivity of *vHL* null and competent RCC4 cells to rapamycin

The sensitivity of *vHL* null and competent RCC4 cells to rapamycin was investigated at 4 time points to optimize the technique. Rapamycin was toxic at concentrations greater than 100μM. The absence of functional *vHL* increased the sensitivity of RCC4 cells to rapamycin at 24, 72 and 96 hours (Figure 5.2). For both *vHL* null and *vHL* competent RCC4 cells, the IC50 value for rapamycin was inversely proportional to the duration of treatment, being over 1000 fold lower at 96hrs (Figure 5.2d) than at 24hrs (Figure 5.2a).



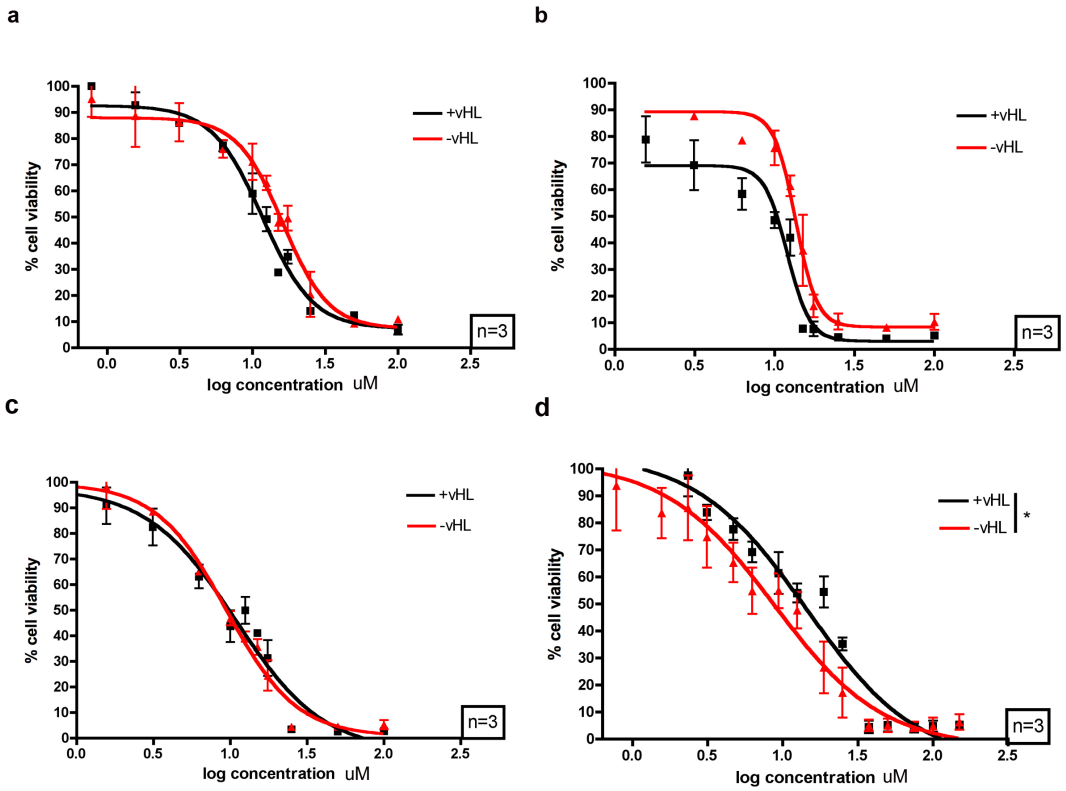
	24 hours	48 hours	72 hours	96 hours
RCC4 *+vHL*	33.3µM	16.5µM	3.5µM	0.03µM
RCC4 *-vHL*	17.9µM	24.3µM	0.09µM	0.0004µM
Significance	p=0.01	n/s	p<0.001	p<0.001

Figure 5-2 Rapamycin sensitivity in RCC4 cells

RCC4 cells were cultured for (a) 24, (b) 48, (c) 72 and (d) 96 hours following treatment with various concentrations of rapamycin. Data are presented as % cell viability of the control population, mean points and standard error of three replicates. A non linear curve of best fit is shown. Two way ANOVA tests were performed to examine differences between cell lines. Statistical significance: * p<0.05, ** p<0.01, *** p<0.001.

5.2.3. Sensitivity of vHL null and competent RCC4 cells to sunitinib

For *vHL* competent RCC4 cells, there was no correlation between the sensitivity of RCC4 cells to sunitinib and the duration of treatment (Figure 5.3). The absence of *vHL* did not affect sensitivity compared to *vHL* competent cells at 24-72 hours; (Figure 5.3a-c). However at 96 hours *vHL* negative cells were modestly more sensitive to sunitinib (Figure 5.3d). It is unclear whether this is a real effect but the lack of consistency at each of the 4 time points suggests it is unlikely *vHL* mutation alters *in vitro* sensitivity to sunitinib. IC50 values of between 5 and 15μM were consistent with those previously published [277]. Dosing of sunitinib according to the FDA approved schedule for renal cancer leads to peak plasma levels of sunitinib of around 200nM [278].



	24 hours	48 hours	72 hours	96 hours
RCC4 *+vHL*	11.9µM	12.0µM	10.8µM	14.3µM
RCC4 *-vHL*	16.1µM	13.5µM	9.4µM	8.7µM
Significance	n/s	n/s	n/s	p=0.02

Figure 5-3 Sunitinib sensitivity in RCC4 cells

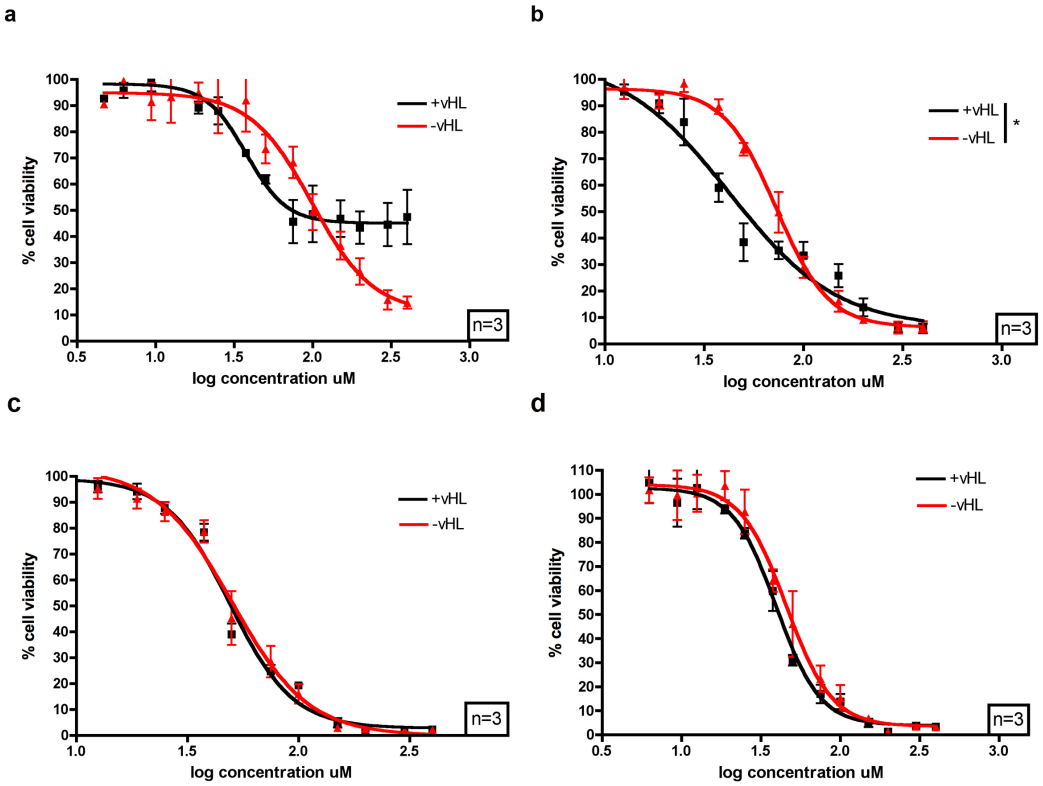
RCC4 cells were cultured for (a) 24, (b) 48, (c) 72 and (d) 96 hours following treatment with various concentrations of sunitinib. Data are presented as % cell viability compared to the control population, mean points and standard error of three replicates. A non-linear curve of best fit is shown. Two way ANOVA tests were performed to examine differences between cell lines. Statistical significance: * $p<0.05$, ** $p<0.01$, *** $p<0.001$.

5.2.4. Sensitivity of *vHL* null and competent RCC4 cells to sorafenib

Published IC50 data for the effects of sorafenib on the activity of individual cellular kinases activity vary from 6nM to 1μM [279]. In contrast, the observed IC50 values for effects on cell viability were 10-100 fold greater (Figure 5.4), similar to values obtained for hepatocellular carcinoma cell lines [280]. There was a trend for *vHL* null RCC4 cells to be more resistant to sorafenib for up to 48 hours of exposure (Figure 5.4a and b). However, this result was not reproduced at later time points (Figure 5.4c and d). For *vHL* competent RCC4 cells, the IC50 values were not proportional to the duration of treatment while for *vHL* null cells, the IC50 decreased by approximately half from 24-96 hours. In the clinical setting the maximum plasma concentration of sorafenib used in the treatment of renal cancer are around 15μM [281].

5.2.5. Sensitivity of *vHL* null and competent RCC4 cells to metformin

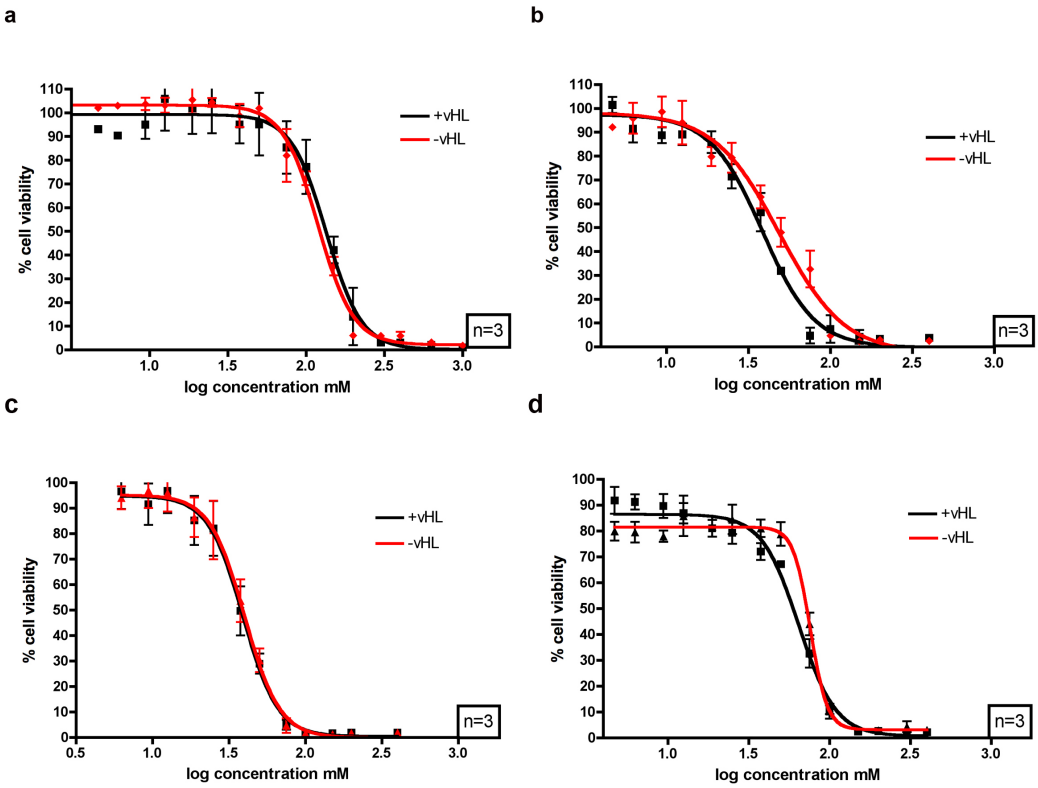
Metformin inhibits cell proliferation by activating AMPK and subsequently leading to the inhibition of mTOR [282]. IC50 in RCC4 cells were similar to those published in other cell lines. Both *vHL* null and *vHL* competent RCC4 cells had similar IC50 values for the different time points. In both cases, cells were more resistant at 24 hours, with moderately increased sensitivity evident at later time points (Figure 5.5). The usual serum concentrations of metformin in clinical use range from 7-31μM [283]



	24 hours	48 hours	72 hours	96 hours
RCC4 *+vHL*	35.9µm	34.9µm	48.9µM	39.4µm
RCC4 *-vHL*	100µm	76.9µm	49.9µM	45.5µm
Significance	n/s	P=0.02	n/s	n/s

Figure 5-4 Sorafenib sensitivity in RCC4 cells

RCC4 cells were cultured for (a) 24, (b) 48, (c) 72 and (d) 96 hours following treatment with various concentrations of sorafenib. Data are presented % cell viability compared to the control cell population, as mean points and standard error of three replicates. A non linear curve of best fit is shown. Two way ANOVA tests were performed to examine differences between cell lines. Statistical significance: * $p<0.05$, ** $p<0.01$, *** $p<0.001$.



	24 hours	48 hours	72 hours	96 hours
RCC4 *+vHL*	134mM	75.3mM	38.8mM	64.4mM
RCC4 *-vHL*	119mM	67.1mM	40.0mM	75.8mM
Significance	n/s	n/s	n/s	n/s

Figure 5-5 Metformin sensitivity in RCC4 cells

RCC4 cells were cultured for (a) 24, (b) 48, (c) 72 and (d) 96 hours following treatment with various concentrations of metformin. Data are presented as % cell viability compared to the control cell population, as mean points and standard error of three replicates. A non linear curve of best fit is shown. Two way ANOVA tests were performed to examine differences between cell lines. Statistical significance: * $p<0.05$, ** $p<0.01$, *** $p<0.001$.

5.2.6. Sensitivity of 786-0 cells to chemotherapeutic agents

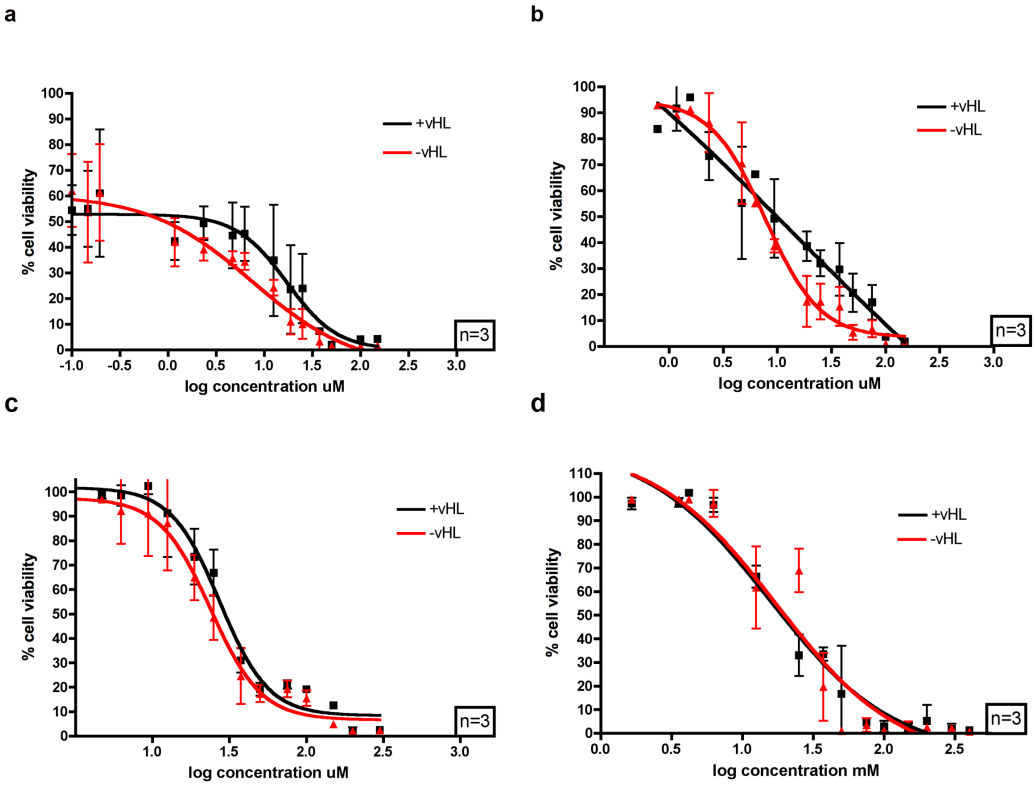
Next, the sensitivity of 786-0 cells to rapamycin, sunitinib, sorafenib and metformin was assessed. Cell viability was quantified using SRB assays at 72 hours, in line with a number of previous similar studies [284].

Even at the lowest doses, 72 hours of exposure to rapamycin led to an approximately 50% decrease in cell viability relative to untreated controls for both *vHL* competent and *vHL* null 786-0 cells. Although the IC50 value for *vHL* null cells was less that *vHL* competent cells, this was not statistically significant (Figure 5.6a).

Sunitinib sensitivity in 786-0 was similar to those in RCC4 cells. While the IC50 value was higher in the *vHL* competent 786-0 cells compared to their null counterparts this was not statistically significant (Figure 5.6b).

The IC50 values for sorafenib were lower in 786-0 when compared to RCC4 cells (50μM) and *vHL* status of these cells did not effect their sensitivity after 72 hours of treatment (Figure 5.6c).

The IC50 values for 786-0 cells treated with metformin were similar for both *vHL* competent and null cells but were lower than those observed in RCC4 (40μM) (Figure 5.6d).



	Rapamycin	Sunitinib	Sorafenib	Metformin
7860 *+vHL*	17.0µM	15.0µM	27.3µM	15.5mM
7860 *-vHL*	7.5µM	7.7µM	23.8µM	17.3mM
Significance	n/s	n/s	n/s	n/s

Figure 5-6 Drug sensitivity in 7860 cells

786-0 cells were treated with (a) rapamycin, (b) sunitinib, (c) sorafenib and (d) metformin for 72 hours. Data are presented as % cell viability compared to the control cell population, mean points and standard error of three replicates. A non linear curve of best fit is shown. Two way ANOVA tests were performed to examine differences between cell lines. Statistical significance: * $p<0.05$, ** $p<0.01$, *** $p<0.001$.

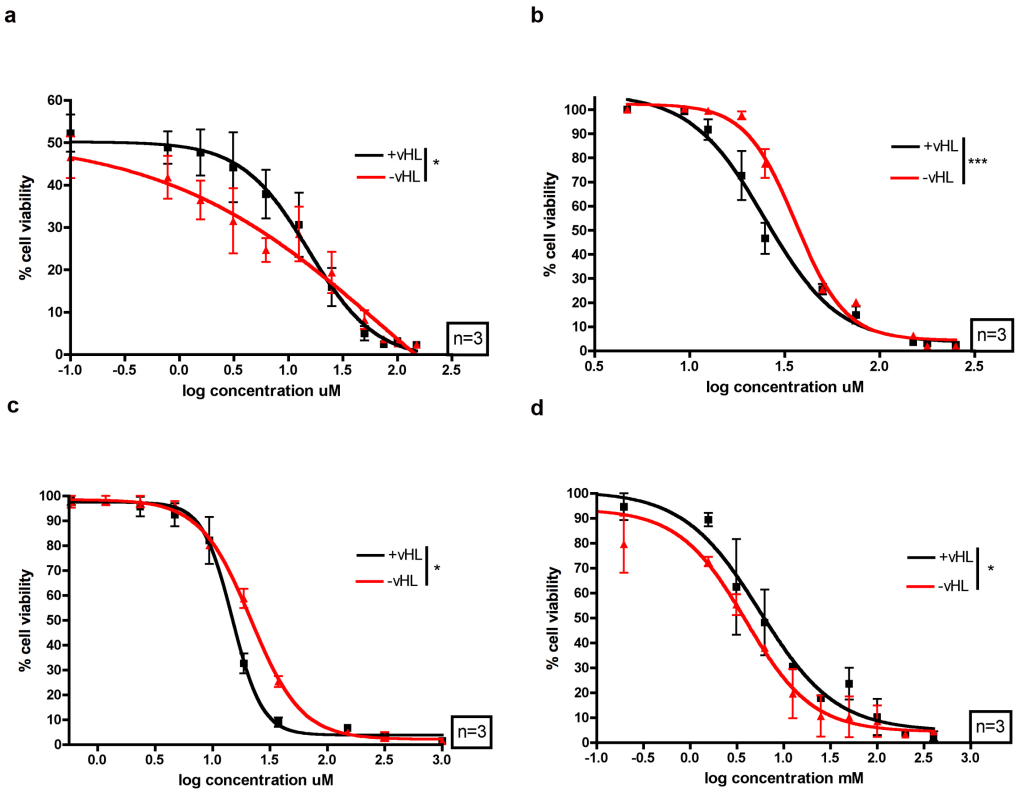
5.2.7. Sensitivity of UMRC2 cells to chemotherapeutic agents

We also assessed the sensitivity of the RCC line UMRC2 cells to rapamycin, sunitinib, sorafenib and metformin. As with the 786-0 cells, cell viability was quantified using SRB assays at 72 hours. The phenotype of UMRC2 cells is thought to be closer to that of RCC4 rather than 786-0 cells [285]. However, like 786-0, even the lowest doses tested led to an approximately 50% decrease in cell viability compared to untreated controls for both *vHL* competent and *vHL* null UMRC2 cells. We found *vHL* null UMRC2 cells were significantly more sensitive to rapamycin than *vHL* competent cells (0.07μM versus 15.3μM respectively (Figure 5.7a).

Contrary to our findings in other cell lines we found that *vHL* competent UMRC2 cells were modestly, but significantly, more sensitive than *vHL* null cells to sunitinib ($p<0.001$), with the IC50 value was approximately 10μM lower (Figure 5.7b). In addition, IC50 values were higher in UMRC2 compared to RCC4 cells.

Like their response to sunitinib, *vHL* competent UMRC2 cells were also more sensitive to sorafenib than *vHL* null cells ($p=0.01$) (Figure 5.7c). Furthermore, the IC50 values for sorafenib in UMRC2 cells were lower than those in RCC4 cells.

While we found *vHL* null UMRC2 cells to be more sensitive to metformin than *vHL* competent cells, the difference in IC50 values was only 2μM and so, is not likely to be biologically relevant (Figure 5.7d). Again, the IC50 values for metformin in UMRC2 cells were lower than those in RCC4 cells.



	Rapamycin	Sunitinib	Sorafenib	Metformin
MMRC2 *+vHL*	15.3µM	24.8µM	14.9µM	5.5mM
MMRC2 *-vHL*	0.1µM	35.9µM	21.5µM	3.9mM
Significance	p= 0.04	p<0.01	p=0.01	p=0.02

Figure 5-7 Drug sensitivity in UMRC2 cells

UMRC2 cells were treated with (a) rapamycin, (b) sunitinib, (c) sorafenib and (d) metformin for 72 hours. Data are presented as % cell viability compared to the control cell population, mean points and standard error of three replicates. A non linear curve of best fit is shown. Two way ANOVA tests were performed to examine differences between cell lines. Statistical significance: * p<0.05, ** p<0.01, *** p<0.001.

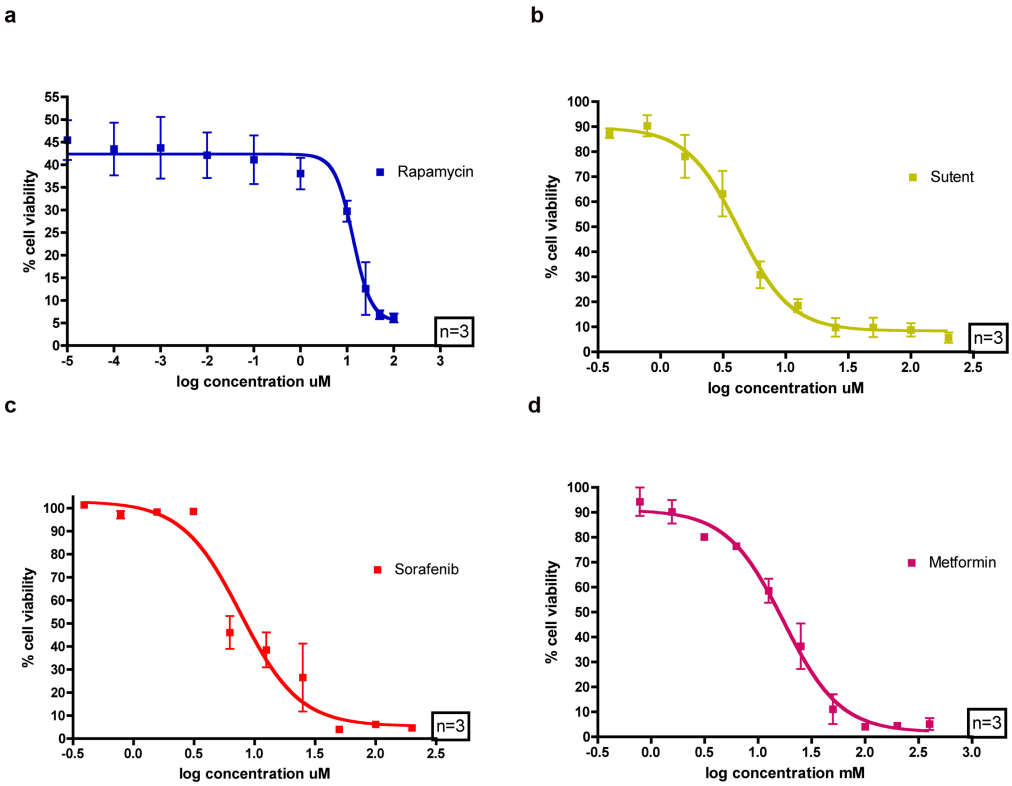
5.2.8. Sensitivity of HUVEC cells to chemotherapeutic agents

To compare the effect of targeted therapies on normal cells with responses in RCC lines, human umbilical vein endothelial cells (HUVECs) cells were treated for 72 hours with rapamycin, sunitinib, sorafenib and metformin and cell viability measured by SRB assays.

HUVECs showed much greater sensitivity to rapamycin than any of the RCC lines including RCC4, with an IC50 value less than 1pM (Figure 5.8a). In addition, they were also more sensitive to sunitinib (Figure 5.8b) and sorafenib (Figure 5.8c) compared to the renal cancer cell lines. While HUVECs were more sensitive to metformin than RCC4 cells (Figure 5.8d), the IC50 value was similar to that obtained for 786-0 cells (Figure5.6d) and was higher than that observed for UMRC2 cells (Figure 5.7d).

5.2.9. Summary

In the established renal cancer cell lines, vHL mutation sensitized RCC4 and UMRC2 cells to rapamycin; there was also a trend towards increased sensitivity with vHL mutation in 786-0 cells. By and large, vHL mutation did not confer increased sensitivity/ resistance to the other drugs tested across the different cell lines. In addition, HUVEC cells were more sensitive to rapamycin, sunitinib and sorafenib compared to established renal cancer cell lines. This is most likely due to the targeting of VEGF, which is critical in HUVEC proliferation.



	Rapamycin	Sunitinib	Sorafenib	Metformin
IC50	<1pM	4.2µM	7.7µM	17.2mM
RCC4 *+vHL*	p<0.001	n/s	p<0.001	p<0.001
RCC4 *-vHL*	p<0.001	p<0.001	p<0.001	p<0.001

Figure 5-8 Drug sensitivity in HUVEC cells

HUVEC cells were treated for 72 hours with (a) rapamycin, (b) sunitinib, (c) sorafenib and (d) metformin. Data are presented as % cell viability compared to the control cell population, as mean points and standard error of three replicates. A non linear curve of best fit is shown. Two way ANOVA tests were performed to examine differences between HUVEC cells and RCC4 cells. This data is shown in the table and green font indicated HUVEC cells were more sensitive to the RCC4 cell line in the comparison.

5.2.10. Sensitivity of primary renal cancer cell lines to targeted therapies

Renal cancer is a heterogeneous disease and individual tumours may have unique characteristics that alter drug sensitivity and set them apart from historic cell lines. To test intertumour variability in drug sensitivity, 10 primary RCC cultures were established from nephrectomy specimens. The microscopic appearance of representative primary renal cancer cells can be seen in Figures 5.9a and b. Positive immunohistochemistry for pancytokeratin and vimentin can diagnose renal cell cancer with a high sensitivity and specificity [286]. Thus primary cultures were initially stained for these markers and found to be positive (Figure 5.9). On average 1 in 4 primary cultures reached passage 4, at which point the cells became senescent. Therefore experiments were performed at passage 2. Growth rates varied, however all results were normalised to a control cell population from the same cell pool.

The tumours from which the primary cultures were established were also screened for the presence of *vHL* mutations. Screening was performed by Dr Claire Taylor, CRUK Cancer Centre Genomics Facility, Leeds Institute of Molecular Medicine. Mutations were identified in 5 of the 10 tumours (Table 5.1).

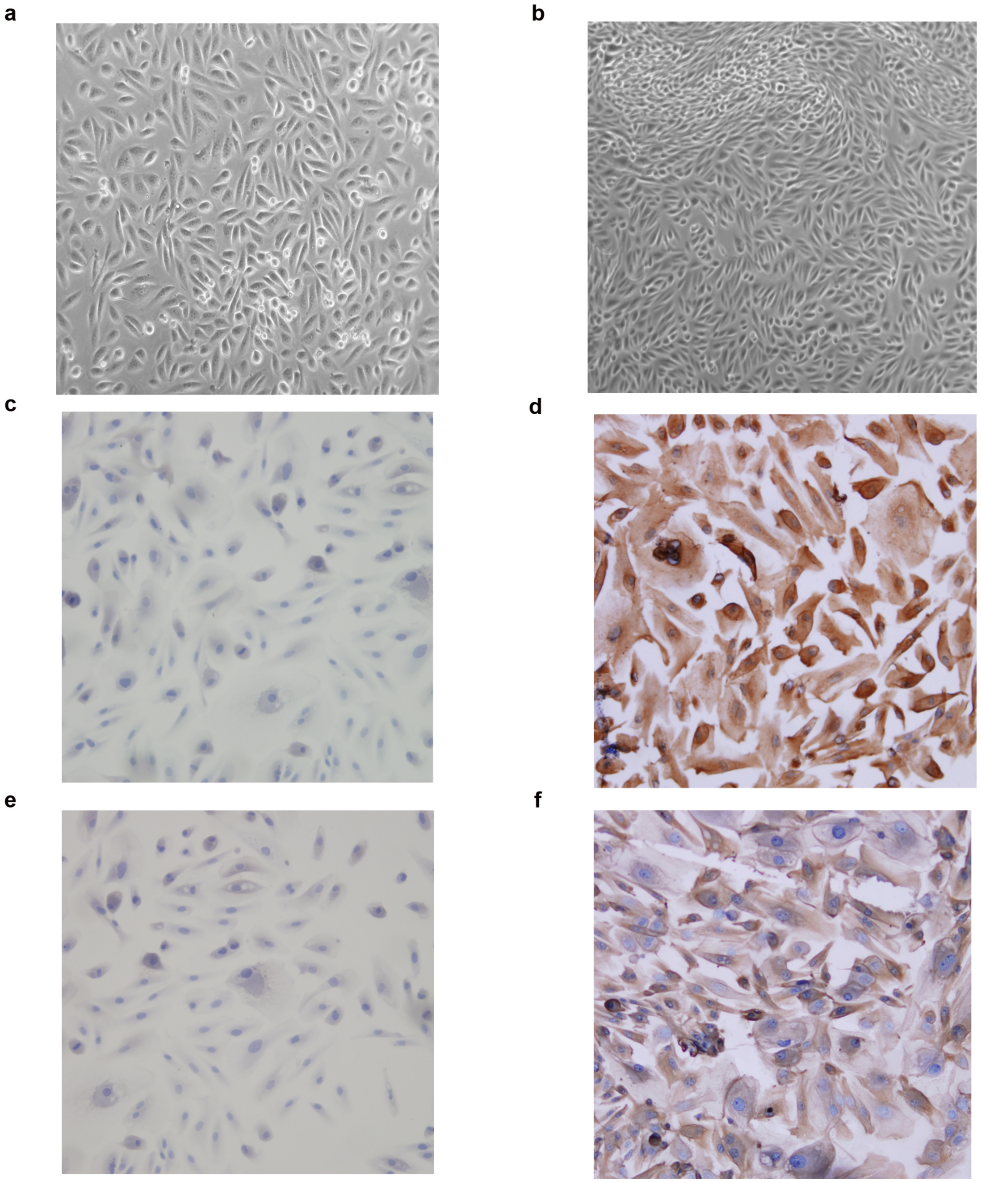


Figure 5-9 Primary renal cancer cell lines

Primary RCC lines were established from nephrectomy samples and representative monolayer culture at (a) 10x magnification and (b) 5X magnification are shown. (c) No primary antibody control for pancytokeratin staining. (d) Pancytokeratin staining in primary RCC cultures. (e) No primary antibody control for vimentin staining. (f) Vimentin staining in primary RCC cultures.

A high degree of variation in drug sensitivity between primary cell lines was observed (Figures 5.10-11). No cell line was consistently more or less sensitive to the panel of drugs than another. The IC50 values and histology from these tumour cell lines are summarized in Table 5.1.

Cell line 17511.11 (no *vHL* mutation detected) was the most resistant cells to sorafenib and the most sensitive to sunitinib when compared to other cell lines (Figure 5.10a). Cell line 27877.10 (*vHL* mutant) was relatively resistant to all therapies and had the highest IC50 value for rapamycin treatment (52.8μM) and the second highest value for sunitinib treatment (Figure 5.10b and Table 5.1). Cell line 35236.10 (no *vHL* mutation detected) was one of the most sensitive cell lines to rapamycin, with even the lowest concentration tested leading to a 50% decrease in cell viability (Figure 5.10c). Cell line 36993.10 (*vHL* mutant) was the most sensitive to both sorafenib and metformin (Figure 5.10d and Table 5.1). In addition, the lowest dose of rapamycin tested led to a 40% decrease in cell viability (Figure 5.10d). Cell line 04134.10 (no *vHL* mutation detected) had similar IC50 values for the drugs tested compared to the other cell lines; however, despite this cells were more sensitive as even the lowest concentrations of drugs caused a 40% reduction in cell growth (Figure 5.10e).

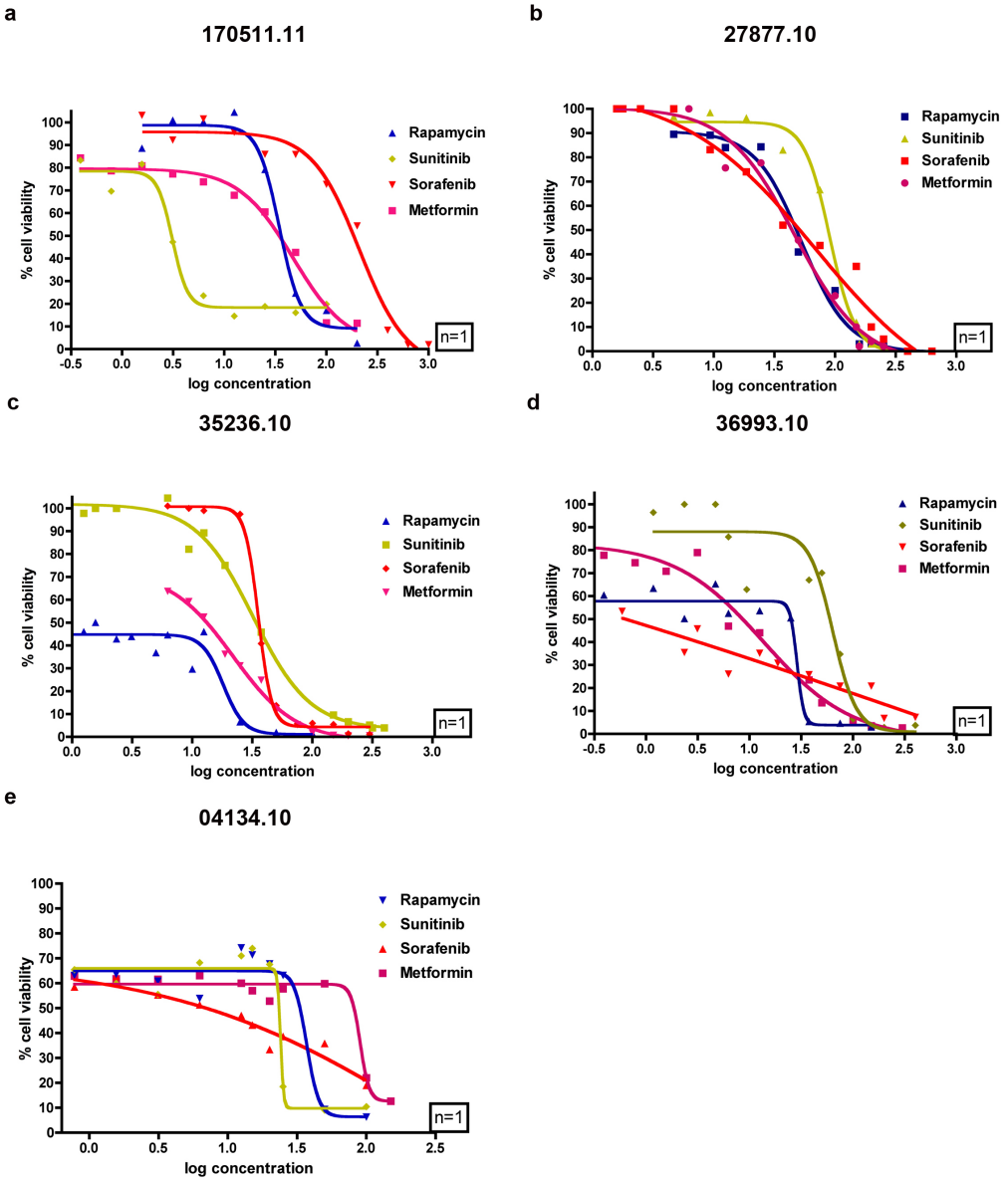


Figure 5-10 Drug sensitivity of primary renal cancer cell lines

Cells were cultured in normoxia for 72 hours after treatment with varying doses of rapamycin (blue), sunitinib (gold), sorafenib (red) and metformin (pink). Data are presented as % of cell viability when compared to the control cell population. The line of best fit is shown through each set of data points.

Cell line 5711.10 (*vHL* mutant) was highly sensitive to rapamycin, with even the lowest concentration tested leading to a 60% decrease in cell viability (Figure 5.11a and Table 5.1). However, this cell line was the most resistant to metformin (Figure 5.11a and Table 5.1). Cell line 00929.11 (no *vHL* mutation detected) was the most resistant cell line to sunitinib (Figure 5.11b and Table 5.1). In addition this cell line was reasonably sensitive to rapamycin, with the lowest concentration tested leading to a 40% decrease in cell viability (Figure 5.11b). Cell line 09885.11 (*vHL* mutant) was the second most sensitive to sorafenib but the second most resistant to rapamycin (Figure 5.11c and Table 5.1). Cell line 34484.11 (no *vHL* mutation detected) was very sensitive to sunitinib but more resistant to sorafenib and metformin (Figure 5.11 d) and Table 5.1). Finally cell line 35285.11 (*vHL* mutant) was relatively sensitive to metformin (Figure 5.11e).

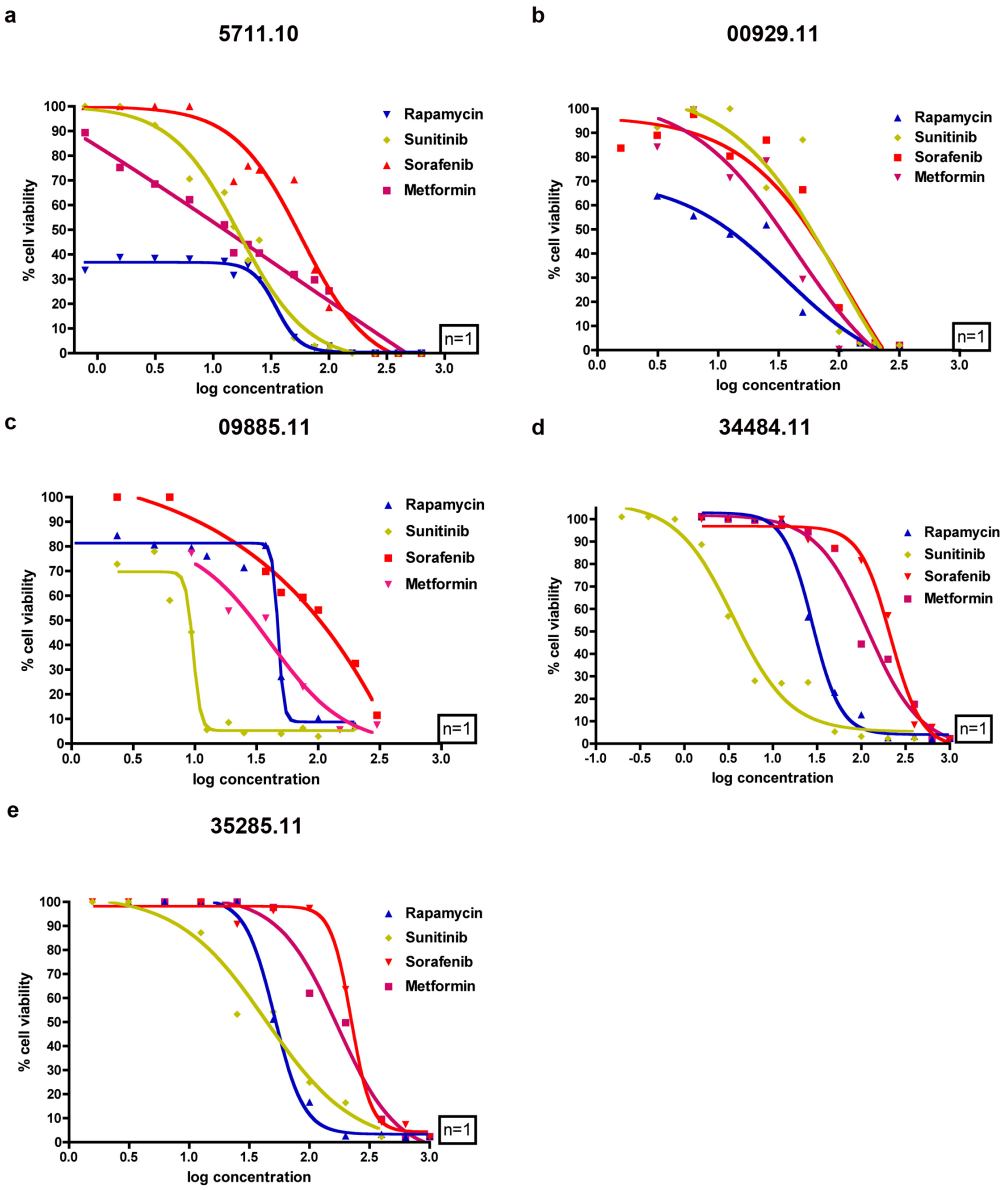


Figure 5-11 Drug sensitivity in primary renal cancer cell lines

Cells were cultured in normoxia for 72 hours after treatment with varying doses of rapamycin (blue), sunitinib (gold), sorafenib (red) and metformin (pink). Data are presented as % of cell viability when compared to the control cell population. A line of best fit is shown.

The IC50 values of the primary cell lines to the different drugs is summarized in Table 5.1 and graphically represented in Figure 5.12. In primary RCC cell cultures treated with rapamycin (Figure 5.12a), there was a range of sensitivities from the most resistant (27877.10, IC50: 52.8μM) to the most sensitive (35236.10, IC50: 1.4μM). In contrast to the established RCC cell lines, *vHL* mutation status did not correlate with sensitivity to rapamycin, sunitinib or metformin in these primary cultures; the two cell lines most resistant to rapamycin (27877.10 and 09885.11) had *vHL* mutations. Sunitinib sensitivity varied from the most resistant (00929.11, IC50: 97.5μM) to the two most sensitive cell lines (34484.11 and 17511.11, IC50: 3μM) (Figure 5.12b). Metformin sensitivities were again in mM concentrations. Sensitivities were spread evenly between the most sensitive (36993.10, IC50: 11.6mM) and the most resistant (34484.11, IC50: 119mM)(Figure 5.12d). Interestingly, the presence of *vHL* mutation increased sensitivity to sorafenib and was significant (T-test, p=0.02), with 4 of the 5 most sensitive cell lines having a mutant *vHL* (Table5.1). Sorafenib had perhaps the widest variation in sensitivities, with an almost 1000 fold difference in sensitivity between the least and most sensitive cell lines (Figure 5.12c).

Cell line	Histology	vHL mutation	Rapamycin	Sunitinib	Sorafenib	Metformin
17511.11	Grade 3 Clear cell RCC		34.5μM	3.1μM	209μM	46.9mM
27877.10	Grade 2 Clear cell RCC	Exon 2 Frameshift (het)	52.8μM	90.5μM	68.7μMM	46.6mM
35236.10	Grade 3 Clear cell RCC		1.4μM	32.0μM	34.6μM	21.8mM
36993.10	Grade 2 Clear cell RCC	Exon 1 Frameshift (het)	28.2μM	67.5μM	0.03μM	11.6mM
04134.10	Grade 2 Clear cell RC		37.0μM	24.0μM	98.5μM	90.2mM
5711.10	Grade 2 Clear cell RCC	Exon 2 Splice (het)	0.3μM	24.4μM	52.1μM	97.7mM
00929.11	Grade 3 Clear cell RCC		35.7μM	97.5μM	121μM	43.5mM
09885.11	Grade 2 Clear cell RCC	Exon 3 Splice (het)	48.5μM	9.6μM	2.8μM	40.2mM
34484.11	Oncocytoma		27.9μM	3.6μM	186μM	119mM
35285.11	Grade 3 Clear cell RCC	Exon 1 Nonsense (het)	18.1μM	32.0μM	34.6μM	21.8mM

Table 5-1 IC50 values for primary renal cancer cells

Data is presented as IC50 values for the 10 primary cell lines to the 4 drugs.
These values are colour coded from the two most sensitive (green) to the two most resistant (red). *vHL* mutations are also indicated. Het-heterozygous.

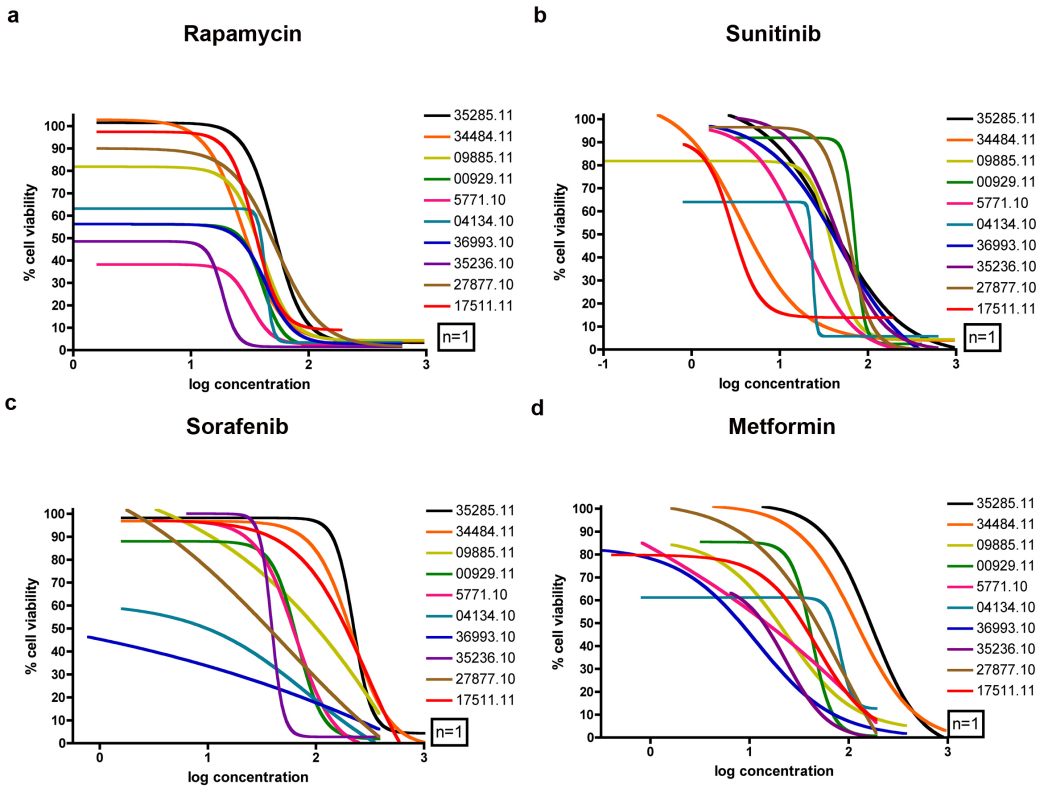


Figure 5-12 Comparison of drug sensitivities in renal cancer cell lines

Ten primary cell lines were treated with (a) rapamycin, (b) sunitinib, (c) sorafenib) and (d) metformin for 72 hours and cultured in normoxia. Data are presented as % cell viability when compared to the control cell population.

5.2.11. Comparison of historic and primary cell lines

To determine the sensitivity of primary cell lines against historic cell lines the mean and median results were compared (Table 5.2). Overall, primary cell lines were more resistant to both rapamycin and metformin, but there was no difference in sensitivity to treatment with sunitinib and sorafenib. The standard deviation in primary cell lines was consistently higher reflecting the heterogeneous nature of renal tumours. In general the data is comparable and would suggest that in the absence of primary cell lines, historic cell lines are a representative model to test drug sensitivity. We found that the IC50 values for these drugs in our experiments were in many cases higher than those that can be achieved clinically. There are a number of possible reasons for this, for example we specifically targeted a cancer cell population and therefore the effects of stromal interaction and endothelial cells proliferation were not appreciated. We also used a single dose protocol and therefore this does not represent a clinical scenario. The experiments were such designed to directly compare the effects of these drugs in different cell lines rather than establish the clinically relevant IC50 values. We therefore maintained a consistent experimental design to achieve this goal.

Cell line		Rapamycin	Sunitinib	Sorafenib	Metformin
Primary cell lines	mean	28.4μM	38.4μM	80.8μM	53.9mM
	median	31.4μM	28.2μM	60.4μM	45.0mM
	Sd	17.6μM	34.7μM	72.6μM	36.1mM
	se	5.6μM	11.0μM	23.0μM	11.4mM
Historic cell lines	mean	7.3μM	17.3μM	31.0μM	20.1mM
	median	5.5μM	12.9μM	25.6μM	16.4mM
	SD	7.4μM	11.0μM	14.8μM	15.8mM
	se	3.0μM	4.5μM	6.0μM	6.5mM
Significance		p=0.01	n/s	n/s	p=0.04

Table 5-2 Sensitivity of renal cancer cells to targeted therapies

A comparison of IC50 data from primary and historic cell lines, data are presented as mean, median, standard deviation (SD) and standard error (se).

5.2.12. Genes involved in the hypoxic and mTOR pathways in renal cancer

In this study, we found that neither *vHL* mutation status nor sensitivity to one drug were suitable for predicting drug sensitivity to other therapies in primary cultures from renal tumours. We, therefore, investigated the expression of a number of genes at the transcript level to determine whether they may provide insights into drug responses. A total of 27 genes were chosen that were involved in either the regulation or output from the mTOR signaling pathway (*REDD1, REDD2, EIF4E, 4EBP1, mTOR, RHEB, RICTOR, RAPTOR, p70S6K* and *AKT*), the regulation or output from the hypoxic pathway (*HIF-1α, HIF-2α, EGLN3, VEGFR2* and *CA9*) or were involved in the cell cycle (the cell cycle promoters *CYCLIN D1* and *MYC* and the cell cycle inhibitors *p21* and *p27*). Additional pathways interrogated were the unfolded protein response and autophagy (*CHOP* and *ULK1*), and stem cell fate (*NANOG* and *OCT4*). Finally, the histone demethylase

JARID1C and the methylase *SETD2* are mutated in around 3% of renal cancer cases [149]; the expression of these two genes was also examined. All expression data was normalized to *ACTIN*. The selected genes are summarized in Table 5.3.

Table 5-3 Genes selected for analysis in renal cancer cell lines

REDD1	Hypoxia induced inhibitor of mTOR pathway via activation of TSC1	**p27**	Cell cycle inhibitor
REDD2	Stress response gene involved in the negative regulation of mTOR	**MYC**	Oncogenic transcription factor that controls metabolism and proliferation
4IF4E	Activator of translation inhibited by 4EBP1	**CHOP**	Transcription factor in UPR (PERK) pathway
4EBP1	Downstream target of mTOR pathway	**ULK1**	Kinase that co-ordinates autophagy from multiple stimuli
mTOR	Kinase that regulates cellular metabolism	**CAIX**	Involved in hydration of CO_2 and therefore regulation of pH
Rheb	GTPase which activates mTOR	**HIF-1α**	Transcription factor that co-ordinates hypoxic response
RICTOR	Rapamycin insensitive component of mTORC1	**HIF-2α**	Transcription factor involved in hypoxic response
P70S6K	Downstream target of mTOR	**EGLN3**	Member of EGLN family of prolyl hydroxylases
Raptor	Rapamycin sensitive component of mTORC1	**VEGFR2**	Receptor for VEGF
TSC1	Promotes hydrolysis of Rheb	**JARID1c**	Histone Demethylase mutated in renal cancer
TSC2	Downstream of AMPK and negatively regulates mTOR	**NANOG**	Transcription factor required for stem cell phenotype
AKT	Oncogenic kinase that activates TOR pathway	**OCT4**	Transcription factor involved in stem cell regulation
CYCLIN	Promotes G1 transition	**SETD2**	Methylase mutated in renal cancer
p21	Cell cycle inhibitor		

5.2.13. Analysis of gene expression data from renal cancer cell lines

Initially, the effect of *vHL* mutation on the expression of these genes in RCC4 and 786-0 cells was examined (Figure 5.13). In RCC4, *REDD1, 4EBP1, CYCLIN D1* and *CA9* and *EGLN3* were significantly upregulated in *vHL* null cells, while *TSC2, ULK1, HIF-2α* and *HIF-1α* were significantly downregulated in these cells (Figure 5.13a). In 786-0 cells, *4EBP1, RHEB, RAPTOR, TSC1* and *2, ULK1, p27, HIF-2α* and *OCT4* were all significantly upregulated, while *JARID1c* was the only gene downregulated in *vHL* null 786-0 cells (Figure 5.13b).

Next, a similar analysis of gene expression was performed in the primary cell lines. The expression of each gene in these cells were compared to the average expression of the gene in 3 separate normal renal cultures derived from parenchymal tissue to establish the variation in expression in cancer cells when compared to normal cells. Gene expression in each of the primary renal cell lines could only be measured in one experiment due to a limited amount of material to work with.

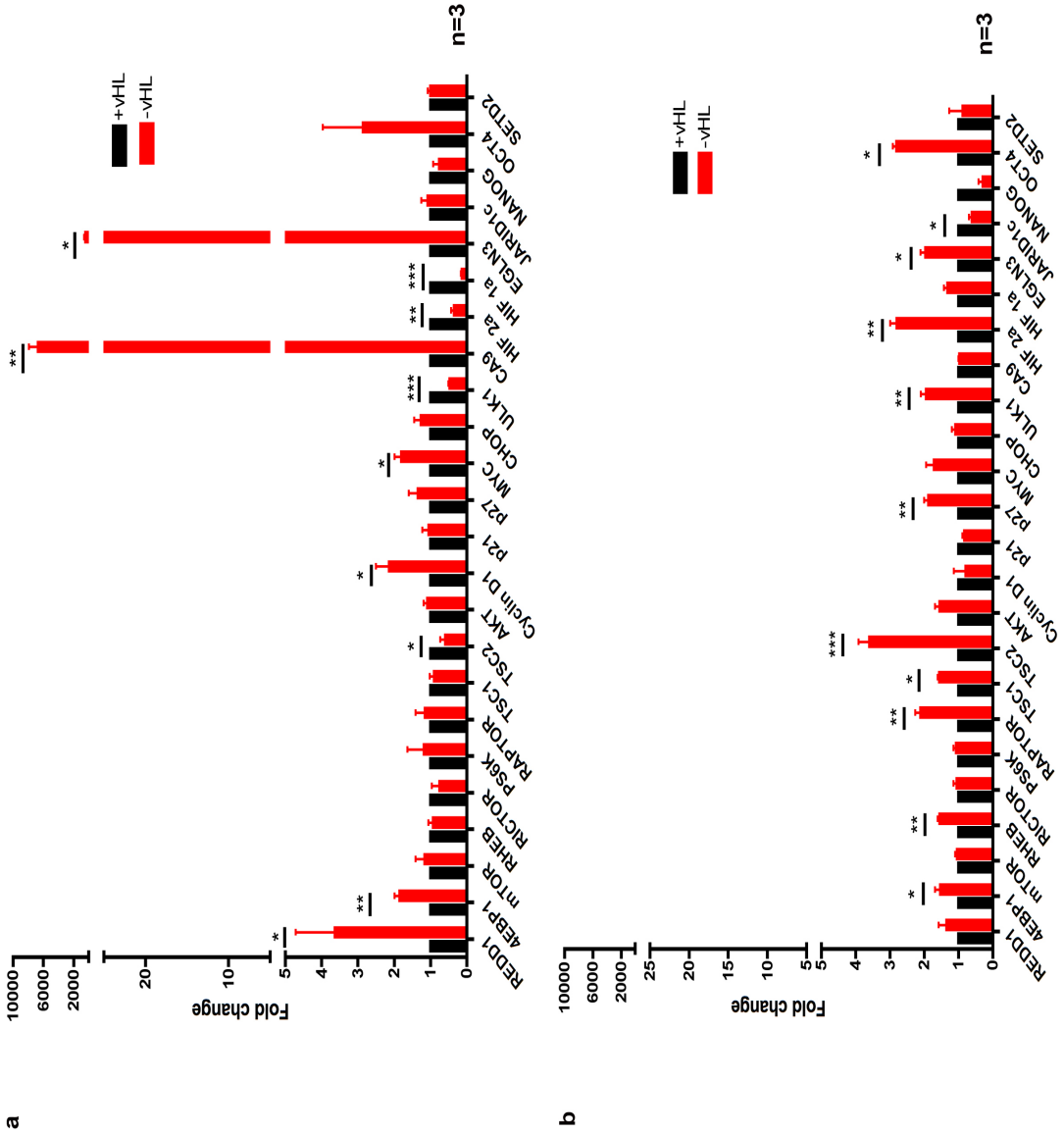


Figure 5-13 Gene expression in RCC4 and 7860 cells

(a) RCC4 *+vHL* and *vHL* null cells were cultured for 24 hours in normoxia, (b) 786-0 *+vHL* and *vHL* null cells were cultured for 24 hours in normoxia. Data are presented as fold change relative to the expression in *vHL* + cells for each line after normalization to *ACTIN* for each sample. Statistical significance: * p<0.05, ** p<0.01, ***p<0.001. Mean ± standard error.

The expression of the target genes in each of the primary RCC cell lines is presented in Figure 5.14 – 5.17 and summarized in Table 5.4. In all cases, a minimum of a two-fold difference in gene expression was considered significant. The most dramatically induced gene was *CA9*, with a mean upregulation of nearly 4000 fold. All of the primary cell lines with *vHL* mutation had elevated levels of *REDD1* and *CA9*. Four of the five *vHL* mutant lines had increased levels of *RAPTOR* and *EGLN3* and 3/5 lines had increased levels of *4EPB1*. In addition, 4/5 *vHL* mutant lines had decreased levels of *HIF-1*α transcript.

In addition to the above genes that were regulated predominantly in a *vHL* dependent manner, the expression of a number of genes was altered in RCC regardless of *vHL* mutation status. For example, the expression *SETD2* was decreased in 5 primary RCC lines, two of which did not have a *vHL* mutation. The expression of *OCT4* was decreased in 8/10 primary RCC lines; half of these had mutations in *vHL*, while the other half did not (Table 5.4).

A number of genes had variable expression across the primary RCC cell lines. For example, the expression of *CYCLIN D1* was unchanged in 5 lines, decreased in 4 (1 *vHL* mutant) and increased in 1 (*vHL* mutant) primary RCC lines. Similarly, the expression of *CHOP* was unchanged in 5 lines, decreased in 4 (3 *vHL* mutant) and increased in 1 (*vHL* mutant) primary RCC lines. The expression of *NANOG* was decreased in 4 RCC lines (3 *vHL* mutant) and increased in 2 (1 *vHL* mutant) primary RCC lines. Finally, the expression of *REDD2* was decreased in 5 (2 *vHL* mutant) and increased in 2 (both *vHL* mutant) primary RCC lines (Table 5.4). By and large, the expression of the other genes was largely unchanged in the primary RCC cell lines.

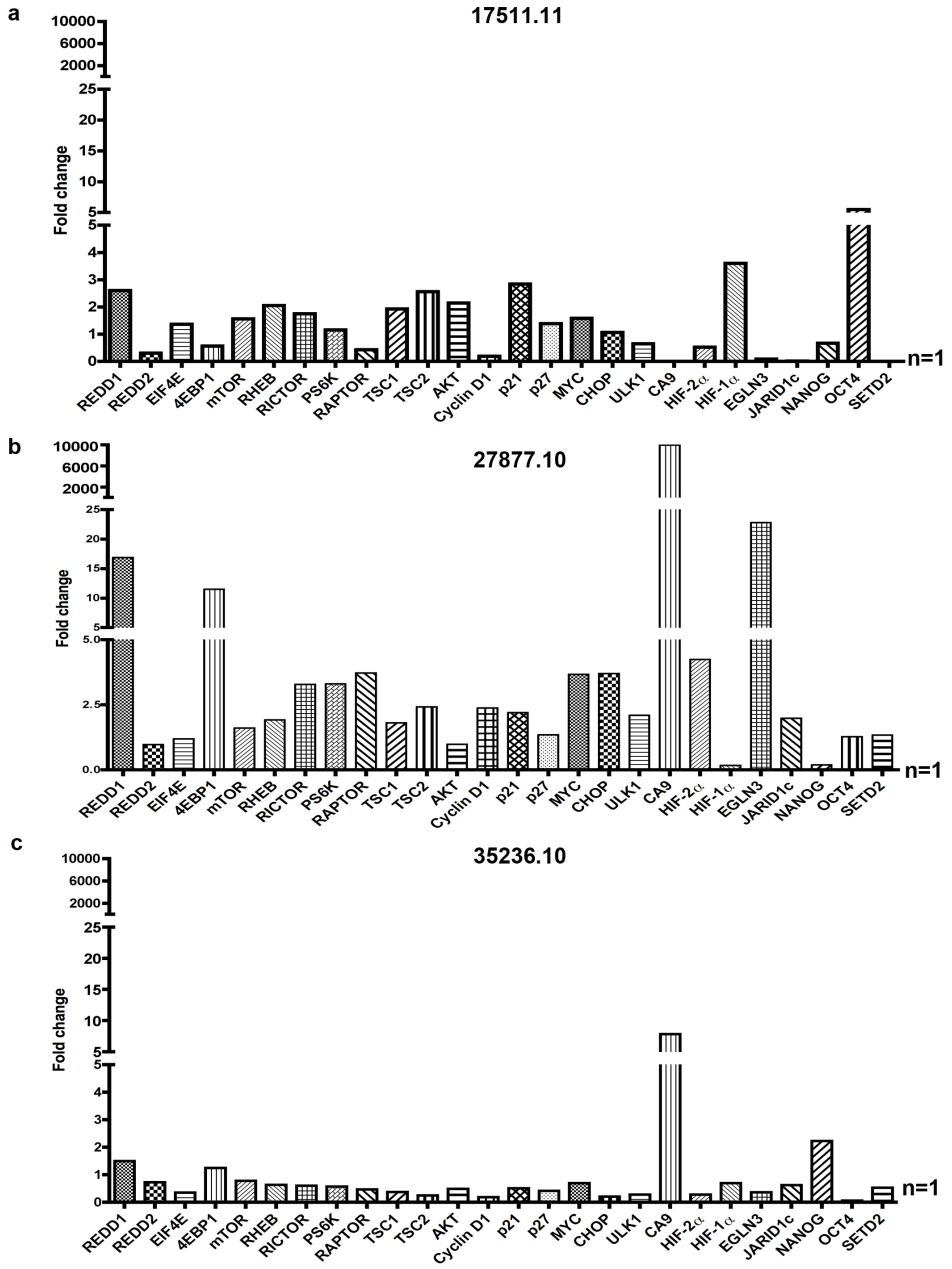


Figure 5-14 Gene expression in cell lines 17511.11, 27877.10 and 35236.10

(a) 17511.11, (b) 27877.10 and (c) 35236.10 cells were cultured in normoxia for 24 hours. Data are presented as fold change compared to average expression in three normal renal cell cultures.

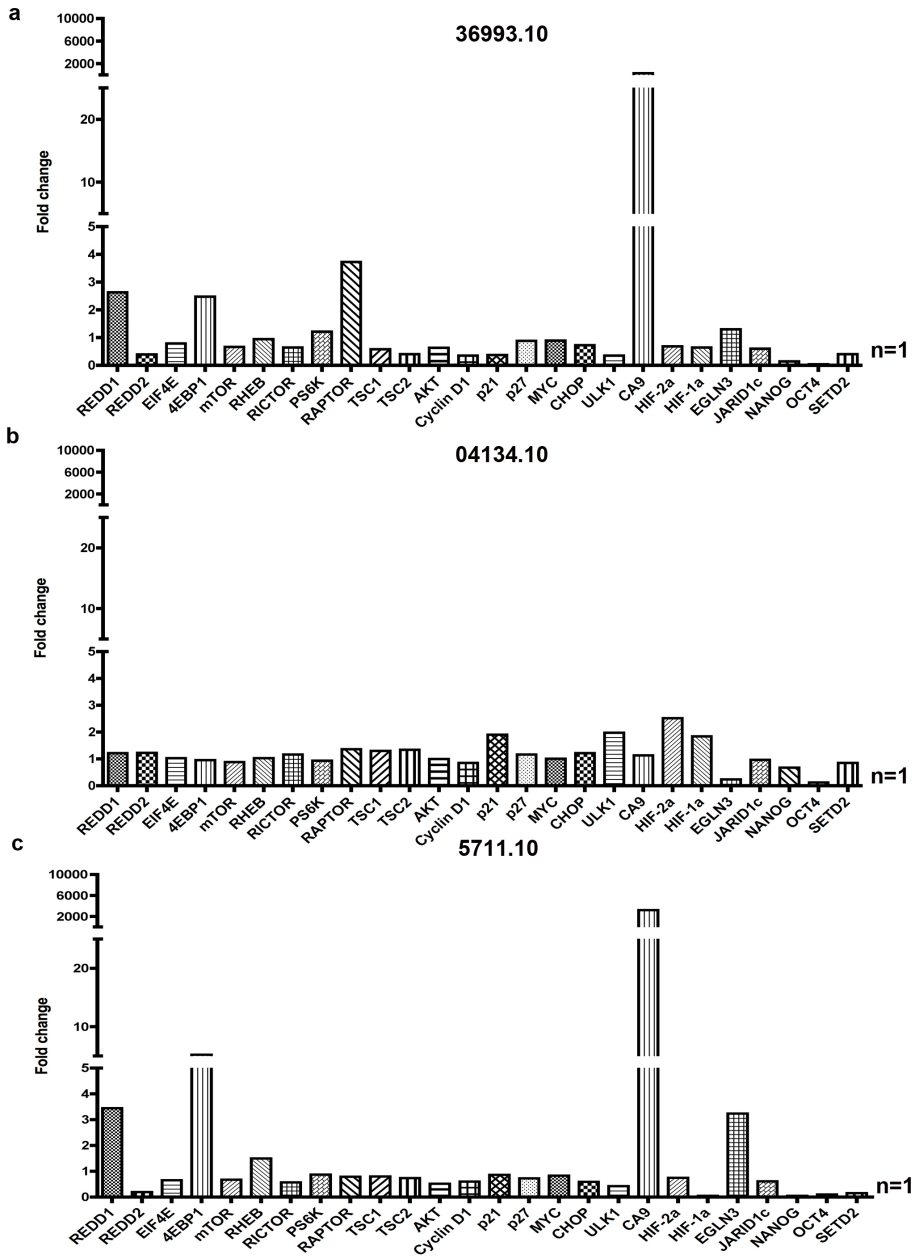


Figure 5-15 Gene expression from cell lines 36993.10, 04134.10 and 5711.10

(a) 36993.10, (b) 04134.10 and (c) 5711.10 cells were cultured in normoxia for 24 hours. Data are presented as fold change compared to average expression in three normal renal cell cultures.

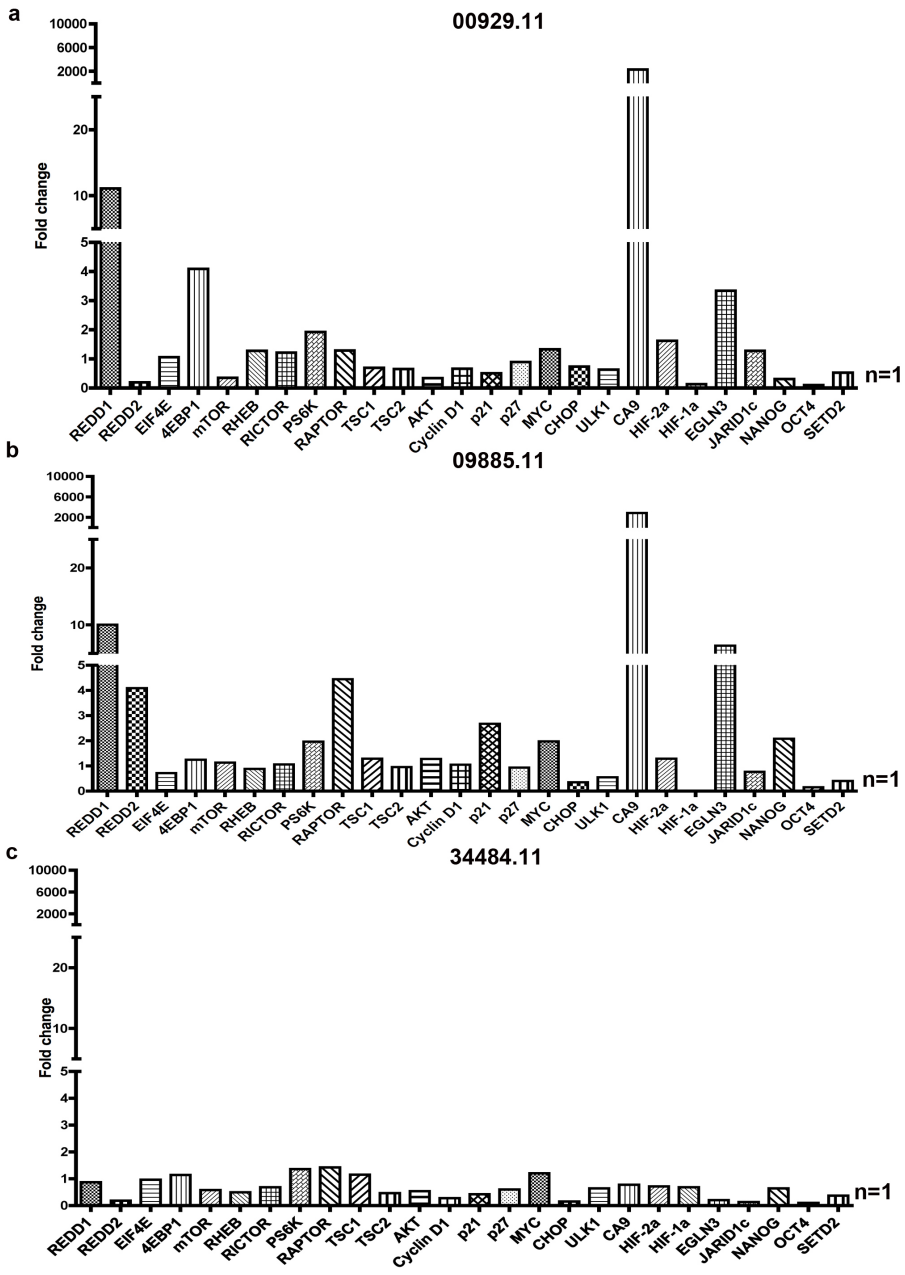


Figure 5-16 Gene expression in cell lines 00929.11, 09885.11 and 34484.11

(a) 00929.11, (b) 09885.11 and (c) 34484.11 cells were cultured in normoxia for 24 hours. Data are presented as fold change compared to average expression in three normal renal cell cultures.

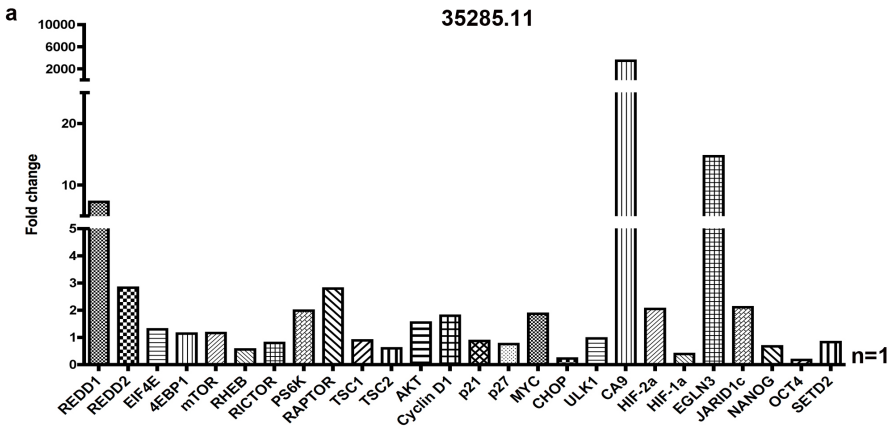


Figure 5-17 Gene expression from cell line 35285.11

(a) 35285.11 cells were cultured in normoxia for 24 hours. Data are presented as fold change compared to average expression in three normal renal cell cultures.

	17511	27877	35236	36993	04134	5711	00929	09885	34484	35285
		vHL mut		*vHL* mut		*vHL* mut		*vHL* mut		*vHL* mut
REDD1	2.6	16.9	1.5	2.6	1.2	3.4	11.1	10.1	0.9	7.3
REDD2	0.3	1.0	0.7	0.4	1.2	0.2	0.2	4.1	0.2	2.8
EIF4E	1.4	1.2	0.4	0.8	1.0	0.7	1.1	0.7	1.0	1.3
4EBP1	0.6	11.5	1.3	2.5	1.0	5.2	4.1	1.3	1.2	1.2
mTOR	1.6	1.6	0.8	0.7	0.9	0.7	0.4	1.1	0.6	1.2
RHEB	2.1	1.9	0.6	0.9	1.0	1.5	1.3	0.9	0.5	0.6
RICTOR	2.8	3.3	0.6	0.6	1.2	0.6	1.2	1.1	0.7	0.8
p70S6K	2.3	3.3	0.6	1.2	0.9	0.9	1.9	2.0	1.4	2.0
RAPTOR	0.4	3.7	0.5	3.7	1.4	0.8	1.2	4.5	1.4	2.8
TSC1	1.9	1.8	0.4	0.6	1.3	0.8	0.7	1.3	1.2	0.9
TSC2	2.6	2.4	0.3	0.4	1.4	0.7	0.7	1.0	0.5	0.6
AKT	2.1	1.0	0.5	0.6	1.0	0.5	0.4	1.3	0.6	1.6
CYCLIN D1	0.2	2.4	0.2	0.4	0.9	0.6	0.7	1.1	0.3	1.8
p21	2.8	2.2	0.5	0.4	1.9	0.9	0.5	2.7	0.4	0.9
p27	1.4	1.4	0.4	0.9	1.2	0.7	0.9	0.9	0.6	0.8
MYC	1.6	3.7	0.7	0.9	1.0	0.8	1.3	2.0	1.2	1.9
CHOP	1.1	3.7	0.2	0.7	1.2	0.6	0.7	0.4	0.2	0.2
ULK1	0.7	2.1	0.3	0.4	2.0	0.4	0.6	0.6	0.7	1.0
CA9	0.1	9970	7.9	335	1.1	3236	2310	2890	0.8	3490
HIF-2	0.5	4.3	0.3	0.7	2.5	0.8	1.6	1.3	0.7	2.1
HIF-1	3.6	0.2	0.7	0.6	1.8	0.1	0.1	0.1	0.7	0.4
EGLN3	0.1	22.8	0.4	1.3	0.2	3.2	3.3	6.4	0.2	14.7
JARID 1C	0.1	2.0	0.6	0.6	1.0	0.6	1.3	0.8	0.1	2.1
NANOG	0.7	0.2	2.2	0.1	0.7	0.1	0.3	2.1	0.7	0.7
OCT4	5.5	1.3	0.1	0.1	0.1	0.1	0.1	0.2	0.1	0.2
SETD2	0.1	1.3	0.5	0.4	0.9	0.2	0.5	0.4	0.4	0.8

Table 5-4 Gene expression in primary cell lines

Data are presented as fold change compared to expression in normal cells. Genes are highlighted if more than 2 fold upregulation (red) or 2 fold downregulation (green).

A primary RCC cell line of note was 0929.11 in which no *vHL* mutation was detected (Table 5.1). However, this line had an expression pattern of genes that was typical of loss of *vHL* function, with elevated levels of *CA9, REDD1, EGLN3* and *4EBP1* and decreased expression of *HIF-1a* (Figure 5.16a and Table 5.4).

5.2.14. Gene co-expression in primary cell lines

Next, the correlation of expression of different genes was examined to identify clusters of genes whose expression was co-regulated. The analysis was limited to genes that had a minimum 2-fold change (either up or down) in at least 4 out of 10 cell lines. Thus, the following genes were chosen - *REDD1, REDD2, 4EBP1, p70S6K, RAPTOR, HIF-1, CYCLIN D1, p21, CHOP, CA9, EGLN3, NANOG, OCT4* and *SETD2*.

We found that REDD1 had significant, positive correlation with *p70S6K, CYCLIN D1, CA9* and *EGLN3*, and significant, negative correlation with *HIF-1α*. The expression of *REDD2* and *CHOP* expression did not correlate with any of the other genes tested. The expression of *4EBP1* had a significant, positive correlation with CA9 and EGLN3, and significant, negative correlation with *HIF-1α* and *NANOG*. In addition to *REDD1*, *p70S6K* had significant, positive with *OCT4*. The expression of *RAPTOR* was positively, and significantly correlated to *CYCLIN D1* and *EGLN3. CYCLIN D1* had significant, positive correlation with *CA9*, *EGLN3* and *SETD2*, in addition to *REDD1* and *RAPTOR*. There was significant, positive correlation between *p21* and *OCT4*. In addition to *REDD1, 4EBP1* and *CYCLIN D1, CA9* expression was significantly, positively correlated with *EGLN3* and negatively correlated with *HIF-1α*. *HIF-1α* expression was strongly, negatively

correlated with *REDD1*, *4EBP1, CA9* and *EGLN3. NANOG* expression was significantly, negatively correlated with *4EBP1. OCT4* expression was significantly, positively correlated with *p70S6K* and *p21* and finally, *SETD2* expression was positively correlated with *CYCLIN D1*. All significant associations are summarized in Table 5.5.

	REDD1	REDD2	4EBP1	P70S6K	RAPTOR	CYCLIN D1	P21	CHOP	CA9	HIF-1	EGLN3	NANOG	OCT4	SETD2
REDD1				0.72 (0.02)		0.72 (0.02)			0.82 (0.004)	-0.68 (0.03)	0.87 (0.001)			
REDD2														
4EBP1									0.73 (0.02)	-0.69 (0.03)	0.67 (0.03)	-0.68 (0.03)		
p70S6K													0.66 (0.04)	
RAPTOR						0.73 (0.02)					0.67 (0.03)			
CYCLIN D1									0.72 (0.02)		0.83 (0.003)			0.7 (0.03)
p21													0.67 (0.03)	
CHOP														
CA9										-0.88 (<0.001)	0.96 (<0.001)			
HIF-1											-0.78 (0.008)			
EGLN3														
NANOG														
OCT4														
SETD2														

Table 5-5 Correlation of gene expression

The expression of each gene used in the screening array was compared to each other. Data are presented based upon significance of correlation. Correlation was quantified using Pearson correlation coefficient and significance presented as red squares $p<0.001$, yellow squares $p<0.01$ and green squares $p<0.05$. Blank squares signify no correlation between genes.

5.2.15. Gene expression and rapamycin sensitivity

As *vHL* mutation status did not appear to be a good predictor of drug response, we examined whether gene expression could correlate with rapamycin sensitivity in the 10 primary RCC cultures. Of the fourteen genes with a minimum 2-fold change in at least 4 out of 10 cell lines, the expression of *REDD1* was significantly positively correlated rapamycin response (Pearson correlation coefficient=0.72) (Table 5.6 and Figure 5.20a for a Spearman correlation). The expression of *p70S6K* expression was also significantly positively correlated rapamycin response (Pearson correlation coefficient=0.73). None of the other genes showed a significant correlation to rapamycin sensitivity.

	Pearson R	R squared	p value		Pearson R	R squared	p value
REDD1	0.72	0.52	0.02*	**CHOP**	0.57	0.32	n/s
REDD2	0.31	0.10	n/s	**CA9**	0.39	0.15	n/s
4EBP1	0.29	0.08	n/s	**HIF-1**	0.10	0.01	n/s
p70S6K	0.73	0.53	0.02*	**EGLN3**	0.38	0.14	n/s
RAPTOR	0.58	0.34	n/s	**NANOG**	-0.09	0.01	n/s
CYCLIN D1	0.44	0.20	n/s	**OCT4**	0.23	0.05	n/s
p21	0.62	0.39	n/s	**SETD2**	0.40	0.16	n/s

Table 5-6 Correlation of gene expression with rapamycin sensitivity

Gene expression was compared with IC50 data for each cell line with rapamycin treatment. Data are presented as the Pearson correlation co-efficient, the R squared value for the data set. Statistical significance: * $p<0.05$, ** $p<0.01$, ***$p<0.001$.

5.2.16. *REDD1* expression in renal cancer cell lines

The role of REDD1 in RCC was explored further as it appeared to be a nexus between the hypoxic and mTOR pathways (Figure 5.18).

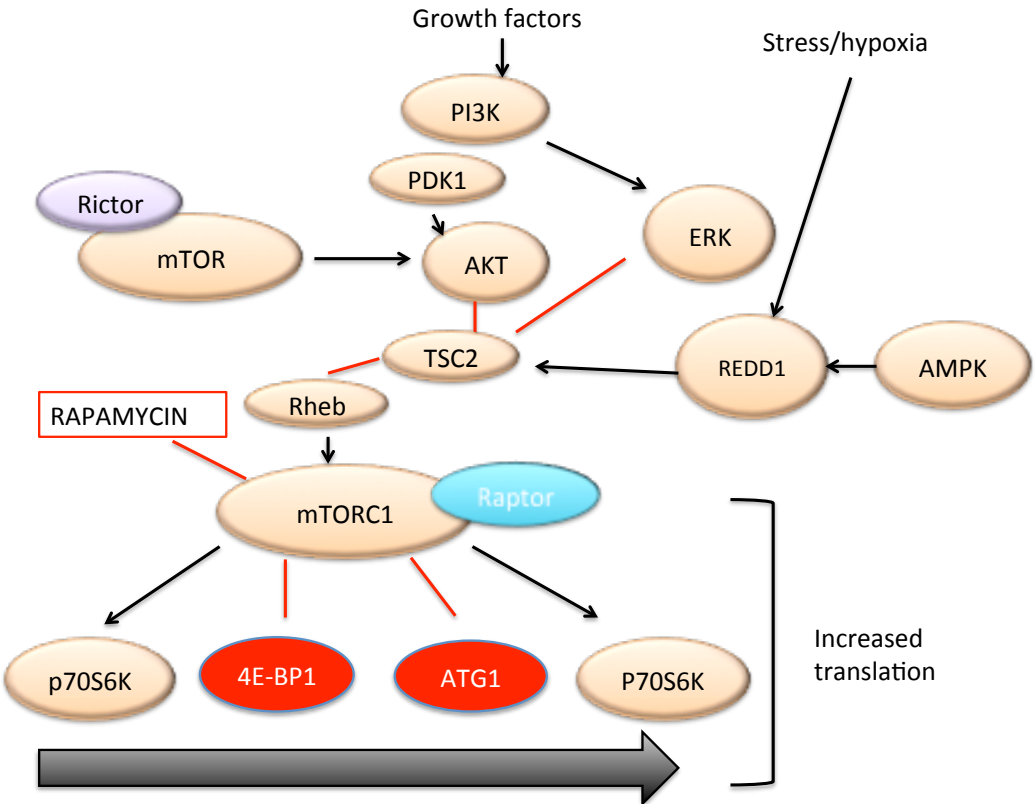


Figure 5-18 Rapamycin, the mTOR pathway and integration of REDD1 and AMPK signaling

Black arrow indicates stimulatory interactions/phosphorylations while red lines indicate inhibitory.

First, the expression of *REDD1* in vHL null/competent RCC4 and 786-0 cells was examined. *REDD1* expression was induced by hypoxia in RCC4 *vHL* competent cells after both 24 and 48 hours (Figure 5.19a and b). Futhermore, the absolute levels of *REDD1* were increased in *vHL* null RCC4 cells (Figure 5.19b), although these levels were not affected by exposure to hypoxia. In 786-0 cells *REDD1* expression was induced in hypoxia at both 24 and 48 hours in both *vHL* competent and *vHL* null cells (Figure 5.19c and d); vHL mutation status per se did not affect *REDD1* expression in this line (Figure 5.19d).

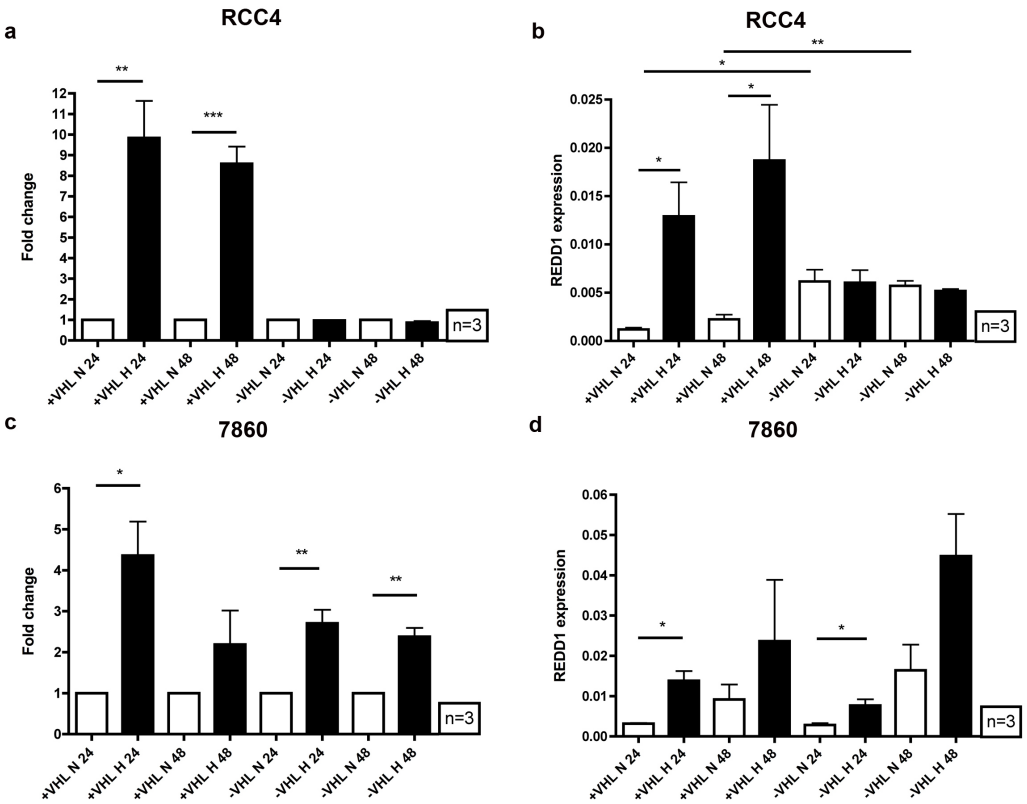


Figure 5-19 *REDD1* expression in RCC4 and 7860 cells

REDD1 expression regulation by hypoxia. RCC4 cells were cultured in normoxia and 0.1% O_2 for 24 and 48 hours. Data are presented as (a) fold change relative to normoxia and (b) expression relative to *ACTIN* at each timepoint. 786-0 cells were cultured in normoxia and 0.1% O_2 for 24 and 48 hours. Data are presented as (c) fold change relative to normoxia and (d) expression relative to *ACTIN* at each timepoint. Data are presented as mean ± standard error. Statistical significance: * $p<0.05$, ** $p<0.01$, *** $p<0.001$.

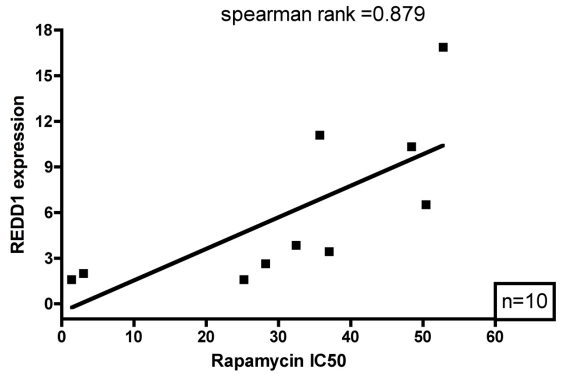
5.2.17. *REDD1* expression and clinical data

We then examined the expression of *REDD1* in mRNA extracted from an additional 23 renal tumours and matching normal renal tissue from the Oxford Biobank. It is published that variation occurs in the expression of control genes in tumour tissue samples [193, 194]. To identify the most consistent control gene for this quantification, the GeNorm version 3.2 applet was used to calculate a gene stability measure (M) value to establish the most consistently expressed control gene [193, 194]. Three internal control genes were tested - *ACTIN, RPL11* and *HPRT1*. All three genes had similar M values with the most stable gene being *ACTIN* (Figure 5.20b); this was, therefore, was used in the remaining experiments.

In 23 matched tumour and normal renal samples, *REDD1* expression, normalized to *ACTIN*, was significantly higher in tumour samples when compared to normal tissue (Figure 5.20c). When analysed as fold change of expression between paired samples, the standard error was greatly reduced, indicating that even samples with low expression of *REDD1* in the normal tissue had significant upregulation in the tumour (Figure 5.20d).

When the RCC samples were subdivided the samples into clear cell and papillary tumours, *REDD1* expression was only upregulated in the clear cell tumours compared to normal tissue and not in papillary tumours, although the numbers of papillary tumour samples was insufficient to draw any real conclusions (Figure 5.21a).

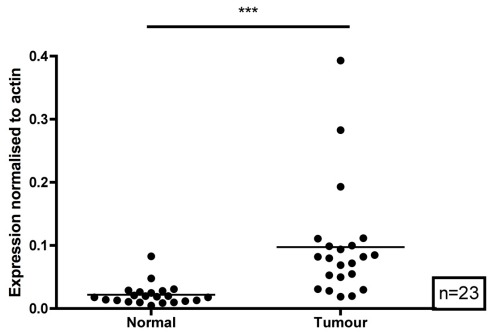
a



b

	Actin	HPRT1	RPL11
M < 0.9	0.79	0.89	0.82

c



d

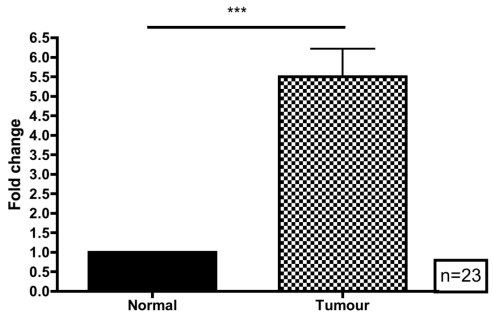


Figure 5-20 *REDD1* correlation with rapamycin sensitivity and expression in tumours

(a) *REDD1* expression in 10 primary tumours was normalised to *ACTIN* and correlation compared to rapamycin sensitivity, correlation was quantified using spearman rank correlation. (b) GeNorm (version 3.2) software was used to establish the most stable control gene to be used in future experiments. The lowest M value identifies the most stable gene. (c) *REDD1* expression in 23 paired clear cell tumours and normal renal tissue, data are presented normalized to *ACTIN*. (d) Fold change in *REDD1* expression in the 23 paired tumour/ normal samples.
Statistical significance: * $p<0.05$, ** $p<0.01$, *** $p<0.001$.

Next, the relationship between *REDD1* expression and a number of markers of prognosis in renal cancer was examined. In the RCC samples used above, *REDD1* expression were higher in tumours reported to contain foci of vascular invasion (Figure 5.21b) but was not associated with the grade of tumour (Figure 5.21c). In the same group of tumours, *REDD1* expression had a positive correlation with miR-210 expression (Figure 5.21d). In a larger, independent, series of RCC tumours from the Oxford Biobank, the expression of *REDD1* and *CA9* were found to correlate significantly (Figure 5.21e).

We then examined survival data for 31 patients in treated at the Churchill hospital, Oxford with long term follow up and from whom tumour biopsies were obtained. Tumour sections were stained for *REDD1* by immunohistochemistry and patients grouped as those with high *REDD1* expression (expression greater than the median) or those with low *REDD1* expression (lower than the median). Expression levels of *REDD1* did not distinguish survival of patients (Figure 5.21f); however repeating this analysis in a larger cohort of patients would be useful.

Finally we stably knocked down *REDD1* in *vHL* null RCC4 cells using 5 different shRNA against *REDD1*. Knockdown efficiency between 5%-75% was achieved with the constructs (Figure 5.22a); shRNA5 gave the weakest knockdown. The sensitivity of RCC4 cells to rapamycin after stably knocking down *REDD1* expression with shRNA1, 3 and 4 was then assessed. Knockdown of *REDD1* with shRNA1, which had the greatest knockdown efficiency, sensitized RCC4 cells to rapamycin, with cells requiring a 10-fold lower dose of rapamycin to reduce cell viability by 50% (Figure 5.22b and c).

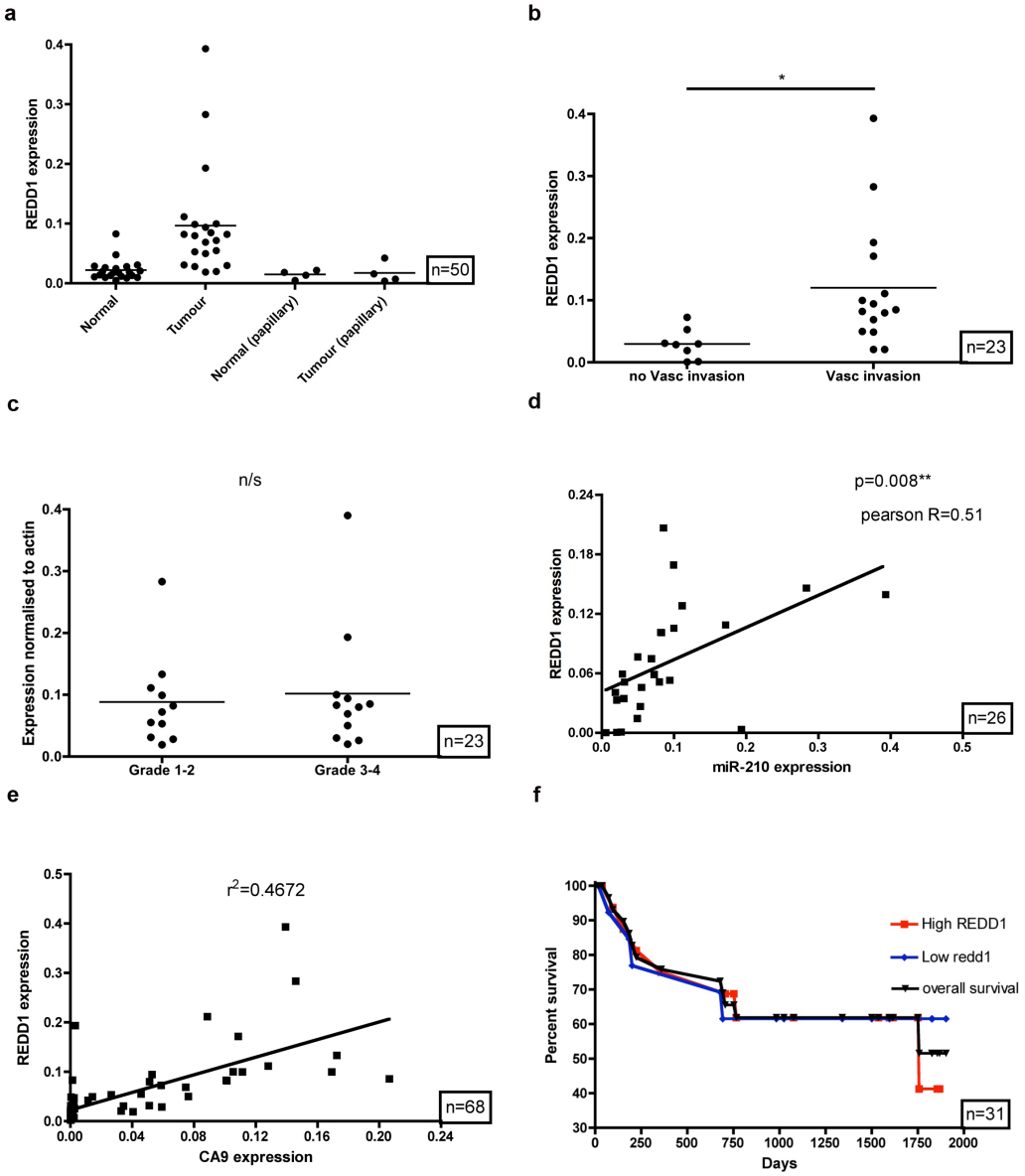
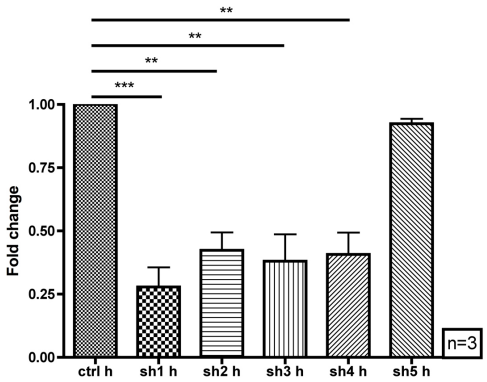


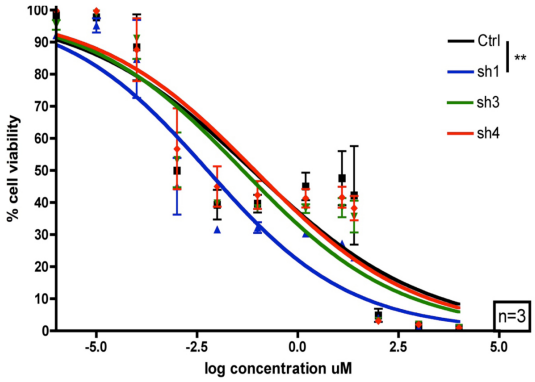
Figure 5-21 REDD1 expression and tumour variables

(a) *REDD1* expression in clear cell renal cell carcinoma compared with normal parenchymal tissue. Data are presented as fold change in a total of 23 paired RCC tumours and normal tissue. (b) Expression of *REDD1* in 23 RCC tumours based on their vascular invasion status. (c) *REDD1* expression based on tumour grade in 23 RCC tumours. (d) Correlation of *REDD1* expression to that of miR-210 in 23 RCC tumours. (e) correlation between *CA9* and *REDD1* expression in an independent series of 68 RCC tumour samples. For a-e, *REDD1* expression was normalised to *ACTIN*. (f) Kaplan Meier survival data from 31 patients with either high or low *REDD1* expression. Statistical significance: * $p<0.05$, ** $p<0.01$, *** $p<0.001$.

a



b



c

	IC50uM
Ctrl	0.07
sh1	0.006
sh3	0.04
sh4	0.09

Figure 5-22 REDD1 knockdown and rapamycin sensitivity

REDD1 expression was quantified in RCC4 *vHL* null cells after transduction with a control lentivirus or transduction with 5 different shRNA against *REDD1*. Cells were incubated for 24 hours in hypoxia before RNA extraction and quantification, expression was normalized to *ACTIN* and data are presented as fold change relative to shcontrol. (b) SRB assays were performed on the above cell lines after treatment with different concentration of rapamycin for 72 hours. Data are presented as the mean and standard error of three replicates, a non-linear curve is also shown. (c) IC50 values for rapamycin sensitivity in RCC4 cells transduced with a control shRNA or three different shRNA against *REDD1*. Statistical significance: * $p<0.05$, ** $p<0.01$, *** $p<0.001$.

5.3. Discussion

5.3.1. miR-100 in renal cancer

We have previously demonstrated hypoxic downregulation of miR-100 in bladder cancer cell lines and also found its expression to be inversely correlated with hypoxia in breast cancer samples. As the hypoxic response is an important feature of RCC, we hypothesized that miR-100 may be downregulated in renal cancer. Furthermore, as miR-100 can target mTOR [240], it could potentially regulate sensitivity to the mTORC1 inhibitor rapamycin in RCC. In this chapter, miR-100 levels were found to be lower in renal tumour tissue when compared to normal renal tissue.

MiR-100 expression was lower in *vHL* null 786-0 cells compared to their *vHL* competent counterparts. However, miR-100 levels were not regulated by hypoxia in *vHL* null or competent RCC4 and 786-0 cells. Thus, the downregulation of miR-100 is not likely to be a direct result of regulation by HIF. In support of this, miR-100 expression could not be suppressed with the hypoxia memetic DMOG (Figure 3.10) and was unaffected by HIF knockdown (Figure 3.11) in the bladder cell line RT4. The decrease in expression of miR-100 seen in RCC may be a result of alternative pathways such as loss of the miR-100 locus on chromosome 11q, as seen in oral cancer [287]. In our hands, overexpression of mimic-100 did not affect rapamycin sensitivity of RT4 cells. However, down regulation of miR-100 may be of clinical significance in other cancer types as in ovarian clear cell cancer, miR-100 increases sensitivity to rapamycin [240].

5.3.2. *vHL* mutation and drug sensitivity

There is an important need to identify predictive factors for response to targeted therapy in RCC. Although others exist, the predominant mutations in renal cancer are those in *vHL*. Loss of functional *vHL* leads to the stabilization of HIF and activation of its target genes. Thus, patients with *vHL* mutations overexpress HIF dependent genes such as *VEGF* and *PDGF* and may respond better than those without *vHL* mutations to therapies that target these pathways. In the first instance, we investigated whether loss of *vHL* could predict response to rapamycin, sunitinib, sorafenib and metformin in RCC.

In all three established cell lines (RCC4, 786-0 and UMRC2), loss of *vHL* increased the sensitivity of cells to growth inhibition by rapamycin. The rapamycin sensitive mTORC1 complex is responsible for increased translation of HIF-1α and HIF-2α in certain circumstances [288]. Thus, cell lines that are "addicted" to the HIF pathway, such as those with *vHL* mutation, would be more sensitive to drugs that attenuate HIF levels, such as rapamycin. In RCC4 cells, sensitivity to rapamycin increased with duration of exposure, irrespective of *vHL* status. Rapamycin is thought to be a selective inhibitor of mTORC1; however, prolonged exposure is known to disrupt assembly of the mTORC2 complex needed to sustain PKB activation [172], and may account for the greater sensitivity at later timepoints.

In contrast to established renal cancer lines, the response of primary RCC cultures was mixed. Of the five primary renal cancer cultures most sensitive to rapamycin, three had mutations detected in *vHL*. However, the two primary cell

lines that were most resistant to rapamycin also had detectable *vHL* mutations. In agreement with this, a study with 20 patients suggested that there was no association between *vHL* status and response to the rapamycin derivative, temsirolimus [289]. Thus, at present, *vHL* status does not appear to be a useful predictive marker of responses to rapamycin and rapamycin analogues.

There was no consistent effect of *vHL* mutation on the response of the established RCC cell lines and primary RCC cultures to sunitinib, suggesting that *vHL* mutation status is not a useful indicator of responsiveness to sunitinib.

For both RCC4 and UMRC2, loss of *vHL* made cells more resistant to sorafenib. Similarly, the presence of wildtype *vHL* was found to render RCC tumours more sensitive to the SRC inhibitor dasatinib [290]. However, in the primary RCC cultures, the loss of *vHL* was found to increase sensitivity to sorafenib; indeed, the five most sensitive primary lines had a *vHL* mutation. This highlights the differences that may exist between established cell lines and primary material and the utility of primary RCC cultures in studying drug responses. However, a larger number of samples are required to definitively confirm a link between *vHL* mutation status and sensitivity to sorafenib. Indeed, a recent study with 123 patients found no correlation between *vHL* mutation/methylation and response to sorafenib or sunitinib [291].

Thus, data from this work suggests that vHL mutation status is not predictive in defining response to current therapeutic agents used in the treatment of RCC. It is likely that mutations in a number of genes and alterations in multiple signaling pathways are likely to contribute to the heterogeneity in chemotherapy responses observed in the primary RCC cultures. Indeed, it is known that

mutations in genes such as *PTEN* and *PIK3CA* affect the response to mTOR inhibitors in different cancer types [292, 293].

5.3.3. Does the absence of competent vHL effect gene expression?

We reasoned that a panel of biomarkers rather than just the *vHL* mutation status would be required to accurately predict response to treatment. With this in mind we selected a panel of genes for expression profiling to identify possible markers of response to targeted therapies in renal cancer.

5.3.2.1. Effect of vHL mutation on HIF target gene expression

Of the genes chosen as markers of hypoxia, the expression of *REDD1*, *EGLN3*, *CYCLIN D1, CA9* and *HIF-1* appeared to be affected by *vHL* mutation status. All primary RCC cultures with *vHL* mutation had elevated levels of *REDD1* and *CA9*. Furthermore, elevated levels of *EGLN3* were also seen in 4 out of 5 primary RCC cultures with *vHL* mutation. The expression of *REDD1, EGLN3* and *CA9* were also increased in *vHL* null RCC4 cells. In 786-0 cells, no differential regulation of *CA9* was observed in *vHL* null cells compared to their wildtype counterparts. *CA9* appears to be an exclusive *HIF-1*α target gene [294]; 786-0 cells only express *HIF-2*α and the lack of *HIF-1*α in these cells accounts for the lack of *CA9* induction in this line.

REDD1 is a HIF target gene that is responsive to both *HIF-1*α and *HIF-2*α [198] Despite this, it is not induced in *vHL* null 786-0 cells. In contrast, the HIF target gene *EGLN3* (PHD3) [295] is responsive to both *HIF-1*α and *HIF-2*α [296] and is upregulated in *vHL* null 786-0 cells. In normoxia, *EGLN3* is one of three prolyl

hydroxylases responsible for hydroxylating HIF-α subunits, leading to their degradation. Its induction under hypoxic conditions serves to prevent excessive HIF signaling that would otherwise lead to cell death [296]. Increased expression of *EGLN3* may be more relevant in RCC as loss of *vHL* leads to HIF accumulation in normoxia when the prolyl hydroxylases are most active, thus establishing a feedback loop to limit HIF activity.

In RCC4, *vHL* null cells had higher levels of *CYCLIN D1. CYCLIN D1* is a known HIF target gene [297], although regulation appears to be either positive or negative in a context dependent manner. It has previously been reported that *CYCLIN D1* levels were upregulated in renal cancer specimens with *vHL* mutations when compared to those without mutations [298]. However, in our study, we did not observe a correlation between *CYCLIN D1* levels and *vHL* status in primary RCC cultures; expression was unchanged in 5 lines, decreased in 4 (1 *vHL* mutant) and increased in 1 (*vHL* mutant) primary RCC lines. Thus, the expression of *CYCLIN D1* does not appear to correlate to *vHL* mutation status and at present, it is unclear whether levels are different in RCC compared to normal renal cells.

Loss of *vHL* in RCC4 led to a dramatic suppression of HIF-1α transcript levels. This occurs despite *HIF-1α* protein levels being elevated in these cells. In addition, decreased HIF-1α mRNA levels were also observed in 4/5 primary RCC lines that had a *vHL* mutation. Consistent with our observation, it has recently been shown that the mRNA destabilizing protein tristetraprolin binds to the 3'UTR of the HIF-1α transcript, leading to its decay after a few hours of hypoxia in endothelial cells [299].

Although *REDD2* is a potent inhibitor of mTOR activity, there is no evidence at present to suggest that it is a hypoxia regulated/HIF target gene. Variable

expression of *REDD2* was observed in the primary RCC lines, with decreased expression in 5 (2 *vHL* mutant) and increased expression in 2 (both *vHL* mutant) lines. Thus, it is unlikely that *REDD2* is involved in the pathogenesis of the majority of RCC.

5.3.2.2 Effect of vHL mutation on the expression of mTOR Signaling components

Of the components of the mTOR signaling pathways chosen for expression analyses at the transcript level, differential regulation of *4EBP1, RAPTOR, TSC1, TSC2* and *RHEB* by *vHL* status was observed. Of the primary RCC lines, 3/5 with *vHL* mutation had increased levels of *4EBP1*. The expression of *4EBP1* was also elevated in *vHL* null RCC4 and 786-0 cells. Under hypoxic conditions, the mTOR pathway is rapidly attenuated, largely by HIF independent mechanisms, that results in decreased phosphorylation of the mTOR substrates *4EBP1* and *p70S6K* [270]. *4EBP1* inhibits protein synthesis on ribosomes; phosphorylation of *4EBP1* by mTOR inhibits its activity, thereby allowing translation to occur [270]. Recently, increased staining for total *4EBP1* by immunohistochemistry has been reported in RCC tumours, and particularly in metastatic tumours [300]. This increase in *4EBP1* immunoreactivity could be a consequence of increased transcript levels of this gene, although the functional consequence of this increase is unclear.

Four out of the five primary RCC lines with vHL mutation had increased levels of RAPTOR. Furthermore, in 786-0, vHL null cells had increased levels of RAPTOR compared to their wildtype counterparts. While this suggests there may be a correlation between *RAPTOR* expression and vHL status, a larger number of

samples is required to confirm this association. 786-0 cells with loss of *vHL* also had increased levels of *TSC1, TSC2* and *RHEB*. However, this was not reproduced in the primary RCC cultures, suggesting either that they are unique to *vHL* null 786-0 cells or that they are responsive to HIF-2α.

5.3.2.3 Effect of vHL mutation on the expression of stem cell markers

In this study, the expression of *NANOG* was decreased in 4 primary RCC lines (3 *vHL* mutant) and increased in 2 (1 *vHL* mutant) and unchanged in the remainder of the primary RCC lines. Thus, the expression of *NANOG* is likely to be regulated in a cell specific manner, irrespective of *vHL* mutation status.

Elevated levels of both *OCT4* and *HIF-2α* were also observed in *vHL* null 786-0 cells. *OCT4* is a known *HIF-2α,* but not *HIF-1α,* target gene [301] and, thus, the elevated levels of *OCT4* in 786-0 cells is not surprising as these cells only express *HIF-2α.* However, *HIF-2α* levels were not consistently regulated in the primary RCC cultures. Furthermore, *OCT4* levels were markedly decreased in the majority of primary RCC cultures (8/10 cell lines), irrespective of *vHL* mutation status. In agreement with this, a recent study found the transcript levels of *OCT4* and *NANOG* to be lower in 30 RCC tumours compared to five normal renal tissue samples [302]. In our study, *NANOG* levels were decreased in four out of 10 primary RCC cultures compared to normal renal cells.

The observation that primary RCC cultures have lower levels of *OCT4* could suggest that RCC stem cells are a smaller percentage of the tumour than adult stem cells in normal renal tissue as increased expression of *OCT4* and *NANOG* are associated with a more "stem cell" like phenotype in breast cancer [270]. Alternatively, decreased expression of *OCT4* may be of functional relevance in

RCC as it has recently been shown that *OCT4* suppresses invasion of MCF7 breast cancer cells [303]. Thus, the role of *OCT4* in RCC warrants further investigation.

5.3.2.4 Effect of vHL mutation on histone modifying genes

Mutations in *JARID1C* and *SETD2* have been identified in around 3% of cases of clear cell RCC [149]. In 786-0 cells we saw a reduction in expression of *JARID1C* with loss of *vHL*. *JARID1C* expression is known to be responsible for the suppression of HIF response genes such as *IGFBP3* in *vHL* null cells [304]. However, there was no consistent regulation of *JARID1C* in the primary renal cancer lines, suggesting that regulation at the mRNA level is not important in determining JARID1C activity.

There was no change in *SETD2* levels in RCC4 or 786-0 cells in *vHL* null cells compared to their wildtype counterparts. However, the expression of *SETD2* was less than 50% of the levels found in normal renal cells in 7/10 of the primary RCC lines, irrespective of *vHL* mutation status. The results from this study suggest that in addition to mutations, decreased *SETD2* expression also occur in RCC that may contribute to the pathology of this cancer. The role of *SETD2* in RCC biology warrants further investigation.

5.3.2.5 Incomplete detection of loss of vHL function

In this study, loss of *vHL* function was detected by mutation screening; of the 10 primary RCC samples used in this study, five were found to have a *vHL* mutation in the heterozygote state. However, two additional primary tumour cell lines, 35236.10 and 00929.11, also had increased levels of CA9, the former by around 8

fold and the latter by over 2000 fold. In addition, 00929.11 exhibited a gene expression profile that was similar to the majority of primary RCC cultures with *vHL* mutation – it had elevated levels *EGLN3, REDD1* and *4EBP1* and decreased levels of *HIF-1α*. This strongly suggests that the primary cell line 00929.11 has loss of *vHL* function that was not detected during sequencing.

A number of factors could account for the negative mutation status by sequencing in cell line 00929.11. A large stromal contamination of the sample would lead to masking of any mutation in *vHL* in the tumour by the wildtype gene in the stroma. In RCC, *vHL* loss occurs as LOH in the majority of cases with loss of function mutation of the remaining allele. This hemizygous state would appear as homozygous by sequencing. In contrast, all of the mutations identified in *vHL* in this study were present in the heterozygous state, suggesting significant contamination from the wildtype allele in the stroma. Other possibilities include mutations in other regions of the gene not sequenced. Alternatively, *vHL* function may be lost by promoter methylation or deletion of both copies of the gene in this cell line. As the primary line 35236.10 only had an 8-fold upregulation of *CA9* levels, there is no evidence to suggest it may have lost *vHL* function. However, it would be worth investigating the status of *vHL* in both these primary lines further.

5.3.3. Correlation of gene expression

It would be expected that the expression of genes in the same pathway would correlate. Indeed, the expression of 4 HIF target genes, *CA9, REDD1*, *EGLN3* and *CYCLIN D1*, were positively correlated with each other. Additionally, there was

strong correlation between *CA9* and *EGLN3* expression and the expression of the mTOR target gene *4EBP1* and good correlation between the expression of *CYCLIN D1* and *EGLN3* and the mTORC1 component *RAPTOR*. To date, neither *RAPTOR* nor *4EBP1* are known to be direct HIF target genes but this possibility warrants further investigation. Of note is the observation that increased expression of *CA9, EGLN3, REDD1* and *4EBP1* were all inversely correlated with the expression of *HIF-1α*. Thus, the coordinated upregulation of *CA9, EGLN3*, *REDD1, CYCLIN D1, 4EBP1* and *RAPTOR*, and downregulation of HIF-1α mRNA appear to be a robust marker of *vHL* inactivation and activation of the hypoxic pathway in renal cell cancer.

We observed a number of correlations between individual genes such as *SETD2* to *CYCLIN D1, OCT4* to *p21* and *p70S6K*. However, all these genes belong to traditionally distinct pathways, and therefore, the relevance of these individual correlations requires validation in a larger number of renal tumour samples.

5.3.4. Can gene expression predict sensitivity to rapamycin?

Intriguingly, *REDD1* expression was correlated to *p70S6K* expression. This may represent a mechanism to overcome *REDD1* dependent reduction in mTOR signaling; indeed, the inhibitory REDD1-mTOR link is often disrupted in cancer, where cell proliferation persists even in the face of sustained expression of *REDD1* [305].

Of note is that the expression of *REDD1* and *p70S6K* had a positive correlation with rapamycin sensitivity of primary RCC cultures. Both these genes are integral components of the mTOR pathway, although they act in opposing

fashion, suggesting that increased activation of mTOR pathway directly predicts the sensitivity to rapamycin. It would appear that increased expression of REDD1 an inhibitor of the pathway decreases the effectiveness of rapamycin. In summary cells with higher activation of the mTORC2 and lower activation of mTORC1 pathways are more resistant to rapamycin.

5.3.5. The role of REDD1 in renal cancer

As previously mentioned, *REDD1* levels were elevated in *vHL* null primary RCC cultures and established cell lines. In paired normal/tumour samples, increased levels of *REDD1* were observed in clear cell RCC samples, most likely as a consequence of *vHL* inactivation and HIF pathway activation in this RCC subtype. Indeed, the expression of *REDD1* was positively correlated to the expression of known markers of hypoxia including *CA9* and miR-210. Intriguingly, increased expression of *REDD1* was seen in tumours with vascular invasion. It is known that hypoxia leads to the induction of the angiogenic factor VEGF; thus, it is likely that tumours that have lost *vHL* function would upregulate VEGF, leading to angiogenesis and vascular invasion, perhaps accounting for the correlation with *REDD1* expression. Although vascular invasion is known to be an adverse prognostic factor in RCC [306], *REDD1* levels did not correlate with tumour grade or overall patient survival. This was somewhat surprising as nucleolar size is a major determinant for Fuhrman grading in RCC [307] and mTORC1 activation is critical in the regulation of ribosomal biogenesis and nucleolar size. This would suggest that *REDD1* on its own is not a sufficient marker for RCC grading/prognosis.

REDD1 is known to be induced by various stresses including hypoxia, in a HIF-1α and HIF-2α dependent manner [305], and DNA damage in a p53/p63 dependent pathway [308]. REDD1 binds to, and sequesters, the 14-3-3 protein, thereby releasing TSC2 to inhibit mTOR. Intriguingly, *REDD1* expression was correlated to *p70S6K* expression. Although final p70S6K activity is regulated by mTORC1 phosphorylation, increased transcript levels may translate to increased protein levels of p70S6K. This may represent a mechanism to overcome REDD1 dependent reduction in mTOR signaling. Indeed, the inhibitory REDD1-mTORC1 link was found to be disrupted in clear cell RCC by mutations in *TSC1* [305].

In *vHL* null RCC4 cells, REDD1 appeared to mediate some level of resistance to rapamycin as knockdown of *REDD1* increased the sensitivity of cells by around 10-fold. This would be in agreement with the correlation between *REDD1* expression and rapamycin sensitivity in primary RCC cultures, with the cells with greater *REDD1* expression being more resistant to rapamycin. In a previous study, knockdown of *REDD1* expression sensitized cells to rapamycin mediated increase in cell volume [309]. Thus, there may be clinical utility for the combination use of inhibitors that target REDD1 (hypoxia pathway) and mTOR simultaneously.

5.3.6 Conclusion

In this chapter, we found that while *vHL* mutation sensitized cells to rapamycin mediated growth arrest in established cell lines, this did not hold true in primary RCC cultures. By looking at gene expression, we found a mRNA signature of 7 genes – high *CA9, EGLN3, REDD1, CYCLIN D1, 4EBP1* and *RAPTOR* and low *HIF-1α*

that could be a surrogate marker for *vHL* inactivation in RCC. Of all the markers investigated in this study, expression of *REDD1* and *p70S6K* were found to correlate with rapamycin sensitivity and may be useful in identifying patients who may respond to mTOR inhibitors.

Chapter 6 Conclusions and future plans

6.1. Hypoxia regulated miRNAs in bladder cancer

In this thesis, I have focused on urological malignancies. Both miRNAs and hypoxia are important players in the oncogenic process. In Chapter 3, hypoxia regulated miRNA (HRMs) were identified that may be important in non-muscle invasive and muscle invasive bladder cancer. We found both miRNAs 210 and 193b to be upregulated by hypoxia in bladder and renal cancer cell lines. Furthermore, we found almost half the members of a miRNA cluster known as the chromosome 19 cluster (C19MC) to be induced by hypoxia in a cell line specific manner. The hypoxic induction of miR-210 is well published and a number of miR-210 targets have been identified and functionally analysed. Relatively little is known about miR-193b and the C19MC cluster, and, therefore, confirmation of hypoxic regulation of these miRNA by functional studies could be a focus for future studies.

We found miR-145 to be robustly induced by hypoxia in the non-muscle invasive line RT4. In this cell line, miR-145 is a novel HIF target gene with two functional HIF response elements. Furthermore, miR-145 was found to contribute to apoptosis after exposure of RT4 cells to hypoxia for an extended period of time. It would be worth examining the expression of miR-145 in clinical samples of bladder cancer and determine if its expression correlated with outcome variables.

The downregulation of miR-100 has been reported in a number of tumour types including bladder cancer. MiR-100 is known to target both FGFR3 and mTOR. In this study, miR-100 expression was found to be decreased by exposure to hypoxia but this was not dependent on HIF, suggesting it may be a stress response. It would be worth examining the expression of miR-100 after other forms of stress such as glucose deprivation. Functionally, miR-100 was found to downregulate both FGFR3 and mTOR and in the case of the former, to affect its activation of ERK and PKB pathways. The novel hypoxic and miR-100 mechanism for regulating *FGFR3* in bladder cancer may provide an additional means for increased expression of this growth promoting pathway that could contribute to the pathogenesis of this disease. This may provide selection for upregulation of *FGFR3* and maintenance of the papillary phenotype, hence preventing progression to muscle invasive disease. An intriguing observation is that mutations in *FGFR3* that occur in dwarfism lead to terminal differentiation of osteoblasts. Therapies targeting *FGFR3* in bladder cancer may lead to the loss of this potentially protective mechanism that promotes a more differentiated (and, therefore, less aggressive tumour) and requires additional studies.

While miR-100 regulates mTOR expression, we did not observe it to impact on rapamycin sensitivity in the non-muscle invasive cell line RT4. However, miR-100 has been shown to affect rapamycin sensitivity in clear cell ovarian tumours; it may be worth exploring a role for miR-100 in regulating this process in additional bladder and RCC lines.

It is likely that altered miRNA expression is likely to have important physiological and pathological implications. It may be worth performing xenografts experiments to uncover the involvement of miR-100 in bladder and

renal cancer tumourigenesis. It would also be worth performing mRNA expression profiling analyses and miRNA pull down experiments to identify other targets for the miRNA of interest found in this study, such as miR-100, miR-145 and miR-193b.

6.2. The role of *vHL* mutation and hypoxia regulated genes in predicting sensitivity to targeted therapies

We were interested in identifying biomarkers that may predict drug sensitivity in historic and primary RCC cell lines. Although the presence of a *vHL* mutation sensitized historic RCC lines to the mTOR inhibitor, this did not hold true in the primary RCC lines, suggesting that loss of *vHL* is not a useful predictor of rapamycin response. However, in this work, the expression of both *REDD1* and *p70S6K* were found to correlate with the response to rapamycin; it would be worthwhile to test the clinical utility of these two markers, either individually or in combination, in a larger series of RCC samples. Furthermore, the expression of phospho- and total *p70S6K* in RCC samples should be investigated, as *p70S6K* activity is known to depend on phosphorylation by mTOR.

By sequencing, a *vHL* mutation was found in 50% of the primary RCC lines used in this study. However, one cell line was found to have all the features of *vHL* inactivation but no mutation was detected. This would suggest that either the sequencing reaction failed to pick up a mutation present in the sample or that *vHL* may be inactivated by other means besides mutation. It would be worth exploring other means of *vHL* inactivation, such as promoter methylation or total gene deletions, in RCC.

We found the coordinated expression of seven genes - high *CA9, EGLN3, REDD1, CYCLIN D1, 4EBP1* and *RAPTOR* and low *HIF-1α* that could be a surrogate marker for *vHL* inactivation in RCC. It would be worth investigating whether this signature was predictive of loss of *vHL* function in a larger series of RCC samples. *4EBP1* and *RAPTOR* are not known to be targets of HIF; this, their induction by *vHL* inactivation warrants further investigation as it would shed light on the crosstalk between the hypoxic and mTOR pathways. An interesting observation is that *vHL* mutation, which would lead to higher protein levels of the HIF-α subunit, is associated with a dramatic decrease in HIF-1α transcript levels. It would suggest that there was an inverse correlation between increased HIF-1α translation in hypoxia and its transcript levels and could be investigated further.

While mutations in the methylase *SETD2* have been reported in around 3% of cases of clear cell RCC, in this study, transcript levels were also found to be low in primary tumour cultures compared to normal renal tissue. This would suggest that loss of *SETD2* plays an important role in the biology of RCC and its function can be inactivated by both mutation and decreased expression. It would be worth exploring the possibility of promoter methylation as a mechanism for decreased *SETD2* expression in RCC.

In this study, immunostaining for *REDD1* was not found to correlate with RCC patient survival. However, it may be worth repeating the analysis in a larger number of patients. *REDD1* expression did appear to play a functional role in regulating mTOR activity as knockdown of *REDD1* sensitised cells to rapamycin. However, these knockdown pools are likely to be heterogeneous mix of cells with very good to very poor knockdown. Thus, it would be worth isolating individual clones with good knockdown with each of the REDD1 shRNA and

repeating the sensitivity to rapamycin experiment. Xenograft studies using individual REDD1 shRNA clones may provide valuable information on the role of *REDD1* in regulating the mTOR pathway *in vivo*.

Publications and presentations

Publications

MicroRNA-210 regulates mitochondrial free radical response to hypoxia and Krebs cycle in cancer cells by targeting iron sulphur cluster protein ISCU.
Favaro E, Ramachandran A, McCormick R, Gee H, Blancher C, Crosby M, Devlin C,Blick C, Buffa F, Li JL, Vojnovic B, Pires das Neves R, Glazer P, Iborra F, Ivan M, Ragoussis J, Harris AL.
PLoS One. 2010 Apr 26;5(4):

Radiosensitization of Renal Cell Carcinoma in vitro through the induction of autophagy
Anbalagan, S. Pires,IM. Blick C. Hill MA. Ferguson DJP. Chan DA. Hammond EM.
Accepted Radiotherapy and oncology

The hypoxic and miR-100 regulation of FGFR3 in non-invasive bladder cancer.
Blick C. McCormick, R. Ramachandran, A. Knowles, MA. Catto, J. Cranston, D. Harris, AL.
Submitted to Clinical Cancer Research

Presentations

Hypoxia regulated miRNAs in bladder cancer.
British Association of Urologists Annual Meeting, Glasgow, 2012.

The potential role of REDD1 as a biomarker in renal cell carcinoma.
American Association of Cancer Research. Chicago, 2012.

The role of miR-100 in the regulation of FGFR3.
MicroRNAs and cancer, Keystone meeting, Banff, Canada, February 2011

References

1. Jemal, A., F. Bray, M.M. Center, J. Ferlay, E. Ward, and D. Forman, *Global cancer statistics.* CA Cancer J Clin, 2011. **61**(2): p. 69-90.
2. Hanahan, D. and R.A. Weinberg, *The hallmarks of cancer.* Cell, 2000. **100**(1): p. 57-70.
3. Hanahan, D. and R.A. Weinberg, *Hallmarks of cancer: the next generation.* Cell, 2011. **144**(5): p. 646-74.
4. Chitnis, M.M., J.S. Yuen, A.S. Protheroe, M. Pollak, and V.M. Macaulay, *The type 1 insulin-like growth factor receptor pathway.* Clin Cancer Res, 2008. **14**(20): p. 6364-70.
5. Cappellen, D., C. De Oliveira, D. Ricol, S. de Medina, J. Bourdin, X. Sastre-Garau, et al., *Frequent activating mutations of FGFR3 in human bladder and cervix carcinomas.* Nat Genet, 1999. **23**(1): p. 18-20.
6. Tomlinson, D.C., O. Baldo, P. Harnden, and M.A. Knowles, *FGFR3 protein expression and its relationship to mutation status and prognostic variables in bladder cancer.* J Pathol, 2007. **213**(1): p. 91-8.
7. Roberts, P.J. and C.J. Der, *Targeting the Raf-MEK-ERK mitogen-activated protein kinase cascade for the treatment of cancer.* Oncogene, 2007. **26**(22): p. 3291-310.
8. Adjei, A.A., *Blocking oncogenic Ras signaling for cancer therapy.* J Natl Cancer Inst, 2001. **93**(14): p. 1062-74.
9. Burchill, S.A., D.E. Neal, and J. Lunec, *Frequency of H-ras mutations in human bladder cancer detected by direct sequencing.* Br J Urol, 1994. **73**(5): p. 516-21.
10. Liu, P., H. Cheng, T.M. Roberts, and J.J. Zhao, *Targeting the phosphoinositide 3-kinase pathway in cancer.* Nat Rev Drug Discov, 2009. **8**(8): p. 627-44.
11. Carpenter, C.L., K.R. Auger, M. Chanudhuri, M. Yoakim, B. Schaffhausen, S. Shoelson, et al., *Phosphoinositide 3-kinase is activated by phosphopeptides that bind to the SH2 domains of the 85-kDa subunit.* J Biol Chem, 1993. **268**(13): p. 9478-83.
12. Balla, T., *Inositol-lipid binding motifs: signal integrators through protein-lipid and protein-protein interactions.* J Cell Sci, 2005. **118**(Pt 10): p. 2093-104.
13. Currie, R.A., K.S. Walker, A. Gray, M. Deak, A. Casamayor, C.P. Downes, et al., *Role of phosphatidylinositol 3,4,5-trisphosphate in regulating the activity and localization of 3-phosphoinositide-dependent protein kinase-1.* Biochem J, 1999. **337 (Pt 3)**: p. 575-83.
14. Bakkar, A.A., H. Wallerand, F. Radvanyi, J.B. Lahaye, S. Pissard, L. Lecerf, et al., *FGFR3 and TP53 gene mutations define two distinct pathways in urothelial cell carcinoma of the bladder.* Cancer Res, 2003. **63**(23): p. 8108-12.
15. Irie, A., T. Uchida, H. Ishida, K. Matsumoto, M. Iwamura, and S. Baba, *p53 Mutation in bladder cancer patients in Japan and inhibition of growth by in vitro adenovirus-mediated wild-type p53 transduction in bladder cancer cells.* Mol Urol, 2001. **5**(2): p. 53-8.

16. Miyamoto, H., T. Shuin, S. Torigoe, Y. Iwasaki, and Y. Kubota, *Retinoblastoma gene mutations in primary human bladder cancer.* Br J Cancer, 1995. **71**(4): p. 831-5.
17. Mitra, A.P., M. Birkhahn, and R.J. Cote, *p53 and retinoblastoma pathways in bladder cancer.* World J Urol, 2007. **25**(6): p. 563-71.
18. Vanhaesebroeck, B., L. Stephens, and P. Hawkins, *PI3K signalling: the path to discovery and understanding.* Nat Rev Mol Cell Biol, 2012. **13**(3): p. 195-203.
19. Kopfstein, L. and G. Christofori, *Metastasis: cell-autonomous mechanisms versus contributions by the tumor microenvironment.* Cell Mol Life Sci, 2006. **63**(4): p. 449-68.
20. Bryan, R.T. and C. Tselepis, *Cadherin switching and bladder cancer.* J Urol, 2010. **184**(2): p. 423-31.
21. Shay, J.W. and W.E. Wright, *Role of telomeres and telomerase in cancer.* Semin Cancer Biol, 2011. **21**(6): p. 349-53.
22. Fujioka, T., M. Hasegawa, Y. Suzuki, T. Suzuki, J. Sugimura, S. Tanji, et al., *Telomerase activity in human renal cell carcinoma.* Int J Urol, 2000. **7**(1): p. 16-21.
23. Chung, I., S. Osterwald, K.I. Deeg, and K. Rippe, *PML body meets telomere: The beginning of an ALTernate ending?* Nucleus, 2012. **3**(3).
24. Baldewijns, M.M., I.J. van Vlodrop, P.B. Vermeulen, P.M. Soetekouw, M. van Engeland, and A.P. de Bruine, *VHL and HIF signalling in renal cell carcinogenesis.* J Pathol. **221**(2): p. 125-38.
25. Yang, J., X. Liu, K. Bhalla, C.N. Kim, A.M. Ibrado, J. Cai, et al., *Prevention of apoptosis by Bcl-2: release of cytochrome c from mitochondria blocked.* Science, 1997. **275**(5303): p. 1129-32.
26. Er, E., L. Oliver, P.F. Cartron, P. Juin, S. Manon, and F.M. Vallette, *Mitochondria as the target of the pro-apoptotic protein Bax.* Biochim Biophys Acta, 2006. **1757**(9-10): p. 1301-11.
27. Powis, G. and L. Kirkpatrick, *Hypoxia inducible factor-1alpha as a cancer drug target.* Mol Cancer Ther, 2004. **3**(5): p. 647-54.
28. Pugh, C.W. and P.J. Ratcliffe, *Regulation of angiogenesis by hypoxia: role of the HIF system.* Nat Med, 2003. **9**(6): p. 677-84.
29. Appelhoff, R.J., Y.M. Tian, R.R. Raval, H. Turley, A.L. Harris, C.W. Pugh, et al., *Differential function of the prolyl hydroxylases PHD1, PHD2, and PHD3 in the regulation of hypoxia-inducible factor.* J Biol Chem, 2004. **279**(37): p. 38458-65.
30. Kaelin, W.G., Jr. and P.J. Ratcliffe, *Oxygen sensing by metazoans: the central role of the HIF hydroxylase pathway.* Mol Cell, 2008. **30**(4): p. 393-402.
31. Semenza, G.L., *Targeting HIF-1 for cancer therapy.* Nat Rev Cancer, 2003. **3**(10): p. 721-32.
32. Harris, A.L., *Hypoxia--a key regulatory factor in tumour growth.* Nat Rev Cancer, 2002. **2**(1): p. 38-47.
33. Ruan, K., G. Song, and G. Ouyang, *Role of hypoxia in the hallmarks of human cancer.* J Cell Biochem, 2009. **107**(6): p. 1053-62.
34. Maxwell, P.H., C.W. Pugh, and P.J. Ratcliffe, *Activation of the HIF pathway in cancer.* Curr Opin Genet Dev, 2001. **11**(3): p. 293-9.

35. Guo, K., G. Searfoss, D. Krolikowski, M. Pagnoni, C. Franks, K. Clark, et al., *Hypoxia induces the expression of the pro-apoptotic gene BNIP3.* Cell Death Differ, 2001. **8**(4): p. 367-76.
36. Ray, R., G. Chen, C. Vande Velde, J. Cizeau, J.H. Park, J.C. Reed, et al., *BNIP3 heterodimerizes with Bcl-2/Bcl-X(L) and induces cell death independent of a Bcl-2 homology 3 (BH3) domain at both mitochondrial and nonmitochondrial sites.* J Biol Chem, 2000. **275**(2): p. 1439-48.
37. Bellot, G., R. Garcia-Medina, P. Gounon, J. Chiche, D. Roux, J. Pouyssegur, et al., *Hypoxia-induced autophagy is mediated through hypoxia-inducible factor induction of BNIP3 and BNIP3L via their BH3 domains.* Mol Cell Biol, 2009. **29**(10): p. 2570-81.
38. Sowter, H.M., P.J. Ratcliffe, P. Watson, A.H. Greenberg, and A.L. Harris, *HIF-1-dependent regulation of hypoxic induction of the cell death factors BNIP3 and NIX in human tumors.* Cancer Res, 2001. **61**(18): p. 6669-73.
39. Gatenby, R.A., K. Smallbone, P.K. Maini, F. Rose, J. Averill, R.B. Nagle, et al., *Cellular adaptations to hypoxia and acidosis during somatic evolution of breast cancer.* Br J Cancer, 2007. **97**(5): p. 646-53.
40. Lu, X. and Y. Kang, *Hypoxia and hypoxia-inducible factors: master regulators of metastasis.* Clin Cancer Res, 2010. **16**(24): p. 5928-35.
41. Bell, E.L., T.A. Klimova, J. Eisenbart, P.T. Schumacker, and N.S. Chandel, *Mitochondrial reactive oxygen species trigger hypoxia-inducible factor-dependent extension of the replicative life span during hypoxia.* Mol Cell Biol, 2007. **27**(16): p. 5737-45.
42. Seimiya, H., M. Tanji, T. Oh-hara, A. Tomida, I. Naasani, and T. Tsuruo, *Hypoxia up-regulates telomerase activity via mitogen-activated protein kinase signaling in human solid tumor cells.* Biochem Biophys Res Commun, 1999. **260**(2): p. 365-70.
43. Song, G., G. Ouyang, and S. Bao, *The activation of Akt/PKB signaling pathway and cell survival.* J Cell Mol Med, 2005. **9**(1): p. 59-71.
44. Zhou, J., T. Schmid, and B. Brune, *Tumor necrosis factor-alpha causes accumulation of a ubiquitinated form of hypoxia inducible factor-1alpha through a nuclear factor-kappaB-dependent pathway.* Mol Biol Cell, 2003. **14**(6): p. 2216-25.
45. Haddad, J.J. and S.C. Land, *A non-hypoxic, ROS-sensitive pathway mediates TNF-alpha-dependent regulation of HIF-1alpha.* FEBS Lett, 2001. **505**(2): p. 269-74.
46. Bergers, G. and L.E. Benjamin, *Tumorigenesis and the angiogenic switch.* Nat Rev Cancer, 2003. **3**(6): p. 401-10.
47. Liu, Y., S.R. Cox, T. Morita, and S. Kourembanas, *Hypoxia regulates vascular endothelial growth factor gene expression in endothelial cells. Identification of a 5' enhancer.* Circ Res, 1995. **77**(3): p. 638-43.
48. Laderoute, K.R., R.M. Alarcon, M.D. Brody, J.M. Calaoagan, E.Y. Chen, A.M. Knapp, et al., *Opposing effects of hypoxia on expression of the angiogenic inhibitor thrombospondin 1 and the angiogenic inducer vascular endothelial growth factor.* Clin Cancer Res, 2000. **6**(7): p. 2941-50.
49. Svastova, E., A. Hulikova, M. Rafajova, M. Zat'ovicova, A. Gibadulinova, A. Casini, et al., *Hypoxia activates the capacity of tumor-associated carbonic anhydrase IX to acidify extracellular pH.* FEBS Lett, 2004. **577**(3): p. 439-45.

50. Robertson, N., C. Potter, and A.L. Harris, *Role of carbonic anhydrase IX in human tumor cell growth, survival, and invasion.* Cancer Res, 2004. **64**(17): p. 6160-5.
51. Teicher, B.A., S.D. Liu, J.T. Liu, S.A. Holden, and T.S. Herman, *A carbonic anhydrase inhibitor as a potential modulator of cancer therapies.* Anticancer Res, 1993. **13**(5A): p. 1549-56.
52. Gatenby, R.A. and R.J. Gillies, *Glycolysis in cancer: a potential target for therapy.* Int J Biochem Cell Biol, 2007. **39**(7-8): p. 1358-66.
53. Draoui, N. and O. Feron, *Lactate shuttles at a glance: from physiological paradigms to anti-cancer treatments.* Dis Model Mech, 2011. **4**(6): p. 727-32.
54. Kroemer, G. and J. Pouyssegur, *Tumor cell metabolism: cancer's Achilles' heel.* Cancer Cell, 2008. **13**(6): p. 472-82.
55. Greijer, A.E., P. van der Groep, D. Kemming, A. Shvarts, G.L. Semenza, G.A. Meijer, et al., *Up-regulation of gene expression by hypoxia is mediated predominantly by hypoxia-inducible factor 1 (HIF-1).* J Pathol, 2005. **206**(3): p. 291-304.
56. Greenberger, L.M., I.D. Horak, D. Filpula, P. Sapra, M. Westergaard, H.F. Frydenlund, et al., *A RNA antagonist of hypoxia-inducible factor-1alpha, EZN-2968, inhibits tumor cell growth.* Mol Cancer Ther, 2008. **7**(11): p. 3598-608.
57. Zhang, H., D.Z. Qian, Y.S. Tan, K. Lee, P. Gao, Y.R. Ren, et al., *Digoxin and other cardiac glycosides inhibit HIF-1alpha synthesis and block tumor growth.* Proc Natl Acad Sci U S A, 2008. **105**(50): p. 19579-86.
58. Blank, M., M. Mandel, Y. Keisari, D. Meruelo, and G. Lavie, *Enhanced ubiquitinylation of heat shock protein 90 as a potential mechanism for mitotic cell death in cancer cells induced with hypericin.* Cancer Res, 2003. **63**(23): p. 8241-7.
59. Barliya, T., M. Mandel, T. Livnat, D. Weinberger, and G. Lavie, *Degradation of HIF-1alpha under hypoxia combined with induction of Hsp90 polyubiquitination in cancer cells by hypericin: a unique cancer therapy.* PLoS One, 2011. **6**(9): p. e22849.
60. Choi, H.J., B.J. Song, Y.D. Gong, W.J. Gwak, and Y. Soh, *Rapid degradation of hypoxia-inducible factor-1alpha by KRH102053, a new activator of prolyl hydroxylase 2.* Br J Pharmacol, 2008. **154**(1): p. 114-25.
61. Yang, J., A. Ahmed, E. Poon, N. Perusinghe, A. de Haven Brandon, G. Box, et al., *Small-molecule activation of p53 blocks hypoxia-inducible factor 1alpha and vascular endothelial growth factor expression in vivo and leads to tumor cell apoptosis in normoxia and hypoxia.* Mol Cell Biol, 2009. **29**(8): p. 2243-53.
62. Kong, D., E.J. Park, A.G. Stephen, M. Calvani, J.H. Cardellina, A. Monks, et al., *Echinomycin, a small-molecule inhibitor of hypoxia-inducible factor-1 DNA-binding activity.* Cancer Res, 2005. **65**(19): p. 9047-55.
63. Kung, A.L., S.D. Zabludoff, D.S. France, S.J. Freedman, E.A. Tanner, A. Vieira, et al., *Small molecule blockade of transcriptional coactivation of the hypoxia-inducible factor pathway.* Cancer Cell, 2004. **6**(1): p. 33-43.
64. Hudson, C.C., M. Liu, G.G. Chiang, D.M. Otterness, D.C. Loomis, F. Kaper, et al., *Regulation of hypoxia-inducible factor 1alpha expression and function*

by the mammalian target of rapamycin. Mol Cell Biol, 2002. **22**(20): p. 7004-14.
65. Grgic, T., L. Mis, and J.M. Hammond, *Everolimus: a new mammalian target of rapamycin inhibitor for the treatment of advanced renal cell carcinoma.* Ann Pharmacother, 2011. **45**(1): p. 78-83.
66. Lee, R.C., R.L. Feinbaum, and V. Ambros, *The C. elegans heterochronic gene lin-4 encodes small RNAs with antisense complementarity to lin-14.* Cell, 1993. **75**(5): p. 843-54.
67. Reinhart, B.J., F.J. Slack, M. Basson, A.E. Pasquinelli, J.C. Bettinger, A.E. Rougvie, et al., *The 21-nucleotide let-7 RNA regulates developmental timing in Caenorhabditis elegans.* Nature, 2000. **403**(6772): p. 901-6.
68. Rodriguez, A., S. Griffiths-Jones, J.L. Ashurst, and A. Bradley, *Identification of mammalian microRNA host genes and transcription units.* Genome Res, 2004. **14**(10A): p. 1902-10.
69. Kim, V.N. and J.W. Nam, *Genomics of microRNA.* Trends Genet, 2006. **22**(3): p. 165-73.
70. Schwarz, D.S., G. Hutvagner, T. Du, Z. Xu, N. Aronin, and P.D. Zamore, *Asymmetry in the assembly of the RNAi enzyme complex.* Cell, 2003. **115**(2): p. 199-208.
71. Yang, J.S., T. Maurin, and E.C. Lai, *Functional parameters of Dicer-independent microRNA biogenesis.* RNA, 2012.
72. Babiarz, J.E., J.G. Ruby, Y. Wang, D.P. Bartel, and R. Blelloch, *Mouse ES cells express endogenous shRNAs, siRNAs, and other Microprocessor-independent, Dicer-dependent small RNAs.* Genes Dev, 2008. **22**(20): p. 2773-85.
73. Coller, J. and R. Parker, *General translational repression by activators of mRNA decapping.* Cell, 2005. **122**(6): p. 875-86.
74. Pillai, R.S., S.N. Bhattacharyya, C.G. Artus, T. Zoller, N. Cougot, E. Basyuk, et al., *Inhibition of translational initiation by Let-7 MicroRNA in human cells.* Science, 2005. **309**(5740): p. 1573-6.
75. Filipowicz, W., S.N. Bhattacharyya, and N. Sonenberg, *Mechanisms of post-transcriptional regulation by microRNAs: are the answers in sight?* Nat Rev Genet, 2008. **9**(2): p. 102-14.
76. Bentwich, I., A. Avniel, Y. Karov, R. Aharonov, S. Gilad, O. Barad, et al., *Identification of hundreds of conserved and nonconserved human microRNAs.* Nat Genet, 2005. **37**(7): p. 766-70.
77. Berezikov, E., V. Guryev, J. van de Belt, E. Wienholds, R.H. Plasterk, and E. Cuppen, *Phylogenetic shadowing and computational identification of human microRNA genes.* Cell, 2005. **120**(1): p. 21-4.
78. Fabbri, M., C.M. Croce, and G.A. Calin, *MicroRNAs.* Cancer J, 2008. **14**(1): p. 1-6.
79. Volinia, S., G.A. Calin, C.G. Liu, S. Ambs, A. Cimmino, F. Petrocca, et al., *A microRNA expression signature of human solid tumors defines cancer gene targets.* Proc Natl Acad Sci U S A, 2006. **103**(7): p. 2257-61.
80. Calin, G.A. and C.M. Croce, *MicroRNA signatures in human cancers.* Nat Rev Cancer, 2006. **6**(11): p. 857-66.
81. O'Donnell, K.A., E.A. Wentzel, K.I. Zeller, C.V. Dang, and J.T. Mendell, *c-Myc-regulated microRNAs modulate E2F1 expression.* Nature, 2005. **435**(7043): p. 839-43.

82. Xiao, C., L. Srinivasan, D.P. Calado, H.C. Patterson, B. Zhang, J. Wang, et al., *Lymphoproliferative disease and autoimmunity in mice with increased miR-17-92 expression in lymphocytes.* Nat Immunol, 2008. **9**(4): p. 405-14.
83. Johnson, S.M., H. Grosshans, J. Shingara, M. Byrom, R. Jarvis, A. Cheng, et al., *RAS is regulated by the let-7 microRNA family.* Cell, 2005. **120**(5): p. 635-47.
84. Childs, G., M. Fazzari, G. Kung, N. Kawachi, M. Brandwein-Gensler, M. McLemore, et al., *Low-level expression of microRNAs let-7d and miR-205 are prognostic markers of head and neck squamous cell carcinoma.* Am J Pathol, 2009. **174**(3): p. 736-45.
85. Musumeci, M., V. Coppola, A. Addario, M. Patrizii, M. Maugeri-Sacca, L. Memeo, et al., *Control of tumor and microenvironment cross-talk by miR-15a and miR-16 in prostate cancer.* Oncogene, 2011. **30**(41): p. 4231-42.
86. Cole, K.A., E.F. Attiyeh, Y.P. Mosse, M.J. Laquaglia, S.J. Diskin, G.M. Brodeur, et al., *A functional screen identifies miR-34a as a candidate neuroblastoma tumor suppressor gene.* Mol Cancer Res, 2008. **6**(5): p. 735-42.
87. Yamakuchi, M., M. Ferlito, and C.J. Lowenstein, *miR-34a repression of SIRT1 regulates apoptosis.* Proc Natl Acad Sci U S A, 2008. **105**(36): p. 13421-6.
88. Burk, U., J. Schubert, U. Wellner, O. Schmalhofer, E. Vincan, S. Spaderna, et al., *A reciprocal repression between ZEB1 and members of the miR-200 family promotes EMT and invasion in cancer cells.* EMBO Rep, 2008. **9**(6): p. 582-9.
89. Huang, Q., K. Gumireddy, M. Schrier, C. le Sage, R. Nagel, S. Nair, et al., *The microRNAs miR-373 and miR-520c promote tumour invasion and metastasis.* Nat Cell Biol, 2008. **10**(2): p. 202-10.
90. Lee, D.Y., Z. Deng, C.H. Wang, and B.B. Yang, *MicroRNA-378 promotes cell survival, tumor growth, and angiogenesis by targeting SuFu and Fus-1 expression.* Proc Natl Acad Sci U S A, 2007. **104**(51): p. 20350-5.
91. Poliseno, L., A. Tuccoli, L. Mariani, M. Evangelista, L. Citti, K. Woods, et al., *MicroRNAs modulate the angiogenic properties of HUVECs.* Blood, 2006. **108**(9): p. 3068-71.
92. Mitomo, S., C. Maesawa, S. Ogasawara, T. Iwaya, M. Shibazaki, A. Yashima-Abo, et al., *Downregulation of miR-138 is associated with overexpression of human telomerase reverse transcriptase protein in human anaplastic thyroid carcinoma cell lines.* Cancer Sci, 2008. **99**(2): p. 280-6.
93. Benetti, R., S. Gonzalo, I. Jaco, P. Munoz, S. Gonzalez, S. Schoeftner, et al., *A mammalian microRNA cluster controls DNA methylation and telomere recombination via Rbl2-dependent regulation of DNA methyltransferases.* Nat Struct Mol Biol, 2008. **15**(3): p. 268-79.
94. Hua, Z., Q. Lv, W. Ye, C.K. Wong, G. Cai, D. Gu, et al., *MiRNA-directed regulation of VEGF and other angiogenic factors under hypoxia.* PLoS One, 2006. **1**: p. e116.
95. Kulshreshtha, R., M. Ferracin, S.E. Wojcik, R. Garzon, H. Alder, F.J. Agosto-Perez, et al., *A microRNA signature of hypoxia.* Mol Cell Biol, 2007. **27**(5): p. 1859-67.
96. Bruning, U., L. Cerone, Z. Neufeld, S.F. Fitzpatrick, A. Cheong, C.C. Scholz, et al., *MicroRNA-155 promotes resolution of hypoxia-inducible factor 1alpha activity during prolonged hypoxia.* Mol Cell Biol, 2011. **31**(19): p. 4087-96.

97. Zhang, Z., H. Sun, H. Dai, R.M. Walsh, M. Imakura, J. Schelter, et al., *MicroRNA miR-210 modulates cellular response to hypoxia through the MYC antagonist MNT.* Cell Cycle, 2009. **8**(17): p. 2756-68.
98. Babar, I.A., J. Czochor, A. Steinmetz, J.B. Weidhaas, P.M. Glazer, and F.J. Slack, *Inhibition of hypoxia-induced miR-155 radiosensitizes hypoxic lung cancer cells.* Cancer Biol Ther, 2011. **12**(10): p. 908-14.
99. Ghosh, G., I.V. Subramanian, N. Adhikari, X. Zhang, H.P. Joshi, D. Basi, et al., *Hypoxia-induced microRNA-424 expression in human endothelial cells regulates HIF-alpha isoforms and promotes angiogenesis.* J Clin Invest, 2010. **120**(11): p. 4141-54.
100. Du, R., W. Sun, L. Xia, A. Zhao, Y. Yu, L. Zhao, et al., *Hypoxia-induced down-regulation of microRNA-34a promotes EMT by targeting the Notch signaling pathway in tubular epithelial cells.* PLoS One, 2012. **7**(2): p. e30771.
101. Gonsalves, C.S. and V.K. Kalra, *Hypoxia-mediated expression of 5-lipoxygenase-activating protein involves HIF-1alpha and NF-kappaB and microRNAs 135a and 199a-5p.* J Immunol, 2010. **184**(7): p. 3878-88.
102. Lei, Z., B. Li, Z. Yang, H. Fang, G.M. Zhang, Z.H. Feng, et al., *Regulation of HIF-1alpha and VEGF by miR-20b tunes tumor cells to adapt to the alteration of oxygen concentration.* PLoS One, 2009. **4**(10): p. e7629.
103. Meng, F., R. Henson, H. Wehbe-Janek, K. Ghoshal, S.T. Jacob, and T. Patel, *MicroRNA-21 regulates expression of the PTEN tumor suppressor gene in human hepatocellular cancer.* Gastroenterology, 2007. **133**(2): p. 647-58.
104. Peng, G., Y. Yuan, Q. He, W. Wu, and B.Y. Luo, *MicroRNA let-7e regulates the expression of caspase-3 during apoptosis of PC12 cells following anoxia/reoxygenation injury.* Brain Res Bull, 2011. **86**(3-4): p. 272-6.
105. Office for National Statistics, C.S.r.R.o.c.d.i., England. Series MB1 no.37. 2009, National Statistics: London.
106. Mistry, M., D.M. Parkin, A.S. Ahmad, and P. Sasieni, *Cancer incidence in the United Kingdom: projections to the year 2030.* Br J Cancer, 2011. **105**(11): p. 1795-803.
107. Madeb, R. and E.M. Messing, *Gender, racial and age differences in bladder cancer incidence and mortality.* Urol Oncol, 2004. **22**(2): p. 86-92.
108. Baris, D., M.R. Karagas, C. Verrill, A. Johnson, A.S. Andrew, C.J. Marsit, et al., *A case-control study of smoking and bladder cancer risk: emergent patterns over time.* J Natl Cancer Inst, 2009. **101**(22): p. 1553-61.
109. Luis, N.M., E. Lopez-Knowles, and F.X. Real, *Molecular biology of bladder cancer.* Clin Transl Oncol, 2007. **9**(1): p. 5-12.
110. Ploeg, M., K.K. Aben, C.A. Hulsbergen-van de Kaa, M.P. Schoenberg, J.A. Witjes, and L.A. Kiemeney, *Clinical epidemiology of nonurothelial bladder cancer: analysis of the Netherlands Cancer Registry.* J Urol, 2010. **183**(3): p. 915-20.
111. Salem, H.K. and S. Mahfouz, *Changing Patterns (Age, Incidence, and Pathologic Types) of Schistosoma-associated Bladder Cancer in Egypt in the Past Decade.* Urology, 2012. **79**(2): p. 379-83.
112. Montironi, R. and A. Lopez-Beltran, *The 2004 WHO classification of bladder tumors: a summary and commentary.* Int J Surg Pathol, 2005. **13**(2): p. 143-53.

113. Castillo-Martin, M., J. Domingo-Domenech, O. Karni-Schmidt, T. Matos, and C. Cordon-Cardo, *Molecular pathways of urothelial development and bladder tumorigenesis.* Urol Oncol. **28**(4): p. 401-8.
114. Goebell, P.J. and M.A. Knowles, *Bladder cancer or bladder cancers? Genetically distinct malignant conditions of the urothelium.* Urol Oncol. **28**(4): p. 409-28.
115. Platt, F.M., C.D. Hurst, C.F. Taylor, W.M. Gregory, P. Harnden, and M.A. Knowles, *Spectrum of phosphatidylinositol 3-kinase pathway gene alterations in bladder cancer.* Clin Cancer Res, 2009. **15**(19): p. 6008-17.
116. Lopez-Knowles, E., S. Hernandez, N. Malats, M. Kogevinas, J. Lloreta, A. Carrato, et al., *PIK3CA mutations are an early genetic alteration associated with FGFR3 mutations in superficial papillary bladder tumors.* Cancer Res, 2006. **66**(15): p. 7401-4.
117. Sjodahl, G., M. Lauss, S. Gudjonsson, F. Liedberg, C. Hallden, G. Chebil, et al., *A systematic study of gene mutations in urothelial carcinoma; inactivating mutations in TSC2 and PIK3R1.* PLoS One, 2011. **6**(4): p. e18583.
118. Jebar, A.H., C.D. Hurst, D.C. Tomlinson, C. Johnston, C.F. Taylor, and M.A. Knowles, *FGFR3 and Ras gene mutations are mutually exclusive genetic events in urothelial cell carcinoma.* Oncogene, 2005. **24**(33): p. 5218-25.
119. Hoglund, M., T. Sall, S. Heim, F. Mitelman, N. Mandahl, and I. Fadl-Elmula, *Identification of cytogenetic subgroups and karyotypic pathways in transitional cell carcinoma.* Cancer Res, 2001. **61**(22): p. 8241-6.
120. Lopez-Beltran, A., J. Alvarez-Kindelan, R.J. Luque, A. Blanca, A. Quintero, R. Montironi, et al., *Loss of heterozygosity at 9q32-33 (DBC1 locus) in primary non-invasive papillary urothelial neoplasm of low malignant potential and low-grade urothelial carcinoma of the bladder and their associated normal urothelium.* J Pathol, 2008. **215**(3): p. 263-72.
121. Williams, S.V., K.D. Sibley, A.M. Davies, H. Nishiyama, N. Hornigold, J. Coulter, et al., *Molecular genetic analysis of chromosome 9 candidate tumor-suppressor loci in bladder cancer cell lines.* Genes Chromosomes Cancer, 2002. **34**(1): p. 86-96.
122. van Rhijn, B.W., T.H. van der Kwast, A.N. Vis, W.J. Kirkels, E.R. Boeve, A.C. Jobsis, et al., *FGFR3 and P53 characterize alternative genetic pathways in the pathogenesis of urothelial cell carcinoma.* Cancer Res, 2004. **64**(6): p. 1911-4.
123. Aveyard, J.S., A. Skilleter, T. Habuchi, and M.A. Knowles, *Somatic mutation of PTEN in bladder carcinoma.* Br J Cancer, 1999. **80**(5-6): p. 904-8.
124. Gottardo, F., C.G. Liu, M. Ferracin, G.A. Calin, M. Fassan, P. Bassi, et al., *Micro-RNA profiling in kidney and bladder cancers.* Urol Oncol, 2007. **25**(5): p. 387-92.
125. Neely, L.A., K.M. Rieger-Christ, B.S. Neto, A. Eroshkin, J. Garver, S. Patel, et al., *A microRNA expression ratio defining the invasive phenotype in bladder tumors.* Urol Oncol. **28**(1): p. 39-48.
126. Catto, J.W., A. Alcaraz, A.S. Bjartell, R. De Vere White, C.P. Evans, S. Fussel, et al., *MicroRNA in Prostate, Bladder, and Kidney Cancer: A Systematic Review.* Eur Urol, 2011.

127. Villadsen, S.B., J.B. Bramsen, M.S. Ostenfeld, E.D. Wiklund, N. Fristrup, S. Gao, et al., *The miR-143/-145 cluster regulates plasminogen activator inhibitor-1 in bladder cancer.* Br J Cancer, 2011.
128. Lin, T., W. Dong, J. Huang, Q. Pan, X. Fan, C. Zhang, et al., *MicroRNA-143 as a tumor suppressor for bladder cancer.* J Urol, 2009. **181**(3): p. 1372-80.
129. Ostenfeld, M.S., J.B. Bramsen, P. Lamy, S.B. Villadsen, N. Fristrup, K.D. Sorensen, et al., *miR-145 induces caspase-dependent and -independent cell death in urothelial cancer cell lines with targeting of an expression signature present in Ta bladder tumors.* Oncogene, 2010. **29**(7): p. 1073-84.
130. Chiyomaru, T., H. Enokida, S. Tatarano, K. Kawahara, Y. Uchida, K. Nishiyama, et al., *miR-145 and miR-133a function as tumour suppressors and directly regulate FSCN1 expression in bladder cancer.* Br J Cancer, 2010. **102**(5): p. 883-91.
131. Wiklund, E.D., J.B. Bramsen, T. Hulf, L. Dyrskjot, R. Ramanathan, T.B. Hansen, et al., *Coordinated epigenetic repression of the miR-200 family and miR-205 in invasive bladder cancer.* Int J Cancer, 2011. **128**(6): p. 1327-34.
132. Hanke, M., K. Hoefig, H. Merz, A.C. Feller, I. Kausch, D. Jocham, et al., *A robust methodology to study urine microRNA as tumor marker: microRNA-126 and microRNA-182 are related to urinary bladder cancer.* Urol Oncol, 2010. **28**(6): p. 655-61.
133. Yamada, Y., H. Enokida, S. Kojima, K. Kawakami, T. Chiyomaru, S. Tatarano, et al., *MiR-96 and miR-183 detection in urine serve as potential tumor markers of urothelial carcinoma: correlation with stage and grade, and comparison with urinary cytology.* Cancer Sci, 2011. **102**(3): p. 522-9.
134. Jakse, G., F. Algaba, P.U. Malmstrom, and W. Oosterlinck, *A second-look TUR in T1 transitional cell carcinoma: why?* Eur Urol, 2004. **45**(5): p. 539-46; discussion 546.
135. McConkey, D.J., S. Lee, W. Choi, M. Tran, T. Majewski, A. Siefker-Radtke, et al., *Molecular genetics of bladder cancer: Emerging mechanisms of tumor initiation and progression.* Urol Oncol, 2010. **28**(4): p. 429-40.
136. Sylvester, R.J., A.P. van der Meijden, W. Oosterlinck, J.A. Witjes, C. Bouffioux, L. Denis, et al., *Predicting recurrence and progression in individual patients with stage Ta T1 bladder cancer using EORTC risk tables: a combined analysis of 2596 patients from seven EORTC trials.* Eur Urol, 2006. **49**(3): p. 466-5; discussion 475-7.
137. Sylvester, R.J., W. Oosterlinck, and A.P. van der Meijden, *A single immediate postoperative instillation of chemotherapy decreases the risk of recurrence in patients with stage Ta T1 bladder cancer: a meta-analysis of published results of randomized clinical trials.* J Urol, 2004. **171**(6 Pt 1): p. 2186-90, quiz 2435.
138. Pawinski, A., R. Sylvester, K.H. Kurth, C. Bouffioux, A. van der Meijden, M.K. Parmar, et al., *A combined analysis of European Organization for Research and Treatment of Cancer, and Medical Research Council randomized clinical trials for the prophylactic treatment of stage TaT1 bladder cancer. European Organization for Research and Treatment of Cancer Genitourinary Tract Cancer Cooperative Group and the Medical Research Council Working Party on Superficial Bladder Cancer.* J Urol, 1996. **156**(6): p. 1934-40, discussion 1940-1.

139. Bohle, A. and P.R. Bock, *Intravesical bacille Calmette-Guerin versus mitomycin C in superficial bladder cancer: formal meta-analysis of comparative studies on tumor progression.* Urology, 2004. **63**(4): p. 682-6; discussion 686-7.
140. Sylvester, R.J., M.A. van der, and D.L. Lamm, *Intravesical bacillus Calmette-Guerin reduces the risk of progression in patients with superficial bladder cancer: a meta-analysis of the published results of randomized clinical trials.* J Urol, 2002. **168**(5): p. 1964-70.
141. Sonpavde, G. and C.N. Sternberg, *Neoadjuvant Chemotherapy for Invasive Bladder Cancer.* Curr Urol Rep, 2012.
142. Nielsen, M.E., G.S. Palapattu, P.I. Karakiewicz, Y. Lotan, P.J. Bastian, S.P. Lerner, et al., *A delay in radical cystectomy of >3 months is not associated with a worse clinical outcome.* BJU Int, 2007. **100**(5): p. 1015-20.
143. Klatte, T., A.J. Pantuck, M.D. Kleid, and A.S. Belldegrun, *Understanding the natural biology of kidney cancer: implications for targeted cancer therapy.* Rev Urol, 2007. **9**(2): p. 47-56.
144. Knudson, A.G., Jr., *Hereditary cancer, oncogenes, and antioncogenes.* Cancer Res, 1985. **45**(4): p. 1437-43.
145. Finley, D.S., A.J. Pantuck, and A.S. Belldegrun, *Tumor biology and prognostic factors in renal cell carcinoma.* Oncologist, 2011. **16 Suppl 2**: p. 4-13.
146. Schmidt, L., K. Junker, N. Nakaigawa, T. Kinjerski, G. Weirich, M. Miller, et al., *Novel mutations of the MET proto-oncogene in papillary renal carcinomas.* Oncogene, 1999. **18**(14): p. 2343-50.
147. Pollard, P.J., J.J. Briere, N.A. Alam, J. Barwell, E. Barclay, N.C. Wortham, et al., *Accumulation of Krebs cycle intermediates and over-expression of HIF1alpha in tumours which result from germline FH and SDH mutations.* Hum Mol Genet, 2005. **14**(15): p. 2231-9.
148. Schmidt, L.S., M.B. Warren, M.L. Nickerson, G. Weirich, V. Matrosova, J.R. Toro, et al., *Birt-Hogg-Dube syndrome, a genodermatosis associated with spontaneous pneumothorax and kidney neoplasia, maps to chromosome 17p11.2.* Am J Hum Genet, 2001. **69**(4): p. 876-82.
149. Varela, I., P. Tarpey, K. Raine, D. Huang, C.K. Ong, P. Stephens, et al., *Exome sequencing identifies frequent mutation of the SWI/SNF complex gene PBRM1 in renal carcinoma.* Nature, 2011. **469**(7331): p. 539-42.
150. Dalgliesh, G.L., K. Furge, C. Greenman, L. Chen, G. Bignell, A. Butler, et al., *Systematic sequencing of renal carcinoma reveals inactivation of histone modifying genes.* Nature, 2010. **463**(7279): p. 360-3.
151. Lam, J.S., J.T. Leppert, A.S. Belldegrun, and R.A. Figlin, *Novel approaches in the therapy of metastatic renal cell carcinoma.* World J Urol, 2005. **23**(3): p. 202-12.
152. Coppin, C., F. Porzsolt, A. Awa, J. Kumpf, A. Coldman, and T. Wilt, *Immunotherapy for advanced renal cell cancer.* Cochrane Database Syst Rev, 2005(1): p. CD001425.
153. Escudier, B., A. Pluzanska, P. Koralewski, A. Ravaud, S. Bracarda, C. Szczylik, et al., *Bevacizumab plus interferon alfa-2a for treatment of metastatic renal cell carcinoma: a randomised, double-blind phase III trial.* Lancet, 2007. **370**(9605): p. 2103-11.

154. Wilhelm, S.M., C. Carter, L. Tang, D. Wilkie, A. McNabola, H. Rong, et al., *BAY 43-9006 exhibits broad spectrum oral antitumor activity and targets the RAF/MEK/ERK pathway and receptor tyrosine kinases involved in tumor progression and angiogenesis.* Cancer Res, 2004. **64**(19): p. 7099-109.
155. Escudier, B., T. Eisen, W.M. Stadler, C. Szczylik, S. Oudard, M. Staehler, et al., *Sorafenib for treatment of renal cell carcinoma: Final efficacy and safety results of the phase III treatment approaches in renal cancer global evaluation trial.* J Clin Oncol, 2009. **27**(20): p. 3312-8.
156. Escudier, B., T. Eisen, W.M. Stadler, C. Szczylik, S. Oudard, M. Siebels, et al., *Sorafenib in advanced clear-cell renal-cell carcinoma.* N Engl J Med, 2007. **356**(2): p. 125-34.
157. Morimoto, A.M., N. Tan, K. West, G. McArthur, G.C. Toner, W.C. Manning, et al., *Gene expression profiling of human colon xenograft tumors following treatment with SU11248, a multitargeted tyrosine kinase inhibitor.* Oncogene, 2004. **23**(8): p. 1618-26.
158. Motzer, R.J., T.E. Hutson, P. Tomczak, M.D. Michaelson, R.M. Bukowski, S. Oudard, et al., *Overall survival and updated results for sunitinib compared with interferon alfa in patients with metastatic renal cell carcinoma.* J Clin Oncol, 2009. **27**(22): p. 3584-90.
159. Sternberg, C.N., I.D. Davis, J. Mardiak, C. Szczylik, E. Lee, J. Wagstaff, et al., *Pazopanib in locally advanced or metastatic renal cell carcinoma: results of a randomized phase III trial.* J Clin Oncol, 2010. **28**(6): p. 1061-8.
160. Sun, M., G. Lughezzani, P. Perrotte, and P.I. Karakiewicz, *Treatment of metastatic renal cell carcinoma.* Nat Rev Urol. **7**(6): p. 327-38.
161. Flaherty, K.T. and I. Puzanov, *Building on a foundation of VEGF and mTOR targeted agents in renal cell carcinoma.* Biochem Pharmacol. **80**(5): p. 638-46.
162. Rini, B.I. and M.B. Atkins, *Resistance to targeted therapy in renal-cell carcinoma.* Lancet Oncol, 2009. **10**(10): p. 992-1000.
163. Shaw, R.J. and L.C. Cantley, *Ras, PI(3)K and mTOR signalling controls tumour cell growth.* Nature, 2006. **441**(7092): p. 424-30.
164. Robb, V.A., M. Karbowniczek, A.J. Klein-Szanto, and E.P. Henske, *Activation of the mTOR signaling pathway in renal clear cell carcinoma.* J Urol, 2007. **177**(1): p. 346-52.
165. Huang, J. and B.D. Manning, *A complex interplay between Akt, TSC2 and the two mTOR complexes.* Biochem Soc Trans, 2009. **37**(Pt 1): p. 217-22.
166. Yellen, P., M. Saqcena, D. Salloum, J. Feng, A. Preda, L. Xu, et al., *High-dose rapamycin induces apoptosis in human cancer cells by dissociating mTOR complex 1 and suppressing phosphorylation of 4E-BP1.* Cell Cycle, 2011. **10**(22): p. 3948-56.
167. Oh, W.J. and E. Jacinto, *mTOR complex 2 signaling and functions.* Cell Cycle, 2011. **10**(14): p. 2305-16.
168. Tremblay, F. and A. Marette, *Amino acid and insulin signaling via the mTOR/p70 S6 kinase pathway. A negative feedback mechanism leading to insulin resistance in skeletal muscle cells.* J Biol Chem, 2001. **276**(41): p. 38052-60.

169. Harrington, L.S., G.M. Findlay, A. Gray, T. Tolkacheva, S. Wigfield, H. Rebholz, et al., *The TSC1-2 tumor suppressor controls insulin-PI3K signaling via regulation of IRS proteins.* J Cell Biol, 2004. **166**(2): p. 213-23.
170. Wan, X., B. Harkavy, N. Shen, P. Grohar, and L.J. Helman, *Rapamycin induces feedback activation of Akt signaling through an IGF-1R-dependent mechanism.* Oncogene, 2007. **26**(13): p. 1932-40.
171. Sun, S.Y., L.M. Rosenberg, X. Wang, Z. Zhou, P. Yue, H. Fu, et al., *Activation of Akt and eIF4E survival pathways by rapamycin-mediated mammalian target of rapamycin inhibition.* Cancer Res, 2005. **65**(16): p. 7052-8.
172. Sarbassov, D.D., S.M. Ali, S. Sengupta, J.H. Sheen, P.P. Hsu, A.F. Bagley, et al., *Prolonged rapamycin treatment inhibits mTORC2 assembly and Akt/PKB.* Mol Cell, 2006. **22**(2): p. 159-68.
173. Livak, K.J. and T.D. Schmittgen, *Analysis of relative gene expression data using real-time quantitative PCR and the 2(-Delta Delta C(T)) Method.* Methods, 2001. **25**(4): p. 402-8.
174. Tickoo, S.K., M.I. Milowsky, N. Dhar, M.E. Dudas, D.J. Gallagher, H. Al-Ahmadie, et al., *Hypoxia-inducible factor and mammalian target of rapamycin pathway markers in urothelial carcinoma of the bladder: possible therapeutic implications.* BJU Int, 2011. **107**(5): p. 844-9.
175. Turner, K.J., J.P. Crew, C.C. Wykoff, P.H. Watson, R. Poulsom, J. Pastorek, et al., *The hypoxia-inducible genes VEGF and CA9 are differentially regulated in superficial vs invasive bladder cancer.* Br J Cancer, 2002. **86**(8): p. 1276-82.
176. Nadaoka, J., Y. Horikawa, M. Saito, T. Kumazawa, T. Inoue, S. Narita, et al., *Prognostic significance of HIF-1 alpha polymorphisms in transitional cell carcinoma of the bladder.* Int J Cancer, 2008. **122**(6): p. 1297-302.
177. Theodoropoulos, V.E., A. Lazaris, F. Sofras, I. Gerzelis, V. Tsoukala, I. Ghikonti, et al., *Hypoxia-inducible factor 1 alpha expression correlates with angiogenesis and unfavorable prognosis in bladder cancer.* Eur Urol, 2004. **46**(2): p. 200-8.
178. Jones, A., C. Fujiyama, C. Blanche, J.W. Moore, S. Fuggle, D. Cranston, et al., *Relation of vascular endothelial growth factor production to expression and regulation of hypoxia-inducible factor-1 alpha and hypoxia-inducible factor-2 alpha in human bladder tumors and cell lines.* Clin Cancer Res, 2001. **7**(5): p. 1263-72.
179. Chai, C.Y., W.T. Chen, W.C. Hung, W.Y. Kang, Y.C. Huang, Y.C. Su, et al., *Hypoxia-inducible factor-1alpha expression correlates with focal macrophage infiltration, angiogenesis and unfavourable prognosis in urothelial carcinoma.* J Clin Pathol, 2008. **61**(5): p. 658-64.
180. Deniz, H., M. Karakok, F. Yagci, and M.E. Guldur, *Evaluation of relationship between HIF-1alpha immunoreactivity and stage, grade, angiogenic profile and proliferative index in bladder urothelial carcinomas.* Int Urol Nephrol, 2010. **42**(1): p. 103-7.
181. Ioachim, E., M. Michael, M. Salmas, M.M. Michael, N.E. Stavropoulos, and V. Malamou-Mitsi, *Hypoxia-inducible factors HIF-1alpha and HIF-2alpha expression in bladder cancer and their associations with other angiogenesis-related proteins.* Urol Int, 2006. **77**(3): p. 255-63.

182. Wang, G., H. Zhang, H. He, W. Tong, B. Wang, G. Liao, et al., *Up-regulation of microRNA in bladder tumor tissue is not common.* Int Urol Nephrol, 2010. **42**(1): p. 95-102.
183. Kulshreshtha, R., R.V. Davuluri, G.A. Calin, and M. Ivan, *A microRNA component of the hypoxic response.* Cell Death Differ, 2008. **15**(4): p. 667-71.
184. Catto, J.W., S. Miah, H.C. Owen, H. Bryant, K. Myers, E. Dudziec, et al., *Distinct microRNA alterations characterize high- and low-grade bladder cancer.* Cancer Res, 2009. **69**(21): p. 8472-81.
185. Wszolek, M.F., K.M. Rieger-Christ, P.A. Kenney, J.J. Gould, B. Silva Neto, A.K. Lavoie, et al., *A MicroRNA expression profile defining the invasive bladder tumor phenotype.* Urol Oncol, 2011. **29**(6): p. 794-801 e1.
186. Dyrskjot, L., M.S. Ostenfeld, J.B. Bramsen, A.N. Silahtaroglu, P. Lamy, R. Ramanathan, et al., *Genomic profiling of microRNAs in bladder cancer: miR-129 is associated with poor outcome and promotes cell death in vitro.* Cancer Res, 2009. **69**(11): p. 4851-60.
187. Slaby, O., M. Svoboda, P. Fabian, T. Smerdova, D. Knoflickova, M. Bednarikova, et al., *Altered expression of miR-21, miR-31, miR-143 and miR-145 is related to clinicopathologic features of colorectal cancer.* Oncology, 2007. **72**(5-6): p. 397-402.
188. Zaman, M.S., Y. Chen, G. Deng, V. Shahryari, S.O. Suh, S. Saini, et al., *The functional significance of microRNA-145 in prostate cancer.* Br J Cancer. **103**(2): p. 256-64.
189. Xu, N., T. Papagiannakopoulos, G. Pan, J.A. Thomson, and K.S. Kosik, *MicroRNA-145 regulates OCT4, SOX2, and KLF4 and represses pluripotency in human embryonic stem cells.* Cell, 2009. **137**(4): p. 647-58.
190. Sachdeva, M. and Y.Y. Mo, *miR-145-mediated suppression of cell growth, invasion and metastasis.* Am J Transl Res. **2**(2): p. 170-80.
191. Sachdeva, M. and Y.Y. Mo, *MicroRNA-145 suppresses cell invasion and metastasis by directly targeting mucin 1.* Cancer Res. **70**(1): p. 378-87.
192. Sachdeva, M., S. Zhu, F. Wu, H. Wu, V. Walia, S. Kumar, et al., *p53 represses c-Myc through induction of the tumor suppressor miR-145.* Proc Natl Acad Sci U S A, 2009. **106**(9): p. 3207-12.
193. Gee, H.E., F.M. Buffa, C. Camps, A. Ramachandran, R. Leek, M. Taylor, et al., *The small-nucleolar RNAs commonly used for microRNA normalisation correlate with tumour pathology and prognosis.* Br J Cancer, 2011. **104**(7): p. 1168-77.
194. Vandesompele, J., K. De Preter, F. Pattyn, B. Poppe, N. Van Roy, A. De Paepe, et al., *Accurate normalization of real-time quantitative RT-PCR data by geometric averaging of multiple internal control genes.* Genome Biol, 2002. **3**(7): p. RESEARCH0034.
195. Neal, C.S., M.Z. Michael, L.H. Rawlings, M.B. Van der Hoek, and J.M. Gleadle, *The VHL-dependent regulation of microRNAs in renal cancer.* BMC Med, 2010. **8**: p. 64.
196. Ren, J., P. Jin, E. Wang, F.M. Marincola, and D.F. Stroncek, *MicroRNA and gene expression patterns in the differentiation of human embryonic stem cells.* J Transl Med, 2009. **7**: p. 20.

197. Bortolin-Cavaille, M.L., M. Dance, M. Weber, and J. Cavaille, *C19MC microRNAs are processed from introns of large Pol-II, non-protein-coding transcripts.* Nucleic Acids Res, 2009. **37**(10): p. 3464-73.
198. Schneider, A., R.H. Younis, and J.S. Gutkind, *Hypoxia-induced energy stress inhibits the mTOR pathway by activating an AMPK/REDD1 signaling axis in head and neck squamous cell carcinoma.* Neoplasia, 2008. **10**(11): p. 1295-302.
199. Li, X.F., P.J. Yan, and Z.M. Shao, *Downregulation of miR-193b contributes to enhance urokinase-type plasminogen activator (uPA) expression and tumor progression and invasion in human breast cancer.* Oncogene, 2009. **28**(44): p. 3937-48.
200. Noh, H., S. Hong, Z. Dong, Z.K. Pan, Q. Jing, and S. Huang, *Impaired MicroRNA Processing Facilitates Breast Cancer Cell Invasion by Upregulating Urokinase-Type Plasminogen Activator Expression.* Genes Cancer, 2011. **2**(2): p. 140-50.
201. Rauhala, H.E., S.E. Jalava, J. Isotalo, H. Bracken, S. Lehmusvaara, T.L. Tammela, et al., *miR-193b is an epigenetically regulated putative tumor suppressor in prostate cancer.* Int J Cancer, 2010. **127**(6): p. 1363-72.
202. Sarkar, S., B.K. Dey, and A. Dutta, *MiR-322/424 and -503 are induced during muscle differentiation and promote cell cycle quiescence and differentiation by down-regulation of Cdc25A.* Mol Biol Cell, 2010. **21**(13): p. 2138-49.
203. Jiang, L., Q. Huang, S. Zhang, Q. Zhang, J. Chang, X. Qiu, et al., *Hsa-miR-125a-3p and hsa-miR-125a-5p are downregulated in non-small cell lung cancer and have inverse effects on invasion and migration of lung cancer cells.* BMC Cancer, 2010. **10**: p. 318.
204. Nishida, N., K. Mimori, M. Fabbri, T. Yokobori, T. Sudo, F. Tanaka, et al., *MicroRNA-125a-5p is an independent prognostic factor in gastric cancer and inhibits the proliferation of human gastric cancer cells in combination with trastuzumab.* Clin Cancer Res, 2011. **17**(9): p. 2725-33.
205. Hatakeyama, H., H. Cheng, P. Wirth, A. Counsell, S.R. Marcrom, C.B. Wood, et al., *Regulation of heparin-binding EGF-like growth factor by miR-212 and acquired cetuximab-resistance in head and neck squamous cell carcinoma.* PLoS One, 2010. **5**(9): p. e12702.
206. Saini, S., S. Yamamura, S. Majid, V. Shahryari, H. Hirata, Y. Tanaka, et al., *MicroRNA-708 induces apoptosis and suppresses tumorigenicity in renal cancer cells.* Cancer Res, 2011. **71**(19): p. 6208-19.
207. Song, T., W. Xia, N. Shao, X. Zhang, C. Wang, Y. Wu, et al., *Differential miRNA expression profiles in bladder urothelial carcinomas.* Asian Pac J Cancer Prev, 2010. **11**(4): p. 905-11.
208. Rippe, V., L. Dittberner, V.N. Lorenz, N. Drieschner, R. Nimzyk, W. Sendt, et al., *The two stem cell microRNA gene clusters C19MC and miR-371-3 are activated by specific chromosomal rearrangements in a subgroup of thyroid adenomas.* PLoS One, 2010. **5**(3): p. e9485.
209. Yoshitomi, T., K. Kawakami, H. Enokida, T. Chiyomaru, I. Kagara, S. Tatarano, et al., *Restoration of miR-517a expression induces cell apoptosis in bladder cancer cell lines.* Oncol Rep, 2011. **25**(6): p. 1661-8.
210. Oneyama, C., J. Ikeda, D. Okuzaki, K. Suzuki, T. Kanou, Y. Shintani, et al., *MicroRNA-mediated downregulation of mTOR/FGFR3 controls tumor*

growth induced by Src-related oncogenic pathways. Oncogene, 2011. **30**(32): p. 3489-501.
211. Brabletz, S. and T. Brabletz, *The ZEB/miR-200 feedback loop--a motor of cellular plasticity in development and cancer?* EMBO Rep, 2010. **11**(9): p. 670-7.
212. Ma, Y., P. Zhang, F. Wang, H. Zhang, J. Yang, J. Peng, et al., *miR-150 as a potential biomarker associated with prognosis and therapeutic outcome in colorectal cancer.* Gut, 2011.
213. Khan, A.P., L.M. Poisson, V.B. Bhat, D. Fermin, R. Zhao, S. Kalyana-Sundaram, et al., *Quantitative proteomic profiling of prostate cancer reveals a role for miR-128 in prostate cancer.* Mol Cell Proteomics, 2010. **9**(2): p. 298-312.
214. Feng, D.D., H. Zhang, P. Zhang, Y.S. Zheng, X.J. Zhang, B.W. Han, et al., *Down-regulated miR-331-5p and miR-27a are associated with chemotherapy resistance and relapse in leukaemia.* J Cell Mol Med, 2011. **15**(10): p. 2164-75.
215. Zhu, Y., F. Yu, Y. Jiao, J. Feng, W. Tang, H. Yao, et al., *Reduced miR-128 in breast tumor-initiating cells induces chemotherapeutic resistance via Bmi-1 and ABCC5.* Clin Cancer Res, 2011. **17**(22): p. 7105-15.
216. An, W.G., M. Kanekal, M.C. Simon, E. Maltepe, M.V. Blagosklonny, and L.M. Neckers, *Stabilization of wild-type p53 by hypoxia-inducible factor 1alpha.* Nature, 1998. **392**(6674): p. 405-8.
217. Mutharasan, R.K., V. Nagpal, Y. Ichikawa, and H. Ardehali, *microRNA-210 is upregulated in hypoxic cardiomyocytes through Akt- and p53-dependent pathways and exerts cytoprotective effects.* Am J Physiol Heart Circ Physiol, 2011. **301**(4): p. H1519-30.
218. Kitazumi, I. and M. Tsukahara, *Regulation of DNA fragmentation: the role of caspases and phosphorylation.* FEBS J, 2011. **278**(3): p. 427-41.
219. Kent, O.A., R.R. Chivukula, M. Mullendore, E.A. Wentzel, G. Feldmann, K.H. Lee, et al., *Repression of the miR-143/145 cluster by oncogenic Ras initiates a tumor-promoting feed-forward pathway.* Genes Dev. **24**(24): p. 2754-9.
220. Pollard, C., S.C. Smith, and D. Theodorescu, *Molecular genesis of non-muscle-invasive urothelial carcinoma (NMIUC).* Expert Rev Mol Med. **12**: p. e10.
221. Botteman, M.F., C.L. Pashos, A. Redaelli, B. Laskin, and R. Hauser, *The health economics of bladder cancer: a comprehensive review of the published literature.* Pharmacoeconomics, 2003. **21**(18): p. 1315-30.
222. L'Hote, C.G. and M.A. Knowles, *Cell responses to FGFR3 signalling: growth, differentiation and apoptosis.* Exp Cell Res, 2005. **304**(2): p. 417-31.
223. Toydemir, R.M., A.E. Brassington, P. Bayrak-Toydemir, P.A. Krakowiak, L.B. Jorde, F.G. Whitby, et al., *A novel mutation in FGFR3 causes camptodactyly, tall stature, and hearing loss (CATSHL) syndrome.* Am J Hum Genet, 2006. **79**(5): p. 935-41.
224. Billerey, C., D. Chopin, M.H. Aubriot-Lorton, D. Ricol, S. Gil Diez de Medina, B. Van Rhijn, et al., *Frequent FGFR3 mutations in papillary non-invasive bladder (pTa) tumors.* Am J Pathol, 2001. **158**(6): p. 1955-9.
225. Mhawech-Fauceglia, P., R.T. Cheney, G. Fischer, A. Beck, and F.R. Herrmann, *FGFR3 and p53 protein expressions in patients with pTa and pT1 urothelial bladder cancer.* Eur J Surg Oncol, 2006. **32**(2): p. 231-7.

226. Foldynova-Trantirkova, S., W.R. Wilcox, and P. Krejci, *Sixteen years and counting: the current understanding of fibroblast growth factor receptor 3 (FGFR3) signaling in skeletal dysplasias.* Hum Mutat, 2012. **33**(1): p. 29-41.
227. Dai, H., R. Holm, G.B. Kristensen, V.M. Abeler, A.L. Borresen-Dale, and A. Helland, *Fibroblast growth factor receptor 3 (FGFR3) - analyses of the S249C mutation and protein expression in primary cervical carcinomas.* Anal Cell Pathol, 2001. **23**(2): p. 45-9.
228. Winter, S.C., F.M. Buffa, P. Silva, C. Miller, H.R. Valentine, H. Turley, et al., *Relation of a hypoxia metagene derived from head and neck cancer to prognosis of multiple cancers.* Cancer Res, 2007. **67**(7): p. 3441-9.
229. Buffa, F.M., A.L. Harris, C.M. West, and C.J. Miller, *Large meta-analysis of multiple cancers reveals a common, compact and highly prognostic hypoxia metagene.* Br J Cancer, 2010. **102**(2): p. 428-35.
230. Cartharius, K., K. Frech, K. Grote, B. Klocke, M. Haltmeier, A. Klingenhoff, et al., *MatInspector and beyond: promoter analysis based on transcription factor binding sites.* Bioinformatics, 2005. **21**(13): p. 2933-42.
231. Cairo, S., Y. Wang, A. de Reynies, K. Duroure, J. Dahan, M.J. Redon, et al., *Stem cell-like micro-RNA signature driven by Myc in aggressive liver cancer.* Proc Natl Acad Sci U S A. **107**(47): p. 20471-6.
232. Zingone, A., C.M. Cultraro, D.M. Shin, C.M. Bean, H.C. Morse, 3rd, S. Janz, et al., *Ectopic expression of wild-type FGFR3 cooperates with MYC to accelerate development of B-cell lineage neoplasms.* Leukemia, 2010. **24**(6): p. 1171-8.
233. Marshall, M.E., T.K. Hinz, S.A. Kono, K.R. Singleton, B. Bichon, K.E. Ware, et al., *Fibroblast growth factor receptors are components of autocrine signaling networks in head and neck squamous cell carcinoma cells.* Clin Cancer Res, 2011. **17**(15): p. 5016-25.
234. Franovic, A., L. Gunaratnam, K. Smith, I. Robert, D. Patten, and S. Lee, *Translational up-regulation of the EGFR by tumor hypoxia provides a nonmutational explanation for its overexpression in human cancer.* Proc Natl Acad Sci U S A, 2007. **104**(32): p. 13092-7.
235. Wang, X. and A. Schneider, *HIF-2alpha-mediated activation of the epidermal growth factor receptor potentiates head and neck cancer cell migration in response to hypoxia.* Carcinogenesis, 2010. **31**(7): p. 1202-10.
236. Pennacchietti, S., P. Michieli, M. Galluzzo, M. Mazzone, S. Giordano, and P.M. Comoglio, *Hypoxia promotes invasive growth by transcriptional activation of the met protooncogene.* Cancer Cell, 2003. **3**(4): p. 347-61.
237. Gauglhofer, C., S. Sagmeister, W. Schrottmaier, C. Fischer, C. Rodgarkia-Dara, T. Mohr, et al., *Up-regulation of the fibroblast growth factor 8 subfamily in human hepatocellular carcinoma for cell survival and neoangiogenesis.* Hepatology, 2011. **53**(3): p. 854-64.
238. Sayan, A.E., B. D'Angelo, B.S. Sayan, P. Tucci, A. Cimini, M.P. Ceru, et al., *p73 and p63 regulate the expression of fibroblast growth factor receptor 3.* Biochem Biophys Res Commun, 2010. **394**(3): p. 824-8.
239. Schodel, J., S. Oikonomopoulos, J. Ragoussis, C.W. Pugh, P.J. Ratcliffe, and D.R. Mole, *High-resolution genome-wide mapping of HIF-binding sites by ChIP-seq.* Blood, 2011. **117**(23): p. e207-17.

240. Nagaraja, A.K., C.J. Creighton, Z. Yu, H. Zhu, P.H. Gunaratne, J.G. Reid, et al., *A link between mir-100 and FRAP1/mTOR in clear cell ovarian cancer.* Mol Endocrinol. **24**(2): p. 447-63.
241. Leite, K.R., J.M. Sousa-Canavez, S.T. Reis, A.H. Tomiyama, L.H. Camara-Lopes, A. Sanudo, et al., *Change in expression of miR-let7c, miR-100, and miR-218 from high grade localized prostate cancer to metastasis.* Urol Oncol, 2011. **29**(3): p. 265-9.
242. Mole, D.R., C. Blancher, R.R. Copley, P.J. Pollard, J.M. Gleadle, J. Ragoussis, et al., *Genome-wide association of hypoxia-inducible factor (HIF)-1alpha and HIF-2alpha DNA binding with expression profiling of hypoxia-inducible transcripts.* J Biol Chem, 2009. **284**(25): p. 16767-75.
243. Wood, S.M., M.S. Wiesener, K.M. Yeates, N. Okada, C.W. Pugh, P.H. Maxwell, et al., *Selection and analysis of a mutant cell line defective in the hypoxia-inducible factor-1 alpha-subunit (HIF-1alpha). Characterization of hif-1alpha-dependent and -independent hypoxia-inducible gene expression.* J Biol Chem, 1998. **273**(14): p. 8360-8.
244. Wiesener, M.S., H. Turley, W.E. Allen, C. Willam, K.U. Eckardt, K.L. Talks, et al., *Induction of endothelial PAS domain protein-1 by hypoxia: characterization and comparison with hypoxia-inducible factor-1alpha.* Blood, 1998. **92**(7): p. 2260-8.
245. Winning, S., F. Splettstoesser, J. Fandrey, and S. Frede, *Acute hypoxia induces HIF-independent monocyte adhesion to endothelial cells through increased intercellular adhesion molecule-1 expression: the role of hypoxic inhibition of prolyl hydroxylase activity for the induction of NF-kappa B.* J Immunol, 2010. **185**(3): p. 1786-93.
246. Park, E.C., P. Ghose, Z. Shao, Q. Ye, L. Kang, X.Z. Xu, et al., *Hypoxia regulates glutamate receptor trafficking through an HIF-independent mechanism.* EMBO J, 2012.
247. Koumenis, C. and B.G. Wouters, *"Translating" tumor hypoxia: unfolded protein response (UPR)-dependent and UPR-independent pathways.* Mol Cancer Res, 2006. **4**(7): p. 423-36.
248. Gong, P., B. Hu, D. Stewart, M. Ellerbe, Y.G. Figueroa, V. Blank, et al., *Cobalt induces heme oxygenase-1 expression by a hypoxia-inducible factor-independent mechanism in Chinese hamster ovary cells: regulation by Nrf2 and MafG transcription factors.* J Biol Chem, 2001. **276**(29): p. 27018-25.
249. Lamont, F.R., D.C. Tomlinson, P.A. Cooper, S.D. Shnyder, J.D. Chester, and M.A. Knowles, *Small molecule FGF receptor inhibitors block FGFR-dependent urothelial carcinoma growth in vitro and in vivo.* Br J Cancer, 2011. **104**(1): p. 75-82.
250. Selbach, M., B. Schwanhausser, N. Thierfelder, Z. Fang, R. Khanin, and N. Rajewsky, *Widespread changes in protein synthesis induced by microRNAs.* Nature, 2008. **455**(7209): p. 58-63.
251. Shi, W., N.M. Alajez, C. Bastianutto, A.B. Hui, J.D. Mocanu, E. Ito, et al., *Significance of Plk1 regulation by miR-100 in human nasopharyngeal cancer.* Int J Cancer, 2010. **126**(9): p. 2036-48.
252. Zheng, Y.S., H. Zhang, X.J. Zhang, D.D. Feng, X.Q. Luo, C.W. Zeng, et al., *MiR-100 regulates cell differentiation and survival by targeting RBSP3, a phosphatase-like tumor suppressor in acute myeloid leukemia.* Oncogene, 2012. **31**(1): p. 80-92.

253. Nagaraja, A.K., C.J. Creighton, Z. Yu, H. Zhu, P.H. Gunaratne, J.G. Reid, et al., *A link between mir-100 and FRAP1/mTOR in clear cell ovarian cancer.* Mol Endocrinol, 2010. **24**(2): p. 447-63.
254. Miyake, M., K. Sugano, H. Sugino, K. Imai, E. Matsumoto, K. Maeda, et al., *Fibroblast growth factor receptor 3 mutation in voided urine is a useful diagnostic marker and significant indicator of tumor recurrence in non-muscle invasive bladder cancer.* Cancer Sci, 2010. **101**(1): p. 250-8.
255. Chen, J., B.H. Lee, I.R. Williams, J.L. Kutok, C.S. Mitsiades, N. Duclos, et al., *FGFR3 as a therapeutic target of the small molecule inhibitor PKC412 in hematopoietic malignancies.* Oncogene, 2005. **24**(56): p. 8259-67.
256. Martinez-Torrecuadrada, J., G. Cifuentes, P. Lopez-Serra, P. Saenz, A. Martinez, and J.I. Casal, *Targeting the extracellular domain of fibroblast growth factor receptor 3 with human single-chain Fv antibodies inhibits bladder carcinoma cell line proliferation.* Clin Cancer Res, 2005. **11**(17): p. 6280-90.
257. Jaakkola, P., D.R. Mole, Y.M. Tian, M.I. Wilson, J. Gielbert, S.J. Gaskell, et al., *Targeting of HIF-alpha to the von Hippel-Lindau ubiquitylation complex by O2-regulated prolyl hydroxylation.* Science, 2001. **292**(5516): p. 468-72.
258. Camps, C., F.M. Buffa, S. Colella, J. Moore, C. Sotiriou, H. Sheldon, et al., *hsa-miR-210 Is induced by hypoxia and is an independent prognostic factor in breast cancer.* Clin Cancer Res, 2008. **14**(5): p. 1340-8.
259. Neal, C.S., M.Z. Michael, L.H. Rawlings, M.B. Van der Hoek, and J.M. Gleadle, *The VHL-dependent regulation of microRNAs in renal cancer.* BMC Med. **8**: p. 64.
260. Patard, J.J., N. Rioux-Leclercq, D. Masson, S. Zerrouki, F. Jouan, N. Collet, et al., *Absence of VHL gene alteration and high VEGF expression are associated with tumour aggressiveness and poor survival of renal-cell carcinoma.* Br J Cancer, 2009. **101**(8): p. 1417-24.
261. Turner, K.J., J.W. Moore, A. Jones, C.F. Taylor, D. Cuthbert-Heavens, C. Han, et al., *Expression of hypoxia-inducible factors in human renal cancer: relationship to angiogenesis and to the von Hippel-Lindau gene mutation.* Cancer Res, 2002. **62**(10): p. 2957-61.
262. Cifola, I., C. Bianchi, E. Mangano, S. Bombelli, F. Frascati, E. Fasoli, et al., *Renal cell carcinoma primary cultures maintain genomic and phenotypic profile of parental tumor tissues.* BMC Cancer, 2011. **11**: p. 244.
263. Wolff, N.C., S. Vega-Rubin-de-Celis, X.J. Xie, D.H. Castrillon, W. Kabbani, and J. Brugarolas, *Cell-type-dependent regulation of mTORC1 by REDD1 and the tumor suppressors TSC1/TSC2 and LKB1 in response to hypoxia.* Mol Cell Biol, 2011. **31**(9): p. 1870-84.
264. Cam, H., J.B. Easton, A. High, and P.J. Houghton, *mTORC1 signaling under hypoxic conditions is controlled by ATM-dependent phosphorylation of HIF-1alpha.* Mol Cell, 2010. **40**(4): p. 509-20.
265. Laughner, E., P. Taghavi, K. Chiles, P.C. Mahon, and G.L. Semenza, *HER2 (neu) signaling increases the rate of hypoxia-inducible factor 1alpha (HIF-1alpha) synthesis: novel mechanism for HIF-1-mediated vascular endothelial growth factor expression.* Mol Cell Biol, 2001. **21**(12): p. 3995-4004.
266. Boulahbel, H., R.V. Duran, and E. Gottlieb, *Prolyl hydroxylases as regulators of cell metabolism.* Biochem Soc Trans, 2009. **37**(Pt 1): p. 291-4.

267. Kaelin, W.G., Jr., *Treatment of kidney cancer: insights provided by the VHL tumor-suppressor protein.* Cancer, 2009. **115**(10 Suppl): p. 2262-72.
268. Flaig, T.W., L.J. Costa, D.L. Gustafson, K. Breaker, M.K. Schultz, F. Crighton, et al., *Safety and efficacy of the combination of erlotinib and sirolimus for the treatment of metastatic renal cell carcinoma after failure of sunitinib or sorafenib.* Br J Cancer, 2010. **103**(6): p. 796-801.
269. Atkins, M.B., M. Hidalgo, W.M. Stadler, T.F. Logan, J.P. Dutcher, G.R. Hudes, et al., *Randomized phase II study of multiple dose levels of CCI-779, a novel mammalian target of rapamycin kinase inhibitor, in patients with advanced refractory renal cell carcinoma.* J Clin Oncol, 2004. **22**(5): p. 909-18.
270. Liu, L., T.P. Cash, R.G. Jones, B. Keith, C.B. Thompson, and M.C. Simon, *Hypoxia-induced energy stress regulates mRNA translation and cell growth.* Mol Cell, 2006. **21**(4): p. 521-31.
271. Gwinn, D.M., D.B. Shackelford, D.F. Egan, M.M. Mihaylova, A. Mery, D.S. Vasquez, et al., *AMPK phosphorylation of raptor mediates a metabolic checkpoint.* Mol Cell, 2008. **30**(2): p. 214-26.
272. Sanchez-Cespedes, M., *A role for LKB1 gene in human cancer beyond the Peutz-Jeghers syndrome.* Oncogene, 2007. **26**(57): p. 7825-32.
273. Woodard, J., S. Joshi, B. Viollet, N. Hay, and L.C. Platanias, *AMPK as a therapeutic target in renal cell carcinoma.* Cancer Biol Ther, 2010. **10**(11): p. 1168-77.
274. Sikka, A., M. Kaur, C. Agarwal, G. Deep, and R. Agarwal, *Metformin suppresses growth of human head and neck squamous cell carcinoma via global inhibition of protein translation.* Cell Cycle, 2012. **11**(7).
275. Deng, X.S., S. Wang, A. Deng, B. Liu, S.M. Edgerton, S.E. Lind, et al., *Metformin targets Stat3 to inhibit cell growth and induce apoptosis in triple-negative breast cancers.* Cell Cycle, 2012. **11**(2): p. 367-76.
276. Klubo-Gwiezdzinska, J., K. Jensen, J. Costello, A. Patel, V. Hoperia, A. Bauer, et al., *Metformin inhibits growth and decreases resistance to anoikis in medullary thyroid cancer cells.* Endocr Relat Cancer, 2012.
277. Huang, D., Y. Ding, Y. Li, W.M. Luo, Z.F. Zhang, J. Snider, et al., *Sunitinib acts primarily on tumor endothelium rather than tumor cells to inhibit the growth of renal cell carcinoma.* Cancer Res, 2010. **70**(3): p. 1053-62.
278. Faivre, S., C. Delbaldo, K. Vera, C. Robert, S. Lozahic, N. Lassau, et al., *Safety, pharmacokinetic, and antitumor activity of SU11248, a novel oral multitarget tyrosine kinase inhibitor, in patients with cancer.* J Clin Oncol, 2006. **24**(1): p. 25-35.
279. Wilhelm, S., C. Carter, M. Lynch, T. Lowinger, J. Dumas, R.A. Smith, et al., *Discovery and development of sorafenib: a multikinase inhibitor for treating cancer.* Nat Rev Drug Discov, 2006. **5**(10): p. 835-44.
280. Liu, L., Y. Cao, C. Chen, X. Zhang, A. McNabola, D. Wilkie, et al., *Sorafenib blocks the RAF/MEK/ERK pathway, inhibits tumor angiogenesis, and induces tumor cell apoptosis in hepatocellular carcinoma model PLC/PRF/5.* Cancer Res, 2006. **66**(24): p. 11851-8.
281. Strumberg, D., H. Richly, R.A. Hilger, N. Schleucher, S. Korfee, M. Tewes, et al., *Phase I clinical and pharmacokinetic study of the Novel Raf kinase and vascular endothelial growth factor receptor inhibitor BAY 43-9006 in patients with advanced refractory solid tumors.* J Clin Oncol, 2005. **23**(5): p. 965-72.

282. Liu, J., M. Li, B. Song, C. Jia, L. Zhang, X. Bai, et al., *Metformin inhibits renal cell carcinoma in vitro and in vivo xenograft.* Urol Oncol, 2011.
283. Liu, A. and S.P. Coleman, *Determination of metformin in human plasma using hydrophilic interaction liquid chromatography-tandem mass spectrometry.* J Chromatogr B Analyt Technol Biomed Life Sci, 2009. **877**(29): p. 3695-700.
284. Wang, D., L. Su, D. Huang, H. Zhang, D.M. Shin, and Z.G. Chen, *Downregulation of E-Cadherin enhances proliferation of head and neck cancer through transcriptional regulation of EGFR.* Mol Cancer, 2011. **10**: p. 116.
285. Gan, B., C. Lim, G. Chu, S. Hua, Z. Ding, M. Collins, et al., *FoxOs enforce a progression checkpoint to constrain mTORC1-activated renal tumorigenesis.* Cancer Cell, 2010. **18**(5): p. 472-84.
286. Truong, L.D. and S.S. Shen, *Immunohistochemical diagnosis of renal neoplasms.* Arch Pathol Lab Med, 2011. **135**(1): p. 92-109.
287. Henson, B.J., S. Bhattacharjee, D.M. O'Dee, E. Feingold, and S.M. Gollin, *Decreased expression of miR-125b and miR-100 in oral cancer cells contributes to malignancy.* Genes Chromosomes Cancer, 2009. **48**(7): p. 569-82.
288. Thomas, G.V., C. Tran, I.K. Mellinghoff, D.S. Welsbie, E. Chan, B. Fueger, et al., *Hypoxia-inducible factor determines sensitivity to inhibitors of mTOR in kidney cancer.* Nat Med, 2006. **12**(1): p. 122-7.
289. Cho, D., S. Signoretti, S. Dabora, M. Regan, A. Seeley, M. Mariotti, et al., *Potential histologic and molecular predictors of response to temsirolimus in patients with advanced renal cell carcinoma.* Clin Genitourin Cancer, 2007. **5**(6): p. 379-85.
290. Suwaki, N., E. Vanhecke, K.M. Atkins, M. Graf, K. Swabey, P. Huang, et al., *A HIF-regulated VHL-PTP1B-Src signaling axis identifies a therapeutic target in renal cell carcinoma.* Sci Transl Med, 2011. **3**(85): p. 85ra47.
291. Choueiri, T.K., S.A. Vaziri, E. Jaeger, P. Elson, L. Wood, I.P. Bhalla, et al., *von Hippel-Lindau gene status and response to vascular endothelial growth factor targeted therapy for metastatic clear cell renal cell carcinoma.* J Urol, 2008. **180**(3): p. 860-5; discussion 865-6.
292. Shi, Y., J. Gera, L. Hu, J.H. Hsu, R. Bookstein, W. Li, et al., *Enhanced sensitivity of multiple myeloma cells containing PTEN mutations to CCI-779.* Cancer Res, 2002. **62**(17): p. 5027-34.
293. Weigelt, B., P.H. Warne, and J. Downward, *PIK3CA mutation, but not PTEN loss of function, determines the sensitivity of breast cancer cells to mTOR inhibitory drugs.* Oncogene, 2011. **30**(29): p. 3222-33.
294. Wykoff, C.C., N.J. Beasley, P.H. Watson, K.J. Turner, J. Pastorek, A. Sibtain, et al., *Hypoxia-inducible expression of tumor-associated carbonic anhydrases.* Cancer Res, 2000. **60**(24): p. 7075-83.
295. Pescador, N., Y. Cuevas, S. Naranjo, M. Alcaide, D. Villar, M.O. Landazuri, et al., *Identification of a functional hypoxia-responsive element that regulates the expression of the egl nine homologue 3 (egln3/phd3) gene.* Biochem J, 2005. **390**(Pt 1): p. 189-97.
296. Henze, A.T., J. Riedel, T. Diem, J. Wenner, I. Flamme, J. Pouyseggur, et al., *Prolyl hydroxylases 2 and 3 act in gliomas as protective negative feedback regulators of hypoxia-inducible factors.* Cancer Res, 2010. **70**(1): p. 357-66.

297. Baba, M., S. Hirai, H. Yamada-Okabe, K. Hamada, H. Tabuchi, K. Kobayashi, et al., *Loss of von Hippel-Lindau protein causes cell density dependent deregulation of CyclinD1 expression through hypoxia-inducible factor.* Oncogene, 2003. **22**(18): p. 2728-38.
298. Ren, Y.Y., L.J. Du, Z.Q. Feng, and J. Leng, *[Correlation of cyclin D1 overexpression to mutations of von hippel-lindau gene in renal clear cell carcinoma].* Ai Zheng, 2006. **25**(2): p. 175-8.
299. Chamboredon, S., D. Ciais, A. Desroches-Castan, P. Savi, F. Bono, J.J. Feige, et al., *Hypoxia-inducible factor-1alpha mRNA: a new target for destabilization by tristetraprolin in endothelial cells.* Mol Biol Cell, 2011. **22**(18): p. 3366-78.
300. Schultz, L., A. Chaux, R. Albadine, J. Hicks, J.J. Kim, A.M. De Marzo, et al., *Immunoexpression status and prognostic value of mTOR and hypoxia-induced pathway members in primary and metastatic clear cell renal cell carcinomas.* Am J Surg Pathol, 2011. **35**(10): p. 1549-56.
301. Covello, K.L., J. Kehler, H. Yu, J.D. Gordan, A.M. Arsham, C.J. Hu, et al., *HIF-2alpha regulates Oct-4: effects of hypoxia on stem cell function, embryonic development, and tumor growth.* Genes Dev, 2006. **20**(5): p. 557-70.
302. Liu, Y., C. Zhang, J. Fan, L. Xiao, B. Yin, L. Zhou, et al., *Comprehensive analysis of clinical significance of stem-cell related factors in renal cell cancer.* World J Surg Oncol, 2011. **9**: p. 121.
303. Hu, J., K. Qin, Y. Zhang, J. Gong, N. Li, D. Lv, et al., *Downregulation of transcription factor Oct4 induces an epithelial-to-mesenchymal transition via enhancement of Ca2+ influx in breast cancer cells.* Biochem Biophys Res Commun, 2011. **411**(4): p. 786-91.
304. Niu, X., T. Zhang, L. Liao, L. Zhou, D.J. Lindner, M. Zhou, et al., *The von Hippel-Lindau tumor suppressor protein regulates gene expression and tumor growth through histone demethylase JARID1C.* Oncogene, 2012. **31**(6): p. 776-86.
305. Kucejova, B., S. Pena-Llopis, T. Yamasaki, S. Sivanand, T.A. Tran, S. Alexander, et al., *Interplay between pVHL and mTORC1 pathways in clear-cell renal cell carcinoma.* Mol Cancer Res, 2011. **9**(9): p. 1255-65.
306. Sanli, O., O.U. Zorba, S. Erdem, M. Tezer, I. Kilicar-Slan, T. Esen, et al., *Microscopic venous invasion is associated with disease free and cancer free survival in renal cell carcinoma.* Minerva Urol Nefrol, 2010. **62**(4): p. 347-53.
307. Fuhrman, S.A., L.C. Lasky, and C. Limas, *Prognostic significance of morphologic parameters in renal cell carcinoma.* Am J Surg Pathol, 1982. **6**(7): p. 655-63.
308. Vadysirisack, D.D., F. Baenke, B. Ory, K. Lei, and L.W. Ellisen, *Feedback control of p53 translation by REDD1 and mTORC1 limits the p53-dependent DNA damage response.* Mol Cell Biol, 2011. **31**(21): p. 4356-65.
309. Sofer, A., K. Lei, C.M. Johannessen, and L.W. Ellisen, *Regulation of mTOR and cell growth in response to energy stress by REDD1.* Mol Cell Biol, 2005. **25**(14): p. 5834-45.